Review of sclerorhynchoids (chondrichthyes: bataoidea) and its phylogenetic and taxonomic implicatons

http://bbktheses.da.ulcc.ac.uk/478/

Version: Full Version

REVIEW OF SCLERORHYNCHOIDS (CHONDRICHTHYES: BATOIDEA) AND ITS PHYLOGENETIC AND TAXONOMIC IMPLICATIONS

Eduardo Villalobos Segura

Supervised by Dr. Charlie J. Underwood and Dr. Philip J.

Hopley

Birkbeck, University of London

Thesis submitted to the Department of Earth and Planetary Sciences for the

degree of Doctor of Philosophy

2020

Declaration

Declaration of originality

I, Eduardo Villalobos Segura, confirm that the work presented in this thesis is my own. Where information has been derived from other sources, I confirm that his has been indicated in the thesis.

Copyright declaration

The copyright of this thesis rest with the author. Researchers are free to copy, redistribute, remix and transform this thesis on the condition that it is appropriately attributed.

Doctoral committee

Dr. Charlie J. Underwood
Department of Earth and Planetary Sciences
Birkbeck, University of London

Dr. Philip J. Hopley
Department of Earth and Planetary Sciences
Birkbeck, University of London

Founding

This thesis is dedicated to my two grandmothers, whichever ethereal plane they are

Acknowledgements

Abstract

Recently molecular analysis shifted long-standing conceptions regarding the taxonomic and phylogenetic relationships of batoids. These changes and current phylogenetic work and classifications of fossil batoids have not been integrated. Sclerorhynchoids are one of most diverse and widely recorded clades of Cretaceous batoids whose phylogenetic relations remain undetermined. With the discovery and description of specimens of sclerorhynchoids from Morocco, the present study revaluates the phylogenetic relations of the group and proposes a new topology and rearrangement of it with respect of other batoids as a suborder of Rajiformes. These changes are contrasted with previous works. Whilst these analyses do not provide the ultimate truth regarding the phylogenetic relations of the sclerorhynchoids they represent an important steppingstone for future phylogenetic works involving fossil batoids and morphological data. With the similar composition of the major clades between molecular analyses and the present study a time-scaling analyses using tip-dating, basic and minimum branch length is carried out, with the objective of stablishing a possible divergence time for sclerorhynchoids and other batoids groups. These results are compared using stratigraphic indices. Overall tip-dating presented slightly better scores. The ages estimated by the morphological data recover later divergence events than those with molecular data. Diversity curves (taxonomic diversity estimate and shareholder quorum subsampling) were used to compare the estimated ages between molecular and morphological data, this comparison resulted in morphological data presenting a better overlap with possible divergence events recovered by the diversity curves. Finally, a taxonomic update of the group is presented. A total of 30 genera and 72 valid species were found as a result of the bibliographic review. The bibliographic review revealed an uneven sampling effort between regions, which needs to be addressed, to properly establish an adequate approximation to the diversity of the group and batoids.

Contents

List of Figures

List of Tables

Chapter 1

General introduction

There are two extant groups of Gnathostomata (jawed vertebrates) (Carroll, 1988). Osteichthyes includes all bony fishes and tetrapods derived from them and Chondrichthyes (ςηονδρος = cartilage and ιςητηψς = fish) that includes all "fishes" whose endoskeletons present tessellated chondral mineralization, sometimes accompanied by more granular calcification (Claeson, 2010), (some of the earliest chondrichthyans had acellular bone calcification associated to the dorsal spines and other dermal or exoskeletal elements). Overall the chondrichthyan skeleton is minimalistic, characterised by the fusion of several skeletal regions (cranial, appendicular, and vertebral) (Miyake *et al*., 1992; Claeson & Hilger, 2011; Johanson *et al*., 2013).

Chondrichthyan placement as sister group of the osteichthyans (bony fishes) leads to the misconception that anatomical features observed in chondrichthyans are primitive. In reality, both skeletal forms are highly divergent (Maisey, 2012; Maisey *et al*., 2019), since both forms have been evolving independently since the late Ordovician-Silurian (Andreev *et al*., 2016; Coates *et al.,* 2018). Currently phylogenetic research into chondrichthyans is active with new discoveries changing the landscape of long-lasting conceptions about chondrichthyan evolution (Maisey, 2012). Presently two large groups are recognized within extant chondrichthyans: one that includes the modern sharks and rays (elasmobranchs) and the holocephalans which includes the rather unusual chimaeras. The identity of elasmobranchs as a taxonomic entity has changed through time. Hay (1902) united all modern elasmobranchs into a single group (Euselachii) along with extinct hybodonts. Regan (1906) followed Hay's observations and placed the clasper-bearing 'Ichthyotomi' (xenacanths) into a polytomy with the Euselachii and Holocephali

but excluded the 'pleuropterygian' sharks (those supposedly lacking pelvic claspers. e.g., †*Cladoselache*) and 'acanthodians' from the group, effectively treating them as stem chondrichthyans. Goodrich (1909) advocated that some extinct sharks (e.g. xenacanths, 'cladodonts', †*Cladoselache*) did not belong inside the group comprising the chondrichthyan crown, which he termed Elasmobranchii, following original usage of the term used by Bonaparte (1838). Maisey (1984) also excluded †*Cladoselache* (and 'symmoriids') from the chondrichthyan crown but included xenacanths (treating them as stem elasmobranchs, along with hybodonts plus a few additional taxa). Compagno (1973, 1977) recognized a monophyletic group of living elasmobranchs (which he termed 'neoselachians'), based on several apomorphic characters that are absent in many extinct shark-like chondrichthyans (although some of his characters occur in hybodonts). Compagno's 'neoselachian' is equivalent of Elasmobranchii *sensu* Huxley (1880) and of the elasmobranch crown. Pradel *et al.* (2011) place numerous Paleozoic chondrichthyans (†*Doliodus*, †*Pucapampella*, symmoriiforms, 'ctenacanths', and xenacanths) outside crown chondrichthyans. Coates *et al.* (2017) place all but a few of these taxa within the chondrichthyan crown, which are again resolved as stem chondrichthyans (†*Doliodus*, †*Pucapampella*, and †*Gladbachus*,).

Regardless of future changes in the composition of the crown chondrichthyans, batoids are still included within Elasmobranchii or Neoselachii (*sensu* Maisey, 2012) and are today one the most diverse group of elasmobranchs with about 665 species (Fricke *et al*., 2019). This clade is first recorded in the late Early Jurassic and became well-established in the Middle-Late Jurassic (Maisey *et al*., 2004; Underwood, 2006). The appearance of this group coincided with a change in overall body form, from compressed or cylindrical to depressed, the enlargement and attachment of the pectoral fins to the head, the loss of subocular shelves and anal fin and an euhyostylic jaw suspension (Cappetta, 1987; Wilga *et al*., 2008; Nelson *et al*., 2016; Aschliman *et al*., 2012a). Elasmobranchii is currently

considered a monophyletic group. However, there are discrepancies regarding the relations within it, mostly because depending on the characters used in the analysis the phylogenetic relations change (i.e. topologies proposed with molecular data and statistical methods (Dunn & Morrissey, 1995; Schwartz & Maddock, 2002; Douady *et al*., 2003; Winchell *et al*., 2004; Aschliman *et al*., 2012b; Naylor *et al.,* 2012; Last *et al*., 2016) contradict most of the groups found with morphological data and parsimony (Brito & Dutheil, 2004; Aschliman et al., 2012a; Brito *et al*., 2013; Claeson *et al*., 2013; Underwood & Claeson, 2017)).

Maisey *et al*. (2004) and Underwood (2006), tried to solve this controversy using the fossil record as an independent test for the accuracy of different topologies and noticed that morphological-based phylogenies, were strongly discordant with the known fossil record, they imply that the time origin of almost every major modern elasmobranch group is underestimated and needs the presence of several extremely long ghost lineages. Molecular phylogenies, on the other hand, suggest an earlier appearance of elasmobranch groups (Underwood, 2006) and are more reconciled with the fossil record (Maisey *et al*., 2004).

With the surge of molecular techniques, more groups of batoids are being studied and their phylogenetic relations continue to change drastically as within highly paraphyletic groups (e.g. Rhinobatidae and Rajiformes) previously unnoticed clades are recognised. Leaving classifications based on morphological analysis uncertain and creating problems for the study of fossil batoids that are forced to fit in to recent clades. The sclerorhynchids are one of those groups, they are a major batoid group with over 16 genera and 40 species (Kriwet & Kussius, 2001; Cappetta, 2012). Despite commonly dominating Late Cretaceous (Barremian-Maastrichtian) Chondrichthyan assemblages (Underwood, 2006; Welton & Farish, 1993), they became extinct after the K/Pg (Cretaceous-Paleogene

extinction event). Among the Cretaceous batoids they are a very peculiar group, as they are one of the three groups of known neoselachians (*sensu* Maisey, 2012) that had developed an elongated rostral blade. The group also present a unique anatomy for the pectoral fins with an enlarged propterygium, mesopterygium and metapterygium (Wueringer *et al*., 2009). Despite these peculiarities they share synapomorphies with batoids (e.g. the presence of a synarcual with lateral stays; pectoral disc connected by tissue to the chondrocranium and gill slits located ventrally) and so are clearly included within the clade, but further from that their phylogenetic relations remain uncertain (Woodward, 1895; Kriwet, 2004; Underwood, 2006, Cappetta, 2012).

As with most of chondrichthyans the fossil record of sclerorhynchoids is composed largely by non-cartilaginous remains (e.g. teeth and denticles), fossilized elements with mineralised cartilage (of some sort) are exceptionally rare and even rarer are articulated skeletons. Almost all articulated sclerorhynchid material described to date is from the to the Cenomanian and Santonian (late Cretaceous) of Lebanon (Cappetta, 1980a). From these sites, articulated and in many respects beautifully preserved remains of the small genera of sclerorhynchids, like †*Sclerorhynchus* Woodward (1889a), †*Libanopristis* Cappetta (1980a) and †*Micropristis* Cappetta (1980a), are known and despite the preservation of fine detail these fossils are dorsoventrally flatted and as a result complex three-dimensional detail of structures such as neurocranium, synarcual and pectoral girdle are poorly known.

Despite the lack of uncrushed skeletal remains of sclerorhynchoids, they are recognised as well-defined clade. However, there is great uncertainty as to the phylogenetic relations of the clade remains elusive. With the discovery of the first three-dimensionally preserved skeletal fossil remains of sclerorhynchoids from the Turonian and Cenomanian (late Cretaceous) the present project seeks to revaluate the phylogenetic affiliation of

sclerorhynchoids with respect to other batoids and within the group, through a review of previous morphological characters (Compagno, 1973; Nishida, 1990; Shirai, 1992; Brito & Seret, 1996; McEachran & Aschliman, 2004; Brito & Dutheil, 2004; Aschliman *et al*., 2012a; Brito *et al*., 2013; Claeson *et al*., 2013; Underwood & Claeson, 2017) and presents an update of the taxonomic classification of sclerorhynchoids, based on the results of those previous analysis and on the description of the material collected from the north of Africa (Morocco), which includes the description of a new genus and species of sclerorhynchoid †*Asflapristis cristadentis* gen et nov. sp. along with the first skeletal record for the genera †*Onchopristis* and †*Ptychotrygon* and describes a new species †*P. rostrispatula*. Along with the phylogenetic and taxonomic update a time-scaling analyses using tip-dating, basic and minimum branch length presented with the objective of stablishing a possible divergence time of the sclerorhynchoids and other batoids groups and their results are compared using stratigraphic indices. The tip-dating estimated divergence ages were compared with those of molecular analysis and diversity curves (taxonomic diversity estimate "TDE" and shareholder quorum subsampling "SQS").

Outline of the thesis

Currently morphological phylogenetic studies of fossil batoids are stagnated, using similar sets of characters from previous analysis, which recover discordant topologies to those of the molecular analysis and the fossil record (Maisey 2004; Underwood, 2006) and groups not currently recognized by the present taxonomic arrangement (Naylor *et al.,* 2012; Fricke *et al*., 2019) (e.g. Rajiformes no longer includes Pristoidei and Rhinobatoidei which are currently placed together int the order Rhinopristiformes).

The present analysis evaluates the phylogenetic relations of sclerorhynchoids by reassessing previously used morphological character, considering the taxonomic changes within batoids. Regardless the inherent biological importance of describing three

dimensional preserved skeletal remains of batoids due to their rarity, the aim this thesis is to clarify and improve the phylogenetic relationships of sclerorhynchids within batoids, and within this group and provide a more extended discussion of the characters used in previous works (Brito & Seret, 1996; Brito *et al*., 2004; 2013; 2019; Claeson *et al*., 2013; Underwood & Claeson, 2017) . This thesis is structured as a series of semi-autonomous article-chapters book ended by a general discussion and conclusion. Because this thesis includes separate article-chapters, each with its own introduction, detailed accounts of background information specific to each chapter are not included in this general introduction. Likewise, this thesis does not include a separate chapter dedicated to the entire methodology as each article-chapter contains its own methodology section. For the published chapters the sections that included participation of co-authors are stated at the start of the chapter along with my contributions.

- Chapter 1 (current chapter): presents an overview of the phylogenetic and taxonomic framework of sclerorhynchoids starting from their class Chondrichthyes, leading to the discovery of the specimens described in the present work.

- Chapter 2: Presents the description of the two species of sclerorhynchoids discovered in (Asfla) Morocco, based on the preparation of eleven specimens currently housed in the Natural History Museum (NHM). Along with these descriptions, there are the palaeontological implications of this discoveries for the zone.

- Chapter 3: Presents the description of the †*Onchopristis numidus* remains collected in the "Kem Kem Beds" Southeast of Morocco.

- Chapter 4: Based on the descriptions made in Chapter 2 and with the incorporation of skeletal information from other sclerorhynchoid genera (†*Sclerorhynchus* and †*Libanopristis*), the phylogenetic relations between sclerorhynchoids and other batoids is reviewed. The results of the analysis are compared with previews works that tried to establish them (Kriwet, 2004) or include them in their analysis (Claeson *et al*., 2013 and

Underwood & Claeson, 2017). The results of the present analysis recovered similar crown groups to those of molecular analysis (Aschliman *et a*l., 2012b) and placed the sclerorhynchoids in a different position to that proposed by previous studies (e.g. Kriwet, 2004, Brito *et al*., 2013 and Underwood & Claeson, 2017). This chapter also includes a detailed description of the characters used for the analysis.

- Chapter 5: Based on the description of Chapters 2 and 3, this chapter presents a phylogenetic analysis of the relationships within the sclerorhynchoids. Based on the results obtained in chapter 4 three taxa were used as outgroups (†*Spathobatis*, rajoids, *Pristis* and *Rhinobatos*). Along with the newly described taxa, this chapter included four additional genera of sclerorhynchoids (†*Libanopristis,* †*Micropristis,* †*Schizorhiza* and †*Sclerorhynchus*) with relatively good skeletal records (not only teeth and enlarged denticles). This chapter also includes a detailed description of the characters used for the analysis and a comparison between different types of optimisation of the characters with and evolutionary discussion of the implications of each optimisation.

- Chapter 6: With the recovery of similar crown group as molecular analysis this chapter presents the first time-scaled phylogeny for batoids using morphological data. The time-scaled analysis used the matrix of Chapter 4, with the inclusion of fossil representatives of each batoid order. Two approaches were used to time scale: Tip-dating and "*a posteriori*" methods (minimum length branch and basic). Trying to firs stablish a divergence time for sclerorhynchoids and subsequently all batoid orders (Rajiformes, Rhinopristiformes, Torpediniformes and Myliobatiformes) using morphological data. The results of this analysis are compared with those obtained by molecular time scaled analysis (Aschliman *et al*. 2012b) and discussed in a geological context.

- Chapter 7: Based on the results obtained Chapters 4 and 5 , this chapter presents an updated taxonomic framework for sclerorhynchoids. This update includes a full taxonomic work for each known sclerorhynchoids species, along with a short description

for each genus. This chapter also presents a descriptive analysis on the number of genera and species of sclerorhynchoids through time and in different geographical regions which are compared with previous ones (Kriwet & Kussius, 2001).

- Chapter 8: puts together the results of previous chapters in from of a general discussion and conclusion and presents some new avenues for future research with sclerorhynchoids and batoids.

Chapter 2

Goulmima assemblage and the description of two new sclerorhynchoids.

This chapter is an extended version of the descriptions published in:

1. Eduardo Villalobos-Segura, Charlie J. Underwood, David J. Ward & Kerin M. Claeson. 2019. **The first three-dimensional fossils of Cretaceous sclerorhynchid sawfish: *Asflapristis cristadentis* gen. et sp. nov., and implications for the phylogenetic relations of the Sclerorhynchoidei (Chondrichthyes).** *Journal of Systematic Palaeontology*, DOI:10.1080/14772019.2019.1578832.

2. Eduardo Villalobos-Segura, Charlie J. Underwood & David J. Ward. 2019. **The first skeletal record of the Cretaceous enigmatic sawfish genus *Ptychotrygon* (Chondrichthyes: Batoidea) from the Turonian (Cretaceous) of Morocco**. *Papers in Palaeontology,* DOI: 10.1002/spp2.1287

Co-authors contributions

- o E. Villalobos Segura: Preparation, description and photography of the specimens. Collaborated in the discussion of geographic and taphonomic characteristic of the area.
- o C.J. Underwood: Stratigraphic column. Locality map. Discussion of geographic and taphonomic characteristic of the area. Part of the acquisition team for the specimens
- o D.J. Ward: Micro-sampling and part of the acquisition team for the specimens
- o K M. Claeson: Computed tomography scan of fragile specimens.

Introduction
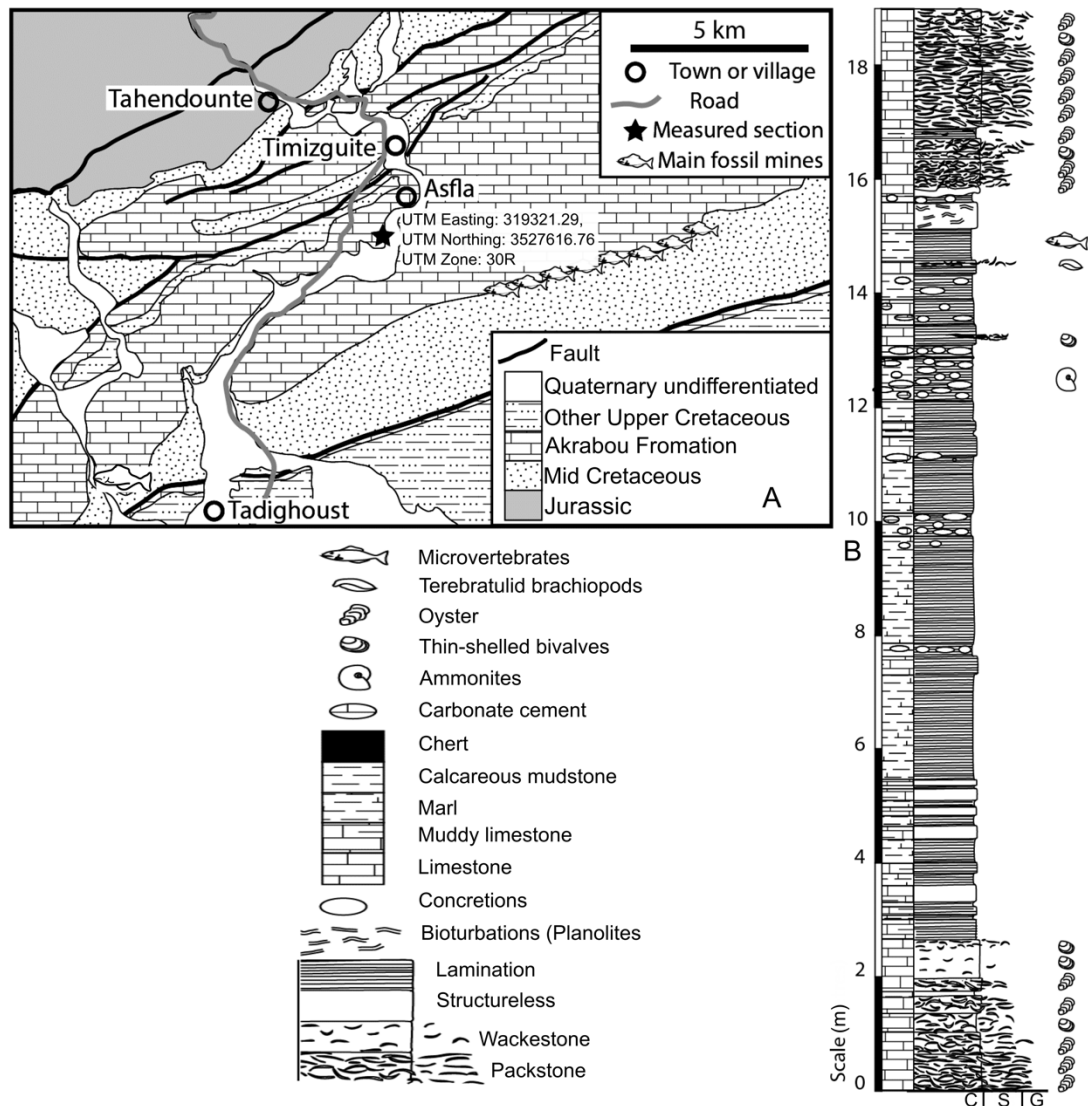
Figure 2.1. A, Map and **B,** Stratigraphic column of the locality in Asfla. Coordinates in figure A correspond to the measured section (UTM Easting: 319321.29, UTM Northing: 3527616.76 and UTM Zone: 30R).

The area North of the town of Goulmima, southeast Morocco, is well known for fossils of ammonites (e.g. Cavin *et al*., 2010, Kennedy *et al*., 2008) and vertebrates (e.g. Ettachfini & Andreu, 2004). In this region fossils are commercially collected, with the trade being centred on the village of Asfla. The fossils in the present study originate from to the Akrabou Formation (Fig. 2.1A), a unit of platform carbonates that ranges from late Cenomanian to Turonian (Cretaceous). These carbonates overlie the famously fossiliferous 'mid' Cretaceous Kem Kem fluvial facies and are overlain by further non-

marine Late Cretaceous rocks. The Akrabou Formation, therefore, presents a strongly transgressive succession and a relatively high sea-level period, followed by a regressive episode. More southern outcrops of the Akrabou Formation form a near-horizontal foreland area to the South of the High Atlas tectonic belt, with successions north of Goulmima being subject to folding and reverse faulting along the southern margin of the High Atlas (Lezin *et al*., 2012). Whilst much of the Akrabou Formation comprises very shallow water facies containing monospecific shell beds, microbial laminites and tepee structures, the ammonites and vertebrates are largely known from a deeper water interval containing ovoid calcareous concretions (Fig. 2.1B). Whilst the deeper water marls are up to 15 metres thick (close to the village of Asfla), fossiliferous concretions are largely limited to near the top of the unit. Where fossils are actively mined, there are typically two distinct units of concretions. A lower concretion bed, up to 1m thick, generally poor in macrofossils. A second concretion bed, about 2m higher in the succession, is somewhat discontinuous (being absent at this level at Asfla itself) and often highly fossiliferous. This level is commonly mined in the cliff face to extract fossils for sale. The concretion-bearing levels are typically finely laminated and trace fossils are limited to rare, fine *Planolites* and other tubular burrows. Benthic fossils are rare other than oval, thin shelled bivalves and very small gastropods (Fig. 2.1B). At least some of the bivalves appear to be members of the Lucinidae. Small cirripede plates and comatulid crinoids are common in some commercially obtained concretions, but their provenance is uncertain.

Fossils are largely restricted to within the concretions themselves, with the only macrofossils in the surrounding rocks being small molluscs. Concretions are typically ovoid and when they enclose a vertebrate fossil, typically take on the general shape of the enclosed fossil. Batoid and actinopterygian skeletons collected from the Asfla area are three-dimensional, with skeletal elements occupying several planes within the concretion (Cavin *et al*., 2010; Underwood *et al*., 2009), although there may be some crushing of

larger elements (Claeson *et al*., 2013). The most abundant larger fossils within the nodules are ammonites (Kennedy & Juignet, 1981; Kennedy *et al*., 2008). Fish fossils are also abundant, with †*Goulmimichthys arambourgi* comprising most of partial to near complete skeletons (Cavin, 1995). †*Ichthyodectes bardacki,* †*Osmeroides rheris* and †*Araripichthys corytophorus* (Cavin *et al*., 2010) are also frequent and *Enchodus sp.* and indeterminate pycnodonts can also be found (Cavin & Dutheil, 1999). Chondrichthyans are far less common and restricted in diversity, microvertebrate sampling suggest a small number of chondrichthyan species are present, with only batoids known from skeletal remains and (Cavin, 1995; Claeson *et al*., 2013; Underwood *et al*., 2016a; text-fig. 3). Teeth of †*Ptychotrygon rostrispatula* are by far the dominant elasmobranch fossils, followed by extremely small teeth resembling those of Rhinobatos. †*Asflapristis cristadentis* teeth are relatively rare. There are also teeth of a small anacoracid and possible †*Cretomanta*.

The marine reptiles include abundant remains of the mosasaur †*Tethysaurus nopcsai* Bardet *et al*., 2003a, several plesiosaurs including †*Thililua longicollis* Bardet *et al.,* 2003b and †*Manemergus anguirostris* Buchy *et al.,* 2005, and undescribed chelonians (Cavin, 2001). The overall fossil composition of the Akrabou Formation, whilst restricted in diversity, contains many of the faunal elements present in other shallow seas of the southern and western Tethys, and shows strong affinities with the South Atlantic and even the Western Interior Seaway in North America (Maisey & Moody, 2001; Cavin, 2001).

The Akrabou Formation typically forms high and steep escarpments, with the concretion beds often within the upper part of these cliffs. The upper nodule bed is the focus of intense commercial collecting activity. The most productive fossil sites are along the large escarpment South and East of Asfla; exposures elsewhere either lack the upper concretion bed or are less fossiliferous and are not commercially exploited. As a result, few fossils

are seen *in situ*, although in the natural screes on the lower parts of the escarpments ammonites and remains of †*Goulmimichthys* can be found. The softer marls, especially those of the level of the Upper Nodule Bed, are suitable for bulk sampling, the results of which have yet to be studied in detail. As with many Moroccan palaeontological investigations, the presence of commercial collecting has proven critical to this study.

Taphonomy

Fossils of dermal elements and teeth of chondrichthyan are often very common in the fossil record as are produced continuously through life. In addition, the enameloid and dentine composition of these elements gives them a high preservation potential. The fossil record of cartilaginous skeleton which is typically strengthened by different degrees of apatite mineralisation, is largely limited to the most intensely mineralised structures such as vertebral centra, jaw cartilages and rostra. The more complete skeletal remains of chondrichthyans are restricted to a small number of *Konservat Lagerstätten* (e.g. Solnhofen, Nusplingen Kriwet & Klug, 2004, Monte Bolca Marramà *et al*., 2018 and Green River Formation, De Carvalho *et al.,* 2004). Cretaceous sites with well-preserved batoids are rare and other than isolated occurrences, largely limited to sites in Lebanon (Cappetta, 1980a) and the Santana Formation of Brazil (Martill, 1988). Of these sites, the outwardly spectacularly preserved fossils of Lebanon are highly compressed, whilst the uncrushed batoid fossils of Brazil are restricted to two species (†*Iansan beurleni* Brito & Seret, 1996 and †*Stahlraja sertanensis* Brito *et al*., 2013).

At Asfla, vertebrate remains are preserved largely uncrushed within large and irregular carbonate concretions. The bony fish are typically preserved with the concretions centred around their trunk, with concretions around smaller fish being ovoid, those around larger skeletons roughly replicating the outline of the enclosed remains. The edges of the concretions rarely reach the extremities of the skeleton, with the caudal area, and often

front of the skull, commonly missing. Specimens of †*Asflapristis cristadentis* and †*Ptychotrygon rostrispatula* are far less complete than those of the bony fishes found in the region.
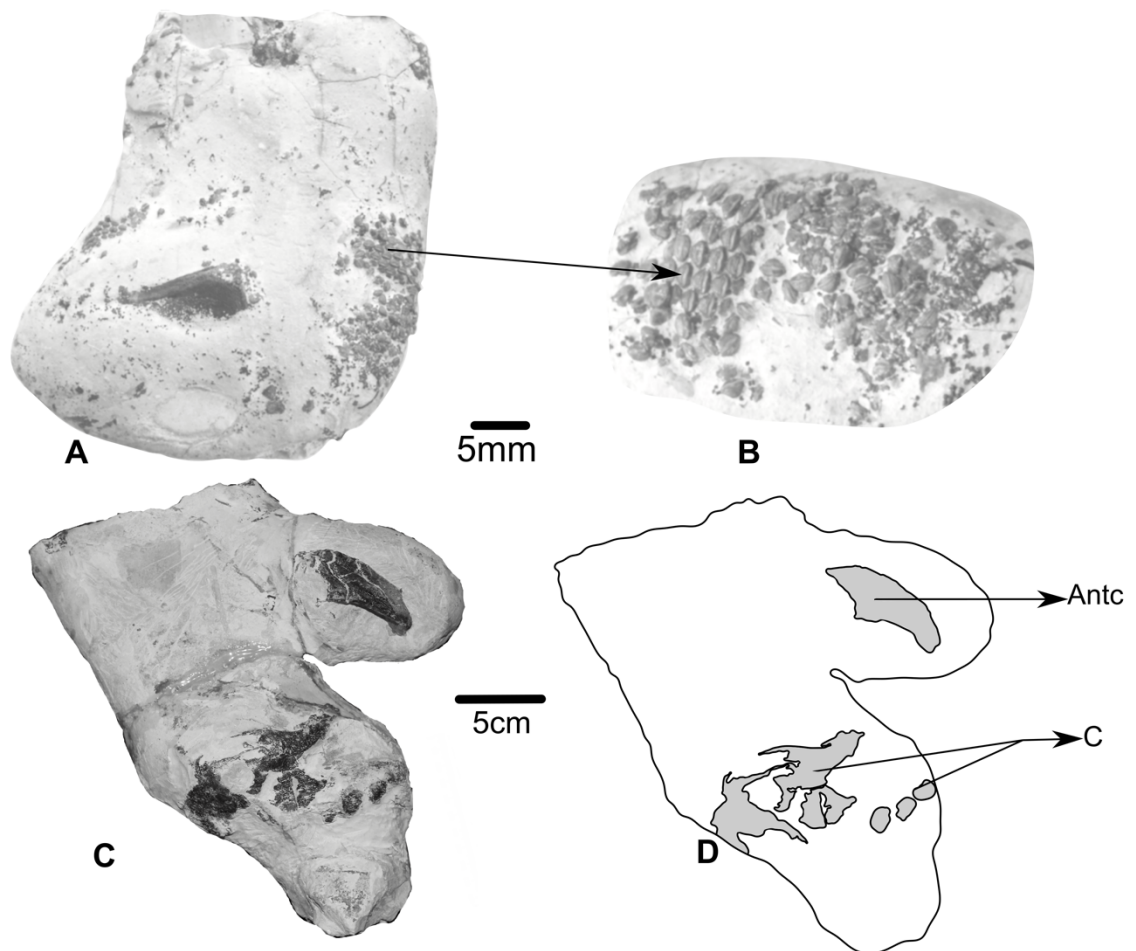
Figure 2.2. Examples of preservation of specimens of †*Asflapristis cristadentis* gen. et sp. nov. found in Asfla. **A-B,** Teeth of NHMUK PV P 75432. **C-D,** Ventral view of NHMUK PV P 75428. **Abbreviations**: Antc, antorbital cartilage. C; undetermined cartilages. Grey colour parts are the exposed cartilage.

Some specimens of †*Asflapristis cristadentis* like NHMUK PV P 75431 were clearly disarticulated prior to burial whereas others like NHMUK PV P 75433, although incompletely preserved, show a skeleton that extends beyond the edges of the concretions and were complete and articulated at the time of burial. In the cases of these articulated specimens, it is likely that parts of the skeleton outside the concretions were lost at the time of collection, with the collectors not recognising the crushed cartilaginous skeleton outside the concretions. The high degree of articulation of even relatively fragile

27

skeletons of batoids suggests that scavenging on the seafloor was absent or minimal, indicative of a hostile seafloor and/or very rapid burial. Whilst the concretion-bearing units of rock are thin, this does not rule out rapid burial by episodic sedimentation, even if the net sedimentation rate was low. Evidence for rapid burial comes from the fact that some of the elements of the skeletons are articulated even though they do not exist on the same bedding plane of the rock. This is clearly seen in the articulated dentitions of specimens like NHMUK PV P 75432 (Fig. 2.2A) where parts of articulated dentition are present in their life position relative to jaw cartilages. This can only have been preserved if burial had occurred prior to decay of dermal tissue supporting the teeth. A similar situation exists with the three-dimensional nature of branchial and jaw elements in some batoid specimens, where connective tissue must have retained the geometry of the skeleton until burial.

The rich biota of the Asfla concretion beds is composed almost entirely of free-swimming taxa, especially ammonites and vertebrates. By contrast, the benthos fauna is very limited and largely occurs sporadically and possibly restricted to certain bedding surfaces, whilst infaunal ichnofossils are largely absent. A likely explanation of this is that the seafloor was generally hostile to life (e.g. Wignall, 1994). The few benthic bivalves appear to be largely limited to lucinids, which possess sulphide-oxidising endosymbionts and thus may have found the conditions favourable when other benthos did not. Whilst there is clear no evidence of scavenging of vertebrate remains (such as bite marks), there are suggestions of scavenging by large organisms on at least one of the specimens (NHMUK PV P 75428) (Fig. 2.2B), which shows a large piece of sheet-like cartilage with ragged edges is present. The affinity of it is unclear, but it appears to be a partially detached piece of the braincase. This displacement cannot easily be explained by burial processes, and therefore it may represent the damage to the skull caused by feeding by a large (presumably reptilian) scavenger.

No soft tissue preservation has been recognised in the specimens of †*Asflapristis cristadentis*, although phosphatised muscle tissue was noted in †*Ptychotrygon rostrispatula* and †*Tingitanius tenuimandibulus* (Claeson *et al*., 2013). This, albeit rare, preservation of soft tissue points towards an environment with poor conditions for organisms responsible for decomposing (Lezin *et al*., 2012) associated with microbially-mediated precipitation of apatite being more rapid than complete decay of soft tissues (Martill, 1988).

Whilst fossils within the concretions are typically preserved in three dimensions, there is evidence of some degree of compaction *prior* to carbonate precipitation to form the concretions. There is some degree of crushing of the neurocranium and pectoral girdle of some specimens and shortening of obliquely orientated elements has previously been noted (Claeson *et al*., 2013). The overall taphonomic environment is thus similar to that of the Santana Formation of Brazil (see, Martill, 1988), despite the lack of similarity of depositional environment, with fully marine environments of Asfla contrasting with the rather more restricted palaeoenvironments of the Santana Formation which lacks fully marine invertebrates (Martill, 1988).

Material and Methods

The specimens described here were obtained from Morocco-based commercial sources, either from fossil collectors in Asfla itself or from larger scale local wholesalers based in Erfoud, Rissani and Rich. The specimens were either totally unprepared, or with only minimal, and typically rather crude, preparation. In all cases some cartilage with tesserae was showing on the surface of the concretion sometimes associated with teeth. Two different tooth morphologies associated with different species and genera were found: †*Asflapristis cristadentis* and †*Ptychotrygon rostrispatula*. To prevent incorrect

attribution of skeletal material between these two species, only specimens associated with teeth were included in the description. †*Asflapristis cristadentis* description is based on six specimens and †*Ptychotrygon rostrispatula* is based on three.

The concretions enclosing the batoid remains are very hard, whilst cartilage elements are often fragile, and tesserae are commonly slightly disarticulated. The somewhat shattered tesserae ruled out acid preparation of the specimens. When necessary, mechanical preparation using air pen, chisel and hammer was carried out to expose characters not seen elsewhere. The mechanical preparation was performed in the Natural History Museum of the United Kingdom (NHMUK) under the supervision of personnel of the Palaeontology Conservation Unit.

One of the specimens (†*Asflapristis cristadentis* NHMUK PV P 75429 a-d) was considered unsuitable for any preparation as the dorsal surface was too fragile, so it was left unprepared but studied as rendered CT scan images. The specimen was scanned at the High-Resolution Computed Tomography Laboratory at The University of Texas at Austin (UTCT) using an NSI scanner. Using the following protocol: GE Titan source, small spot, 370 kV, 1.1 mA, 1 brass filter, Perkin Elmer detector, 2 pF gain, 1 fps (999.911 ms integration time), no binning, no flip, source to object 853.276 mm, source to detector 1421.23 mm, continuous CT scan, 3 frames averaged, 0 skip frames, 3099 projections, 7 gain calibrations, 15 mm calibration phantom, data range (-2, 15) (rescaled from NSI default). Voxel size = 0.1316 mm, beam-hardening correction = 0.5. Post-reconstruction ring correction applied by Jessie Maisano using parameters oversample = 3, bin-width = 21, sectors = 60. Total slices = 1904. Slice data were further analysed using VGStudio MAX 2.0 in the University of Texas Digital Methods Laboratory and using AVIZO in the Department of Biomedical Sciences at Ohio University.

Results

†*Asflapristis cristadentis* Villalobos-Segura, Underwood, Ward and Claeson, 2019a.

Material

Holotype: NHMUK PV P 75433, presents most of the dorsal surface neurocranium, the whole synarcual and pectoral girdle, although distal pectoral elements are missing.

Paratypes: NHMUK PV P 73925, in dorsal view presents most of the mid-posterior regions of the neurocranium (posterior to nasal capsules) and both hyomandibular cartilages. The ventral surface shows both antimeres of the Meckel cartilage, the right antimere palatoquadrate and anterior part of the right second hypobranchial. NHMUK PV P 75428 a-e, specimen composed of five fragments, on ventral view shows a small tooth patches close to the mouth region, fragments of the anterior section of the second hypobranchial and antorbital cartilages. NHMUK PV P 75429 a-d, specimen composed of four fragments on its dorsal surface shows most of the middle portion of the neurocranium along with fragments of the rostrum, most of the anterior portion of the synarcual is preserved, parts of the medial crest and lateral stays exposed, and on the ventral surface a patch of teeth is exposed. NHMUK PV P 75431, complete synarcual. It was assigned after preparation work revealed a characteristic tooth in the rock matrix. NHMUK PV P 75432, articulated teeth set without associated identifiable skull material.

Systematic Palaeontology

Class **Chondrichthyes** Huxley,1880.
Superorder **Batomorphii** Cappetta, 1980b.
Order **Rajiformes** *sensu Naylor et al.*, 2012.
Suborder **Sclerorhynchoidei** Cappetta 1980b.
Family **Ptychotrygonidae** Kriwet *et al*., 2009a.

Genus *Asflapristis* nov. gen.
Species *Asflapristis cristadentis* gen. et. nov. sp.
Figures 2.3-2.11.

- **Derivation of genus Name**: After the town of Asfla, where the specimens were found.
- **Derivation of species Name**: From the presence of several ridges in the teeth.

Type species: †*Asflapristis cristadentis*.

Diagnosis of genus

Sclerorhynchid batoid with estimated total length in excess of two meters. Rostrum of uncertain length but robust and apparently lacking enlarged rostral denticles or 'wood-like' cartilage (external layer of fibrous cartilage that resembles wood cortex with several vertical, parallel and well mineralized ridges). Neurocranium (posterior to nasal capsules) of similar length and width. Palatoquadrate and Meckel's cartilages wide and stout and with a thin outer layer of 'wood-like' cartilage. Second hypobranchial without an anterior process. Synarcual long well beyond the scapulocoracoid, with a well-developed medial crest and dorsally directed lateral stays, no direct joint to the pectoral girdle was observed. Synarcual lip large and fits within the chondrocranium. Vertebral centra fail to reach the middle of the synarcual. Lateral facet of scapulocoracoid thick and compact and articulates to the pectoral elements (propterygium, mesopterygium and metapterygium). Dentition relatively homodont, teeth oval in occlusal view and lacking a medial cusp or well-developed uvulae, and with large pulp cavity. Occlusal ornament with a strong transverse ridge with fine and irregular branching ridges, mostly linguo-labial and around margins. A fine ridge along labial edge of occlusal face is present in many teeth. Root low with widely spaced root lobes with rounded basal face.

Diagnosis of species

As for genus.

Description

Measurements and body proportions are difficult to establish since no complete specimen has been found. Six specimens of skeletal material can unambiguously be referred to †*Asflapristis cristadentis* based on tooth morphology, between them they provide data on the neurocranium and proximal part of the rostrum, jaws and dentition, synarcual, brachial skeleton, pectoral girdle, proximal part of the pectoral fins, and the trunk vertebral column. The pelvic girdle and fins, claspers, dorsal fins, caudal skeleton, distal parts of the pectoral fins and tip of rostrum are missing.

Chondroskeleton

The exposed skeletal elements are composed of a layer of tesserae and prismatic cartilage. The mouth of the specimen NHMUK PV P 75433 shows a small layer or wood-like perichondrium similar to that observed in the rostrum of *Onchopristis* and *Schizorhiza* (Kirkland & Aguillón-Martínez, 2002). The wood-like perichondrium is absent in other regions of the skeleton including the rostrum. Its presence in the jaw cartilages may be an adaptation to durophagy.

Chondrocranium

Box-shaped structure that seems to lack the characteristic bottle shape of other batoids (Fig. 2.3A-B). The antorbital cartilages are scythe-shaped (curved posteriorly towards the distal end) with a wide base and become narrower towards the tip. The chondrocranium in its middle portion presents the supraorbital crests that are slightly elevated from the rest of the roof. Posterior to the postorbital process the chondrocranium widens and progressively narrows until it reaches its end (Figs. 2.4C-D). At the posterior region there is a deep concave indentation where the synarcual lip (odontoid process) fits. The occipital condyles are large and present a broad articular surface for the lateral anterior

facets of the synarcual. The lateral and basal faces of the chondrocranium were not clearly

visible on any specimen.
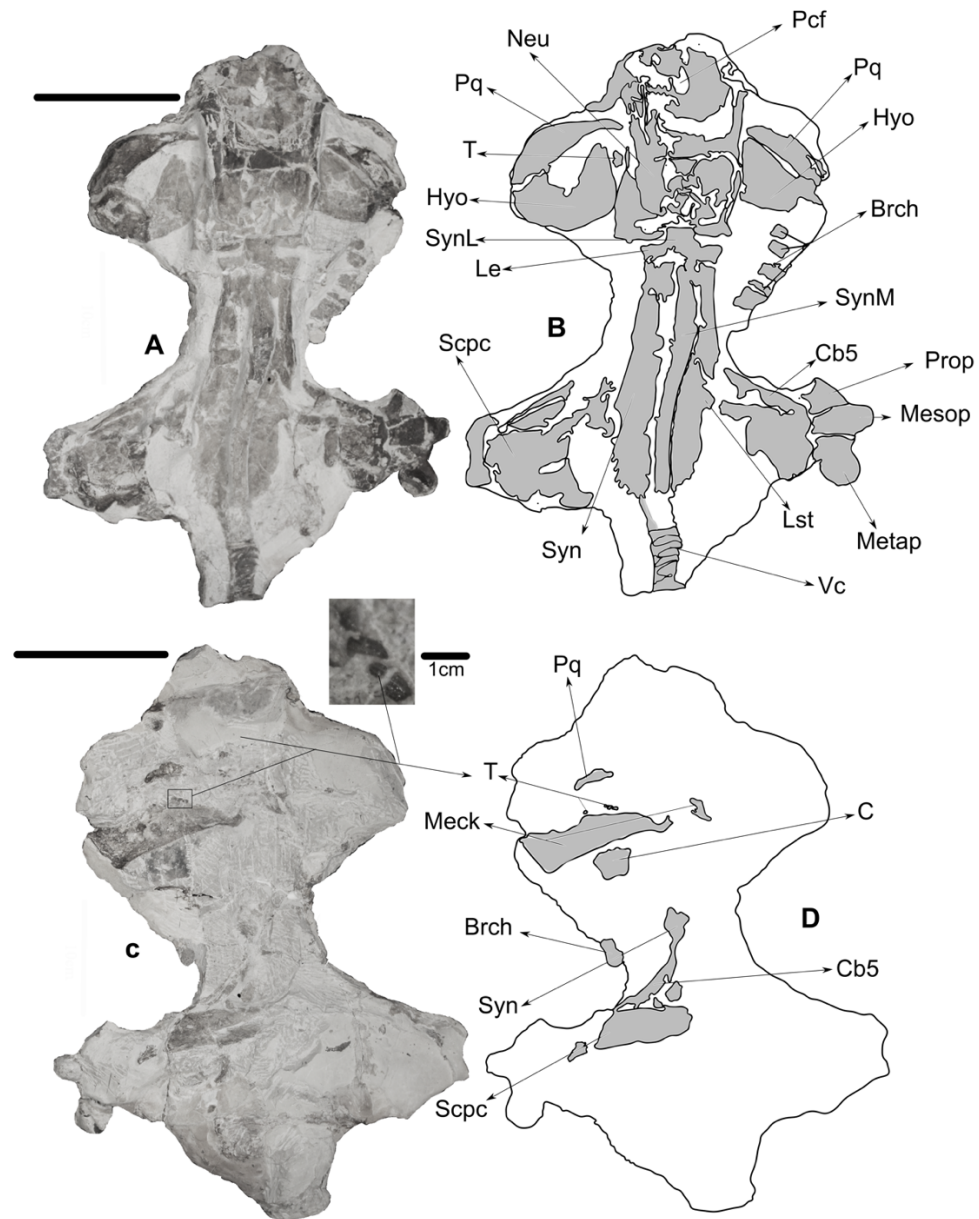
Figure 2.3. †*Asflapristis cristadentis* gen. et sp. nov. holotype NHMUK PV P75433. **A-B**, dorsal view of the anterior skeleton. **C-D**, ventral view of the specimen. **Abbreviations**: Brch, branchial elements; **C**, undetermined cartilages; Cb5, fifth ceratobranchial; Hyo, hyomandibula; Le, lateral extensions; Lst, lateral stays; Meck, Meckel's cartilages; Mesop, mesopterygium; Metap, metapterygium; Neu, neurocranium; Pcf, precerebral fenestra; Pq, palatoquadrate; Prop, propterygium; Scpc, scapulocoracoid; Syn, synarcual; SynL, synarcual lip; SynM, synarcual medial crest; T, teeth; Vc, vertebra centra. Scale bar: 10 cm. Grey colour parts are the exposed cartilage.
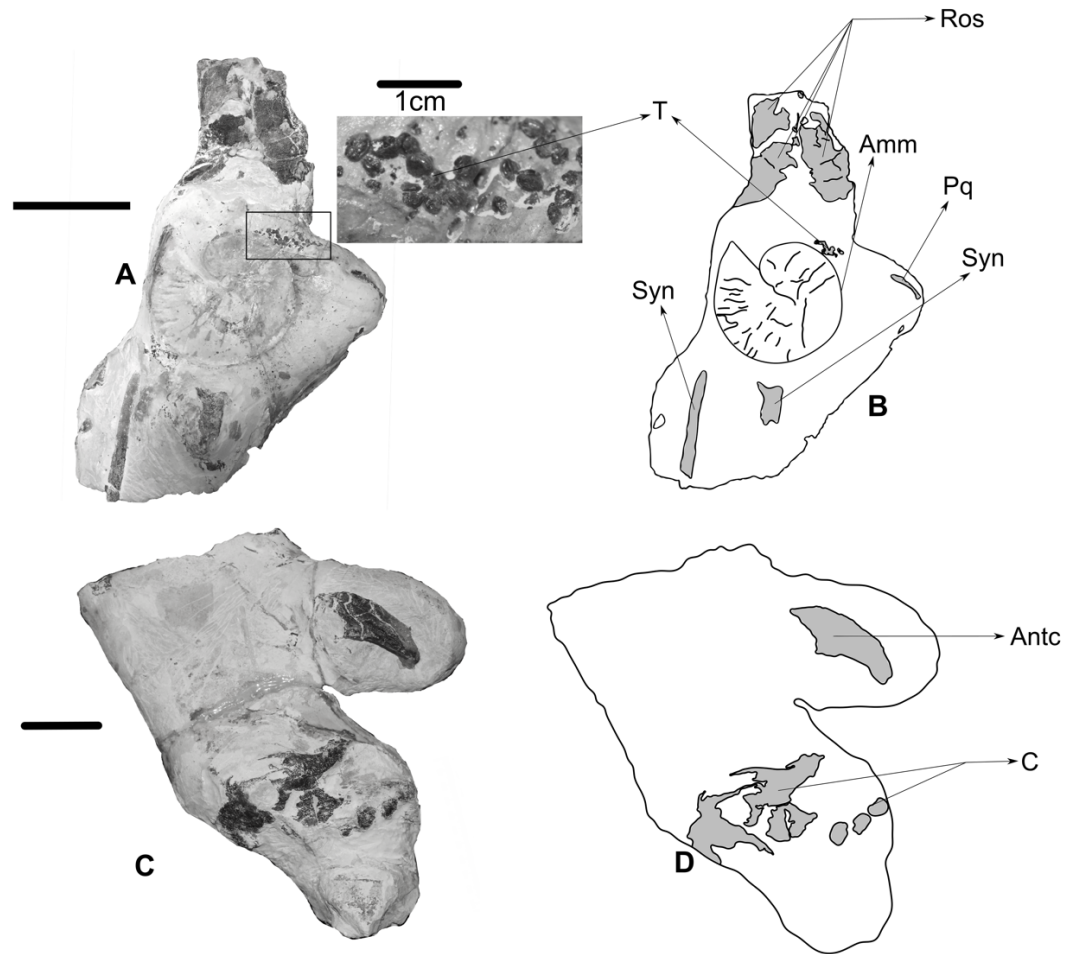
Figure 2.4. †*Asflapristis cristadentis* gen. et sp. nov. NHMUK PV P 75428 a–e. **A-B**, ventral view of part of the anterior skeleton (Scale bar: 10cm). **C-D**, ventral view of another section of the specimen (Scale bar: 5cm). **Abbreviations**: Ros, rostrum; T, teeth; Amm, ammonite; Pq, palatoquadrate; Hypo II, second hypobranchial; Syn, synarcual; Antc, antorbital cartilage; C, undetermined cartilages. Grey colour parts are the exposed cartilage.

Rostrum

Despite the lack of a complete rostrum, some specimens preserve fragments of it. In the holotype the basal portion is preserved and shows an oval-shaped precerebral fontanelle, in similar position and shape to that of †*Libanopristis* and †*Micropristis.* Fragmentary remains of the specimen (NHMUK PV P 75429 a-d) suggest the presence a of stout and hypertrophied rostrum probably twice as long as the neurocranium (Fig 2.5A-B) without 'wood-like' cartilage. None the remains showed enlarged rostral dermal denticles nor cavities/canals.
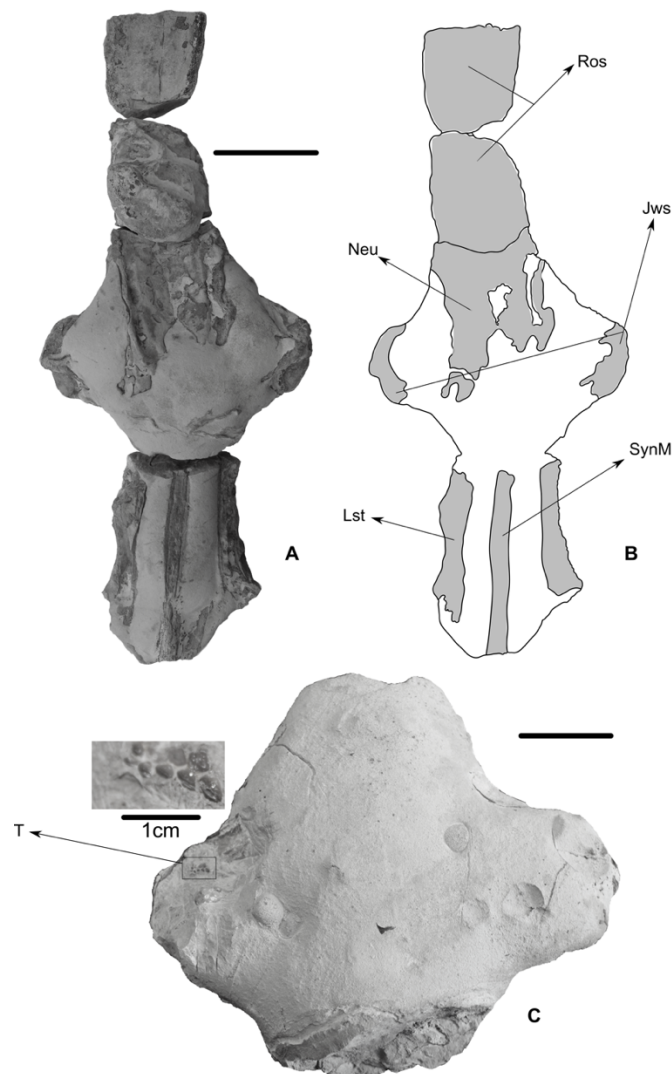
Figure 2.5. †*Asflapristis cristadentis* gen. et sp. nov. NHMUK PV P75429a–d. **A-B**, dorsal view of the neurocranium and part of the synarcual and of rostral cartilage (Scale bar: 10 cm). **C**, ventral view of neurocranium (Scale bar: 4 cm). **Abbreviations**: Lst, lateral stays; SynM, synarcual medial crest; Syn, synarcual; Jws, jaws; Neu, neurocranium; Ros, rostrum; T, teeth. Grey colour parts are the exposed cartilage.

Visceral Skeleton

The mouth cavity is broad (twice the width of the postorbital region in holotype specimen). The Meckel's and palatoquadrate cartilages are straight and broad, and their antimeres are not fused (Fig. 2.6C-D). The palatoquadrate width is approximately 22% of the length of the cartilage, while the Meckel's cartilages width is approximately 32% of its length. The Meckel's cartilages are twice as deep as the palatoquadrate and have a lateral tab-like process that articulates with the notched distal end of the palatoquadrate (Fig. 2.7A). The Meckel's cartilages lack any process or flange in the ventral lateral region flange for muscle articulation. The hyomandibular cartilages are triangular and present a strong medial crest for the articulation of muscles. They become slender towards their distal tip which articulates between the palatoquadrate and Meckel's cartilages (Fig. 2.6A-B). The basihyal is fragmented in two parts, but still reveals a broad, crescent shape, similar to that found in †*Ptychotrygon rostrispatula* (NHMUK PV P73630). The basihyal and first hypobranchial are not articulated, whether they were separated in life or this disarticulation occurred during fossilisation is unknown (Fig. 2.7C). The first hypobranchial is separated from the pseudohyoid and has a roughly arrow shape with an acute proximal edge followed by two process, one dorsal and another ventral. The mid region of the first hypobranchial is narrow and rectangular with an expanded distal edge (Fig. 2.7C). The pseudohyal is triangular with its proximal edge wider than its distal edge. Only the anterior part of the second hypobranchial is preserved (Fig. 2.6C-D), its distal edge is convex and wide, with no evidence of articulation with an anterior process.
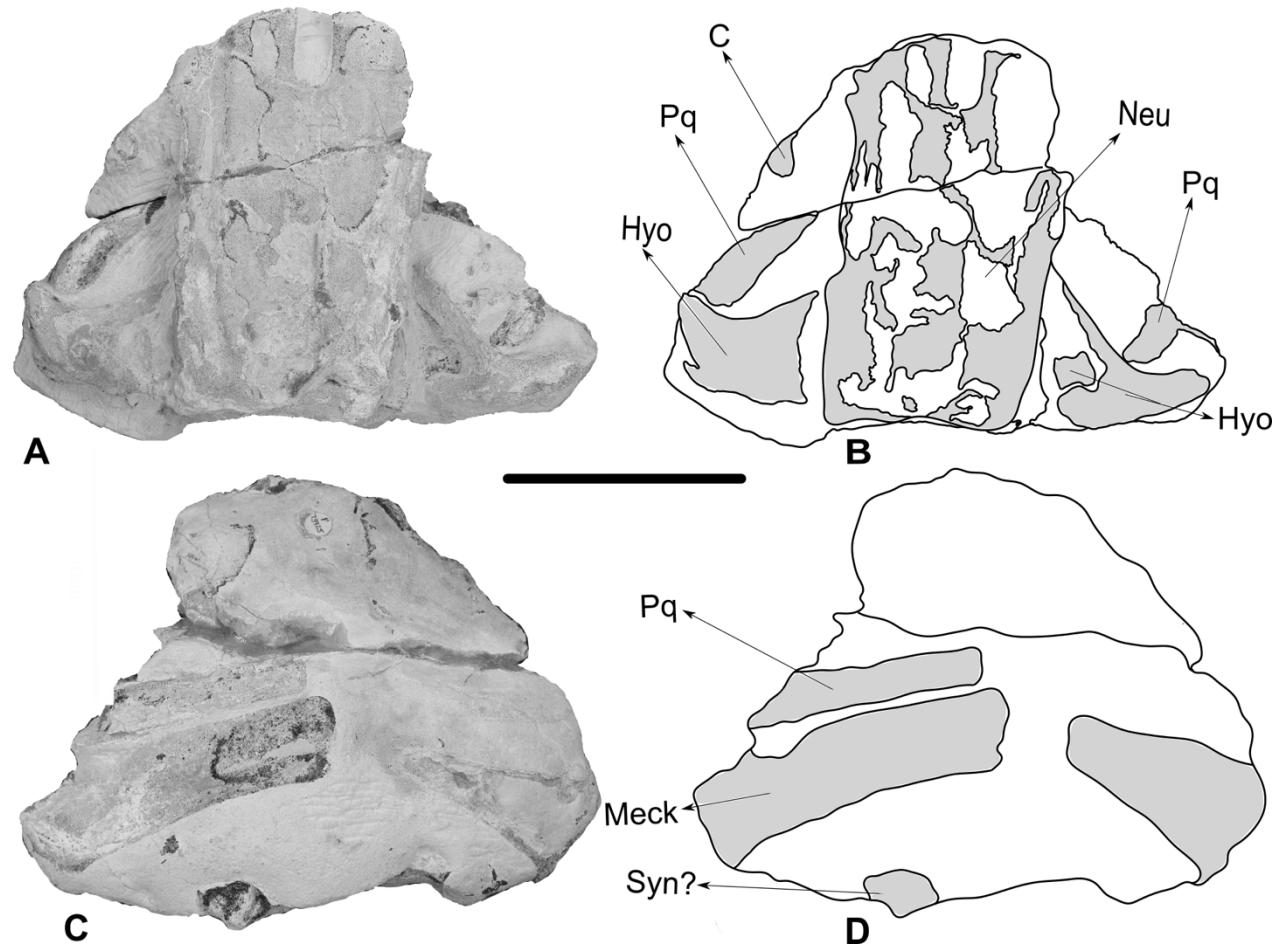
Figure 2.6. †*Asflapristis cristadentis* gen. et sp. nov. NHMUK PV P73925. **A-B**, dorsal view of chondrocranium; **C-D**, ventral view of chondrocranium. **Abbreviations:** Neu, neurocranium; Hyo, hyomandibula; Pq, palatoquadrate; Meck, Meckel's cartilage; Syn?, possible synarcual. Grey colour parts are the exposed cartilage.
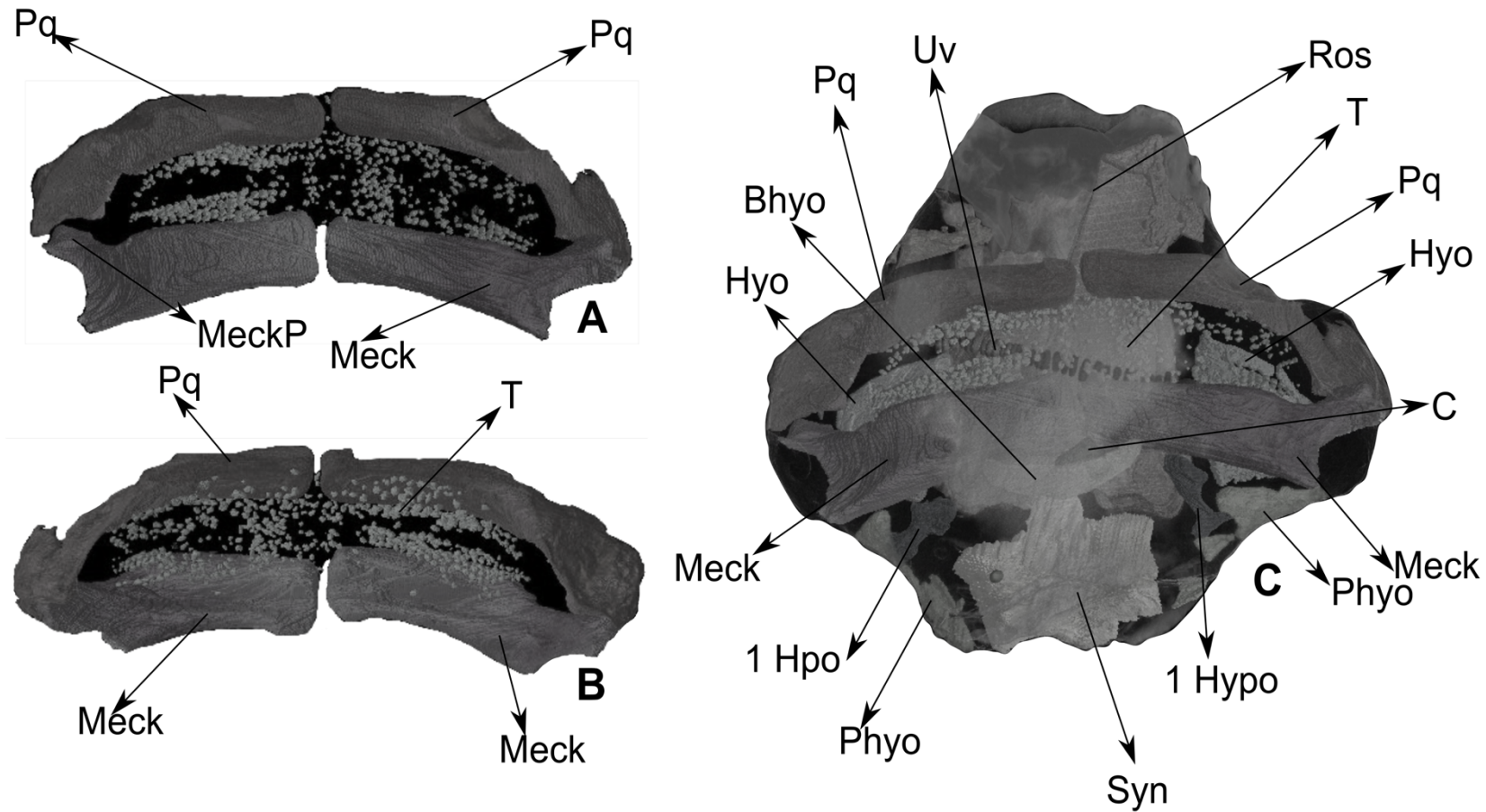
Figure 2.7. †*Asflapristis cristadentis* gen. et sp. nov. CT scan of NHMUK PV P75429b. **A,** frontal view. **B,** rear view of the jaw. **Abbreviations**: Bhyo, basihyoid; C, undetermined cartilage; Hyo, hyomandibula; I Hypo; first hypobranchial; Meck, Meckel's cartilage; MeckP, Meckel's tab-like process; Phyo, pseudohyoid; Pq, palatoquadrate; Ros, rostrum; T, teeth; Uv, undetermined vertebrate remains.

Synarcual and vertebrae

The synarcual extends posteriorly well-beyond the scapulocoracoid. It is about three times longer than its maximum width and twice the length of the preserved portion of the neurocranium in the holotype specimen. The synarcual lip (odontoid process) is large and articulates with the posterior part of the neurocranium. The superior lateral facets of the synarcual are thick and project laterally mirroring the occipital condyles of the neurocranium suggesting a tight interaction between these elements despite being slightly dislocated in the holotype (Fig. 2.8F). The medial crest of the synarcual is wide and well developed. No evidence for either fusion or articulation between the synarcual and suprascapula was observed, although whether the suprascapula was present or not remains unknown. The lateral stays of the synarcual are present and dorsally directed (Fig. 2.8C-D and F). The first exposed vertebral centrum fails to reach the mid-point of the synarcual cartilage (Fig. 2.8A-B). Post synarcual vertebrae are preserved and revealed a dense notochord centre with appositional rings of areolar cartilage, which is consistent with seasonal growth of elasmobranchs (NHMUK PV P 75431). Neural arches and spines are poorly preserved and yield no useful characters.
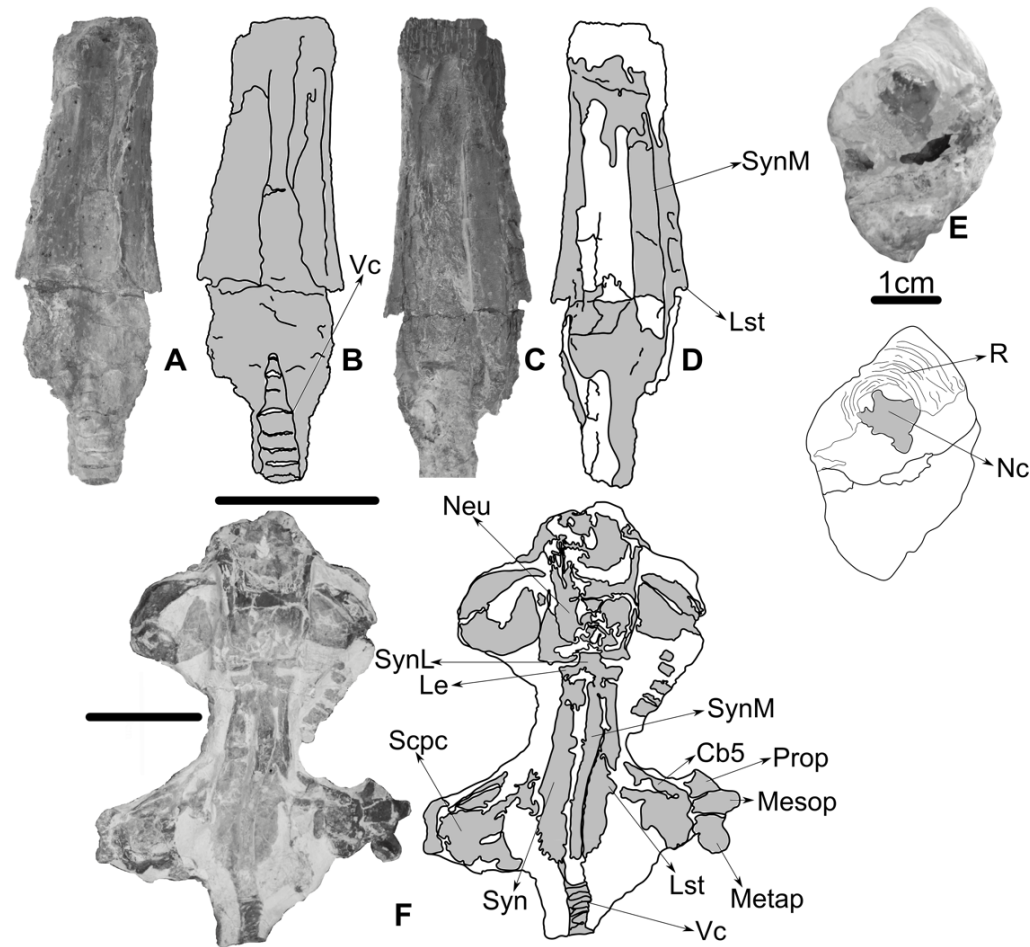
Figure 2.8. †*Asflapristis cristadentis* gen. et sp. nov. **A–E**, NHMUK PV P75431. **A-B,** ventral view of the synarcual; **C-D**, dorsal view of the synarcual; **E**, vertebra on distal end of synarcual. **F**, holotype NHMUK PV P75433 in dorsal view. **Abbreviations**: Cb5, fifth ceratobranchial; Le, lateral extensions; Lst, lateral stays; Mesop, mesopterygium; Metap, metapterygium; Nc, notochordal centre; Neu, neurocranium; Prop, propterygium; R, appositional rings; Scpc, scapulocoracoid; Syn, synarcual; SynL, synarcual lip; SynM, synarcual medial crest; Vc, vertebra centra. Scale bar 10 cm. Grey colour parts are the exposed cartilage.

Appendicular skeleton

The scapulocoracoid is thick and short (the same length as the synarcual in the holotype specimen). The scapular processes are broken and separated from the basal portion of the scapulocoracoid. Regardless they are long, slender and probably dorsally directed, no evidence of a union between the synarcual cartilage and the scapulocoracoid at least on the dorsal surface was observed. The lateral facet of the scapulocoracoid is compact and robust with no enlargement between the proximal pectoral elements (procondyle, mesocondyle or metacondyle) and with no direct articulation of the pectoral radials. There are three condyles for the articulation of the proximal pectoral elements. Between the procondyle and the mesocondyle is the anterior dorsal fenestra. The posterior dorsal fenestra is located between the mesocondyle and metacondyle. Although most of the distal part of pectoral proximal elements is missing their base is preserved and show the characteristic sturdy and paddle-like shape as those of other sclerorhynchoids.

Teeth

Descriptive tooth terminology largely follows that of Cappetta, 1987. The dentition is relatively homodont, with some variation in tooth size and width-depth ratio across the jaw, but the greatest variation occurs within the details of the occlusal ornamentation, with differences appearing to show no systematic variation with jaw position. The teeth are generally robust and up to 5 mm (millimetres) wide (Fig. 2.9C). Teeth are oval, or slightly expanded labially, in occlusal view and wider than deep (Fig. 2.9A). The tooth crown overhangs the root on all sides and the tooth is linguo-labially deeper than high. There is a very weakly developed lingual uvula but no lateral uvulae. The overall form of the tooth occlusal face is flat to weakly domed with no defined cusps; the margins of the occlusal face are rounded except where fine ridges are present at the edge of the occlusal face. The tooth occlusal face is highly ornamented with the ornament being variable in

detail, even within adjacent teeth in the dentition. A narrow and sharp-edged transverse ridge bisects the occlusal crown face, with a shorter parallel ridge labial to this. Other ornament is highly variable and not all elements are present in all teeth. A somewhat irregular ridge may be present at the lingual edge of the occlusal face, and short longitudinal or irregularly orientated ridges may occur across the face but are often concentrated near the crown edge or along the lingual margin. These may bifurcate or break up into tubercles, and rarely join with the main transverse ridges (Fig. 2.9B). The root is low with equal sized and well separated root lobes. The basal faces of the root lobes are convex and there is no sharp edge between the lateral and basal faces. Teeth have a very large and well-developed pulp cavity that may occupy over half of the crown height in section (Fig. 2.10). There is a relatively thin surrounding layer of orthodentine, but the enameloid is rather thick, especially where ornament is present (Fig. 2.10). The is no osteodentine present in the root with the exception of a thin band observed between the crown and root.

The tooth morphology is highly distinctive and unlike that of other batoids, although the highly ornamented occlusal face bears some superficial resemblance to that of *Rhina, Rhynchobatus,* †*Pucabatis* and even †*Ptychodus*. In all cases, though, the overall tooth shapes and morphology of the root are rather different. Teeth of †*Ptychotrygon,* †*Texatrygon,* †*Micropristis* and †*Libanopristis* are considerably more gracile than those of †*Asflapristis cristadentis* but show many similarities in detail. In each of these genera, a well-defined transverse ridge is present, with shorter ridges on the labial and/or lingual sides of it. In some species of †*Ptychotrygon*, more complex occlusal ornamentation is also present (e.g. Cappetta & Case, 1999) but not comparable with that of †*Asflapristis*. Roots are similarly low and with rounded edges. Despite this, teeth of *Ptychotrygon,* †*Texatrygon,* †*Micropristis* and †*Libanopristis* all possess a low and triangular main cusp, are diamond shaped to triangular in occlusal view, have a less complex

ornamentation, possess a weak labial apron and more distinct uvula, and have root lobes with more flattened bases. Teeth most closely resemble those of †*Ptychotrygon gueveli* Cappetta (2004) but can be differentiated by the presence of small crest between the transverse ridges and the lack of a medial cusp suggesting a close relation between these two genera.
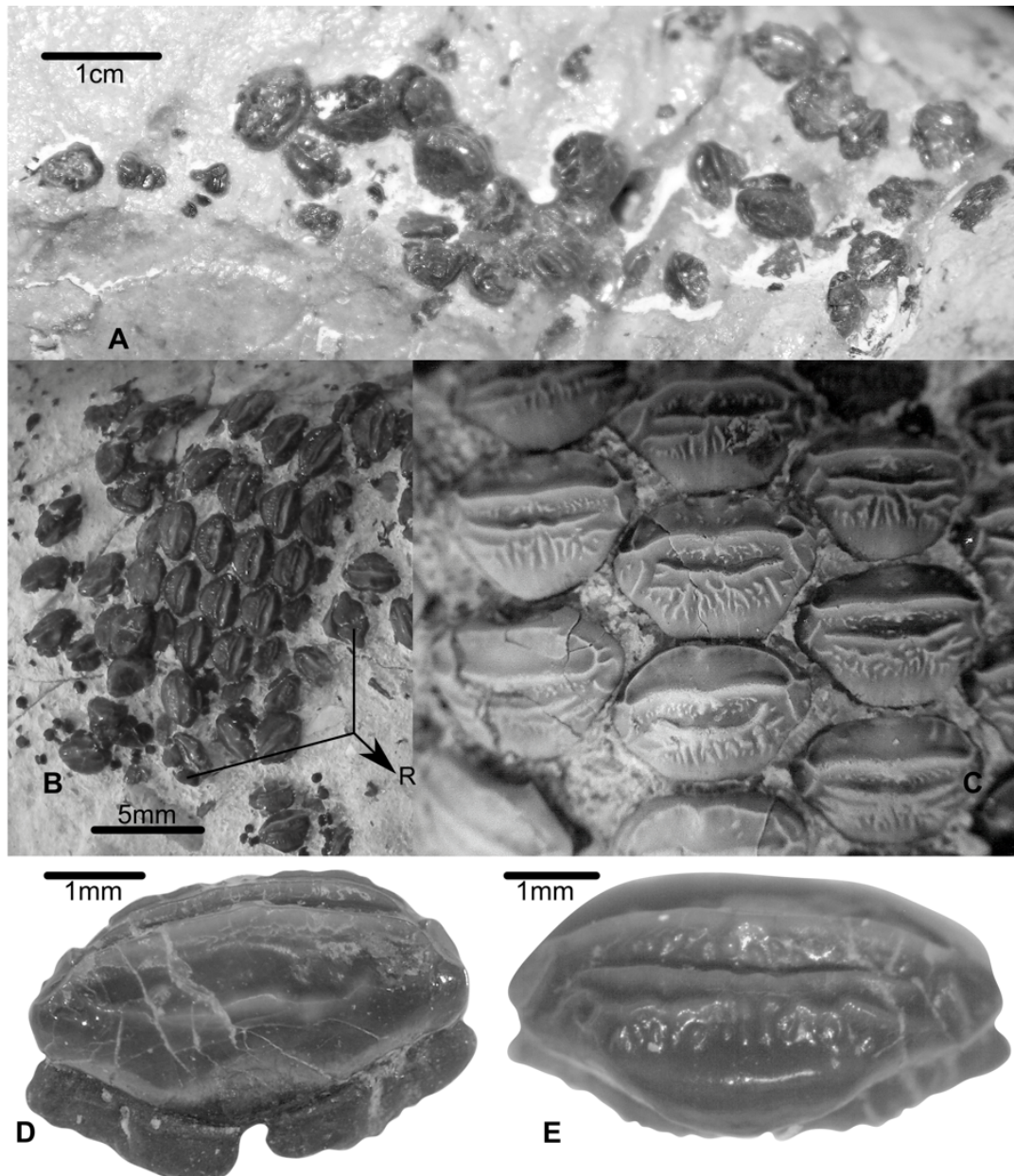
Figure 2.9. †*Asflapristis cristadentis* gen. et sp. nov., tooth sets of different specimens and disarticulated tooth from the preparation of these specimens. **A,** tooth set of NHMUK PV P75428a–e. **B-C**, occlusal view of tooth set of NHMUK PV P75432. **D**, lingual view and E, labial view of separated tooth of NHMUK PV P75432. **Abbreviation**: R, root.
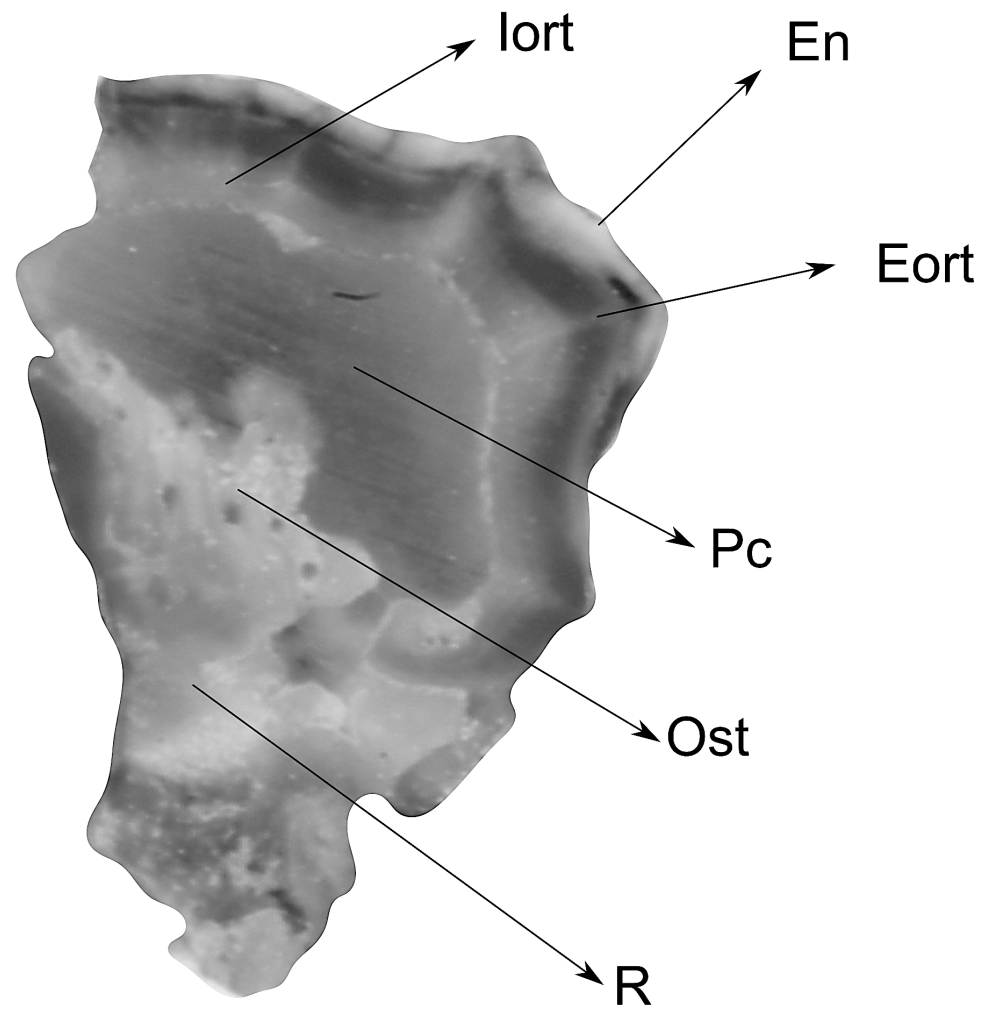
Figure 2.10. †*Asflapristis cristadentis* gen. et sp. nov., lateral section of a tooth found during the preparation of NHMUK PV P75431. **Abbreviations**: En, enameloid; Eort, external orthodentine; Iort, internal orthodentine; Os, Osteodentine; Pc, pulp cavity; R, root.

Denticles

 No extensive areas of skin with articulated denticles were found associated with any of the specimens. Although the majority of denticles were recovered as isolated specimens, collected from treating matrix surrounding the specimens with acid, some denticles were found directly associated with the mouth region and could be observed *in situ*. Five distinct denticle morphologies were found.

Around the mouth, circular denticles with a smooth dorsal surface were found (Fig. 2.11A-D). In lateral view this denticles are tall and become narrower in the middle and expand towards the stem. The stem presents several fringes over the margins (Fig. 2.11B-C).

The other indirect associated morphotypes of denticles were: 1) Leaf shaped with a smooth dorsal surface (Fig. 2.11E-G), these denticles present irregular terminations on their posterior edge and on lateral view are significantly shorter that the circular denticles (Fig. 2.11G); 2) Arrow-shaped (Fig. 2.11H-J), these denticles present ridges on the dorsal surface, of similar shape to those found on the dorsal surface of some sharks as well as 'rhinobatid' rays; 3) Rostral denticles (Fig. 2.11D-L), taller than the rest, crown is posteriorly directed and highly similar to those found on the ventral surface of the rostrum of †*Sclerorhynchus atavus* (Welten *et al*., 2015): 4) a single specimen of a large triangular denticle of unknown provenance was recovered (Fig. 2.11N).

The CT scan also reveals several high-density structures on the ventral surface of the neurocranium (Fig. 2.6C) and clusters found during the preparation of specimens (Fig. 2.11M) suggest that †*Asflapristis cristadentis* was uniformly covered with denticles.
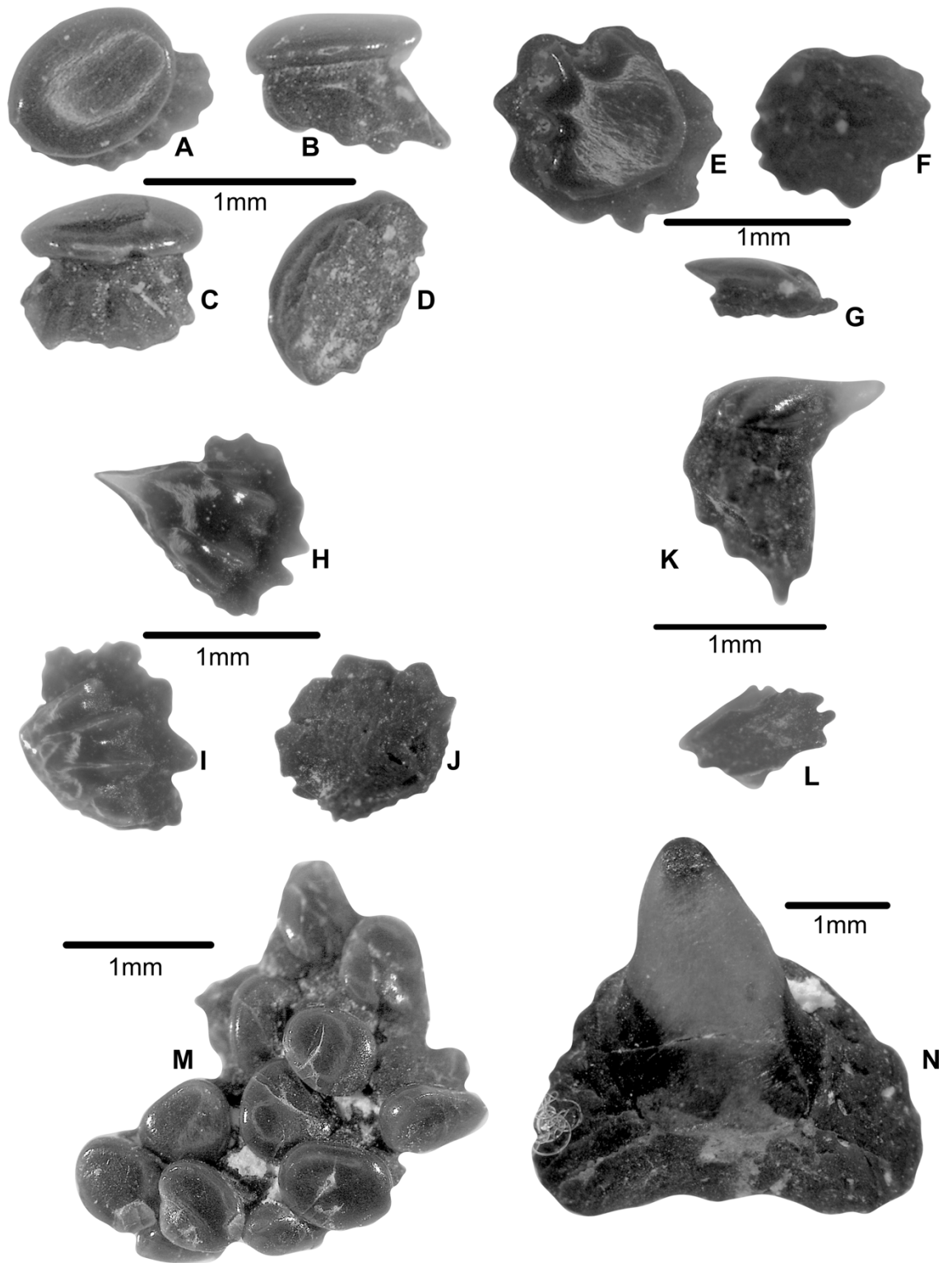
Figure 2.11. †*Asflapristis cristadenti*s gen. et sp. nov., dermal denticles from the preparation of NHMUK PV P75432 (**A–G** and **M**) and NHMUK PV P75428 (**H–L** and **N**).

†Ptychotrygon rostrispatula Villalobos-Segura, Underwood and Ward, 2019b

Material

Holotype: NHMUK PV P 73630, almost complete specimen with only the right pectoral fin, pelvic and caudal fin missing and the ventral surface exposed (Fig. 2.17).

Paratypes: NHMUK PV P 75496, almost complete male specimen, with most of the ventral surface and proximal part of the left clasper exposed. The appendicular skeleton (pectoral and pelvic fins) are missing along with the pelvic gridle and dorsal and caudal fin. NHMUK PV P 75498, almost complete juvenile specimen with the dorsal surface of the synarcual, neurocranium and part of the pectoral griddle exposed after preparation. On the posterior region of the specimen a tooth was found that allowed its identification. NHMUK PV P 75497, an incomplete specimen that preserves the rostrum, neurocranium and part of the jaw, with the ventral surface exposed. Part of the lower jaw was prepared and revealed a single tooth. NHMUK PV P 75500, fragmented specimen with only the ventral surface of the branchial skeleton and parts of the jaw cartilages with teeth preserved.

Systematic Palaeontology

Class **Chondrichthyes** Huxley,1880.
Superorder **Batomorphii** Cappetta, 1980b.
Order **Rajiformes** *sensu* Naylor *et al*., 2012.
Suborder **Sclerorhynchoidei** Cappetta, 1980b.
Family **Ptychotrygonidae** Kriwet *et al*., 2009a.
Genus *Ptychotrygon* (Jaekel,1894).
Species *Ptychotrygon rostrispatula.*
Figures 2.12-2.19.

- **Derivation of genus Name**: From the resemblance in the crown ornamentation of the teeth with the genus *Ptychodus* and *Trygon.*

Type species: †*Ptychotrygon triangularis* (von Reuss, 1844).

Emended diagnosis

Hypertrophied rostrum with no enlarged denticle series attached to it and with two parallel ventral canals, one on each side of the rostrum. Palatoquadrate and Meckel's cartilages slim. Second and third hypobranchials well-developed, close to each other and with no articulation surface with the basibranchial. Teeth are small and oval-shaped, with a sharp strong enamelled pyramidal crown and transverse crests (in some cases short transverse ridges are present on the labial crown face). Labial apron variably developed and in some cases with a straight sagittal ridge on the upper part. The apron is bent basally with a truncated projection. The lingual uvula is short and broad with central interlocking depression. In profile view, the labial face is sigmoidal. Root of holoaulacorhizous type with a single pair of margino-lingual foramina.

†*Ptychotrygon rostrispatula* sp. nov.

Synonymy: Holotype specimen was first illustrated in Underwood *et al*. (2016a, text-fig. 3a).

- **Derivation of species Name**: Making reference to the presence of the flat and hypertrophied rostrum.

Diagnosis of species

Sclerorhynchoid batoid with estimated total length (TL) more than one metre. Hypertrophied rostrum (31% of total preserved length in holotype specimen), that reaches maximum width away from the base giving it a leaf shape. No enlarged rostral denticles associated to the rostrum were observed. Chondrocranium rectangular-shaped, reaches its maximum width at the nasal capsules and posterior to this region becomes narrower. Chondrocranium roof flattened. Palatoquadrate and Meckel's antimeres are separated and slender. Dentition relatively homodont, teeth oval in occlusal view and present two well-developed transversal crests, with a variably developed medial cusp between them. Narrow but well-developed labial apron with is distal edge slightly convex. Transversal crest on labial edge peaks in the mid. Lingual uvulae variably developed. Root low with widely spaced root lobes with rounded and flat basal face. Second hypobranchial long and show a pillar-shape, without an anterior process and no articulation surface with the basibranchial. Ventral portion of the scapulocoracoid is narrow and bar-like, the lateral facet of scapulocoracoid is compact and articulates to the distally expanded and paddle-like proximal pectoral pterygia (propterygium, mesopterygium and metapterygium). The mesopterygium is square shaped and lack of any process. All pectoral radials articulate directly with the proximal element of the pectoral fin. Pelvic girdle slender and bar like without any process.

Description

Five specimens can unambiguously be referred to †*Ptychotrygon rostrispatula* based on tooth morphology. Between them they provide data on the neurocranium rostrum, jaws and dentition, synarcual, brachial skeleton, pectoral girdle, proximal part of the pectoral fins, and the trunk vertebral column. The claspers, pelvic and caudal fins are unknown.

Chondroskeleton

The exposed skeletal elements show a sclerorhynchoid body-shape, with several characteristic features for the group (e.g. hypertrophied rostrum, paddle-like pectoral elements and lack of articulation surface between second hypobranchials and basibranchial). All skeletal elements are formed by a layer of small of prismatic calcified cartilage blocks. Unlike †*Asflapristis* the palatoquadrate and Meckel's cartilage of †*Ptychotrygon rostrispatula* sp. nov. lack 'wood-like cartilage'.

Chondrocranium.

A box-shaped structure, that reaches its maximum width at the nasal capsules and its minimum at the orbital region. The nasal capsules are oval shaped, slightly anteriorly directed and laterally expanded with a flat anterior edge. The antorbital cartilages are connected to the nasal capsules and have a crescent shape with smooth margins and project posterolaterally, with its acute tip directed towards the pectoral fins. In dorsal view the supraorbital crest is flatted and at the same level of the rest of the chondrocranium, but this could be the result of dorsoventral deformation. The posterior edge of the chondrocranium is exposed and presents a deep cavity for the insertion of the odontoid process (synarcual lip) and large occipital condyles that project laterally (Fig. 2.14 and 2.17).
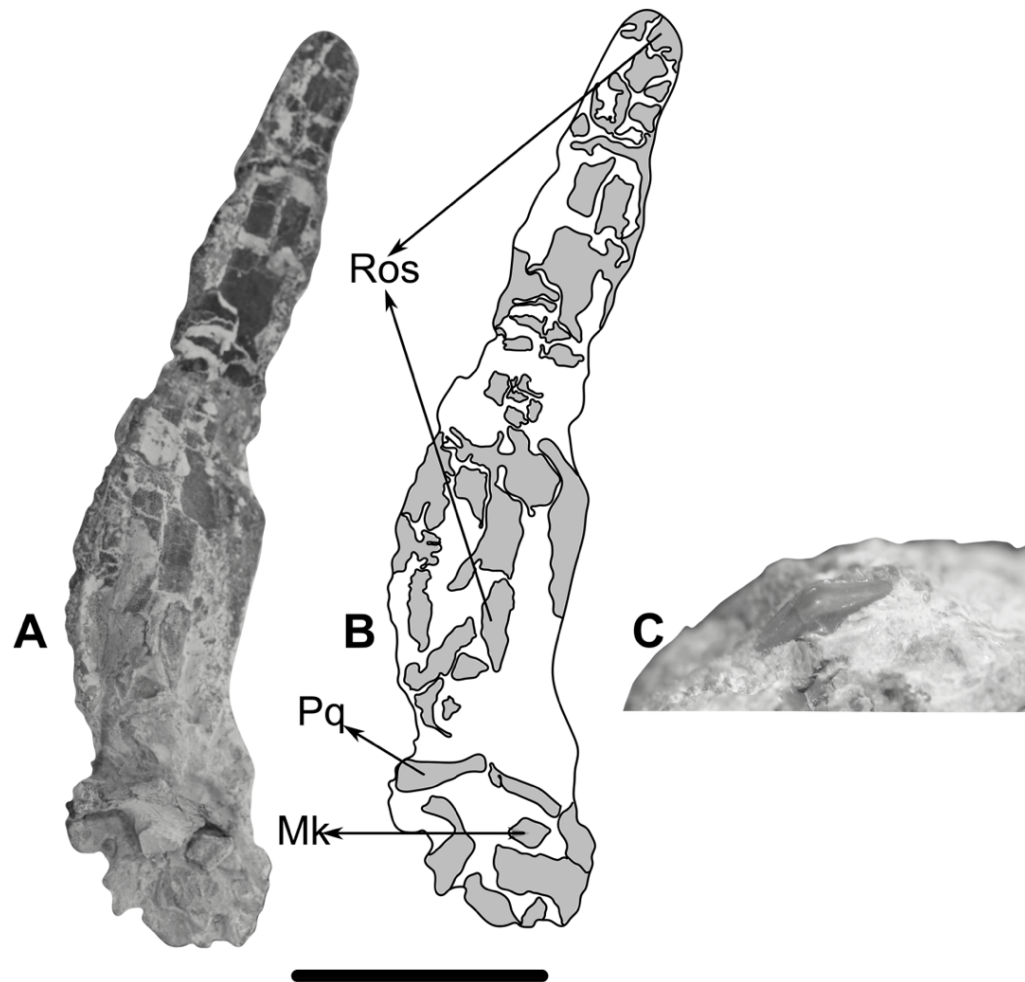
Figure 2.12. †*Ptychotrygon rostrispa*tula sp. nov. NHMUK PV P 75497. **A**, Ventral surface of rostral cartilages. **B**, Interpretative drawing. **C,** teeth. **Abbreviations**: Mk, Meckel's cartilage; Pq, palatoquadrate; Ros, rostrum. Scale bar: 10 cm. Grey colour parts are the exposed cartilage.

Rostrum

Is hypertrophied and thin extends well-beyond the chondrocranium (Fig. 2.12), reaches its maximum width before the base giving it a leaf shape. Ventral surface with two parallel deep grooves that run all the way from the base of the rostrum to the tip (Fig. 2.13). It is hypothesised that on these groves the ophthalmic and buccopharyngeal nerves were placed in other sclerorhynchoid species (Kriwet, 2004). No evidence of rostral denticles directly associated with it was observed.
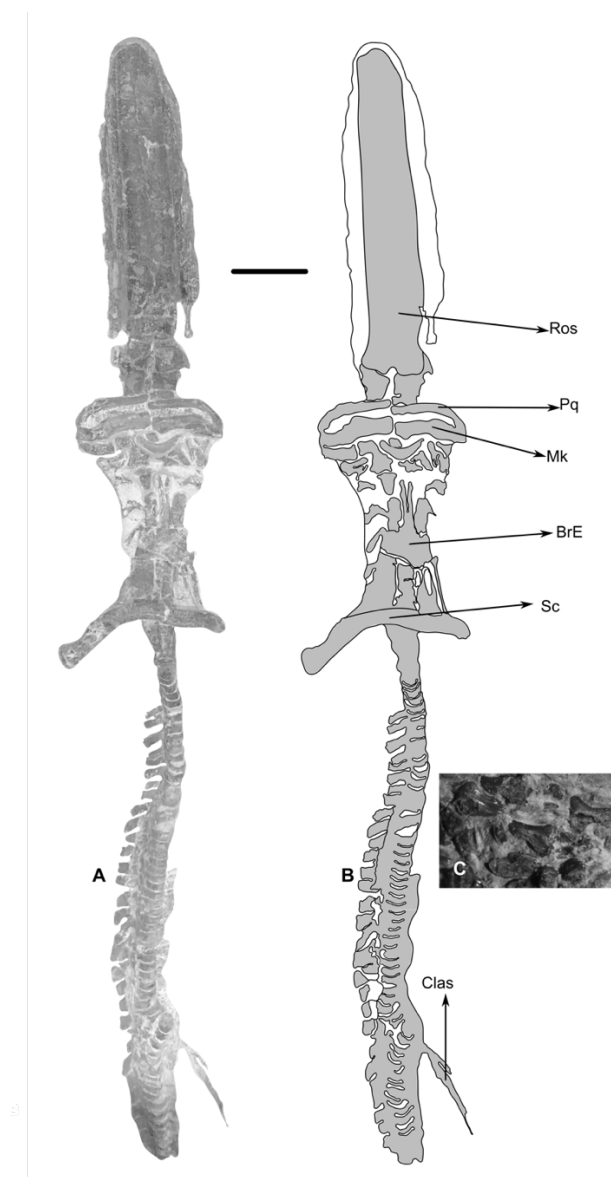
Figure 2.13. †*Ptychotrygon rostrispatula* sp. nov. NHMUK PV P 75496. **A**, ventral surface of axial and part of appendicular skeleton. **B**, interpretative drawing. **C**, teeth. **Abbreviations**: BrE, branchial elements; Clas, clasper; Mk, Meckel's cartilage; Pq, palatoquadrate; Ros, rostrum; Sc, scapulocoracoid. Scale bar: 5 cm. Grey colour parts are the exposed cartilage.
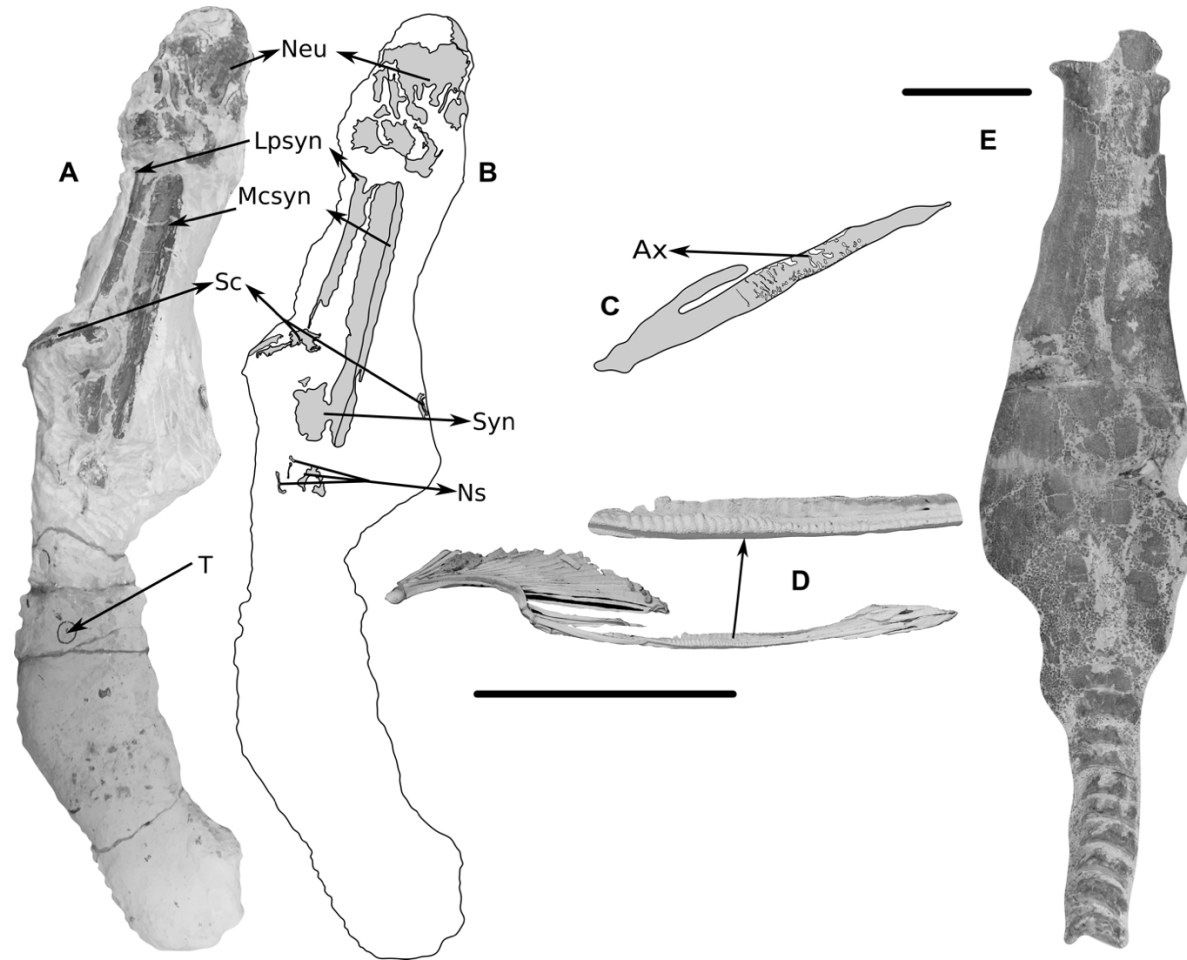
Figure 2.14. †*Ptychotrygon rostrispatula* sp. nov NHMUK PV P75498. **A**, Dorsal surface of axial skeleton. **B**, Interpretative drawing. **C**, Clasper details of NHMUK PV 75496. **D**, Clasper and clasper's axial cartilage of *Zapteryx brevirostris* UERJ 1240. **E**. Synarcual (New specimen collected form Asfla possible †*Ptychotrygon*). **Abbreviations**: Ax, axial cartilage; Lpsyn, lateral process of synarcual; Mcsyn, medial crest of synarcual; Neu, neurocranium; Ns, neural spines; Sc, scapulocoracoid; Syn, synarcual; T, teeth. Scale bar: 10 cm. Grey colour parts are the exposed cartilage.

Synarcual, axial skeleton and claspers

The synarcual cartilage is long and surpasses the scapulocoracoid, suggesting that if present the scapulocoracoid will probably articulate to the synarcual. The synarcual anteriorly narrows after the anterior lateral articular facets that project laterally and are attached to a deep groove on the posterior portion of the neurocranium suggesting a tight interaction between these structures. After one third its length the synarcual progressively widens until reaching its maximum width behind its middle point (Figs 2.14A-B). The medial crest of the synarcual is well-developed and projects dorsally (Figs 2.14A-B). In ventral view the vertebral centra fail to reach the middle of the synarcual.

Several thoracic and caudal vertebrae are preserved and show a dense notochordal centrum with appositional rings of areolar cartilage, which are consistent with the episodic growth rings seen in other elasmobranchs.

Only a portion of the axial cartilage of the left clasper is preserved. This cartilage is ribbed (Fig. 2.14C), similar to that of †*Kimmerobatis* Underwood & Claeson, 2017 and *Zapteryx brevirostris* (Müller & Henle, 1841) (Fig. 2.14D)
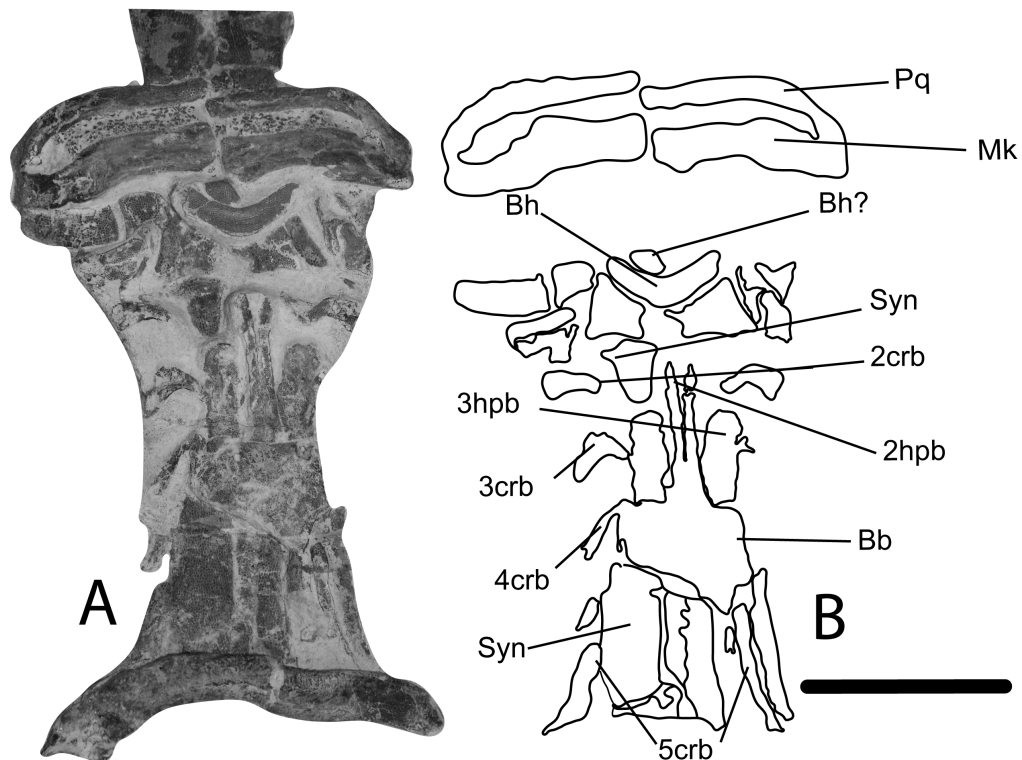
Figure 2.15. †*Ptychotrygon rostrispatula* sp. nov. NHMUK PV P75496. **A**, ventral view of visceral skeleton (mouth and branchial). **B**, interpretative drawing. **Abbreviations**: Mk, Meckel's cartilage; Pq, palatoquadrate; Bh, basihyal; Bb, basibranchial; 2crb, second ceratobranchial; 3crb, third ceratobranchial; 4crb, fourth ceratobranchial; 5crb, fifth ceratobranchial; 2hpb, second hypobranchial; 3hpb, third hypobranchial. Scale bar: 5 cm. Surrounding matrix is not drawn and so no colouring of the exposed cartilages is applied.

Visceral Skeleton

Labial cartilages are not present on this specimen. The mouth cavity is large. The paired Meckel's and palatoquadrate cartilages are straight and slender (Fig. 2.15A). In the holotype (NHMUK PV P73630) and paratype (NHMUK PV P 75496) there is damage on the posterior surface of the Meckel's cartilage but there seems to have been a socket for articulation with the palatoquadrate. The hyomandibula is triangular shaped, with its acute distal edge facing the Meckel's cartilage and its wide posterior edge is directed towards the otic region of the chondrocranium.
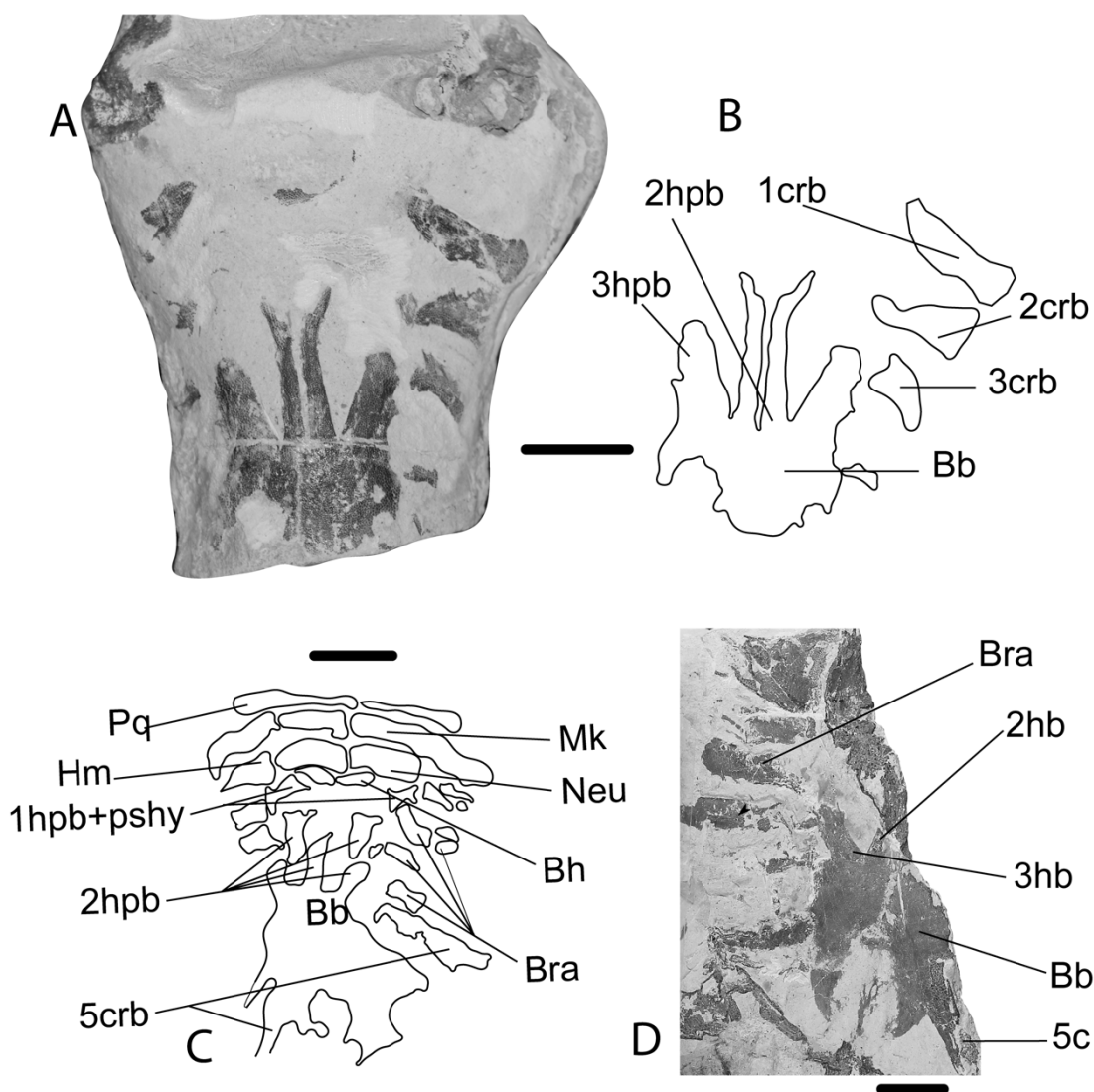
Figure 2.16. A-C, ventral view and interpretative drawing of branchial skeletons of †*Ptychotrygon rostrispatula* sp. nov. NHMUK PV P 75500 (A-B. scale bar: 5 cm). **C**, interpretative drawing of NHMUK PV P 73630 (scale bar: 4cm). **D**, branchial skeletons of †*Sclerorhynchus atavus* NHMUK PV P 49546 (scale bar: 1cm). **Abbreviations**: Bb, basibranchial; Bh, basihyal; Bra, branchial elements; 1crb, first ceratobranchial; 2crb, second ceratobranchial; 3crb, third ceratobranchial; 4crb, fourth ceratobranchial; 5crb, fifth ceratobranchial; 1hpb, first hypobranchial; 2hpb, second hypobranchial; 3hpb, third hypobranchial; Hm, hyomandibula; Mk, Meckel's cartilages; Pq, palatoquadrate; Pshy, pseudohyal. Surrounding matrix is not drawn and so no colouring of the exposed cartilages is applied.

The branchial cartilages are thick and well mineralised. The basihyal is wide, crescent shaped and fragmented in two parts; it is located behind the neurocranium and under the synarcual (Figs 2.15-2.16A-C). The basihyal and first hypobranchial were probably disarticulated as a result of the fossilisation process (Fig. 2.16C), as they are joint in most batoids. The first hypobranchial is T-shaped with regular edges and with its wide edge (distal end) facing the pseudohyal (Fig. 2.16C). The fork-like anterior processes that project from the basibranchial are the second and third hypobranchials, which present a

57

similar configuration to modern rajoids and *Sclerorhynchus atavus* (Fig. 2.16D). At least two ceratobranchial cartilages articulate with the third hypobranchial and there is no evidence of articulation between the ceratobranchials and second hypobranchial. The fourth to fifth ceratobranchials are directed towards the scapulocoracoid and at least the fifth ceratobranchial reaches the scapulocoracoid (Fig. 2.15). The basibranchial and base of the fifth hypobranchial cannot be distinguished from each other.

Appendicular skeleton

The scapular process projects dorsally, whether the process was long or short is unknown. Ventrally the scapulocoracoid is straight and bar-like. The lateral facet of the scapulocoracoid is compact and square-shaped, with no direct articulation with the pectoral radials scapulocoracoid (Fig. 2.17A-C). There are three pectoral condyles (procondyle, mesocondyle and metacondyle) for the articulation of the proximal pectoral elements (propterygium, mesopterygium and metapterygium). The proximal pectoral elements are sturdy and paddle-like: the propterygium anterior process is missing and its posterior section does not extend behind the procondyle (Fig. 2.17C), the distal edge of its preserved portion supports twelve pectoral radials. The mesopterygium is trapezoid shaped and narrower than the rest of the proximal elements with several pectoral radials connected to its distal edge. The metapterygium is long, curved and directed towards the tail and supports 27 pectoral radials. It is uncertain if the paired fins were aplesodic or plesodic as only the first series of pectoral radials is preserved. However, the condition in all other known fossils of sclerorhynchids is plesodic. Most of the pelvic skeleton is missing, only the ventral face of the puboischiadic bar is exposed, which is narrow, plate like with smooth edges and slightly arched in the middle (Fig. 2.17).
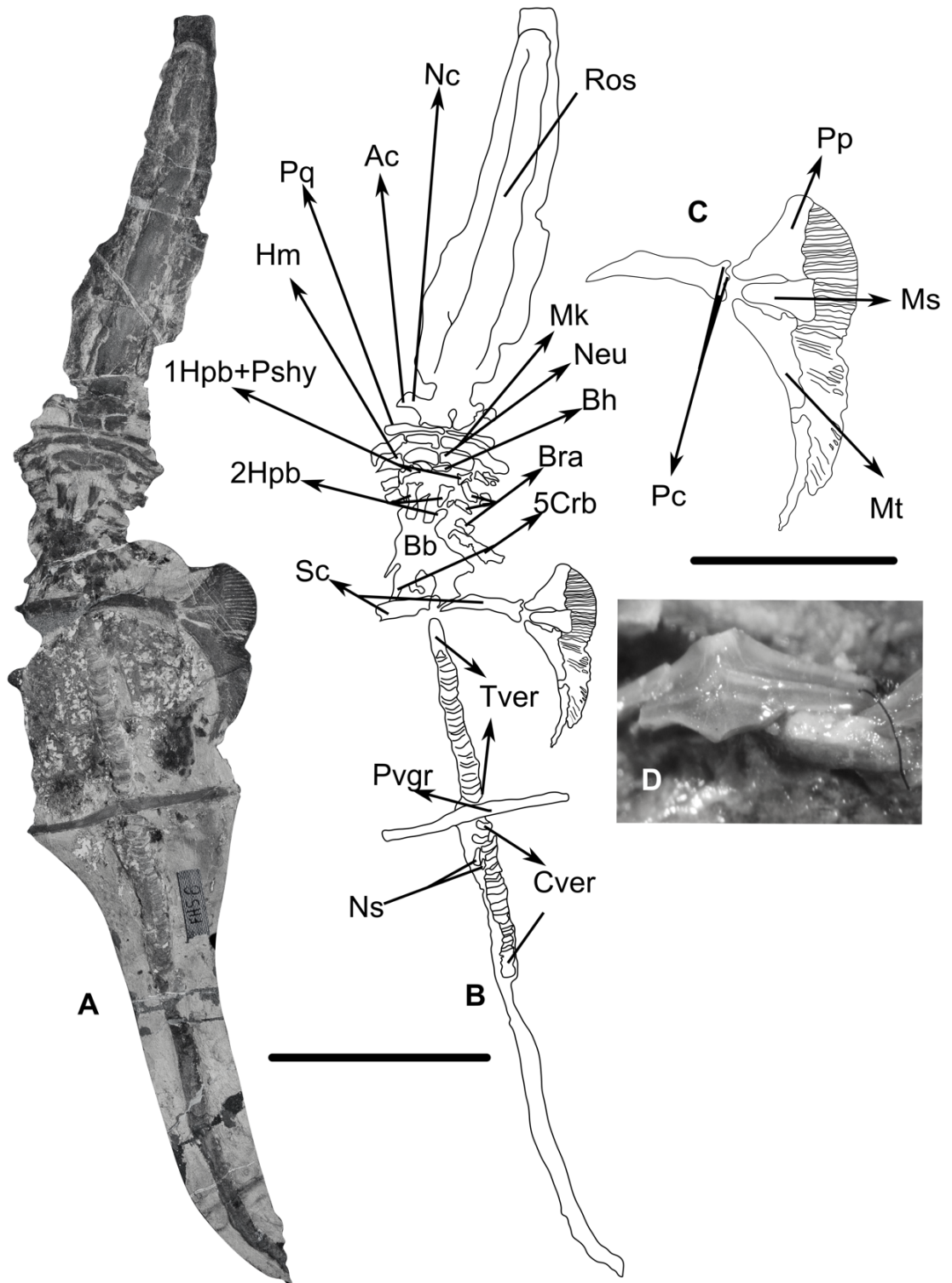
Figure 2.17. †*Ptychotrygon rostrispatula* sp. nov. NHMUK PV P73630 (holotype). **A-B**, ventral surface of specimen (scale bar: 20 cm). **C**, pectoral fin (scale bar: 10 cm). D, teeth. **Abbreviations**: Ac, antorbital cartilage; Bb, basibranchial; Bh, basihyal; Bra, branchial elements; 5crb, fifth ceratobranchial; Cver, caudal vertebras; Hm, hyomandibula; 1hpb; first hypobranchial; 2hpb, second hypobranchial; Mk, Meckel's cartilages; Ms, mesopterygium; Mt, metapterygium; Nc, nasal capsules; Neu, neurocranium; ns, neural spines; Pc, pectoral condyles; Pp; propterygium; Pq, palatoquadrate; Pshy, pseudohyal; Pvgr; Pelvic gridle; Rros, rostrum; Dc, scapulocoracoid; Tver, thoracic vertebras. Surrounding matrix is not drawn and so no colouring of the exposed cartilages is applied.
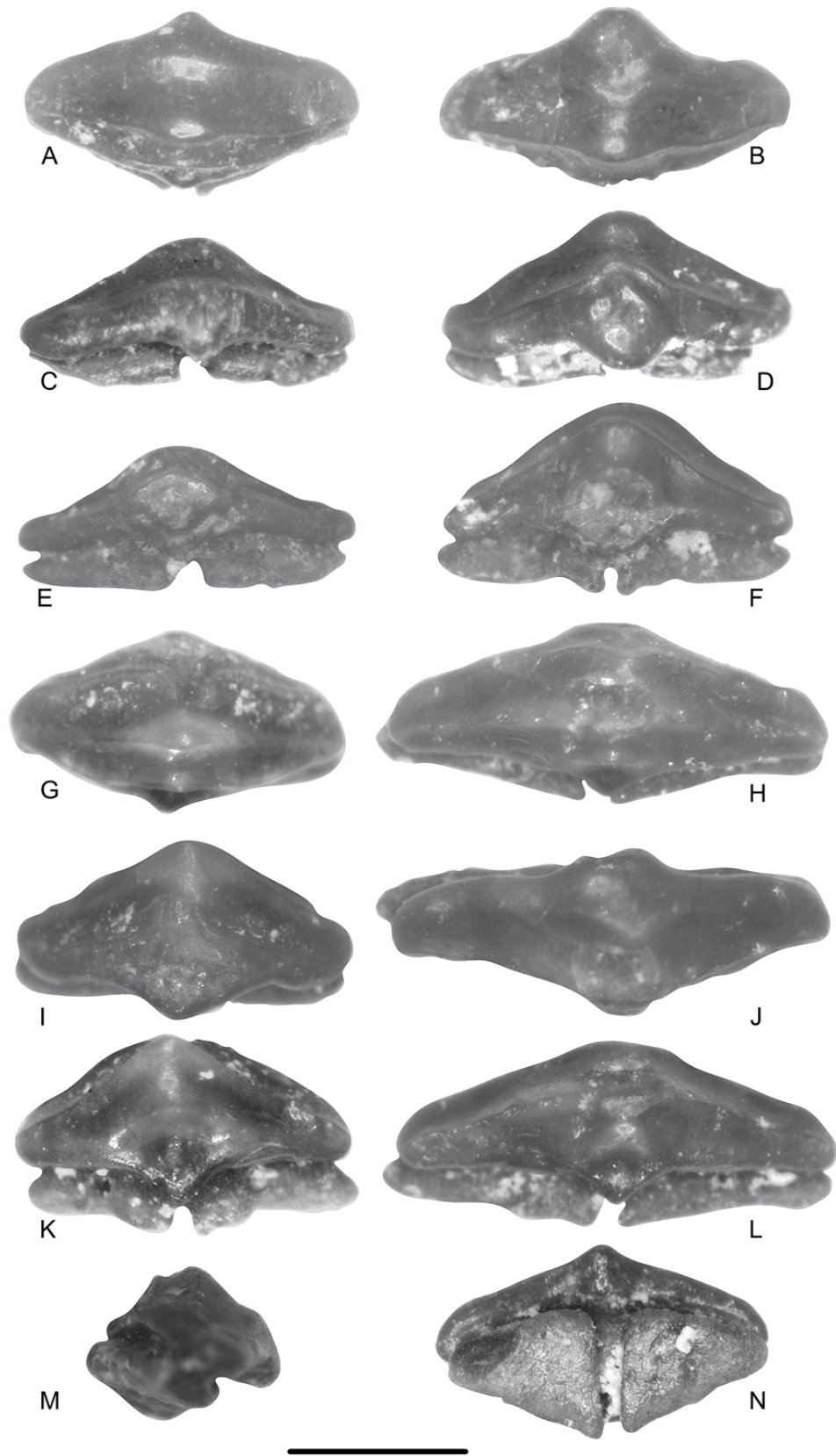
Figure 2.18. Teeth of †*Ptychotrygon rostrispatula* sp. nov**. A-B** and **G-H**, occlusal view. **C-D** and **I-J**, labial face. **E-F** and **K-L**, lingual face. **M**, profile. **N**, root. Scale bar: 2 mm.

Teeth

Descriptive tooth terminology follows that of Cappetta (1987). The dentition is relatively homodont, with some variation in tooth size. The teeth are gracile (up to 2 mm wide) and generally oval-shaped, slightly expanded labially. In dorsal view, tooth crown surpasses the root on all sides (Fig. 2.18), with a strong enamelled medial crest and transverse crests on the labial and lingual sides (Figs. 2.18A-B, G-H). The medial crest is pyramidal-shaped, and its development varies among teeth. The transverse crest on the labial apron is generally well-developed and steeps in the middle towards the medial crest. Smaller ridges at the base of the labial apron extending towards the middle of the labial face are also present (Figs. 2.18D, I, L). In lingual view, there is a small lingual uvula, with a central interlocking depression, that connects with the lingual transverse crest (Figs. 2.18E-F, K-L). On lateral view the apron projects anteriorly and the ligula profile is slightly sigmoidal (Fig. 2.18M). The roots are bilobed, and the lobes are equal sized and rounded. The basal faces of the root lobes are convex and there is no sharp edge between the lateral and basal faces (Fig. 2.18N).

The five specimens are placed in the new species †*Ptychotrygon rostrispatula* sp. nov. as the ornamentation of the teeth differs from other congeneric species of †*Ptychotrygon* (Leriche, 1940; McNulty & Slaughter, 1972; Welton & Farris, 1993; Cappetta 2006 and 2012; Kirkland *et al.*, 2013; Cicimurri *et al.*, 2014):

- †*P. boothi* Case, 1987a lacks a concave lingual uvula and the steep mid portion of the transverse crest in labial apron.

- †*P. henkeli* Werner, 1989 lacks a labial transverse crest.

- †*P. triangularis* (von Reuss, 1844) presents a more ornamented labial apron with generally more than one transverse crest and a straight lingual profile.

- †*P. agujaensis* McNulty & Slaughter, 1972 and †*P. chattahoocheensis* Case *et al.,* 2001 present more than one transverse crest on the labial apron all of which lack the steep mid portion.

- †*P. blainensis* Case, 1978 presents several branching ridges on the labial apron that extend from the cusp of the medial crest to the base of the crown and presents a straight lingual profile.

- †*P. cuspidata* Cappetta & Case, 1975a lacks transversal ridges and present a prominent medial cusp and several ridges restrained to its labial apron.

- †*P. ellae* Case, 1987a present a more developed lingual uvula that extends into the root, along with a much more prominent lingual transverse crest.

- †*P. eutawensis* Case *et al.,* 2001 presents a more ornamented labial apron with several longitudinal ridges reaching into the transverse crest.

- †*P. geyeri* Kriwet, 1999a lacks transversal ridges and a more ornamented labial apron with several branching ridges.

- †*P. pustulata* Kriwet *et al.,* 2009a lacks the chevron crest pattern on the labial apron and presents conical ridges on the transverse and medial crests.

- †*P. rugosa* (Case *et al.,* 2001) presents a large labial apron with several transverse ridges and lack of a well-developed medial crest.

- †*P. striata* Kriwet *et al*., 2009a presents a more ornamented labial face with several straight ridges some of which have a chevron pattern and present a straight lingual profile.

- †*P. texana* (Leriche, 1940) presents a more ornamented labial face with several transverse crest which have a chevron pattern and present a straight lingual profile.

- †*P. ledouxi* Cappetta, 1973*,* †*P. slaughteri* Cappetta & Case, 1975b and †*P. vermiculata* Cappetta, 1975b lack the chevron pattern of the labial apron transverse crest, and †*P. winni* Case & Cappetta 1997 also by the its concave lingual profile.

Discussion

All of the eleven of the specimens collected in Asfla Morocco present a tooth morphology corresponding to the family Ptychotrygonidae (*sensu* Kriwet *et al*., 2009a) (i.e. transversal crest differentiating the labial crown face and a very well-developed labial visor). Six present a previously unknown morphology that belongs to a new species and genus †*Asflapristis cristadentis* Villalobos *et al.* (2019a) and five correspond to the new species †*Ptychotrygon rostrispatula* Villalobos *et al.* (2019b). These remains represent the first reported skeletal remains for the genus.

The absence of enlarge denticles in the rostrum was previously proposed for †*Ptychotrygon* (Cappetta & Case, 1999). This observation is confirmed by †*Ptychotrygon rostrispatula* and extended to †*Asflapristis cristadentis* suggesting that this character was more widely distributed in the group. The long and robust rostrum lacking enlarged rostral denticles suggest that †*Ptychotrygon rostrispatula* and †*Asflapristis cristadentis* used it as a sensory structure (Wueringer *et al*., 2011). This is further supported by the peculiar and highly ornamented teeth occlusal face with a variably developed medial crest and considerable wear found on their teeth which suggest a strong and hard food source probably invertebrates with a shell in poor visibility conditions such as night or in turbid water.

Palaeoecological implications

The restricted overall diversity of the Asfla biota suggests that the environment was not that of a 'normal' open carbonate shelf, and as a result its fauna may have been somewhat specialised. Large vertebrates are highly mobile and so may have lived, or at least fed, away from the depositional site, but the large number of shed teeth of †*Ptychotrygon rostrispatula* in the marl matrix would suggest that it at least spent a significant time in

the area of deposition. Whilst sclerorhynchoids are often common and diverse in shallow marine environments of the Cretaceous of Tethys (Kriwet & Kussius, 2001), the extreme dominance of the chondrichthyan fauna by only two sclerorhynchid species is unusual; elsewhere they are typically associated with diverse 'rhinobatid-like' batoids (e.g. Cappetta, 1987) and often nectobenthic sharks. The rarity of other batoids may be an indication of a hostile seafloor inhibiting nectobenthic taxa (e.g. Underwood & Cumbaa, 2010), which would be consistent with the rarity of benthic shelly fossils. If the restriction of most batoids were due to a hostile seafloor, it would suggest that these sclerorhynchoids were more pelagic than other coeval batoids, living largely within the water column along with the co-occurring fish, reptiles and ammonites. Despite this, sclerorhynchoids appear to have had a very small caudal fin (Cappetta, 1980b) with small and rather rigid pectoral fins containing long, stiff, radial elements. They would therefore be unlikely to have been either fast or powerful swimmers. Most modern batoids, other than planktivorous taxa, feed on relatively small benthic organisms, with many having robust teeth that show considerable wear from processing shelled food. The considerable wear found on the teeth of †*Asflapristis cristadentis* and †*Ptychotrygon rostrispatula* suggest a food source that is strong and hard. Whether both species shared feeding habitats remains unknown, however the size of the teeth and the thickness of its enameloid layer suggest that *Asflapristis cristadentis* feed of different food items possibly larger and with thicker shells, which could have been problematic for the more gracile teeth of †*Ptychotrygon rostrispatula*. Both species present a long and robust rostrum lacking enlarged rostral denticles which suggest a different usage to that of modern Pristidae and Pristiophoridae. However, this structure has a range of functions (Wueringer *et al.*, 2009), and it is highly supplied with sense organs. Even without enlarged denticles the rostrum is still highly functional as a sensory structure (Wueringer *et al.*, 2011). It is possible that in both species this structure was used as sensory appendage. Considering

the unusual occurrence of †*Asflapristis cristadentis*, its poor swimming and durophageous diet, it may have fed on ammonites; slow-moving, pelagic and armoured. It is also possible that the large sensory rostrum allowed hunting of ammonites, which may have relied a lot on sight as in many modern cephalopods. in poor visibility such as at night or in turbid water.

Conclusion

†*Asflapristis cristadentis* and †*Ptychotrygon rostrispatula* provide the first recorded examples of sclerorhynchid batoids with the skeleton preserved in three dimensions. Both taxa present a suite of morphological characters that associates them with sclerorhynchoids (e.g. enlarged proximal pectoral elements, lack of suprascapula) and place them as members of Ptychotrygonidae (*sensu* Kriwet *et al*., 2009a) (e.g. hypertrophied rostrum with no evidence of enlarged dermal denticles a transversal crest differentiating the labial crown face and very well-developed labial visor). The absence of enlarge denticles in the rostrum in both species suggest that this feature was widely distributed within Ptychotrygonidae (*sensu* Kriwet *et al*., 2009a) and probably was used as a sensory structure (Wueringer *et al*., 2011).

The extreme dominance of the chondrichthyan fauna by only two sclerorhynchoid species is unusual and suggest a specialised biotic association of Asfla indicating that the environment was not that of a 'normal' open carbonate shelf, in which †*Ptychotrygon rostrispatula* were a common element. The rarity of other batoids may be an indication of a hostile seafloor inhibiting nectobenthic taxa (e.g. Underwood & Cumbaa, 2010), which would be consistent with the rarity of benthic shelly fossils. †*Asflapristis cristadentis* and †*Ptychotrygon rostrispatula* peculiar teeth morphology and considerable

wear suggest a strong and hard food source probably invertebrates with a shell. Whether

both species shared feeding habitats remains unknown.

Chapter 3

Onchopristis (Batoidea: Sclerorhynchoidei) of the "Kem Kem Beds": The first cranial and synarcual remains reported and its palaeontological implications.

Introduction

†*Onchopristis* (Haug, 1905) is a puzzling Cretaceous batoid taxon, with most of its fossil record composed of fragmentary remains of rostral cartilages, rostral denticles and teeth. Currently the genus classified in the suborder Sclerorhynchoidei within de family Sclerorhynchidae (Cappetta 2012) , although its phylogenetic affinities remain uncertain.

The genus is restricted to the Barremian-Cenomanian time frame (Kriwet, 1999b) and includes only two valid species (Table 3.1): †*O. numidus* (Haug, 1905) found in the Albian of Djoua, Algeria (Cappetta, 1987), in the Albian-Cenomanian of Egypt (Stromer, 1927; Slaughter & Thurmond, 1974; Werner, 1989) and Morocco (Cappetta, 1980b) and †*O. dunklei* (McNulty & Slaughter, 1962) found in the Cenomanian and Middle-Upper Albian of Texas. Plus, an unnamed older species from Spain (Kriwet, 1999b).

Type of remains	Orignial description	Current taxonomic status
Oral	*Squatina aegyptiaca* Stromer, 1927	Syn. *O. numidus* (Cappetta, 2006)
Oral	*Sechmetia cruciformis* Werner, 1989	Syn. *O. dunklei* (Cappetta, 2006)
Oral	*Sechmetia aegyptiaca* Stromer, 1927	Syn. *O. numidus*
Oral and Rostral	*O. dunklei* McNulty & Slaughter, 1962	Valid (Cappetta, 2006)
Vertebra	*Platyspondylus foureaui* Haug, 1905	*Syn. O. numidus* (Cappetta, 2006)
Rostral	*O. dunklei/praecursor* (Thurmond, 1971)	Syn. *Australopristis wiffeni* Martill & Ibrahim, 2012*
Oral, Rostral and Cranial	*O. numidus* (Haug, 1905)	Valid (Cappetta, 2006)

Table 3.1. List of species assigned to the genus *Onchopristis* with its current taxonomic status.

The genus †*Onchopristis* is differentiated for other sclerorhynchoids by the shape and size of the rostral denticles (up to 7 cm in length). Of special significance for its determination is the presence of barbs (hook-like protuberance directed downward) and the numerous rectilinear folds on the posterior margin of the rostral denticles. According to present literature, the two species of †*Onchopristis* are differentiated from each other by the number of barbs of their rostral denticles (one in †*O. numidus* and several in †*O. dunklei*) (Cappetta, 2012). Numerous hypotheses have been proposed for the development of this feature: Slaughter & Steiner (1968) suggest an evolutionary tendency to increase the number of barbs in the rostral denticles, although a secondary loss cannot be discarded. McNulty & Slaughter (1962) propose that the number of barbs is related to the size of the rostral denticles, and as the denticles grows the number of barbs increases.

The finding of multiple barbed denticles (usually double) from Morocco and Egypt (Stromer, 1917, plate 1) (Fig. 3.1), makes the use of the number of barbs as a valid character for species determination within †*Onchopristis* problematic. From recently collected material in the "Kem Kem Beds" the present study describes previously

unknown anatomic features for †*Onchopristis numidus* and compared them to what has been described for †*O. dunklei*. The "Kem Kem" remains revealed a peculiar arrangement of the lateral rostral enlarge denticles series with intercalation of sizes, along with the first reported synarcual and cephalic remains of the genus †*Onchopristis*.
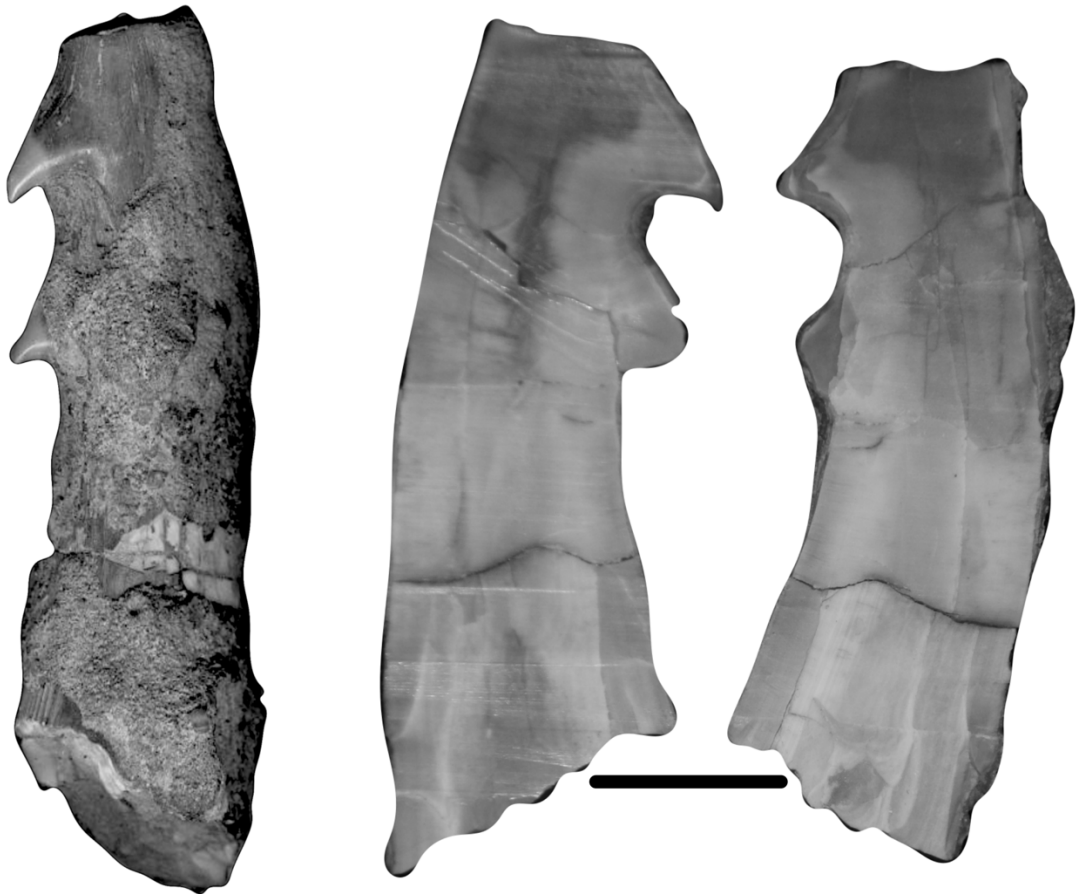
Figure 3.1. Double barbed rostral denticle of †*Onchopristis numidus* found in the Kem Kem Beds. Scale bar: 1cm.

Study area and Taphonomy

Geological setting

The "Kem Kem Beds" is the informal term used for many mid to late Mesozoic non-marine successions of North Africa (Kilian, 1931), the term was subsequently adopted by Sereno *et al.* (1996) for Morocco, and later restricted to a succession of mid Cretaceous age units (Cavin *et al.*, 2010) and are one of the one of the most studied Cretaceous vertebrate-bearing units. With its highly diverse aquatic, semi-aquatic and terrestrial vertebrate faunas have been the subject of several of publications (e.g. Dutheil, 1999; Cavin & Forey, 2004; Rage & Dutheil, 2008; Belverde *et al.*, 2013; Mannion & Barret, 2013). These units form an escarpment along the north-eastern, eastern and south-eastern margins of the Moroccan Anti Atlas, and are underlain by folded Palaeozoic rocks and overlain by Cretaceous marine limestones that form the top of the escarpments. The southern escarpment is typically divided in two: the sandstone-dominated Ifezouane Formation and the overlying mudstone-dominated Aoufous Formation (Cavin *et al.,* 2010, Ettachfini & Andreu, 2004). Most vertebrate fossils from the southern part of the area come from the Ifezouane Formation. In the northern part of the area, close to the mouth of the gorge of the River Ziz, well-preserved fish fossils and amphibian and squamate remains are known from the Aoufous Formation (Dutheil, 1999). However, currently there is no stratigraphic control on the fossil assemblages and hence whether the faunas found in the region share a common time age or are an assemblage of multiple ages is unknown.

The majority of the publications describing fossils from the "Kem Kem Beds" have been based on commercially collected material with relatively few publications dealing with material collected *in situ* (Dutheil, 1999, Rage & Dutheil, 2008). As a result,

palaeoecology studies of the unit might be heavily biased by collection (e.g. higher value specimens) and taphonomic bias (e.g. merging of stratigraphically, environmentally and geographically isolated faunas). Some studies have assumed a rather homogeneous palaeoenvironment (Cavin *et al.,* 2010) or noted some stratigraphical variation in the faunas but did not link that to palaeoenvironment (Läng *et al.*, 2013). There is a general dominance of small remains (vertebrae, teeth and scales fish) of actinopterygian and lepisosteid fishes. Toothplates of the lungfish have also been found although more irregularly. Chondrichthyan remains are also common, largely composed of †*Onchopristis numidus* rostral denticles and teeth, with rarer occurrences of teeth from hybodont and lamniform sharks. Tetrapod bone fragments are also extremely common (e.g. chelonian carapace fragments, spinosaurid teeth). Plant macrofossils are sporadically found in some localities and are especially common in northern localities of the channel sandstone facies (e.g. Aghanbou). Non-vertebrate remains include multiple gastropod species, small bivalves and carapace fragments of decapod crustaceans. This fossil assemblages suggest a fluvial association, with little to none no evidence for marine influence although the presence of common †*Onchopristis numidus* may suggest a link to related to coastal facies within which it is known elsewhere (Werner, 1989) and occurrence of several species of lamniform sharks (typically considered as marine) may suggest a direct and possibly close connection to the sea.

The channel structures within fluvial facies in Moroccan localities (e.g. Boufaddouz) are extremely large suggesting a large scale of the channel which might have been part of a meandering river system as very large and sinuous channels persist in this direction in both Morocco and Libya indicating continuity of an extremely large river system.

Material and Methods

The specimens were obtained from Morocco-based commercial sources and one of them was brought on site (Boufza). Mechanical preparation was carried out in all specimens to remove sediment and reveal features concealed in it. Specimens NHMUK 75502 and 75503 were prepared and currently housed in the Natural History Museum in the United Kingdom (NHMUK). Specimen UV 353500 was prepared and is currently housed in the University of Vienna. Further preparation of the disarticulated specimens involved cutting and polishing in order to check their internal morphological features.

The histology patterns of three isolated rostral denticles were examined at the Department of Palaeontology, University of Vienna with a desktop micro-computed tomography (micro-CT) device (Bruker SkyScan 1173). The following settings for each specimen were used: Pixel size [μm] (10.01486, 17.882692, 26.109324), Source-voltage [kv] (100, 130), Source current [μa] (Al 1.0 mm, brass 0.25 mm), Rotation step [°] (0.2), Frame averaging (8). The generated micro-CT slice file stacks were loaded into the software packages DataViewer (Bruker, version 1.5.1.2) and Amira (FEI Visualization, version 5.4.g) to generate 3D volume renderings of the fossil material and to digitally dissect it using clipping planes of different angles.

Institutional abbreviations

NHMUK: Natural History Museum United Kingdom. UV: University of Vienna

Material examined

Fossil material. †*Libanopristis hiram:* NHMUK PV P 63610, 108708, 13857, 13858. †*Shizorhiza stromeri*: NHMUK PV P 73625.

†Onchopristis numidus

- NHMUK PV P 75502: Anterior portion of a rostrum, concealed in a soft sediment concretion in which the denser components (rostrum) sunk deeper in the sediment while the lightweight elements (dermal spines) are superficial. Ventral and dorsal suggesting that they were not tightly connected during burial. Mechanical preparation was carried on the specimen to expose dorsal and ventral surface.

- NHMUK PV P 75503: Fragment of the right part of the rostrum with the base of several denticles of the lateral rostral cartilage series still attached, the specimen was completely prepared specimen to expose both ventral and dorsal surface.

- Universität Wien (University of Vienna) 353500: Specimen presents an almost complete rostrum, jaws and neurocranium and attach to it a fragmented synarcual. The specimen was mechanically prepared to reveal both ventral and dorsal view of all structures. The rostrum presents most of the lateral series of enlarge rostral denticles and the most anterior part (tip missing) present few ventral denticles attach to it. The neurocranium present most of the mid posterior region (behind nasal capsules).

Results

Systematic Palaeontology

Class **Chondrichthyes** Huxley,1880.
Superorder **Batomorphii** Cappetta, 1980b.
Order **Rajiformes** *sensu* Naylor *et al*., 2012.
Suborder **Sclerorhynchoidei** Cappetta, 1980b.
Genus *Onchopristis* Stromer, 1917.
Species *Onchopristis numidus* (Haug, 1905).
Figs. 3.2-3.15

Description
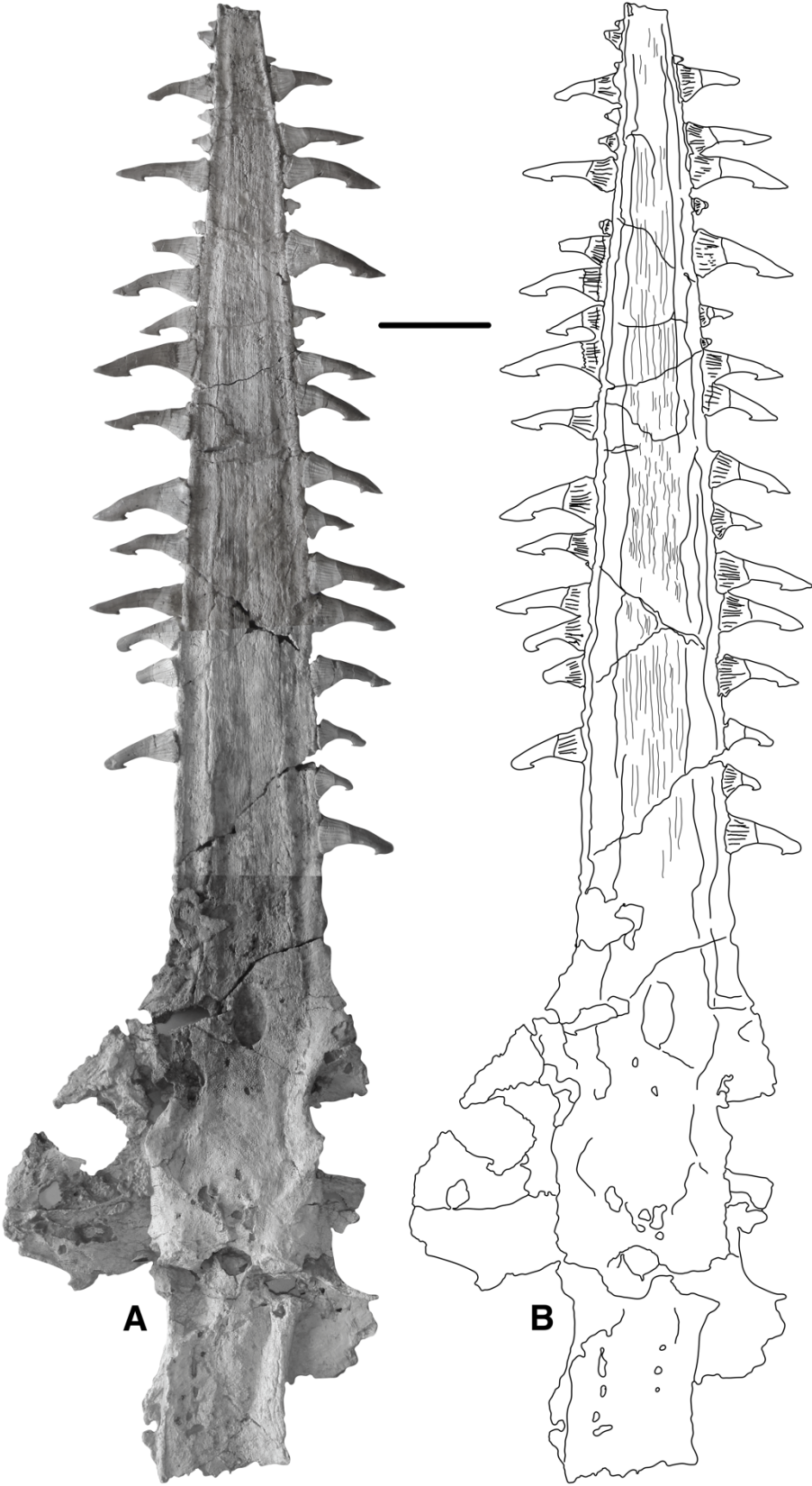
Figure 3.2. Rostrum of †*Onchopristis numidus* (UV 353500). Scale bar: 5 cm

Rostrum

Rostrum–Hypertrophied (837 mm), robust and triangular shaped, reaching its widest point at the base (Length-width at base ratio: 0.0186) and narrows towards the tip (Length-width at the tip ratio: 0.0042) (Fig. 2). The base of the rostrum progress smoothly into the neurocranium. After the removal of the sediment the specimens revealed the presence of a 'wood-like' layer of cartilage covering the inner layer of tessellate (mosaic-like) cartilage on the central part of the rostral cartilages. In addition, a thick layer of heavily vascularised cartilage on sides of the rostral cartilages supporting the lateral series of enlarged rostral denticles is present. Suggesting a constant development of rostral denticles which is corroborated by the presence of fully functional (erect) enlarged rostral denticles of different sizes. †*Schizorhiza* presents a similar rostral arrangement with a thin layer of 'wood-like' cartilage and thick cartilages on the sides. However, in †*Schizorhiza* the thick layer of cartilages on the sides of the rostrum is much less vascularised. These features and the differences in the replacement of the lateral rostral denticles series suggest that these species used their rostrum in a different manner.

Below the highly vascularised lateral layer of cartilage, on both the dorsal and ventral surface of the rostral cartilages are two canals, one on each side (Fig. 3A-C). The supraophtalmic nerve canal runs on the dorsal surface and is covered by a thin layer of cartilage and seems to terminate in a cavity next to the supraorbital crest. On the ventral side the buccopharyngeal nerve canal terminates at the base of the nasal capsules and becomes narrower towards the tip of the rostrum and at some points is covered by wood like cartilage (tip of UV 353500) suggesting that this canal was covered by cartilage.
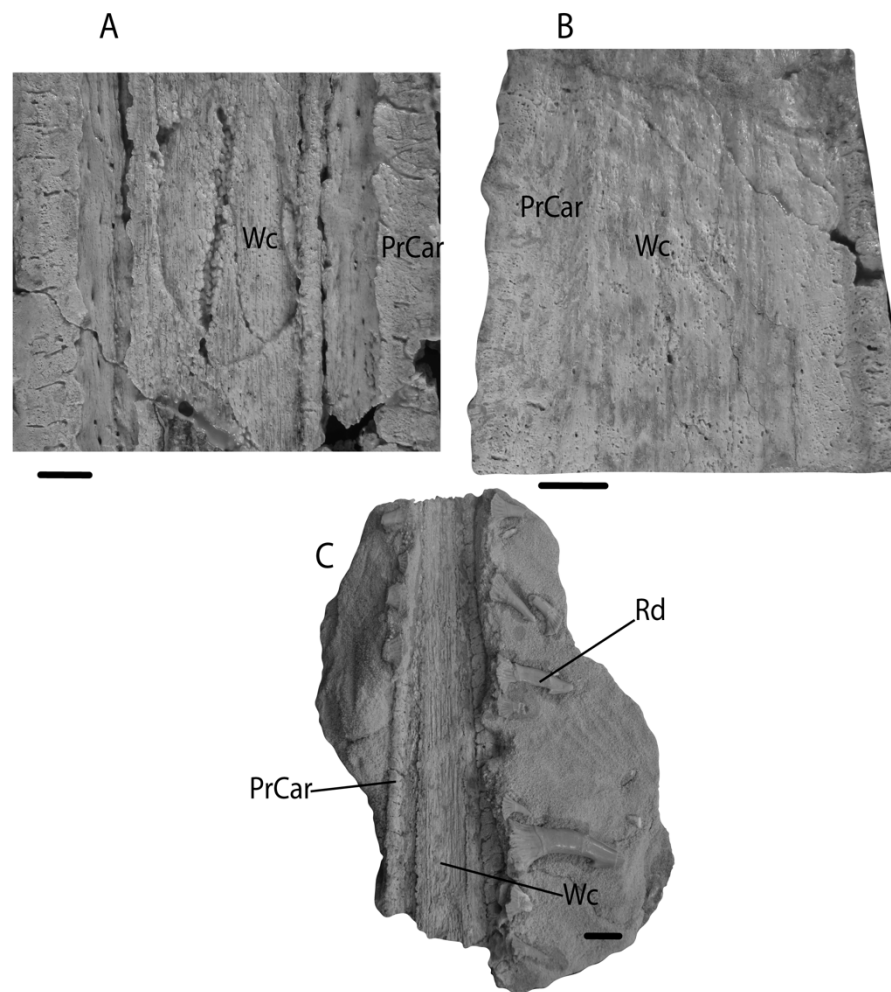
Figure 3.3. A-C Rostrum of † *Onchopristis numidus*. **A**, Ventral surface of UV 353500. **B**, Dorsal surface of UV 353500. **C**, NHMUK PV P 75502. **Abbreviations**: Ld, Lateral denticle series; PrCar, periphery cartilage; Rd, rostral denticle; Wc, Wood-like cartilage. Scale bar: 1cm.

Lateral enlarged rostral denticles

 All lateral rostral denticles in specimen (NHMUK 75502 and UV 353500), and disarticulated ones found elsewhere in the "Kem Kem Beds" display a small, flat base composed mostly of osteodentine and a large cap composed entirely of orthodentine with an external cover of enameloid and a base with the characteristic barb on the apical posterior margin of the denticle. On both anterior and posterior faces of the denticle strongly marked cutting edge follow by rectilinear crest were observed (Fig 3.4). The presence of this cutting edges and the lack of abrasion in the cap of the denticles suggests no close interaction with the sediment.
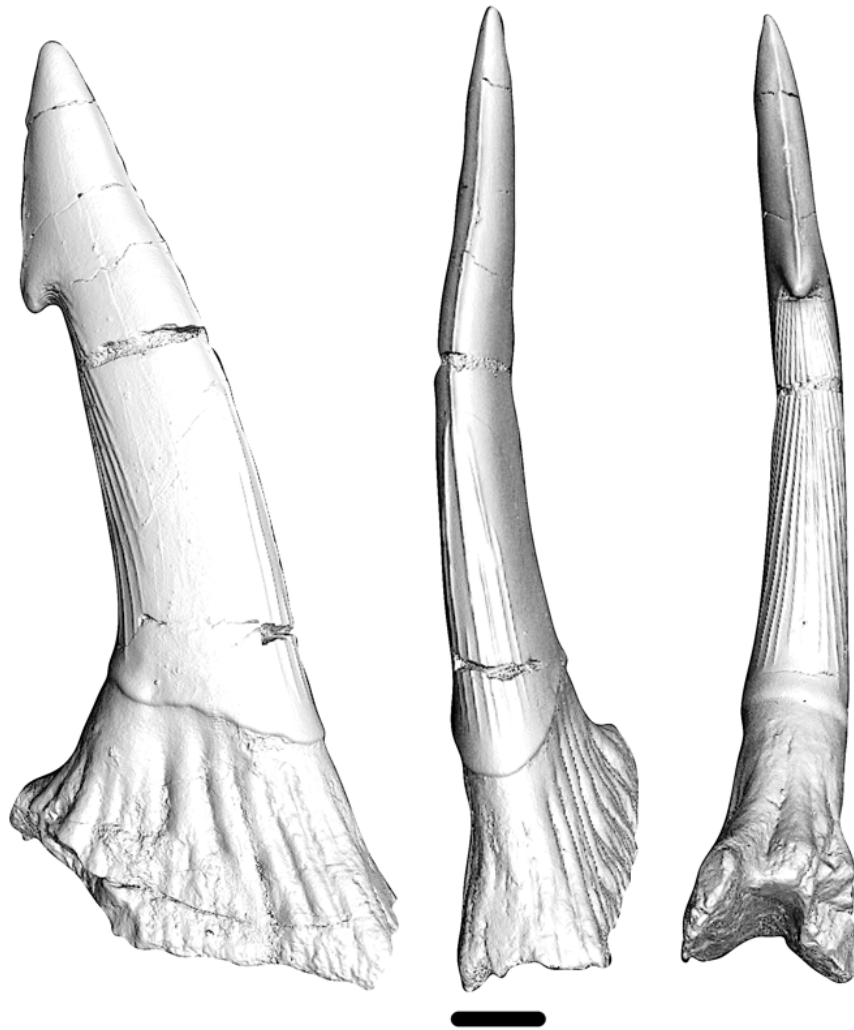
Figure 3.4. Enlarge rostral denticles collected along with the specimen UV 353500 (scale bar: 1mm).

Denticles with multiple number of barbs have been sporadically collected in Morocco (Fig 3.5) (Martill & Ibrahim, 2012), these denticles present similar dimensions to single barbed ones, suggesting no correlation with the size and the partial doctoring of a triple barb denticle (Fig. 3.5A) by commercial dealers might suggest that they might not be that rare. Multiple barb denticles have also been reported in Egypt (Stromer, 1917, plate 1 fig. 9 and 1; Werner, 1989, plate 20, fig. 1a and 1b, 3 and 6-7) along with a three barbed one (Wegner, 1989, plate 20, fig. 5). The presence of multiple barded denticles in the Egyptian and Moroccan localities suggest there is sporadic development of double barbed denticles.
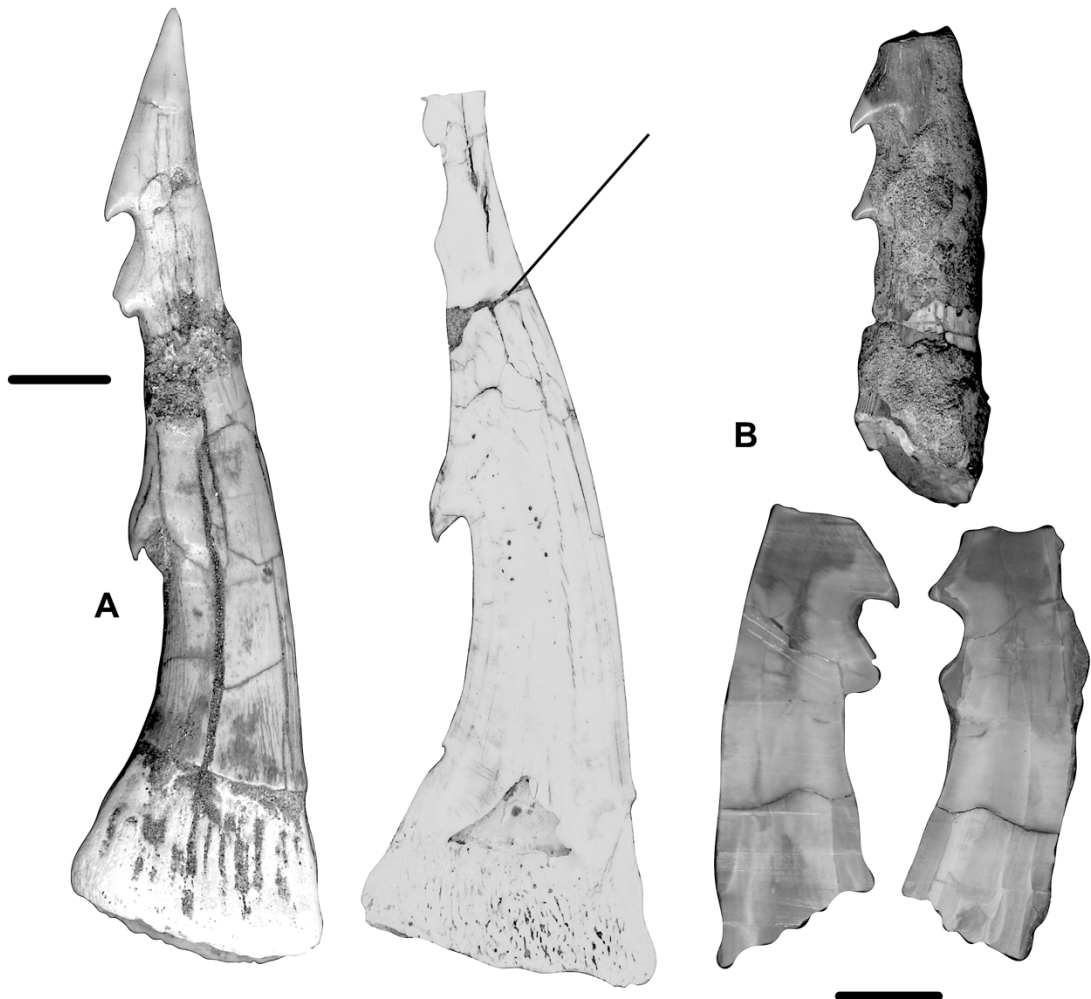
Figure 3.5. A-B, Multiple barb enlarge rostral denticles bought in Morocco. **A,** Partial doctored denticle as the tip actually present two barbs. Scale bar: 1 cm.

Disarticulated denticles recovered present variable developed barb despite some of them being of similar size (Fig. 6C), this suggest that the size of the barb could be a result of the position of the denticles, in cases where the barb develops it seems to grow with the denticle. Section and CT scan of denticles showed a pulp cavity projecting beyond the base and becoming almost a hair size canal when it reaches the barb region, suggesting that barb could reach a fixed size faster than the remaining sections of the cap (Fig 3.6A-B).
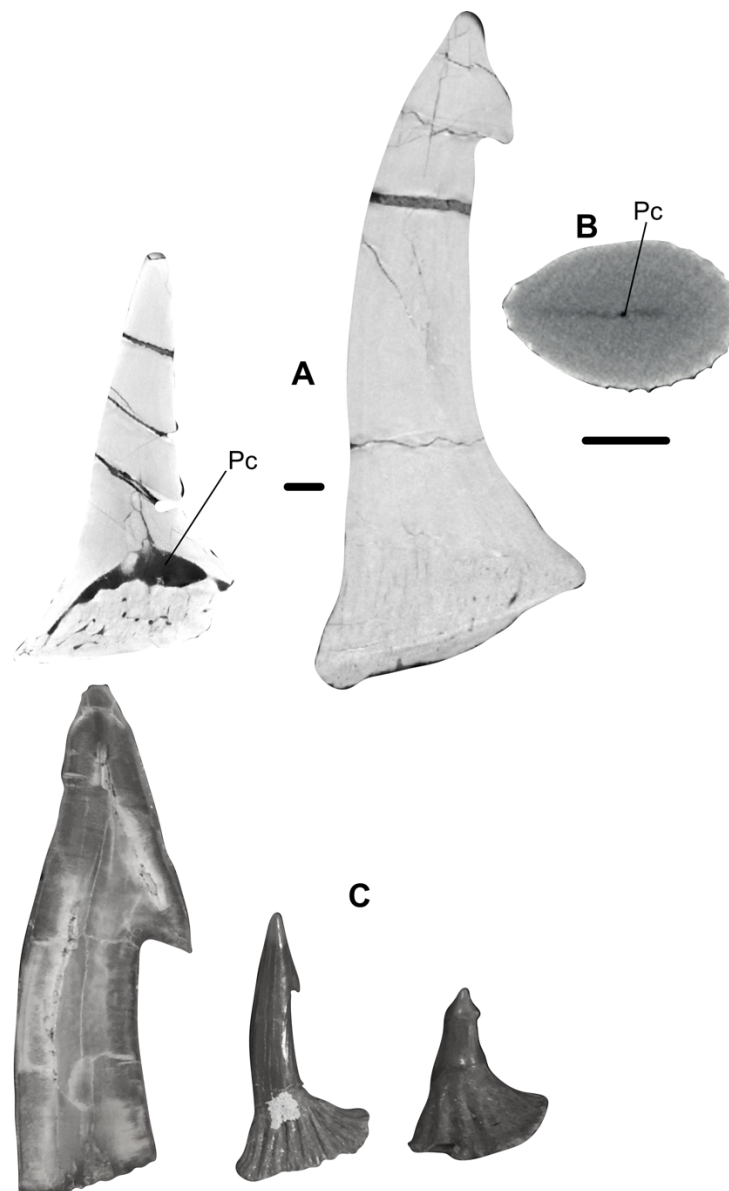
Figure 3.6. A-B, Rostral denticles of † *Onchopristis numidus* found in the "Kem Kem Beds". **A**, CT scan of denticles (scale bar: 1mm). **B**, Transverse section of denticle (scale bat: 2 mm). **C,** Lateral section and complete denticles (scale bar: 1cm). **Abbreviations**: Pc, pulp cavity.
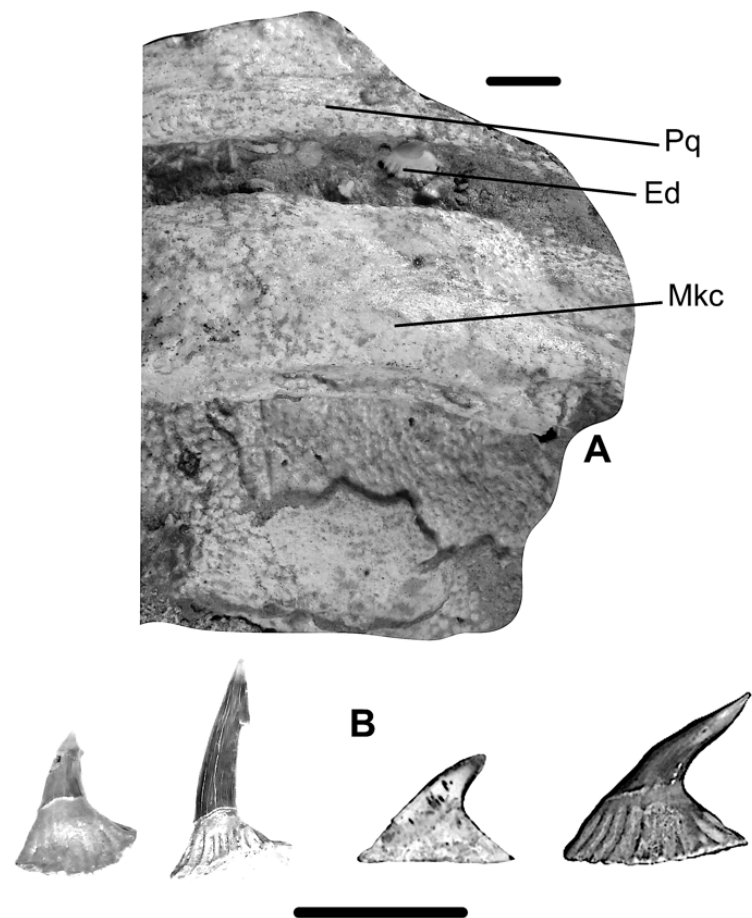
Figure 3.7. A, Mouth of UV 353500. **B**, Disarticulated denticles found in the "Kem Kem Beds" with similar morphology. **Abbreviations**: Ed, enlarge denticle; Pq, palatoquadrate; Mkc, Meckel cartilage. Scale bar: 1cm.

Enlarged denticles series

Different morphologies of enlarged denticles of †*Onchopristis numidus* have been collected in Morocco (Fig. 3.7B) and reported in Egypt (e.g. Stromer, 1927, plate 1, fig. 30b-32b; Werner, 1989, plate 20, fig 8-9). These morphologies suggest the presence of different enlarged series of denticles in †*O. numidus* which probably varies according to their position as indicated for other sclerorhynchoids (Welten *et al*., 2015; Underwood *et al.*, 2016a). The lateral section of the barbless denticles show no evidence of a developing a projection of the posterior margin that could suggest the eventual formation of barbs (Fig. 3.7B). This suggest that the shape of the denticles (Fig. 3.7B) and that the development of the barb seems to be restricted to the lateral series of the rostrum. Furthermore, in the specimen UV 353500 some of the denticles of the anterior cephalic series are located between the jaws (Fig. 3.7A) and indicating the presence of this series of enlarged denticles in this genus as in other sclerorhynchoids (Welten *et al.,* 2015; Underwood *et al.,* 2016a).

Replacement of enlarged rostral denticles

 The lateral series of enlarged denticles of the rostral cartilage presents different sizes, with large denticles intercalated with smaller ones and vice versa in a single line. This type of arrangement has not been seen in other batoid group including Pristidae in which the denticles present a continuous size. The presence of highly vascularised cartilage on the sides of the rostrum suggest that denticles are added as the rostral cartilage grow and develop over time (Fig. 3.8A-B). The presence of a pulp cavity in both large and small denticles suggest some sort of growth of the denticles with the incorporation of orthodentine.

Specimen UV 353500 present fully erect small denticles, suggesting a seriation in the appearance of the rostral denticles starting with smaller denticles at first (Fig. 3.8C; G1) with the addition of larger ones as the organism grows (Fig. 3.8C; G2 and G3). This dynamic is different to what has been previously reported for other sclerorhynchoids (e.g. Sternes & Shimada, 2018; Welten *et al.,* 2015; Underwood *et al.,* 2016a; Smith *et al.,* 2015).
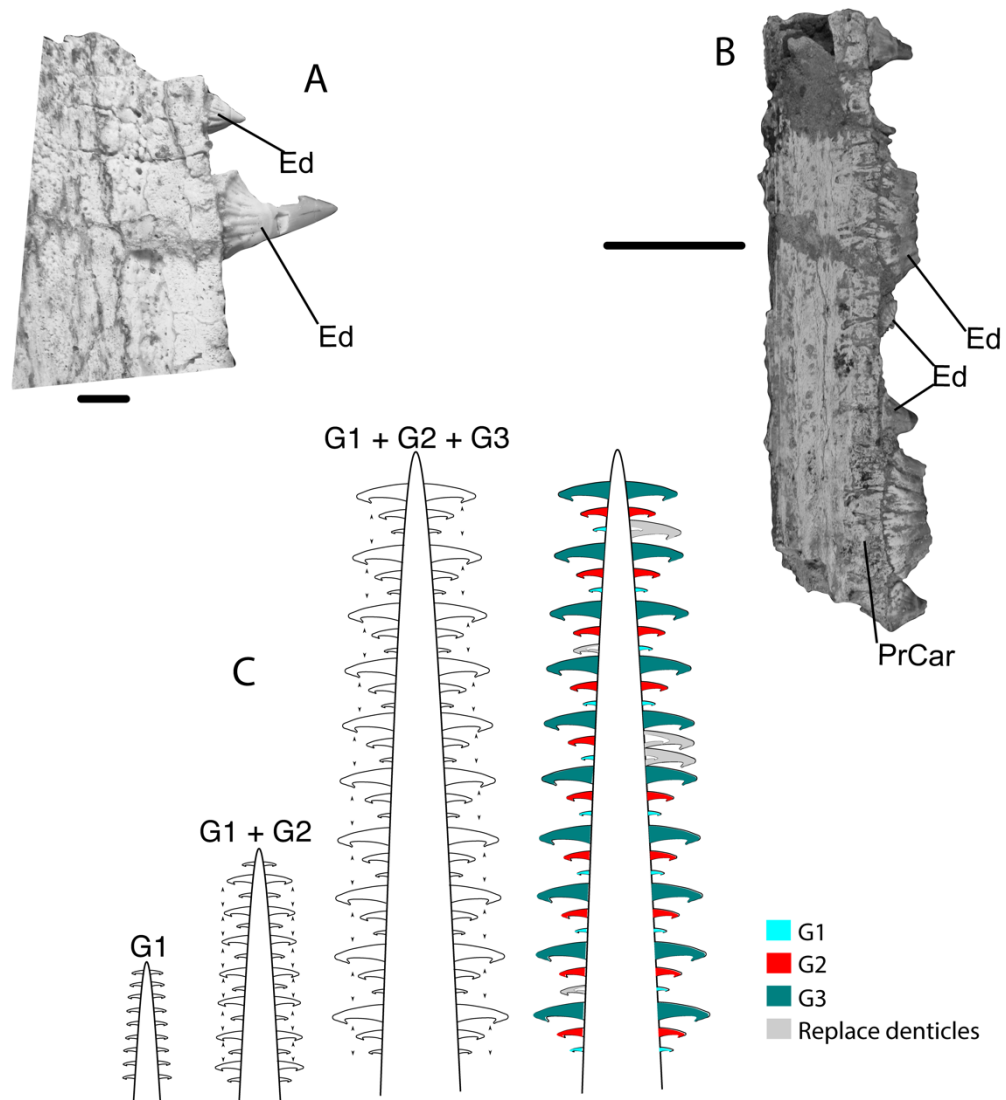
Figure 3.8. Fragment of rostrum of †*Onchopristis numidus*. **A,** CV 353500 (scale bar: 1cm). **B,** NHMUK PV P 75503 (scale bar: 5cm). **C,** Hypothetical scheme of the growth and addition of rostral denticles in †*Onchopristis.* **Abbreviations**: Ed, enlarge dermal denticles. PrCar, highly vascularise peripherical cartilage. Marked in figure B are denticles being displaced by new ones. Denticles in grey in figure C are larger denticles replacing smaller ones that fell.

Neurocranium

Only the postnasal region and part of the posterior edge of the nasal capsules are described as the most anterior part of the nasal capsules is missing. The neurocranium is box-like and rectangular shaped with an oval-shaped precerebral fenestra located in center of the anterior part of the neurocranium near the base of the rostrum (Fig. 3.9). Dorsally no surface of the left nasal capsules is observable (crushed). On ventral view the posterior region of the right nasal capsule is preserved and presents a deep nasal fenestra that smoothly progress into the rostrum. The buccopharyngeal nerves cavities are located on the ventral surface anterior to the nasal capsules (Fig, 3.10A-B). The silhouette of the antorbital cartilage is distinguishable and presents a triangular shape with its acute distal edge pointing posteriorly and the wide proximal edge articulated to the nasal capsule (Fig. 3.10A-B). Even though the neurocranium is slightly crushed dorsoventrally, the supraorbital is well-developed but does not cover the eye crest and stands above the chondrocranium. The orbital cavity is large and contains a well-mineralised optic peduncle, further nerves foramens were not observed (Fig. 3.10C-D). Next to the supraorbital crest is the cavity for the supraophtalmic nerve (Fig. 3.9). The post-orbital region is rectangular and narrow with a small triangular post-orbital process. In the otic region the orbital fissure stands above the lateral commissure underneath the postorbital crest and the lateral commissure covers part of the hyomandibular branch of the facial nerve foramen (Fig. 3.10C-D). The lymphatic foramina are present in the posterior part of the neurocranium. The jugal arches follow the otic region and are located anterior to the occipital condyles which are well-developed expanded laterally and form a large and deep articulation surface for the anterior lateral process of the synarcual (Fig. 3.9).

The hyomandibula is triangular (length: width at base ratio = 0.51, length: width at tip ratio = 0.018), with its proximal end articulated to neurocranium, and the acute distal end

possibly connected between palatoquadrate and Meckel's cartilage. Part of the dorsal surface of the hyomandibula is missing, however it is slightly elevated from the rest suggesting the presence of a process for muscle articulation (Fig 3.9).
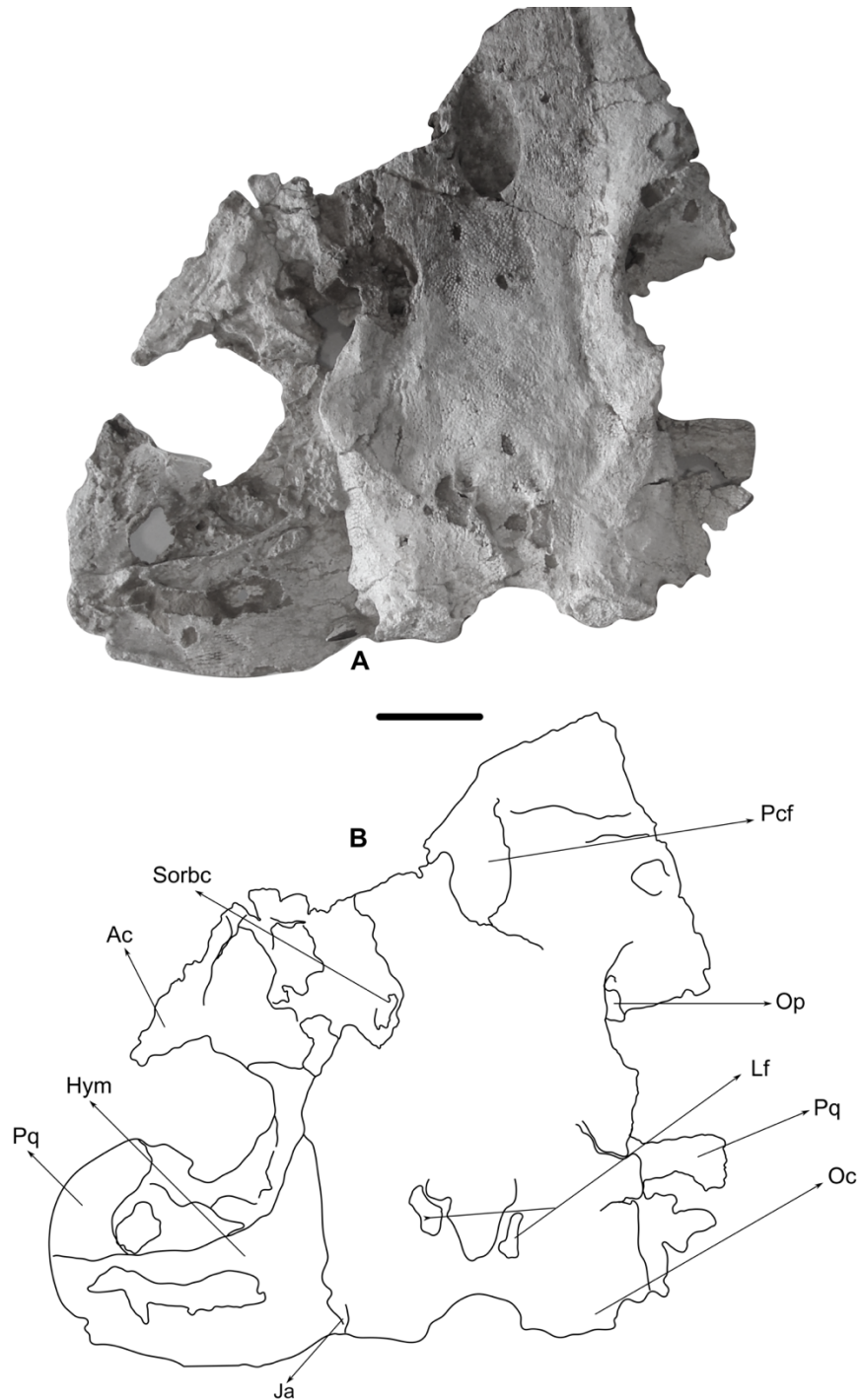
Figure 3.9. A-B, Neurocranium of †*Onchopristis numidus*. **A**, picture of CV 353500, **B**, line drawing. **Abbreviations**: Ac, antorbital cartilage. Hym, hyomandibula. Ja, jugal arch. Lf, lymphatic foramina. Oc, occipital condyle. Op, optic pedicel. Pcf, precerebral fenestra. Pq, palatoquadrate. Sorbc. supra orbital nerve cavity. Scale bar: 5cm.
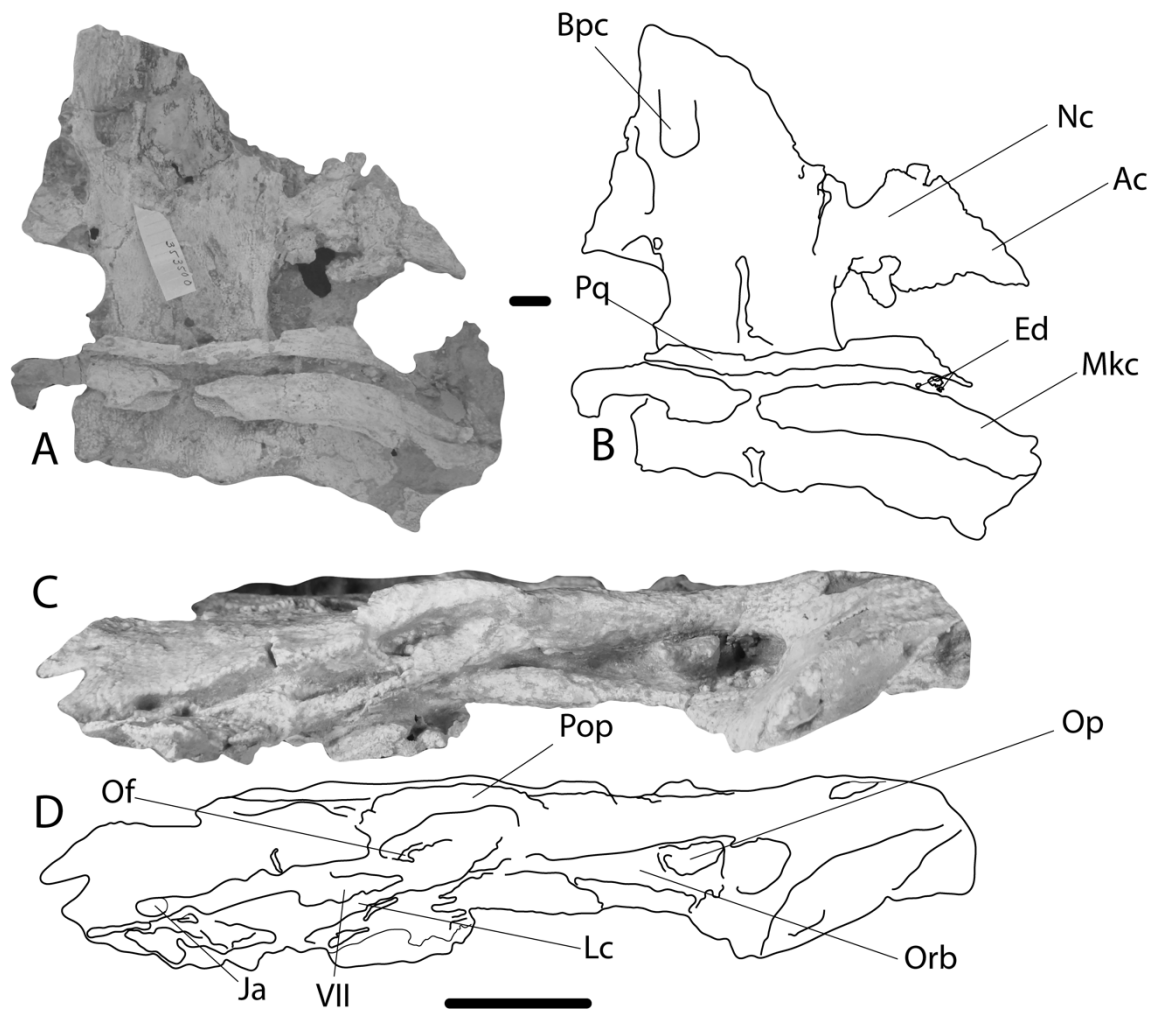
Figure 3.10. Neurocranium of †*Onchopristis numidus* (UV 353500). **A**, Ventral view. **B**, Line draw. **C** Lateral view. **D**, Line draw. (A-B, scale bar: 2 cm). (C-D, scale bar: 5 cm). **Abbreviations**: Ac, antorbital cartilage. Bpc, buccopharyngeal nerve cavity. Ed, enlarge dermal denticle. Ja, jugal arch. Lc, lateral commissure. Mkc, Meckel´s cartilage. Of, orbital foramen. Op, optic pedicel. Orb, orbital cavity. Pop, postorbital process. Pq, palatoquadrate. VII, hyomandibular branch of the facial nerve foramen.

Jaw cartilages

Only part of the Meckel's and palatoquadrate cartilages are observable from ventral view (Fig. 3.10A-B). The palatoquadrate is curved distally and narrows towards the symphysis (Fig. 3.10A-B). In ventral view no apparent articulation to the neurocranium between the Meckel's cartilage and palatoquadrate, both seem to be supported by the hyomandibula. The palatoquadrate and Meckel's cartilage antimeres are not fused and connected at the

symphysis; Meckel's cartilage is wider than the palatoquadrate and become narrower towards the symphysis (Fig. 3.10A-B).

Oral teeth

†*O. numidus* teeth (Fig. 3.11A-L) are similar to those of †*Onchopristis dunklei* (Welton & Farish, 1993; Kriwet & Kussius, 2001, Fig. 4; Cappetta, 2012; Fig. 370M-R). Both species present a strong an acute cusp bent lingually (Fig. 3.11C, G, K). The labial apron is slim and with a bunt end that projects anteriorly beyond the root several teeth collected from Morocco present a double lobed labial apron (Fig. 3.11A, E, D, H). The lateral cusplests were observed on all the specimens (Fig. 3.11A, E). The cutting edge of the medial crest extends towards the lateral cusplets (Fig. 3.11A). The lingual uvula is absent (Fig 3.11C, G) . The root is bilobed and laterally projected (Fig. 3.11B,F). Teeth have been figured multiple times (Stromer, 1927, Plate I, Figs 1-4 (under the name †*Squatina aegyptiaca)*; Werner, 1989, plates 21 & 22 (belonging to a different sclerorhynchid species possibly †*Renpetia.* Plates 35-37 described as †*Sechmetia aegyptiaca* resembling those described as †*O. numidus*).
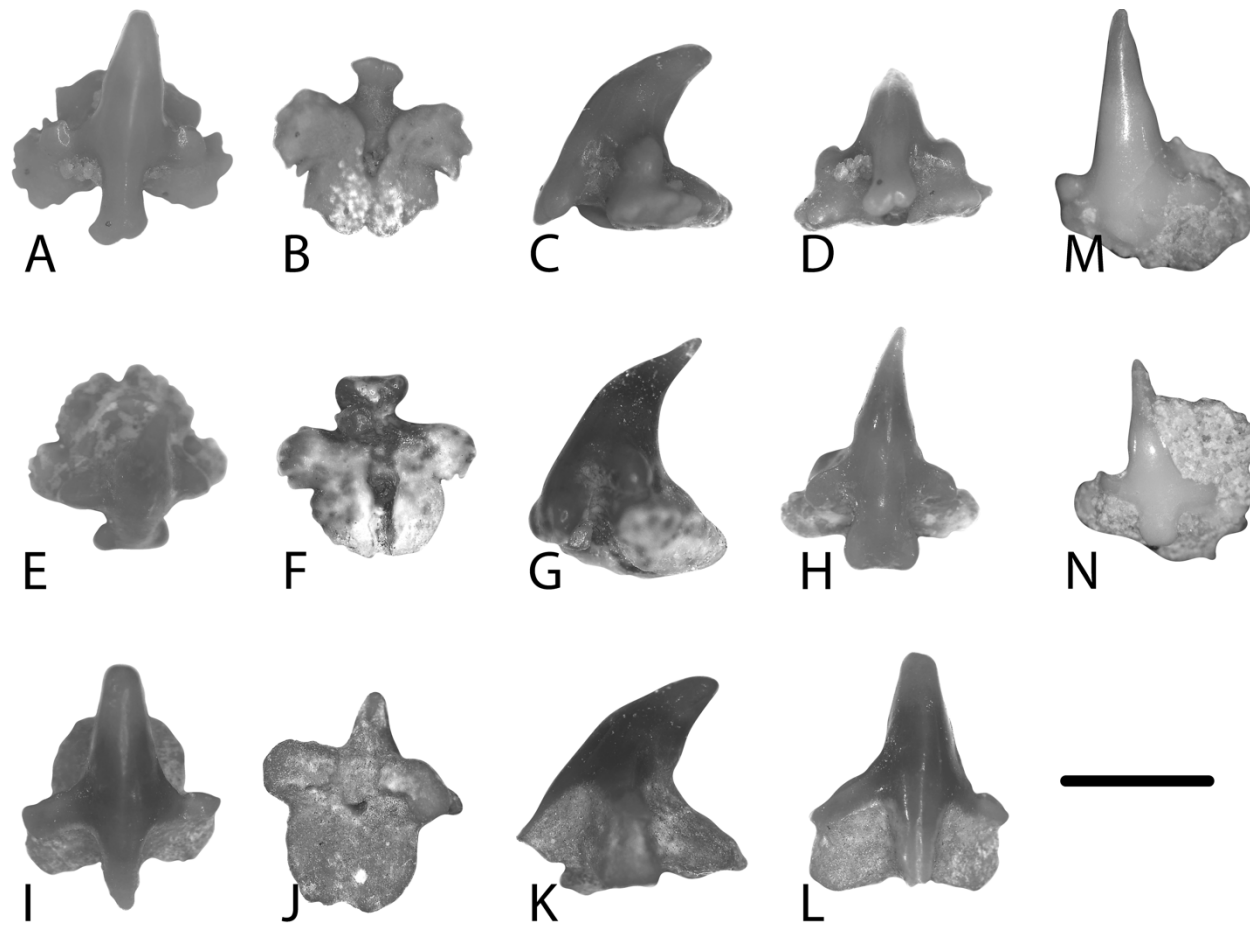
Figure 3.11. A-L, Oral teeth of †*Onchopristis numidus* found in the "Kem Kem Beds". **M-N**, Teeth extracted from the preparation of specimen UV 353500.

Synarcual
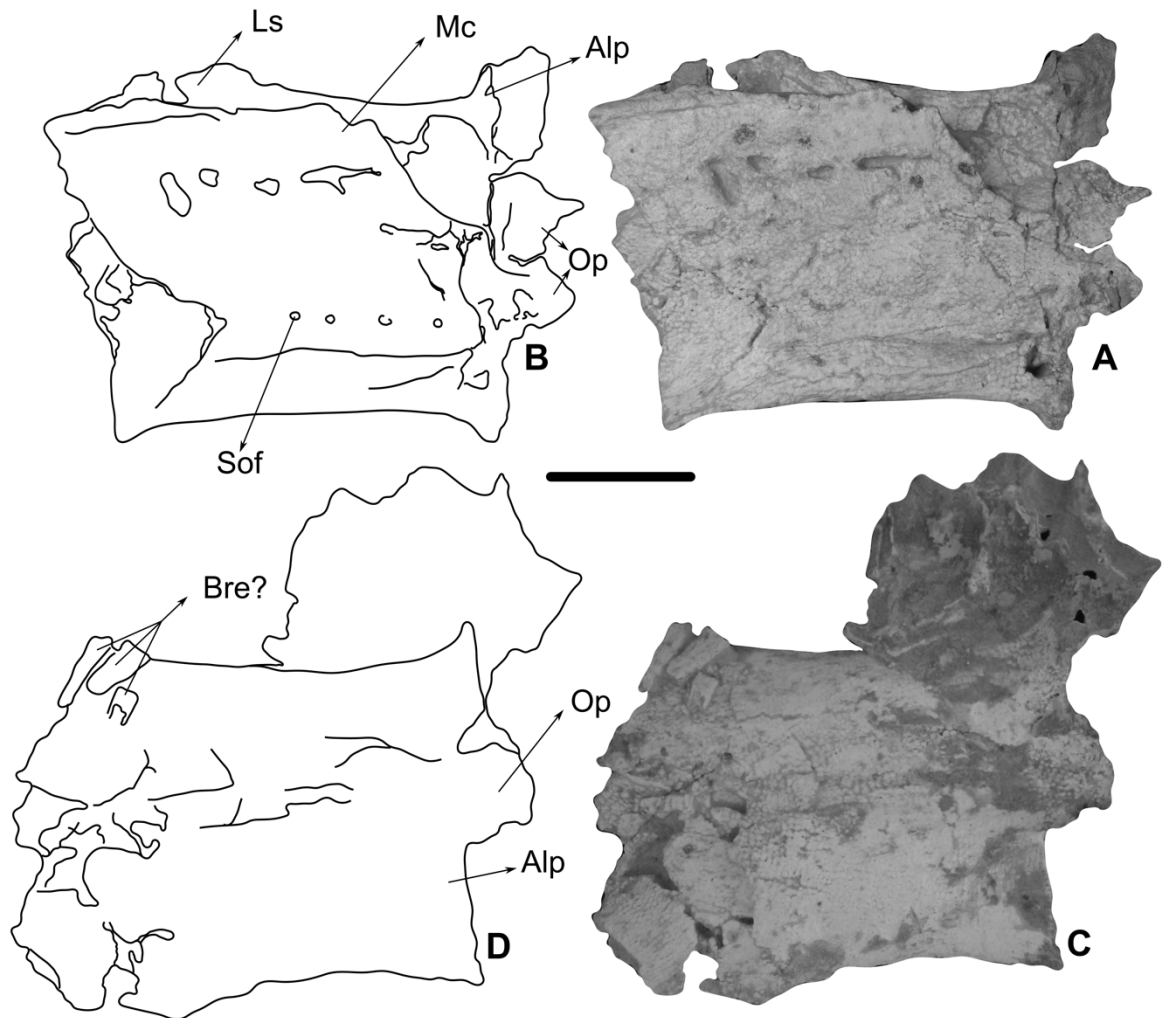
Figure 3.12. Synarcual of †*Onchopristis numidus* (UV 353500). **A**, dorsal view. **B**, line draw. **C**, ventral view. **D**, line draw (scale bar: 5 cm). **Abbreviation**: Alp, anterior lateral process. Bre, branchial elements. Op, odontoid process. Ls, lateral stays. Mc, medial crest. Sof, spino-ochipital foramina.

Only the anterior part of the synarcual is preserved and presents a well-developed odontoid process (synarcual lip) that fits well within the articulation surface for the synarcual in the neurocranium. The synarcual presents large anterior lateral processes that mirror the odontoid processes this and the deepness of the odontoid process suggest a close and not very mobile articulation with the neurocranium (Fig. 3.12). The medial crest is well-developed and thin, at its base presents four easily visible spino-ochipital foramina (actual number remains unknown as only a portion of the synarcual was preserved). The

medial crest was flatted during compaction and its anterior part missing it is unknow whether it presented an anterior process. Only the right lateral stay is visible, and it becomes progressively narrower towards the rear. Its distal end is well-developed and flatted probably dorsally directed in life (Fig. 3.12A-B). In ventral view no vertebra centra were observed which suggest that the vertebral centra do surpass the midpoint of the synarcual as in other sclerorhynchoids (Fig. 3.12C-D) (Villalobos *et al*., 2019a)

Vertebral centra

The vertebral centra of †*O. numidus* as with other chondrichthyans show the corpus calcareum and the intermedialia. The corpus calcareum is well mineralized and shows a clear and opaque band suggesting a cyclical deposition of mineral. Whether or not this was yearly as with other chondrichthyans remains unknown (Fig. 3.13A-B).
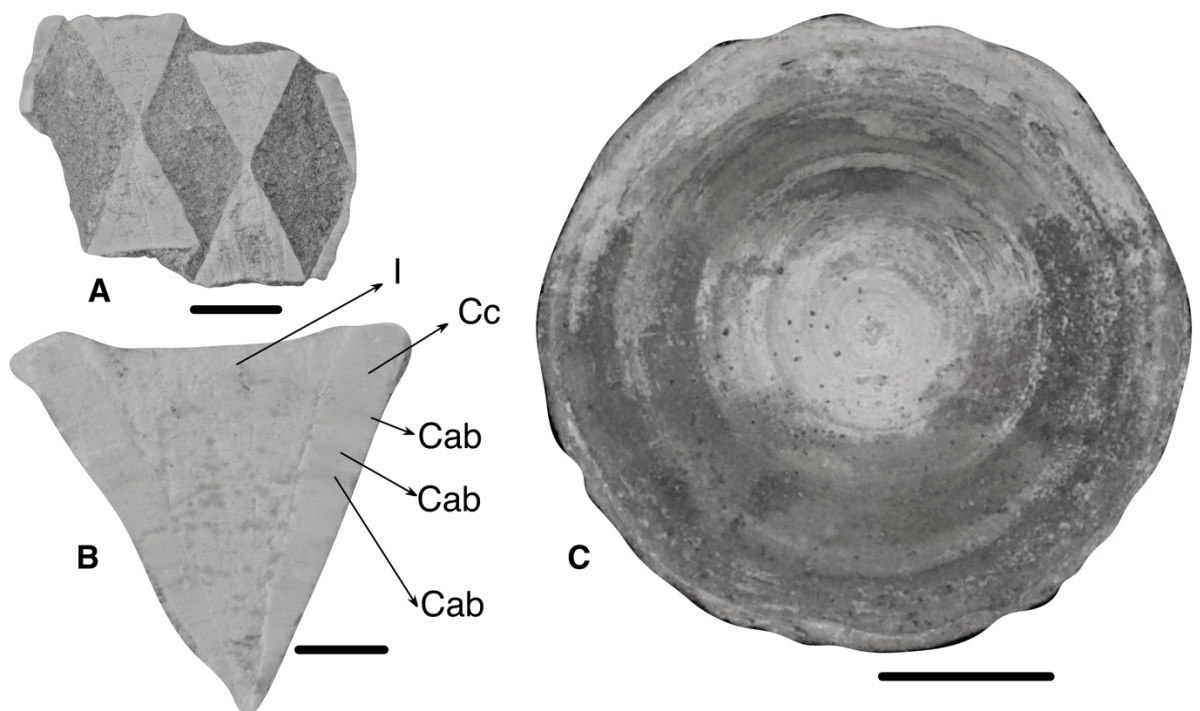
Figure 3.13. A-B, Longitudinal section of a vertebra centre of †*Onchopristis numidus* from the "Kem Kem Beds". **C,** complete vertebra (scale bars: 1 cm). **Abbreviations:** Cc, corpus calcareum; I, Intermedialia.

Dermal denticles

The rostrum also presents a small series of denticles at the base of the enlarged rostral denticles and in the ventral surface (Fig. 3.14G). Two morphologies were identified both of which present a rounded well enamelled cap and a stellated base with fringes that projects beyond the cap and are distinguished by the present of a central cusp (Fig. 3.14A-F)
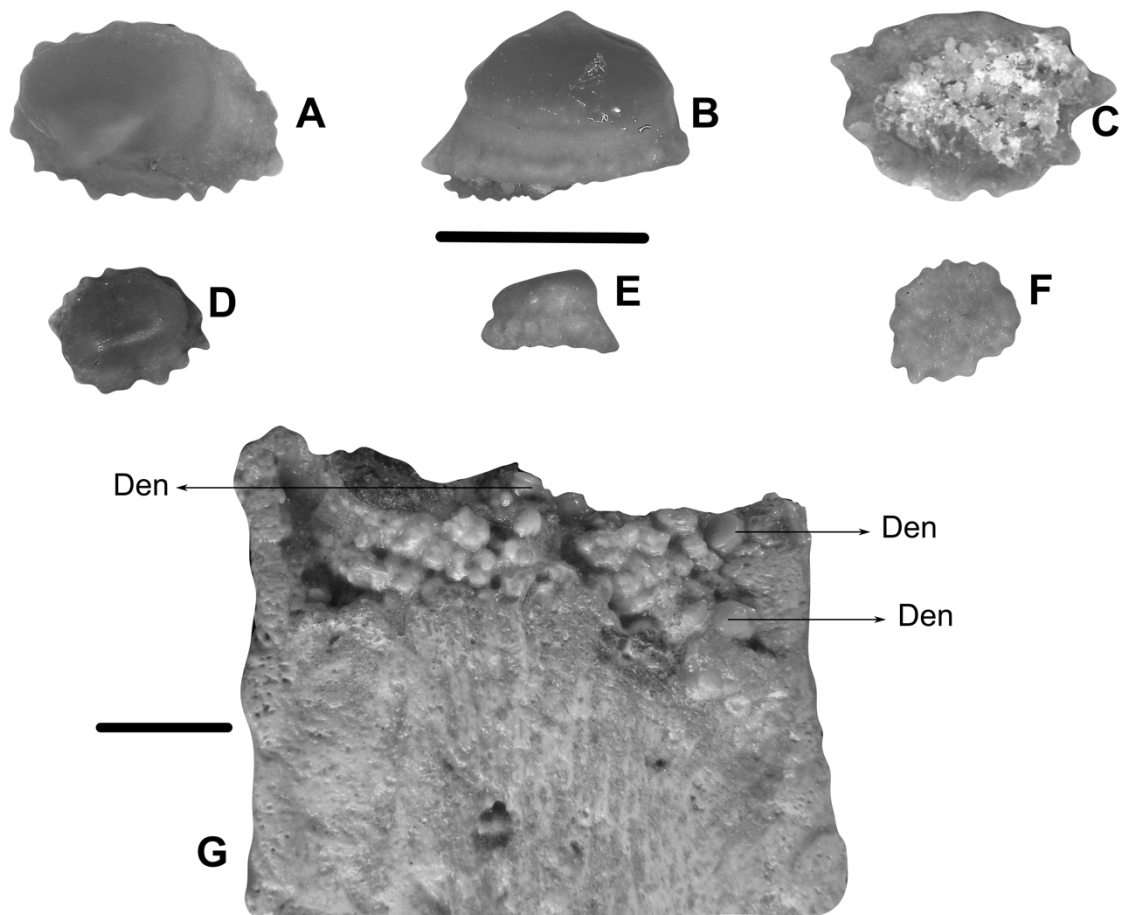
Figure 3.14. A-F, Ventral rostral denticles from the section of the rostrum of †*Onchopristis numidus* (NHMUK PV 75502). **A-C**, Morpho 1. **D-F**, Morpho 2 (scale bar: 2 mm). **G**, anterior part of the ventral surface of CV353500 rostrum. **Abbreviations**. Den, dermal denticle.

As in other fossil assemblages (Werner, 1989), the occurrence of †*Onchopristis* in the "Kem Kem Beds" coincides with "*Peyeria*-like" remains of (Fig. 3.15). Cappetta (2012) noted these two batoid elements are commonly found together and suggested that †*Peyeria* Werner, 1989 remains are in fact dermal denticles of †*Onchopristis.* Recently

similar enlarged dermal denticles have been reported for †*Ischyrhiza mira* Leidy, 1856b (Sternes & Shimada, 2018), suggesting that this feature could be more widespread among sclerorhynchoids. The discovery of these enlarged body denticles agrees with Cappetta's (2012) and Sternes & Shimada's (2018) interpretations and report the presence of enlarge dermal denticles in †*O. numidus*.

The dermal denticles of †*O. numidus* from Morocco are unique compared to what has been previously reported to other sclerorhynchids (Werner, 1989; plate 41, figs. 1-4; Sternes & Shimada, 2018;text-fig. 4e-f). They present a thick enameloid layer on the anterior edge of the denticles. Further longitudinal sections revealed a small pulp cavity followed by a thin not very porous laminar layer, followed by a thick layer of highly vascularised osteodentine that reaches the tip of the denticle (Fig. 3.15C).

As hybodonts are also present in the assemblage the enlarge denticles were compared to Maisey's (1978) observations. The tissue arrangement is very similar in both groups in *O. numidus* the laminar layer pores reach well beyond in to the osteodentine. Only one layer of osteodentine was recognised for †*O. numidus* (compared to the two in hybodonts). Hybodonts present a thick layer of orthodentine between the centre of the hybodont's spine and the osteodentine layers which is absent in †*O. numidus* (Fig. 3.15C).
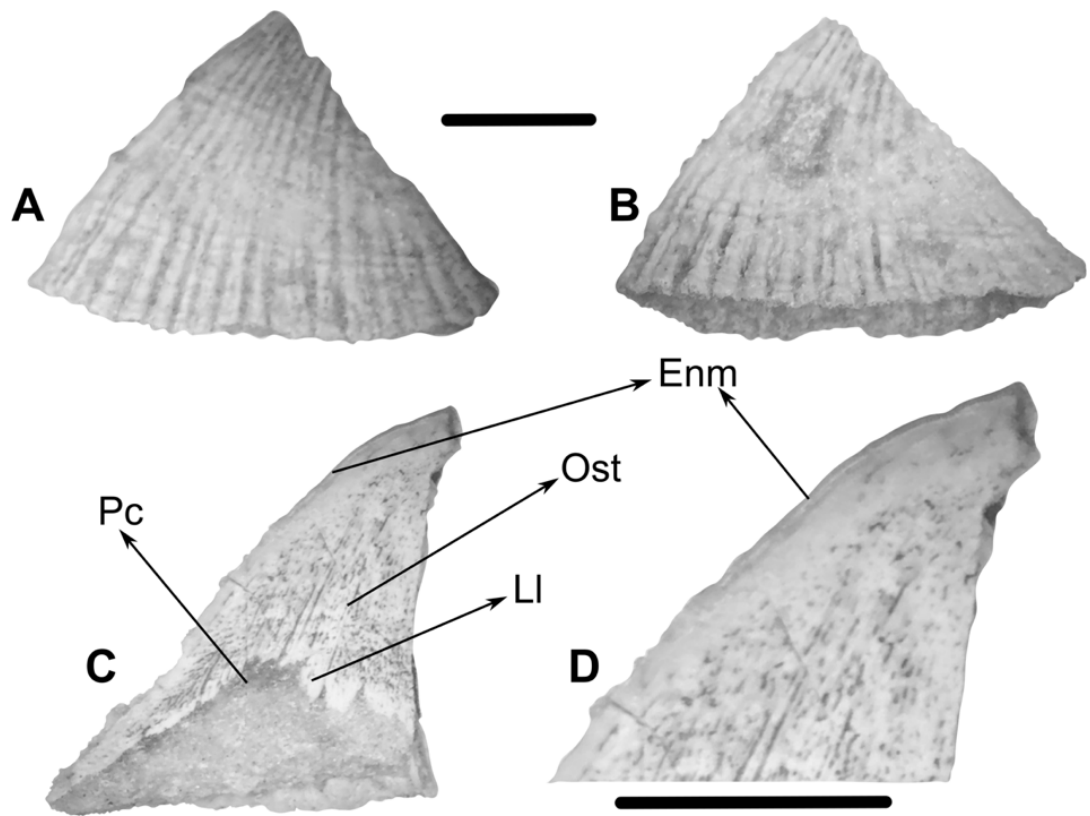
Figure 3.15. Enlarged dermal denticles of †*Onchopristis numidus* from the "Kem Kem Beds". **A,** right side. **B,** left side. **C,** lateral section. **D,** enlarge apical section of lateral section. Scale bar: 1cm. **Abbreviations**. Enm, enameloid; Ll, laminar layer; Ost, osteodentine; Pc, Pulp cavity.

Discussion

Currently there are two species within †*Onchopristis* (†*O. numidus* and †*O. dunklei*) which seem to be restricted to the Early to 'mid' Cretaceous (Barremian-Cenomanian). These two species possess extremely similar oral teeth but can be differentiated in the internal structure of the enlarge rostral denticles. †*O. numidus* presents an orthodentine filled cap, with a smaller pulp cavity that extends into the denticle cap. †*O. dunklei* presents a larger pulp cavity that extends well in to the denticles cap and a thin orthodentine layer (McNulty & Slaughter 1962; text-fig. 1 c-d). What differentiates †*O. numidus* from other sclerorhynchoids and †*O. dunklei* is the presence of a thick enameloid layer at the tip of the cap of the lateral rostral denticles and the presence of a densely orthodentine filled cap with a small pulp canal in the centre (Figs.

3.6) although some exceptions to this condition have been reported (Underwood *et al.*, 2016a; text-fig. 4C).

The cranial remains collected in Morocco (UV353500) are the first published skeletal remains reported for the genus †*Onchopristis*. The peculiar neurocranium anatomy with a rectangular shape of the post-nasal region, a reduced post-orbital process and anterior fenestra located at the base of rostral cartilages suggested the classification of the group within the Sclerorhynchoidei as proposed by Cappetta (2012). However, its affiliation with the family Sclerorhynchidae is doubtful as the rostrum anatomy, replacement and arrangement of the enlarged rostral denticles is different from other members of the group (e.g. †*Sclerorhynchus* and †*Libanopristis*) and resemble those of †*Shizorhiza* and †*Ischyrhiza*. Of significance are characters like the presence of wood-like cartilage in the rostrum centre, the thick peripheric layer of vascularise cartilage at the sides of the rostrum, the different size arrangement of the lateral rostral denticles series and its particular replacement which make †*Onchopristis* a very peculiar taxon within sclerorhynchoids and batoids.

The use of the rostral cartilages seems to vary among the sclerorhynchoids as suggested by the difference on the anatomy of this structure (see Chapter 2). The thick and vascularised peripherical layer of cartilage in the rostrum of †*Onchopristis* suggest a different use of this structure when compared with the thin rostrum of †*Sclerorhynchus* and †*Libanopristis* which also lacks the "wood-like" cartilage and the thick peripherical cartilage.

Conclusion

Currently there are two species within †*Onchopristis* (†*O. numidus* and †*O. dunklei*) which seem to be restricted to the (Barremian-Cenomanian). These two species are extremely similar in their oral teeth but can be differentiated in the internal structure of the enlarge rostral denticles. †*O. numidus* presents a smaller pulp cavity that extends in to the denticle cap as a thin canal and a densely orthodentine filled cap. †*O. dunklei* presents a larger pulp cavity that extends well in to the denticles cap and a thin orthodentine layer.

Rostral remains collected confirm Cappetta's (2012) classification of †*Onchopristis* within the Sclerorhynchoidei. This is suggested by the peculiar neurocranium anatomy with a rectangular shape of the post-nasal region, a reduced post-orbital process and anterior fenestra located at the base of rostral cartilages. The genus affiliation with the family Sclerorhynchidae is doubtful as the rostrum anatomy replacement and arrange of the enlarge rostral denticle series are different from other members of the group (e.g. †*Sclerorhynchus* and †*Libanopristis*) and resembles that of †*Shizorhiza* and †*Ischyrhiza.*

Chapter 4

Phylogenetic relations between Sclerorhynchoids and other Batoids

Results presented in this chapter were published in:

- Eduardo Villalobos-Segura, Charlie J. Underwood, David J. Ward & Kerin M. Claeson (2019): **The first three-dimensional fossils of Cretaceous sclerorhynchid sawfish:** *Asflapristis cristadentis* **gen. et sp. nov., and implications for the phylogenetic relations of the Sclerorhynchoidei (Chondrichthyes).** *Journal of Systematic Palaeontology*, DOI:10.1080/14772019.2019.1578832.

Co-authors contributions

- o E. Villalobos Segura: Description of character used. Participated in the discussion of the characters used. Phylogenetic analysis.
- o C.J. Underwood: Participated in the discussion of the characters used.
- o D.J. Ward: Participated in the discussion of the characters used.

Introduction

Historically parsimony has been the preferred method in phylogenetic analysis for morphological data (Goloboff, 2003) and the analysis of fossil batoids are not the exception (e.g. Brito & Seret, 1996; Brito & Dutheil, 2004; Claeson *et al.,* 2013). However, the use of statistical methods has gained popularity (Lewis, 2001; Wright & Hillis, 2014; O'Reilly *et al.,* 2016 & 2018) and could be useful for the analysis of problematic groups with morphological data. Recently a debate between which methods capture phylogenetic relations more accurate has resurface, simulation studies have suggested that Bayesian analysis using Mk-models are more accurate for morphology analysis than parsimony (Wright & Hillis, 2014; O'Reilly *et al.,* 2016 & 2018). Parsimony methods tend to recover more stratigraphically congruent phylogenies, which means that if the stratigraphic data is used as an independent parameter, for accuracy, parsimony is the better method (Sansom *et al*., 2018). Because of this, in the present analysis both methods were used.

Sclerorhynchoids are currently considered a monophyletic group, classified within Rajiformes as the suborder "Sclerorhynchoidei" (Cappetta, 2012). Despite this, their superficial similarities with sawfish (Pristidae) and saw-sharks (Pristiophoridae) (Wueringer *et al.,* 2009) (e.g. Rostrum-associated structures), have influenced their phylogenetic position. As a result, sclerorhynchoids have been recovered in different positions by different woks (e.g. Kriwet, 2004, Claeson *et al.,* 2013, Underwood & Claeson, 2017).

Kriwet (2004) is the direct antecedent for the present study, representing the most extensive review of the phylogenetics of the sclerorhynchoids to date. This analysis proposed several characters that distinguish the sclerorhynchoids from other batoids (e.g.

buccopharyngeal and supraophthalmic nerves not embedded in the rostral cartilage and lack of connection between the rostral cartilages and rostral denticles). In addition, Kriwet (2004) also included several characters from previous morphological studies (Nishida, 1990; Brito & Seret, 1996; De Carvalho, 1996; Lovejoy, 1996; McEachran *et al*., 1996; Shirai, 1996) that supported the Hypnosqualea hypothesis (Shirai, 1992), within which batoids were considered to be derived squalean sharks, which has been extensively refuted by Dunn & Morrissey, 1995; Schwartz & Maddock 2002; Douady *et al*., 2003; Winchell *et al.,* 2004; Aschliman *et al.,* 2012b; Naylor *et al.,* 2012; Last *et al.,* 2016). Kriwet's (2004) study also included several errors in matters of character definitions and coding (Aschliman *et al., 2012a*).

Recently several extremely well-preserved three-dimensional remains of sclerorhynchoids with previously unseen morphological details have been discovered in the region of Asfla in the northeast of Morocco corresponding to the Late Cretaceous (Chapter 2), allowing a restudy of the phylogenetic relations and taxonomic classification of the group. Of these specimens five present a similar tooth morphology to †*Ptychotrygon* providing the first skeletal record for the genus and a new species †*Ptychotrygon rostrispatula* sp. nov. and six present a previously unknown morphology that belongs to a new species and genus †*Asflapristis cristadentis*.

The present analysis aims to assess the phylogenetic relations between sclerorhynchoids and other batoids. Because of this it includes extant representatives of all extant batoid orders. Aschliman's *et al.* (2012a) observations were used and reviewed using extant material from different collections. In cases where extant material was not available, published images (e.g. Nishida, 1990; Alfonso & Gallo, 2001; Schaefer & Summers, 2005; Domínguez & González-Isaís, 2007; Claeson, 2010; Da Silva & De Carvalho, 2015) and electronic material (https://sharksrays.org; to access this image bank contact

Gavin Naylor). The results of the present analysis are discussed on the context of the phylogenetic relations proposed by Naylor *et al.* (2012) and Last *et al.* (2016), which are currently the ones followed for the taxonomic arrangement of batoids (Fricke *et al.*, 2019). Five fossil taxa were used to complete the data matrix (four representatives of the Jurassic batoids (†*Spathobatis,* †*Belemnobatis,* †*Kimmerobatis* and †*Asterodermus*) and †*Britobatos primarmatus*). As sclerorhynchoids phylogenetic position varies in different works: Kriwet (2004), places them as an intermediate group between Pristidae and Pristiophoridae. Claeson *et al.* (2013) recovers them as an intermediate group between the Jurassic genus †*Spathobatis* and Pristidae. Underwood & Claeson (2017) placed them within Rhinopristiformes.

Material

Institutional abbreviations

AMNH: American Museum of Natural History. BHN: Muséum d'Histoire Naturelle de Boulogne-Sur-Mer. BRC: Birkbeck Reference Collection. BSP: Bayerishe Staatssammling fur Paläontologie und Geologie, Munich, Germany. CNPE-IBUNAM: National Collection of Fishes, Biology Institute, Universidad Nacional Autónoma de México (UNAM). JM-SOS: Jura Museum Eichtätt, Germany. MNHN: Muséum national d'Histoire naturelle, Paris. NHMUK: Natural History Museum United Kingdom, London. UERJ: Universidade do Estado do Rio de Janeiro.

Material examined

Fossil material. †*Asflapristis cristadentis* (NHMUK PV P 73925, 75428 a-e, 75429 a-d*,* 75431, 75432, 75433). †*Asterodermus platypterus* (NHMUK PV P 12067, 10934, JM-SOS 3647). †*Belemnobatis morinicus* (BHN 2P1). †*Britobatos primarmatus* (MNHN

1946.18.94; NHMUK PV P 4015, 4016, 49517). †*Ischyrhiza mira* (AMNHFF 20388, Specimen figured in Sternes & Shimada 2018, Fig, 2 A-I). †*Kimmerobatis etchesi* (K874, K1894). †*Libanopristis hiram*: (NHMUK PV P 108705, 108706, 13858, 63610, 75075). †*Micropristis solomonis (*Cappetta (1980, pl. 1, fig. 1-4; pl. 2, fig. 1). †*Ptychotrygon rostrispatula* (NHMUK PV P73630, 75496, 75497, 75498, 75500). †*Shizorhiza stromeri* (Smith *et al*. 2015, text-fig. 1a-l; 2a-f; NHMUK PV P 73625). †*Sclerorhynchus atavus* (NHMUK PV P4017, 4776, 49546, 49518, 49533, 49547). †*Spathobatis bugesicus* (NHMUK PV P 6010, 2099 (2), BSP AS I 505, BSP 1952 I 82).

Extant material. *Amblyraja radiata* (BRC-Amblyraja, skeleton). *Aptychotrema vincentian*a (CT-Scan available in https://sharksrays.org). *Glaucostegus typus* (NHMUK 1967.2.11.3, CT-Scan). *Hydrolagus affinis* (BRC-*Hydrolagus*, skeleton). *Chimaera cubana* (CT-Scan available in https://sharksrays.org). *Gymnura altavela* (CT-Scan available in https://sharksrays.org). *Heptranchias perlo* (CT-Scan available in https://sharksrays.org). *Hexanchus nakamurai* (CT-Scan available in https://sharksrays.org). *Hypnos monopterygius* (CT-Scan available in https://sharksrays.org). *Irolita waitil* (CT-Scan available in https://sharksrays.org). *Mobula munkiana* (CT-Scan available in https://sharksrays.org). *Narcine brasiliensis* (CNPE-IBUNAM 9280, skeleton). *Narcine entemedor* (CNPE-IBUNAM 5807, CT-Scan). *Narcine tasmaniensis* (NHMUK 1961, CT-Scan). *Platyrhina* (BRC-*Platyrhina*, CT-Scan). *Platyrhinoidis triseriata* (MNHN 4329, CT-Scan available in https://sharksrays.org). *Pristis* (BRC-*Pristis*, CT scan). *Raja clavata* (BRC-*Raja*, CT-Scan). *Raja eglanteria* (CT-Scan available in https://sharksrays.org). *Rajella fyllale* (BRC-*Rajella*, skeleton). *Rhina ancylostoma* (NHMUK 1884, 1925, CT-Scan). *Rhinobatos glaucostigma* (CNPE-IBUNAM 17810, CT-Scan). *Rhinobatos horkelli* (UERJ 1397, skeleton). *Rhinobatos lentiginosus* (CNPE-IBUNAM 17827, CT-Scan). *Rhinobatos leucorhynchus* (CNPE-IBUNAM 1039, X-ray). *Rhinobatos percellens*

(UERJ 1240, skeleton). *Rhinobatos productus* (CNPE-IBUNAM 17829, CT-Scan; 17821 X-ray). *Rhinoptera bonansus* (BRC-*Rhinoptera,* skeleton; CT-Scan available in https://sharksrays.org). *Rhynchobatus djiddensis* (MNHN 7850, X-ray). *Rhynchobatus lübberti* (MNHN 50-22-04.80). *Rhynchobatus sp.* (BCR-*Rhynchobatus,* skeleton). *Tetronarce nobiliana* (CNPE-IBUNAM 9869, CT-Scan). Torpedo (NHMUK 72261). *Trygonorrhina fasciata* (MNHN 1372; BRC-*Trygonorrhina*, CT-Scan). *Urobatis jamaicensis* (AMNH 30385). *Urolophus aurantiacus* (CT-Scan available in https://sharksrays.org). *Urotrygon chilensis* (CT-Scan available in https://sharksrays.org). *Zanobatus sp.* (MNHN 1989.12.91, X-ray; CT-Scan available in https://sharksrays.org). *Zapteryx brevirostris* (UERJ-PMB 35, skeleton; UERJ 1234, 1237, skeleton). *Zapteryx exasperata* (CNPE-IBUNAM 17822, 17823, 17824, 17826, 17825, 20528, CT- Scan and skeleton). *Zapteryx xyster* (CNPE-IBUNAM 1666, 19790, CT-Scan & skeleton).

Methods

Phylogenetic analysis

A matrix of 37 taxa and 95 characters based on Aschliman and collaborators (2012a) analysis and characters from Brito & Seret (1996); McEachran *et al*., (1996); Brito & Dutheil (2004); Kriwet (2004); McEachran & Aschliman (2004); Claeson *et al*., (2013); Brito *et al*., (2013); Johanson *et al.,* (2013); Claeson (2014); Underwood & Claeson (2017), using reductive coding (Brazeau, 2011) was assembled in Mesquite 3.31 (Maddison & Maddison, 2018) (Appendix 4.1) and analysed on TNT 1.1 (Goloboff *et al*., 2013), PAUP (Swofford, 2001) and Mr. Bayes (Ronquist & Huelsenbeck, 2003) using CIPRES (Miller *et al.,* 2010). Aschliman's and collaborators observations were reviewed using extant material from different collections. In cases were extant material was not

available, published images (e.g. Nishida, 1990; Alfonso & Gallo, 2001; Domínguez & González-Arias, 2007; Claeson, 2010; Da Silva & De Carvalho, 2015) and electronic material (https://sharksrays.org, to access this image bank contact Gavin Naylor) were used. In cases were no image was available, the coding of the literature was retained. The sclerorhynchiod taxa included in this analysis are †*Libanopristis* Cappetta (1980b), †*Sclerorhynchus atavus* Woodward (1889a,b) as they are the species with the most complete skeletal remains of the group and the Turonian of Morocco taxa †*Asflapristis cristadentis* and †*Ptychotrygon rostrispatula*.

For the mapping of characters WinClada (Nixon, 2002) phylogenetic software was used, as reductive coding, could lead to ambiguous optimisation of characters, only those present in the unambiguous optimisation were considered when describing the synapomorphies for the clades.

Outgroup Justification

Representatives of the chimaerids and hexanchids were used as outgroups. Chimaerids were used to contrast the differences in ontogenic development and composition of the synarcual between these two groups (batoids and chimeras). As the presence of a synarcual cartilage is generally placed as a shared characteristic with batoids by previous analyses (e.g. Aschliman *et al.*, 2012a). Hexanchids where selected as they are usually place at the base of shark phylogenies (e.g. Naylor *et al.,* 2012) and present a contrasting morphology to that of batoids.

Parsimony

For the parsimony analysis in TNT, the menu interface was used (Appendix 4.3) with a similar search protocol to Mannion *et al*. (2013) which involves:

- A first search with new technology and the following parameters; search algorithm Ratchet with 10 initial add sequences (replications), 1000 random starting points and 1000 iterations of the perturbations phase (Appendix 4.3).

- A second search using the most parsimonious trees (MPT) found in the first search using tree bisection and reconnection algorithm (TBR) with 1000 random seed, 10000 replications and 10 trees saved per replication.

The objective of this protocol is to produce a set of MPT with a method that explores in a more complete way the space of possible trees (avoiding the island problem) in this case Ratchet. Those trees are used as a starting point for TBR analysis to gain extra arrangements of possible equally parsimonious trees or find even more parsimonious trees. The trees found in that search are used to produce a strict or majority rule consensus.

To compare the results obtained with TNT, a heuristic search with PAUP was performed with TBR as the swapping algorithm with the following parameters: 1000 random addition sequences.

To estimate the support of the groups in the parsimony analysis a Bootstrap and Bremer analyses were used. For the Bootstrap analysis the relative frequency values were used (GC value) (Goloboff *et al*., 2003), under these parameters the analysis includes groups with less than 50% of support.

Bayesian inference

The Bayesian analysis was performed using the Mk model for five million generations which resulted in a 50% majority-rule consensus. The selection of the parameters followed: (Dembo *et al*., 2015; Maztke & Wright, 2016; Bapst *et al*., 2016) (Appendix 4.2).

Datatype: What kind of data is being analysed (STANDAR = morphological traits).

Rates: Sets the model for character rate variation (gamma = rates were allowed to vary, permitting the model to estimate evolutionary rates for each character independently from a gamma distribution). Ratepr: This parameter allows you to specify the rates model between partitions (fixed, as there is only one partition (morphological) there was no need to vary across partitions). Samplefreq: Specifies how often the Markov chain is sampled in this case 1000. Printfr: How often information about the chain is printed to the screen (1000). Diagnfreq: number of generations between the calculation of MCMC diagnostics (2000). Nruns: Determines how many files from independent analyses will be summarized (4). Nchain: many chains are run for each analysis for the MCMC (Default setting = 4). Temp: Parameter for heating the chains. These parameters facilitate the change of states between the con and heated chains (Dembo *et al.,* 2015 recommendation = 0.2). relburnin: a proportion of the sampled values will be discarded (Default = yes). Burninfrac: proportion to be discarded (Defautl = 0.25) savebrlens=yes.

Character discussion

Literature: BS1996= Brito & Seret (1996); MD1998= McEachran & Dunn (1998); Kw2004= Kriwet (2004); AMC2012= Aschliman, McEachran & Claeson (2012); CUW 2013= Claeson *et al.* (2013). Br 2013= Brito *et al.* (2013).

1.   **Upper eyelid:** (0) present, (1) absent (AMC2012, char. 1).

2.   **Palatoquadrate:** (0) articulates with neurocranium, (1) does not articulate with neurocranium (AMC2012, char. 2; CUW2013, char. 16).

3.   **Pseudohyal:** (0) absent, (1) present (AMC2012, char. 3; CUW2013, char. 30. Outgroup and *Kimmerobatis* based on Underwood & Claeson, 2017).

4.   **Last ceratobranchial:** (0) free, (1) articulates (AMC2012, char. 4; CUW2013, char. 29).

5.   Synarcual product of lateral expansion of vertebral centra: (0) Absent, (1) Present (Modified from AMC2012, char. 5; CUW2013, char. 38 state).

The modification of this character from its binary coding (presence and absence), proposed by Aschliman *et al.* (2012a), char. 5 and Claeson *et al.* (2013), char. 38, follows observations made by Johanson *et al.* (2013) about the ontogenic development and composition of the synarcual: In holocephans (chimaeras) and placoderms, the synarcual is composed of the neural/basidorsal and haemal/basiventral elements with no evidence of involvement of free vertebral centra that characterize the batoids. The centra are replaced by arcocentra in placoderms and by notochordal rings in holocephalans.

6.   Calcified suprascapula: (0) absent, (1) present (Based on AMC2012, char. 6).
As the present study involves fossil species, states such as 'fused medially' and 'not fused medially' can be difficult to be defined in fossil taxa. The absence or presence of a cartilage connecting the antimeres of the scapulocoracoid of Jurassic batoids and sclerorhynchoids cannot be proven under current fossil data. The lack of preservation of this cartilage in these groups could be caused by the absence of mineralization in the whole cartilage. Embryological series of *Zapteryx brevirostris* shown a late calcification of this cartilage (Fig. 4.1) which could be the case for Jurassic batoids and sclerorhynchoids in which this tissue was not calcified.

†*Libanopristis* present a cartilage that resembles the suprascapula found in Raja. Regardless due to the damage observed in the specimen it was not possible to determinate if this cartilage is in fact the suprascapula, because of this Claeson *et al.* (2013) coding was kept for this.
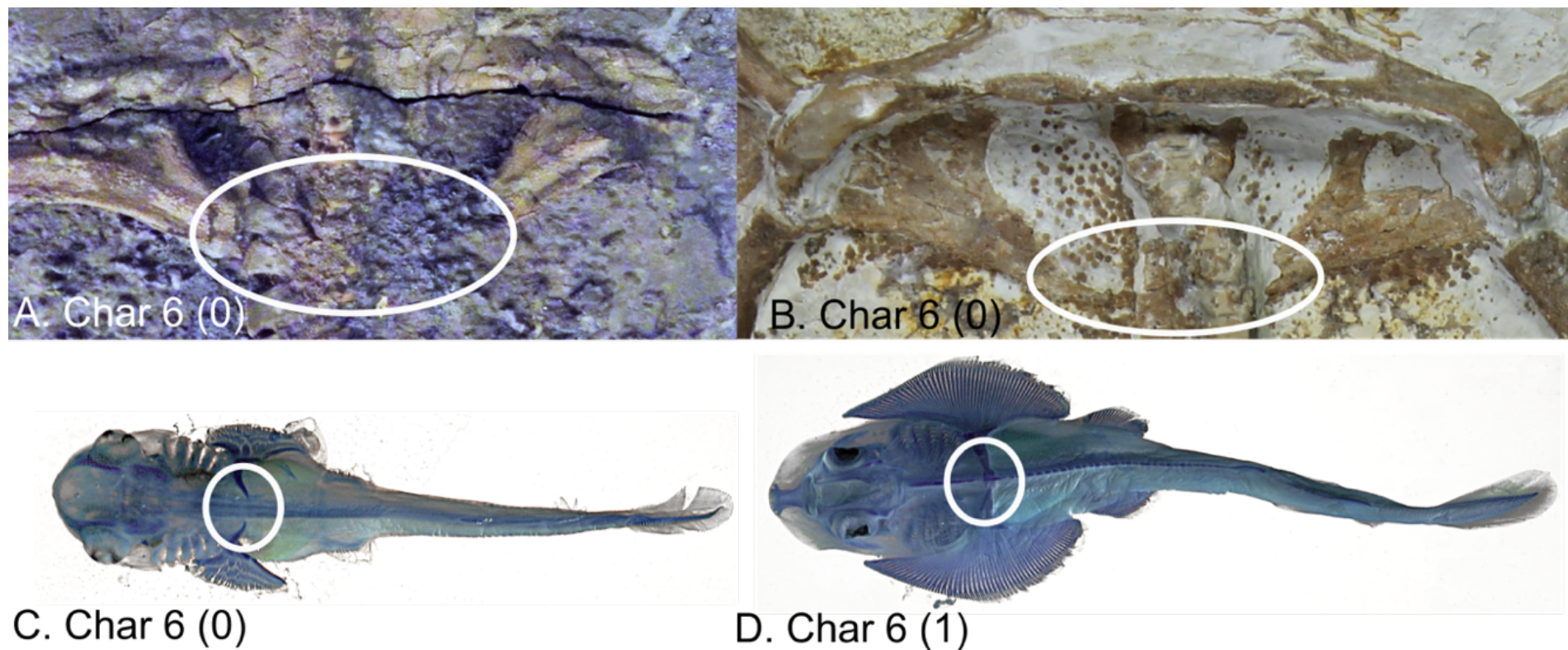
Figure 4.1. Suprascapula region of: **A,** †*Kimmerobatis etches*i (K874). **B**, †*Spathobatis bugesiacus* (PV P 10934). **C,** Early developmental stage of *Zapteryx brevirostris* (Unpublish data). **D,** Later developmental stage of *Z. brevirostris* (Unpublish data). Marked with a white ellipse is the suprascapula zone.

7. **Synarcual lip (Odontoid process):** (0) absent, (1) present (Modified from CUW2013, char. 39).

Aschliman *et al.* (2012a) coding for this character (char. 7: 'short or long'), was modified with the inclusion of fossils (Sclerorhynchoidei) in which the proper length of the structure might be difficult to observe. Besides this the use of quantitative characters as a qualitative character without a proper scale might be subjective. This coding also further differentiates the synarcual found in batoids from that of holocephans.

8. **Antorbital cartilage:** (0) absent, (1) present (CUW2013, char. 5).

9. **Antorbital cartilage:** (0) well-developed, triangular shaped with regular outline), (1) well-developed, variously shaped and with an irregular outline, (2) reduced, triangular shaped and with regular edges (Modified from CUW2013, char. 6).

Claeson *et al.* (2013) character 6 coding was modified, to provide a shared feature between Platyrhinidae and electric rays. Platyrhinidae present a triangular antorbital cartilage with an anterior and posterior processes giving it an irregular outline. The irregular outline is not observed in other batoids with the exception of some electric rays (e.g. *Narcine*).

10. **Cephalic lobes:** (0) absent, (1) present (AMC2012, char. 10).

11. **Cephalic lobes if separated from pectoral fin:** (0) single, (1) two lobes (Modified from AMC2012, char. 10).

Aschliman *et al.* (2012) character 10 multistate coding 'absent, single and two lobes', was separated in to two characters (10 & 11). Seeking to add grouping information regarding the presence of the cephalic lobes and the posterior modification of the lobes (single or double).

12. **Spiracular tentacle:** (0) absent, (1) present (AMC2012, char. 12).

13. **Radial cartilages in cauda fin:** (0) present, (1) absent (AMC2012, char. 13).

14. **Serrated tail sting:** (0) absent, (1) present (AMC2012, char. 14; CUW2013, char. 50).

15. **Placoid scales:** (0) absent, (1) present (Modified from AMC2012, char. 15; CUW2013, char. 51).

With the inclusion of fossils species whether the placoid scales are sparsely or uniformly present is difficult to observe. What has been recovered from this groups are disarticulated scales, so at least their presence or absence can be inferred.

16. **Alar and malar thorns:** (0) absent, (1) present (AMC2012, char. 17; CUW2013, char.48).

17. **Osteodentine:** (0) absent, (1) present (Modified from AMC2012, char. 19; CUW2013, char. 19).

18. **Osteodentine:** (0) present in some roots, (1) spread across the teeth (Modified from AMC2012, char. 19; CUW2013, char. 19).

The separation of this character in to two characters (17 & 18), is based on that the codification of three states without order assumes that the modification from one state to other is equivalent between all three (e.g. 0-2 = 1-0). Ignoring grouping information regarding the presence of Osteodentine.

19. **Infraorbital loop of suborbital and infraorbital canals:** (0) absent, (1) present (AMC2012, char. 21).

20. **Subpleural loop of the hyomandibular canal:** (0) broad rounded, (1) loop forms a lateral hook (AMC2012, char. 22).

21. Lateral tubes of subpleural loop: (0) unbranched, (1) branched (AMC2012, char. 23).

22. Abdominal canal on coracoid bar: (0) absent, (1) present (Modified from, AMC2012, char. 24).

23. Abdominal canal on coracoid bar: (0) groove, (1) pores (Modified from, AMC2012, char. 24).

As stated previously, the separation of this character in to two characters (22 & 23), seeks to increase the grouping information overseen by multistate unorder characters (i.e. this coding seeks to establish a previous shared state: presence or absence of the abdominal canals on coracoid bar. Which is followed, by the modifications to the shape of those canals if they are present).

24. Scapular loops of scapular canals: (0) absent, (1) present (AMC2012, char. 25).

25. Hypobranchials: (0) well developed, (1) reduced (new).

Character proposed with two states. It is based on observations from Myliobatiformes, which hypobranchials are reduced and fused (see Nishida 1990, Figs. 27 and 28 and Miyake 1991 Figs. 8 and 9).

26. Second hypobranchial-basibranchial: (0) free, they are separated from the basibranchial, (1) the second hypobranchial is fused with the basibranchial (†*Sclerorhynchus* and †*Ptychotrygon* present a second hypobranchial fused with the basibranchial (Fig. 4.2), (2) second hypobranchial is articulated with the basibranchial (Modified from MD1998, char. 4).

Character modified form McEachran & Dunn (1998) char. 4, to include the state observed in the outgroup Hexanchidae (0).
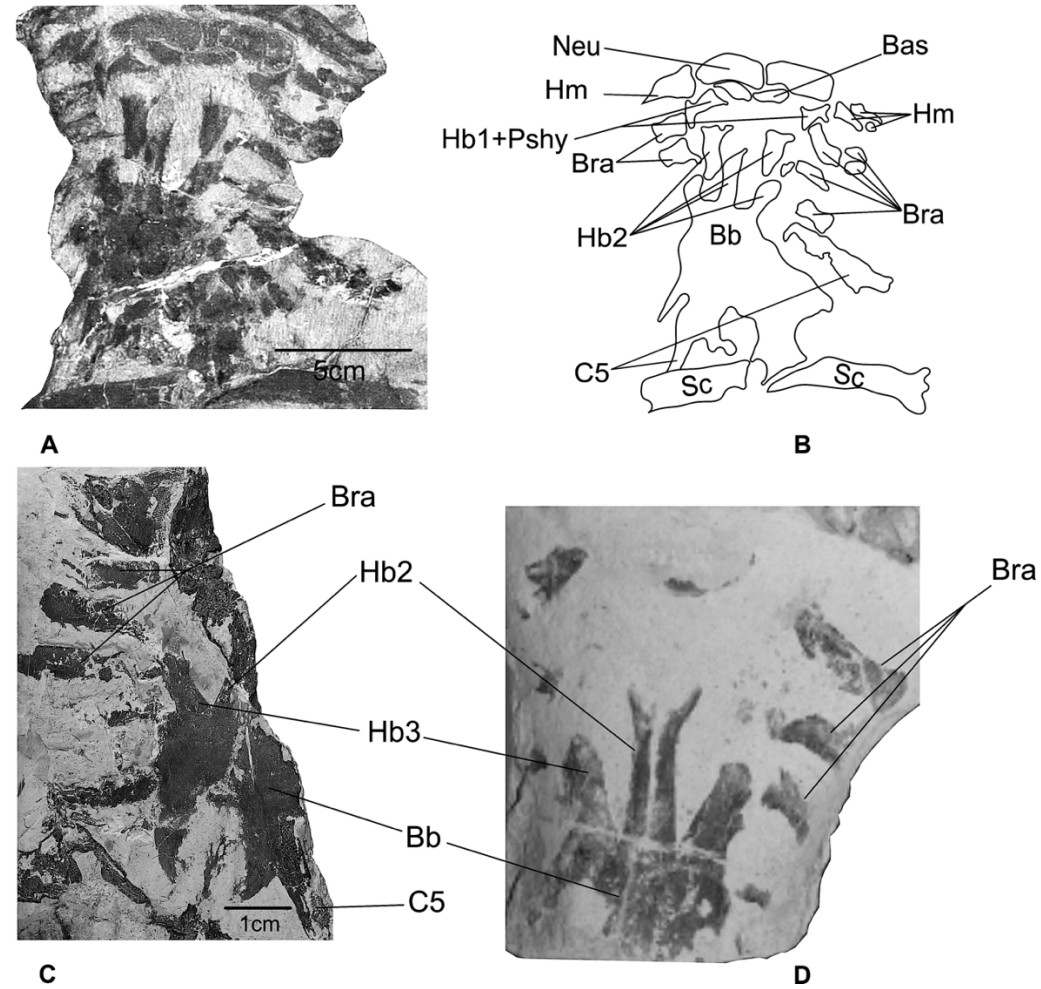
Figure 4.2. Branchial skeleton of sclerorhynchoids (Char 26 (1)). **A-B** and **D**, †*Ptychotrygon rostrispatula* (NHMUK PV P 73630, 75500). **C,** †*Sclerorhynchus atavus* (NHMUK PV P 49546). **Abbreviations**: Bb, basibranchial; Bas, basihyal; Bra, branchial elements; 5C, fifth ceratobranchial; Hb1, first hypobranchial; Hb2, second hypobranchial; Hb3, third hypobranchial; Hm, hyomandibula; Pshy, pseudohyal: Sc, suprascapula.

27. **Rostral cartilages:** (0) absent, (1) present (Modified form AMC2012, char. 26 and UC2017, char. 1).

28. **Rostral cartilages:** (0) reach the tip of the snout, (1) fail to reach the tip of the snout (Modified form AMC2012, char. 26; CUW2013, char. 1; UC2017, char 1 & 2).

The separation of this character in to two: 27-28. Is based, in that previous unordered multistate codifications (e.g. UC2017, character 1: stout, filamentous, absent and subtriangular), considered the modification from one state to another equivalent among all three states, losing grouping information regardless of the presence of rostral cartilages, (i.e. Regardless the 'subtriangular' shape rostral cartilages in *Platyrhina* and *Platyrhinoidis*, they are present and represent shared feature with other groups). Furthermore, UC2017 coding unintentionally weights character as the absence in character 1 (stout, filamentous, absent and subtriangular) is linked to the absence of character (complete, fail to reach tip of the snout and absent).

Claeson (2014) recognises two characters related to the rostral cartilages in Torpediniformes (Char. 48. Median rostral cartilage: (0) trough-shaped and expanded; (1) slender; (2) inconspicuous or absent; Char. 49. Lateral rostral cartilages: (0) absent; (1) articulated with nasal capsule; (2) continuous with chondrocranium). The present characters (27-28) correspond to what Claeson (2014) describes as median rostral cartilages (char. 48). The coding for Hypnos, Temera and Torpedo was changed from Aschliman's observations following the review of the specimens and Claeson (2010; 2014) observations. The codification of character 28 for †*Kimmerobatis* Underwood & Claeson (2017) was changed as the tip of the rostrum is missing (?).

29. **Rostral node:** (0) not expanded laterally, (1) expanded laterally (AMC2012, char. 27).

30. **Rostral appendices:** (0) absent, (1) present (AMC2012, char. 28; CUW2013, char. 3).

31. **Rostral appendices:** (0) calcified, (1) poorly calcified (new).

Based on observations of extant species: In rajids although being present the rostral appendices are a really thin sheet of cartilage almost transparent whereas for example in Rhinopristiformes these cartilages are thicker and often preserved in fossil remains (Fig. 4.3).

In *Platyrhina* and *Platyrhinoidis*, the rostral appendix is replaced by the rostral processes (-). In Myliobatiformes this structure is absent but whether or not it is present in early developmental stages is unclear and requires further study, as such it was code as missing (?).
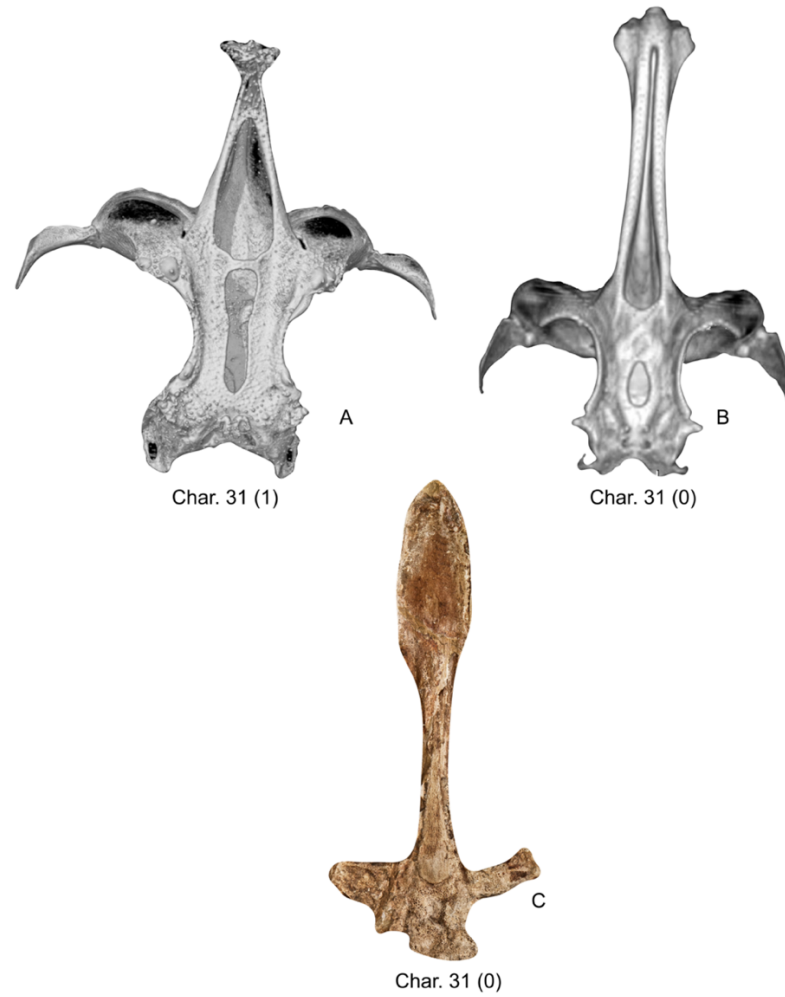
Figure 4.3. Neurocranium of: **A,** *Raja clavata* (BRC-Raja) (rostral appendix poorly calcified). **B,** *Rhinobatos productus* (CNPE-IBUNAM 17829) (rostral appendix calcified). **C,** †*Spathobatis bugesiacus* ((NHMUK PV P 6010) (rostral appendix calcified).

32.   **Rostral process:** (0) absent, (1) present (AMC2012, char. 29).

33.   **Dorsolateral components of the nasal capsule:** (0) absent, (1) present (AMC2012, char. 30).

34.   **Nasal capsules:** (0) laterally expanded, (1) ventrolaterally expanded (AMC2012, char. 3; CUW2013, char. 10).

35.   **Preorbital process:** (0) present, (1) absent (AMC2012, char. 33).

36.   **Supraorbital crest:** (0) present, (1) absent (AMC2012, char. 34; CUW2013, char. 11).

37.   **Anterior preorbital foramen:** (0) dorsally located, (1) anteriorly located (AMC2012, char. 35).

38.   **Postorbital process:** (0) narrow in otic region, (1) absent, (2) broad and shelf like (AMC2012, char. 36).

39.   **Postorbital process:** (0) separated from triangular process, (1) fused with triangular process (AMC2012, char. 37).

40.   **Postorbital process:** (0) projects laterally, (1) projects ventrolaterally (AMC2012, char. 38).

41.   **Antimeres of upper and lower jaws:** (0) separated, (1) fused (AMC2012, char. 40).

42.   **Meckel's cartilage:** (0) not expanded laterally, (1) expanded medially (AMC2012, char. 41).

43.   **Winglike process on Meckel's cartilage:** (0) absent, (1) present (AMC2012, char. 42).

44.   **Labial cartilages:** (0) present, (1) absent (AMC2012, char. 43; CUW2013, char. 17).

45. **Medial section of hyomandibula:** (0) narrow, (1) expanded (AMC2012, char. 44).

46. **Hyomandibula-Meckelian ligament:** (0) absent, (1) present (AMC2012, char. 45).

47. **Small cartilages associated with hyomandibular-Meckelian ligament:** (0) absent, (1) present (AMC2012, char. 47).

48. **Basihyal:** (0) absent, (1) present (Modified from, AMC2012, char. 48; CUW2013, char. 27).

49. **First hypobranchial:** (0) absent, (1) present (Modified from, AMC2012, char. 48; CUW2013, char. 27).

Previous codifications place both basihyal and first hypobranchial together and then codify for the presence or absence of one or the other independently (i.e. AMC2012, char. 48 and CUW2013, char. 27; Basihyal and first hypobranchial: (0) both present and unsegmented, (1) basihyal segmented, (2) basihyal absent and (3) basihyal and first hypobranchial absent. Suggesting independence among these structures, as such they here were coded as separate characters (48-49).

50. **Ceratohyal:** (0) fully developed, (1) reduced (AMC2012, char. 49; CUW2013, char. 28).

51. **Suprascapula-axial skeleton:** (0) free of vertebral column, (1) articulates with vertebral column, (2) fused medially to synarcual, (3) fused medially and laterally to synarcual (CUW2013, char. 40).

52. **Lateral stays:** (0) absent, (1) present (New).

This coding further differentiates the synarcual found in batoids from that of holocephans in which the synarcual does not present lateral stays.

53. **Orientation of lateral stays:** (0) dorsally directed, (1) laterally directed (Torpediniformes, and Platyrhinidae) (Modified from AMC2012, char. 51).

The lateral stay in *Pristis* were previously coded as posteriorly directed. But in this species these gracile processes are also dorsally orientated (Fig. 4.4). More peculiar is that *Pristis* lateral stays are composed by two parts a blunt base with a very similar "V" shape to the one present on myliobatiods, rajoids and guitarfishes which articulates to a slender and gracile cartilage that is posterodorsally directed.

The coding for Platyrhinidae was also modified as their lateral stays are far more open than other "guitarfishes" and even present a flat surface on top of them similar to some electric rays Fig. 4.4).
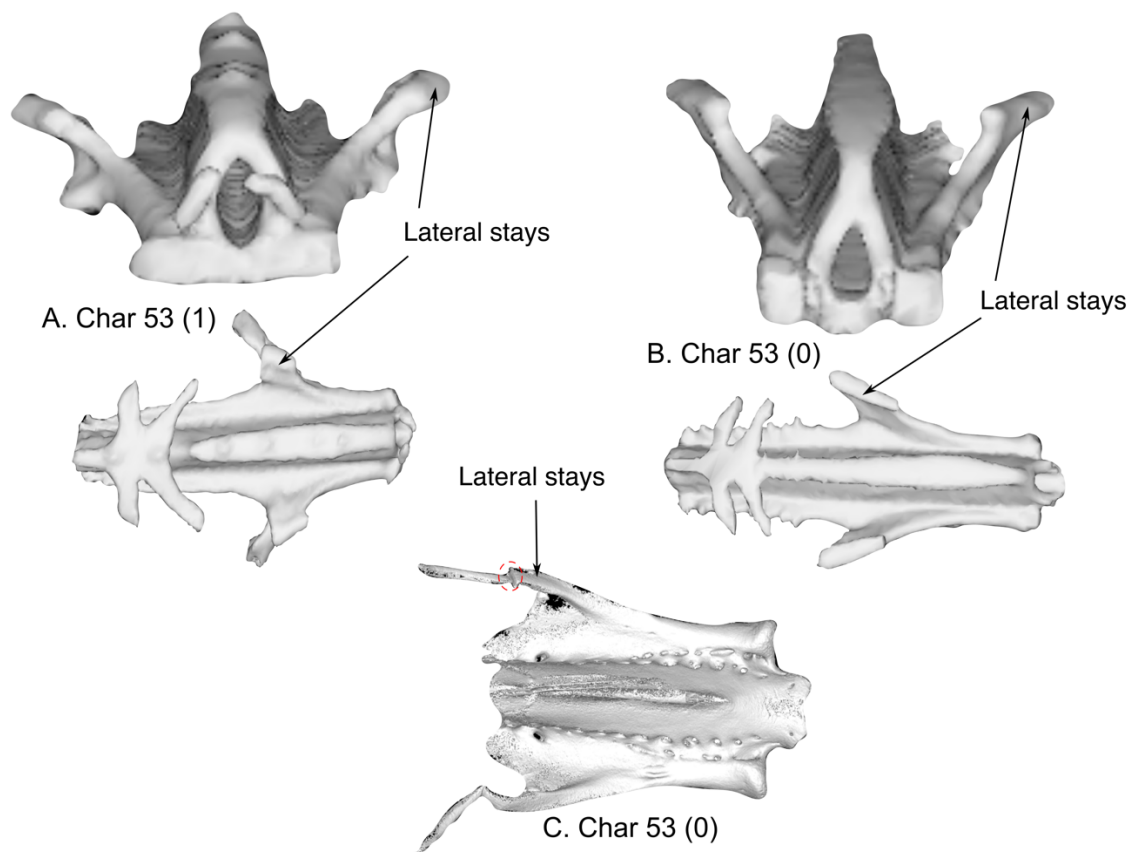
Figure 4.4. Synarcual comparison between: **A,** *Platyrhinoidis triseriata* (lateral stays, laterally directed). **B,** *Rhinobatos lentiginosus* (CNPE-IBUNAM 17827) (lateral stays, dorsally directed). **C,** *Pristis sp.* (BRC-*Pristis*, CT scan) (lateral stays, dorsally directed). Lateral stays signal with arrows. Red circle indicates extra cartilage of *Pristis.*

115

54.   Ventral occipital articulation: (0) synarcual lip fitted into notch in basicranium, (1) synarcual lip rest in foramen magnum (AMC2012, char. 52).

55.   Second synarcual: (0) absent, (1) present (AMC2012, char. 54).

56.   Scapular process: (0) short, (1) long (AMC2012, char. 56).

57.   Scapular process: (0) without fossa, (1) with fossa (AMC2012, char. 57).

58.   Scapulocoracoid condyles: (0) not horizontal, (1) horizontal (AMC2012, char. 58).

59.   Mesocondyle: (0) equidistant, (1) Scapulocoracoid is elongated between the mesocondyle and metacondyle, (2) Scapulocoracoid is elongated between the procondyle and the mesocondyle, (3) replaced with a ridge (AMC2012, char. 59; CUW2013, char. 43).

60.   Anterior extension of propterygium: (0) pectoral propterygium fails to reach anterior margin of disc, (1) extends to near the anterior margin of the disc (AMC2012, char. 62).

61.   Segmentation of propterygium: (0) fails to surpass the mouth, (1) proximal segment extends beyond the mouth (Modified form, AMC2012, char. 63).

The modification of this character seeks to increase grouping information and reduce errors in the interpretation of this character in fossil species. Some of the species coded in Aschliman *et al*. 2012 (Char 63, 3) are erroneous (*Urolophus, Urotrygon* and *Urobatis*) as further review for this character is needed but they seem to present a similar state to that of (*Mobula* and *Myliobatis*) in which the segmentation reaches the anterior margin of the antorbital cartilage.

62.   Proximal section of propterygium: (0) does not surpass the procondyle, (1) extends behind procondyle (AMC2012, char. 64).

63.   **Pectoral fin radials:** (0) articulate to pterygia, (1) some articulate directly with scapulocoracoid (AMC2012, char. 65; CUW2013, char. 43).

64.   **Mesopterygium:** (0) present, (1) absent (CUW2013, char. 45).

65.   **Pectoral fin radials:** (0) not expanded distally, (1) some pectoral fin radials expanded distally (AMC2012, char. 67).

66.   **Paired fin rays:** (0) aplesodic, (1) plesodic (AMC2012, char. 68).

Aschliman's coding for this character is corrected. Few dissections of pristids (sawfishes) are available in the literature, but the present coding follows observations made by Da-Silva & De Carvalho (2015, Fig. 19).

67.   **Puboischiadic bar:** (0) plate like, (1) is narrow and moderately to strongly arched without distinct lateral process narrow (2) strongly arched with a triangular medial prepelvic process narrow, (3) moderately arched with a bar like medial prepelvic process (CUW2013, char. 46).

Reductive coding was not used in this character, as mostly focuses on modifications occurring in the puboischiadic bar in Myliobatiformes. Because the group was already established by other characters, the coding for this feature was kept as in the literature. For the remaining groups on the present analysis the puboischiadic bar is plate like (0).

68.   **First pelvic radial:** (0) band like, (1) slightly expanded distally, articulating with several segments in a parallel fashion, (2) rod-like and articulates with a single radial segment (AMC2012, char. 71).

69.   **Pelvic girdle condyles:** (0) close together, (1) separated (AMC2012, char. 72).

70.   **Clasper length:** (0) short, (1) long (AMC2012, char. 73).

71.   **Dorsal margin clasper cartilages:** (0) lacks medial flange, (1) possesses medial flange (AMC2012, char. 75).

72.   Cartilages forming component claw: (0) present, (1) absent (AMC2012, char. 77).

73.   Ventral terminal cartilages: (0) simple, (1) ventral terminal cartilages are free distally and forms components sentinel or is fused with ventral marginal cartilages, (2) ventral terminal cartilages folded ventrally along its long axis to form a convex flange

Reductive coding was not used in this character, as I was only able to observe a few specimens (Rajidae) and could not contrast Aschliman's observations. Because of this the codification of the character was kept as in the literature.

74.   Ventral terminal cartilages: (0) attached over length to axial cartilages, (1) free of axial (AMC2012, char. 79).

75.   Caudal vertebrae: (0) diplospondylus (1) fused (AMC2012, char. 80).

76.   Ligamentous sling on Meckel's cartilage: (0) absent, (1) present (AMC2012, char. 83).

77.   Depressor mandibularis: (0) present, (1) absent (AMC2012, char. 84).

78.   Spicularis: (0) undivided, (1) divided (AMC2012, char. 85).

79.   Coracobrachialis: (0) consists of three to five components, (1) single component (AMC2012, char. 87).

80.   Coracohyomandibularis: (0) single origin, (1) separate origins (AMC2012, char. 88).

81.   Arcualia dorsalis: (0) absent, (1) present (Modified from Br2013 char.30)

These extra sets of cartilages between the synarcual and the chondrocranium were first described as a synapomorphy of *Zapteryx brevirostris* and the fossil species †*Stahlraja sertanensis* by Brito *et al.* (2013). However further review showed that these cartilages are also present in *Platyrhina* and *Platyrhinoidis* (Nishida, 1990, Fig. 7 F-H), further observations to NHMUK and CNPE (Mex) specimens proved Nishida's observations

and added the remaining species of *Zapteryx* along with *Trygonorrhina* and *Aptychotrema* to the list of extant taxa with these cartilages.

82. **Vertebra centrum in the synarcual:** (0) entire length, (1) reaches half of the length, (2) less than half of the length (new).

This character is proposed with three states. The centra of some vertebra can be observed in the ventral surface of the synarcual or by sagittal sectioning it. The depth to which these structures can be found within batoids varies. In the all the Jurassic batoids and *Platyrhinoidis* fully formed vertebral centra can be observed through most of the synarcual length (0). In *Narke, Rhynchobatus, Glaucostegus, Rhina, Rhinobatos, Zapteryx, Trygonorrhina, †Britobatos*, the centra reach the middle of the synarcual (1). In the rest of batoids in the present study the centra fail to reach the middle of the synarcual (2) (fig. 4.5).
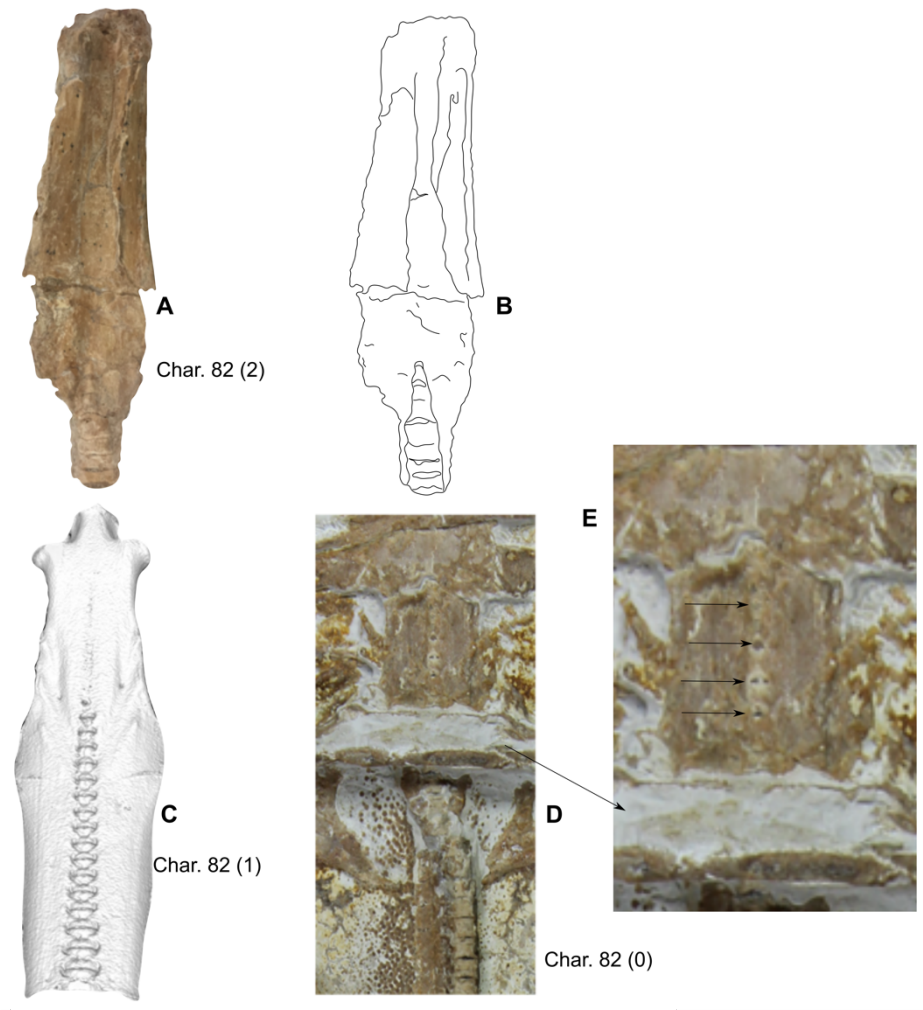
Figure 4.5.Synarcual of: **A**, †*Asflapristis cristadentis* (NHMUK PV P75431). **C**, *Glaucostegus typus* (NHMUK 1967.2.11.3). **D**, †*Spathobatis bugesiacus* NHMUK PV P 2099.   **E**, magnification of the top region of the synarcual of †*Spathobatis*. The vertebra centra marked with arrows.

83. **Nasal capsule margin:** (0) Straight, (1) horn-like process (CUW2013, char. 9).

84. **Parallel rows of enlarged denticles:** (0) absent, (1) present (CUW2013, char. 49).

85. **Ventral antimeres of scapulocoracoid:** (0) fused, (1) separate (new).

Character proposed with two states. The ventral part of the suprascapula is not fused in juveniles of Platyrhinidae and juveniles and adults of Torpediniformes. In the remaining taxa these cartilages are fused (0). In Platyrhinidae the antimeres are fused later in their development (0,1) (Fig. 4.6)
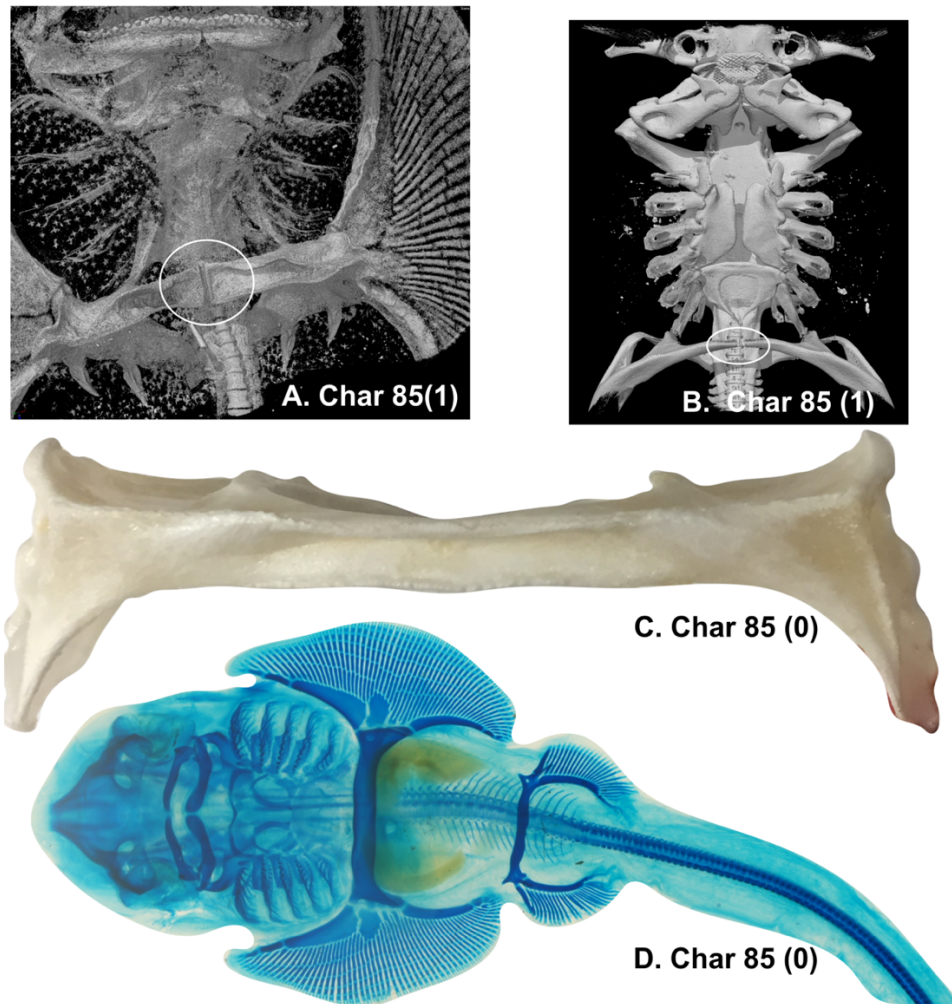
Figure 4.6. Ventral surface of pectoral girdle: **A**, Juvenile of *Platyrhinoidis triseriata* (MNHN 4329); **B**, Adult of *Narcine* (NMHUK 1961). **C**, Adult (CNPE- IBUNAM 20528) and **D**, Juvenile of *Zapteryx*. Ventral articulation zone of the antimeres of the pectoral girdle marked with a white ellipse.

86.   Suprascapula-scapula: (0) curved, (1) crenate/long, (2) crenate/short, (3) ball socket, (4) straight (Modified from AMC2012, char. 53).

There are different types of articulation between the suprascapula and scapula. The suprascapula in Trygonorrhinidae presents a short indentation where the distal edges of the scapula fit and articulate (2). In *Rhinobatos, Rhynchobatus, Rhina, Pristis* (state in *Pristis* see Compagno 1977, Fig. 11) and Platyrhinidae the suprascapula present a deep indentation where the distal edges of the scapula fit and articulate (1). In Rajiformes the scapulocoracoid presents a cotyle for the articulation of the condyle of the suprascapula (0). In Torpediniformes the articulation between these two cartilages is straight and lack of any process (4). Myliobatiformes presents the ball socket articulation (3).

87.   Differentiated lateral uvulae on teeth: (0) absent, (1) present (CUW2013, char. 22).

88.   Anterior projection of second hypobranchial: (0) present, (1) absent (MD1998, char. 5).

89.   Anterior projection of second hypobranchial (if present): (0) present/no loop (1) present/loop (BS1996, char. 41).

90.   Rostral dermal denticles: (0) absent, (1) present (Modified from Kw2004, char. 52).

The coding of this character was modified to increase the grouping possibilities within sclerorhynchoids as the present study included two genera: †*Ptychotrygon rostrispatula* and †*Asflapristis cristadentis,* that so far does not present evidence of the rostral denticle series.

91.   Enlarged rostral dermal denticles series: (0) one, (1) two or more (new, see Welten *et al*., 2015, figs 8-9.).

Based on observations made by Welten *et al.,* (2015) this character is proposed with two states (0 = absent and 1 = two or more). Some sclerorhynchids, Pristiophoridae and Pristidae present rostral cartilages with rostral spines. Pristidae present a single lateral series (1). †*Libanopristis,* †*Sclerorhynchus,* †*Micropristis* and Pristiophoridae (not included in the present analysis) present at least two series of rostral spines one on the side of the rostral cartilages, at the sides of the head and in the ventral surface of the rostral cartilages, with the difference that in sclerorhynchoids the ventral series are on the middle and lateral portions of the rostrum (Fig. 4.7 A-B, 1-4), whereas in Pristiophoridae is only on the sides. For the remaining taxa in the analysis this state is (0).
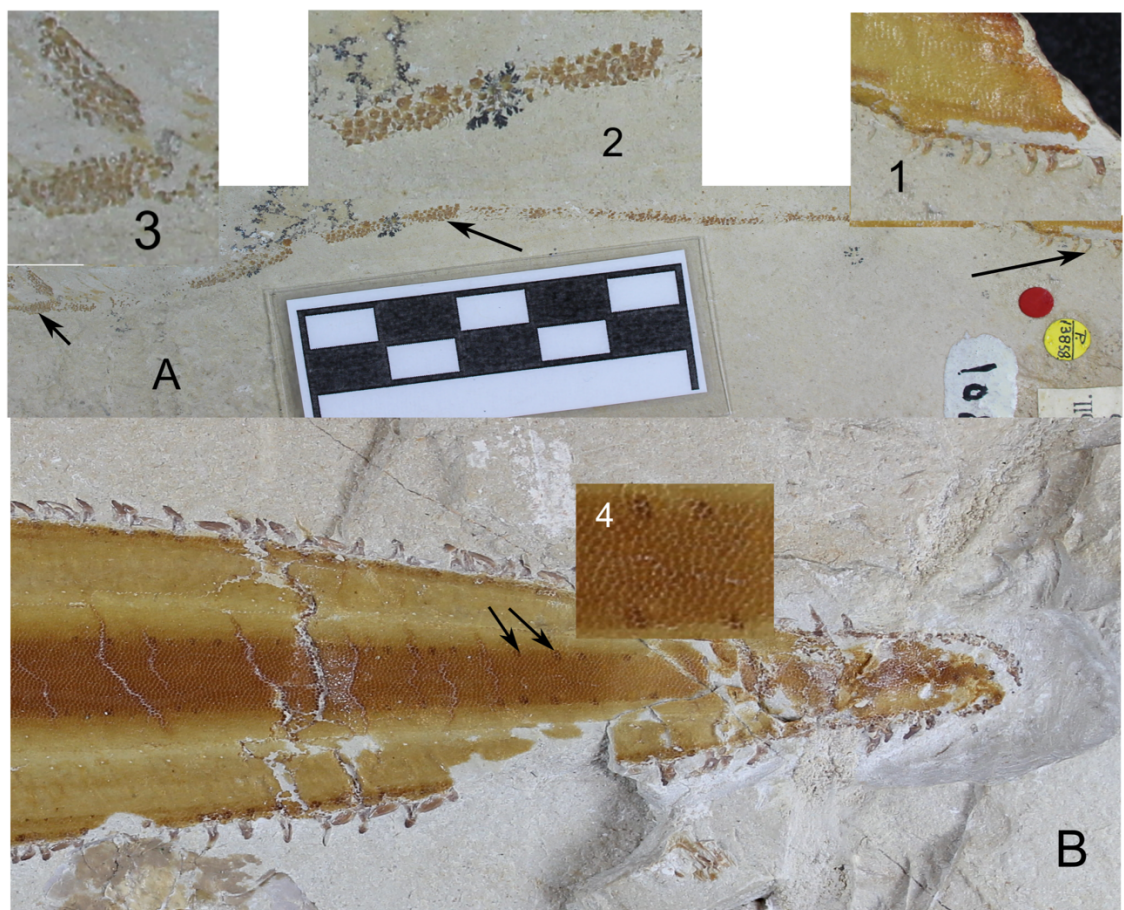
Figure 4.7. A-B, Rostral cartilage of †*Libanopristis hiram* (NHMUK PV P 13858; 75075). Different enlarge denticle series signal with arrows, expanded and marked with numbers : 1. Rostral series, 2. Lateral cephalic series, 3. Normal denticles, 4. Base of denticles in the ventral series.

92.   **Proximal pectoral elements expanded (propterygium, mesopterygium, metapterygium) distally and paddle-like:** (0) absent (1) present (Modified from Kw2004, char 39).

Not to be confuse with Kriwet (2004) char. 39 and Aschliman *et al.* (2012) char. 67 which seems to be refereeing to the presence of some fin radials in the propterygium which are expanded and articulate with the surface of adjacent radials (see Nishida, 1990, Fig. 34). This character has not been observed in sclerorhynchoids so far and is coded as character 65 in the present study (Fig. 4.8).
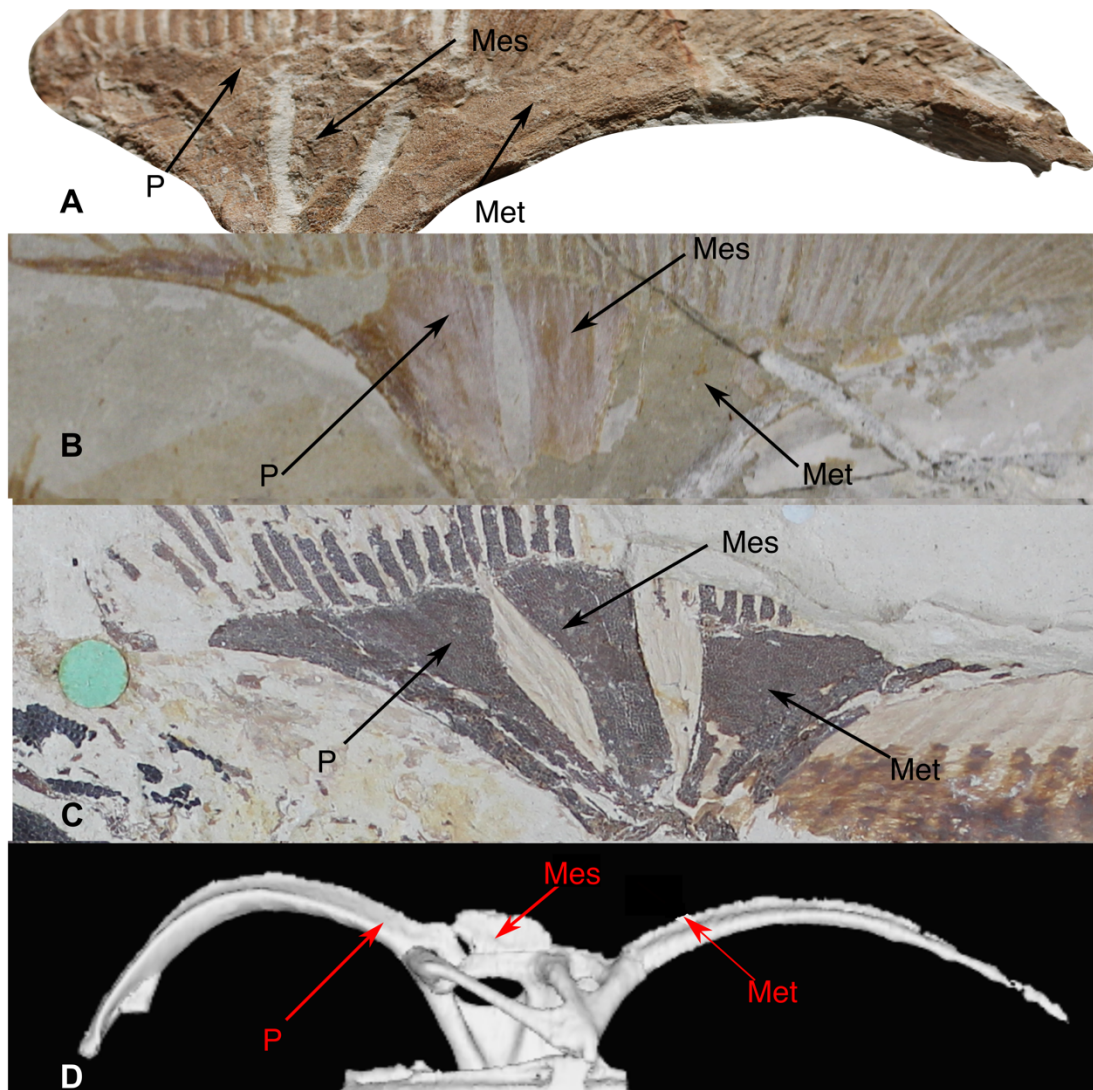
Figure 4.8. Proximal pectoral elements of: **A**, †*Ptychotrygon rostrispatula* NHUMK PV P 73630. **B**, †*Libanopristis hiram* NHUMK PV P NHMUK PV P 75075. **C**, †*Sclerorhynchus atavus* NHUMK PV P 46547, Char. 92 (1); **D**, *Gymnura*, Char. 92 (0). **Abbreviations**: P, Propterygium; Mes, Mesopterygium; Met, Metapterygium.

93. **Propterygium-mesopterygium:** (0) differently shaped, (1) similarly shaped (new).

All Jurassic batoids included in the present study presented an enlarged mesopterygium anteriorly projected in a similar fashion as the propterygium (Fig. 4.9A-B). In the remaining taxa the propterygium is curved and thin and differently shaped to the metapterygium (Fig, 4.9C). In sclerorhynchoids the propterygium are expanded distally and present a process that runs parallel to the body axis, the mesopterygium trapezoid shaped and lacks any process (Fig. 4.8 A-C).
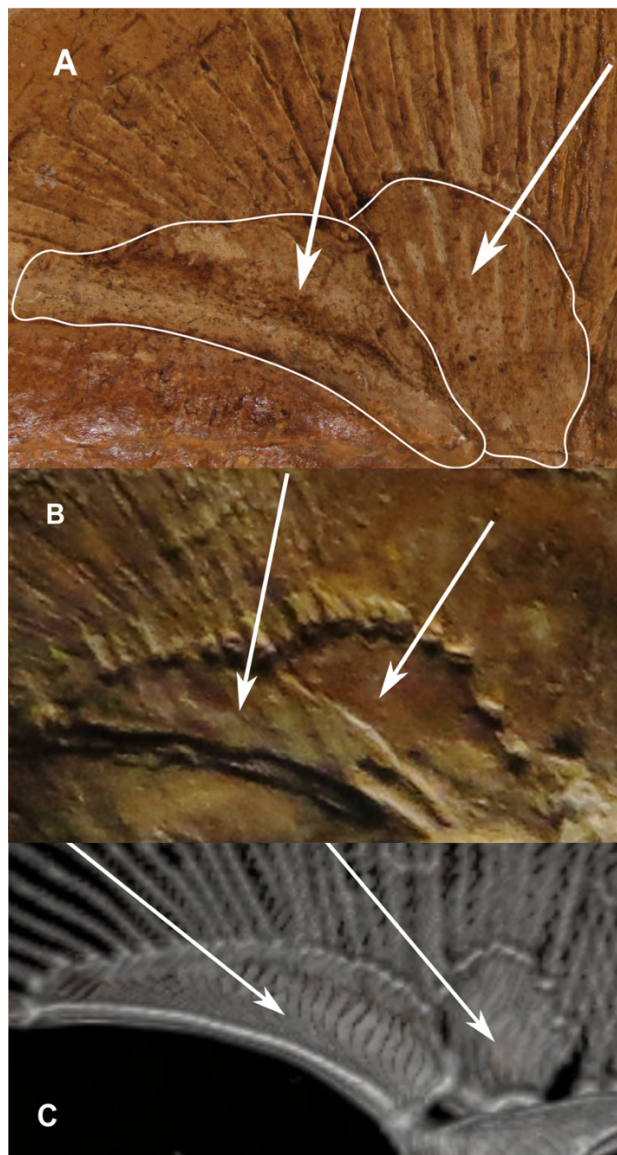
Figure 4.9. Propterygium and Mesopterygium of: **A,** †*Spathobatis bugesiacus*. **B,** †*Belemnobatis sismondae*, Char. 93 (0). **C,** *Zapteryx exasperata*, Char. 93 (1). Propterygium and Metapterygium marked with arrows.

94.   Branchial electric organs: (0) absent, (1) present (AMC2012, char. 86).

95.   Lateral prepelvic process: (0) absent, (1) present (Modified from MD1998 char. 36).

The modification of this character from the multistate coding used in McEachran and Dunn (1998; char. 36), is based on that the three states proposed by the authors (i.e. short, to moderately long, extremely long with acute tips and extremely long with biramous tips) are difficult to interpret in the fossil specimens. Because of this a binary annotation (presence and absence) was used.

Results

Phylogenetic analysis

The TNT analysis resulted in 12 MPT's (most parsimonious trees) of 183 steps. The PAUP search, resulted in 100 MPT's of the same length. The analyses in PAUP and in TNT analyses resulted in the same strict consensus tree (Figs 4.11) with values of Consistency Index = 0.59, Retention Index = 0.85.
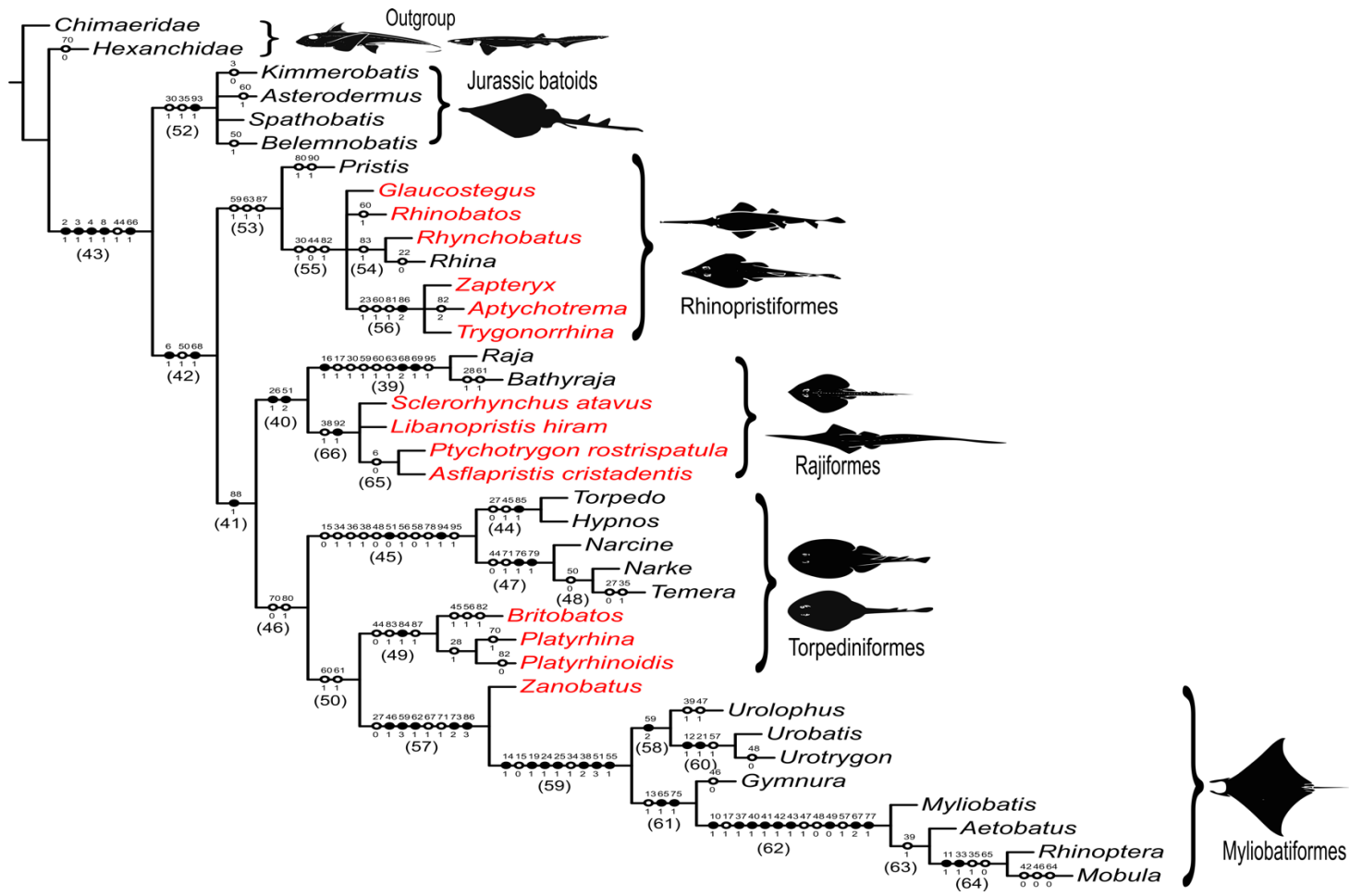
Figure 4.10. Character mapped on strict consensus tree obtained in the parsimony analyses. Characters were mapped in WinClada (Nixon, 2002). Number in parenthesis are the nodes. Non-homoplastic synapomorphies represented by black points, character number is on top and state of character in on bottom. White circles are relevant characters with a consistency index < 1.00 (homoplastic synapomorphies). In red taxa with Rhinobatoid-like shape (i.e. strong tail and well-developed pectoral disk).

127
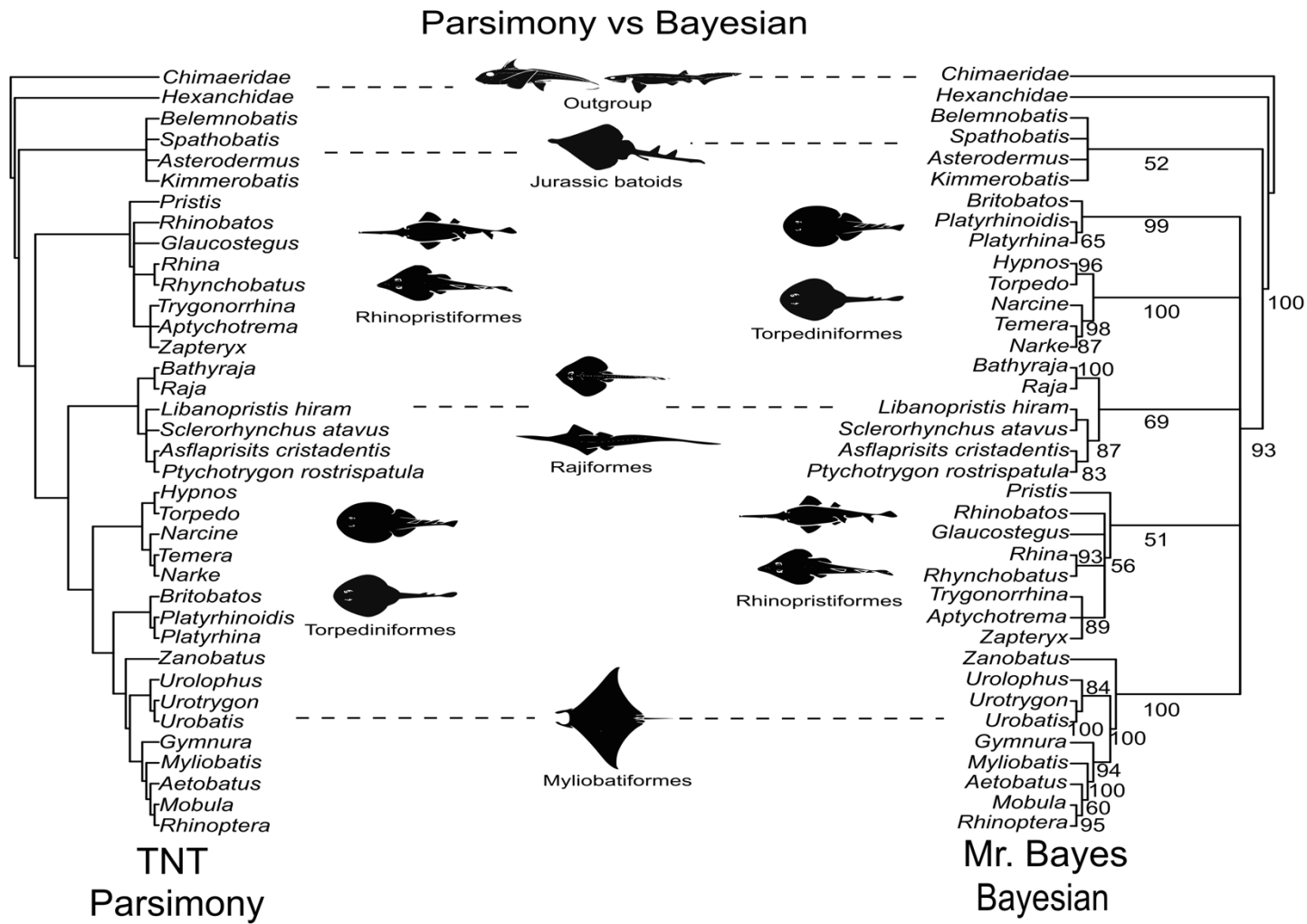
Figure 4.11. Phylogenetic trees obtained on the different analysis: Strict consensus from parsimony analysis compared to Posterior probability tree from Bayesian inference.
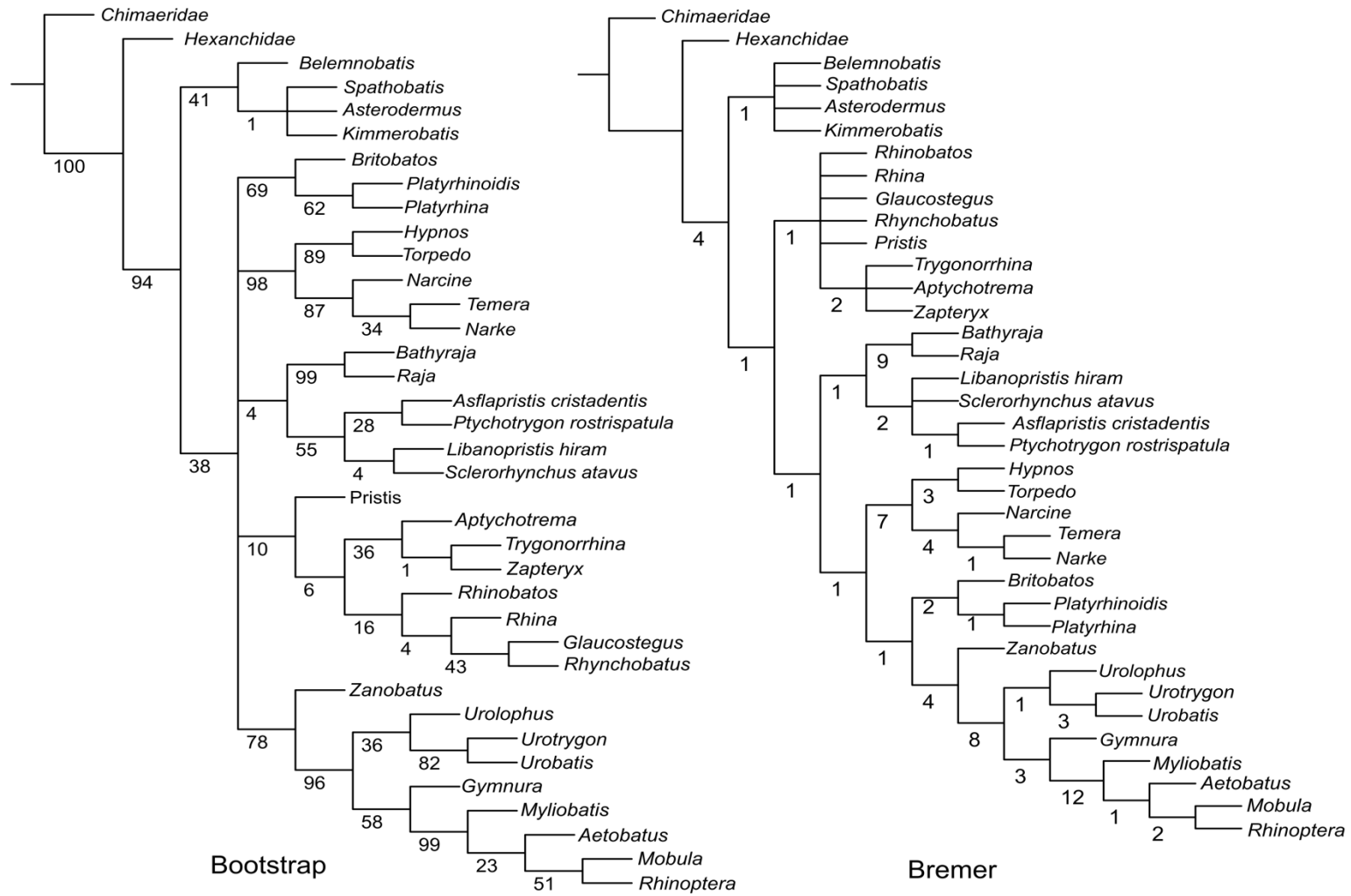
Figure 4.12. Topologies recovered from the clade support analyses. **A,** Bootstrap analysis with the relative frequency (Goloboff, 2003) of the clades. **B,** Bremer analysis.

129

Phylogenetic analysis

All of the phylogenetic analyses recovered the Jurassic genera †*Asterodermus,* †*Kimmerobatis,* †*Spathobatis* and †*Belemnobatis* as poorly supported clade (Node = 52, Bremer = 1, Bootstrap= 41, Posterior probability (Pp) = 52%), sister group to the remaining batoids. Node 52 presents one unambiguous synapomorphy (Char. 93) which refers to the similarity in the shape between propterygium and mesopterygium (Fig. 4.10). The placement recovered by the present analysis differs from that of previous phylogenies (Claeson *et al*., 2013; Underwood & Claeson, 2017) which placed the Jurassic batoids within modern batoids in a close relation with Rhinopristiformes. Our results suggest that their similarity with Rhinopristiformes is superficial. All remaining batoids included in the present study are grouped in node 42 which is characterised by the presence of a calcified suprascapula (Char. 6), a reduced ceratohyal, (Char. 50) and the shape of the first pelvic radial (Char. 68)

The placement of the remaining groups of batoids varied depending on the analysis. These different topologies reflect the variation in the methods of reconstruction. The bayesian analysis found a polytomy that comprises all of the modern orders (Naylor *et al.,* 2012) and remaining groups (Fig. 30). Whilst, in the parsimony analysis recovered a more resolved tree (O'Reilly *et al*., 2016).

Rhinopristiformes forms a sister relationship with the remaining taxa in the Parsimony analysis (Fig. 4.11). Its placement as the sister group of remaining batoids, is supported by the presence an anterior projection of the second hypobranchial (Char. 89, 0). However, the coding of the character requires further work, as in *Pristis* the hypobranchials are fused in a plate (Nishida, 1990, fig. 28g), and during their ontogenetic development the medial plate is divided in two (Miyake & McEachran, 1991, Fig. 5). The

anterior process of the second hypobranchial could be involved in the development of the upper plate but this cannot be clearly demonstrated due to the lack of material available. As a result of this, *Pristis* was coded as "?". In the remaining batoids, there seem to be different and non-homologous processes leading to the loss of this structure which could be coded as separate characters. In electric rays there seems to be several arrangments of the hypobranchials (Miyake & McEachran, 1991, Fig. 6) and for Myliobatiformes there seems to be a reduction and fusion of branchial elements (Nishida, 1990, Figs. 27-28)

The placement of *Pristis* with other Rhinopristiformes has only recently been recovered in molecular analysis. Although this grouping is present in all the analyses (Node = 53, Bremer = 1, Bootstrap= 10, Pp = 51%) (Figs. 4.10-4.11), the present study did not find an exclusive synapomorphy for Rhinopristiformes, but rather this clade is supported by a combination of characters (e.g. Scapulocoracoid is elongated between the mesocondyle and metacondyle with the direct articulation (Char. 59) with the direct articulation of pectoral radials to the scapulocoracoid (Char. 63) and the presence of lateral uvula in teeth (Char. 87)), which could be the cause of lower Bootstrap value for the Rhinopristiformes clade (Fig. 4.12A).

All analyses place sclerorhynchoids as a member of the Rajiformes (Fig. 4.11), based on similarities in the branchial skeleton (Node 40). Although being recovered in all parsimonious trees in the present analysis, the support values for the sclerorhynchiod-rajoids relationship are relatively low (Bremer = 1, Bootstrap = 4, Pp = 69%) (Figs. 4.11-4.12), possibly caused by the presence of missing characters and the rather extensive morphological differences between these groups, such as the unique pectoral skeleton of sclerorhynchoids (Char. 92) and the absence in some sclerorhynchoids of a suprascapula (Char. 6). The present placement varies from previous phylogenies; that places the sclerorhynchoids as an intermediate group between Pristidae and Pristiophoridae (Kriwet,

2004); or recovers them as an intermediate group between the Jurassic genus †*Spathobatis* and Pristidae (Claeson *et al*., 2013); and placed them within Rhinopristiformes (Underwood & Claeson, 2017).

All analyses support the placement of †*Asflapristis cristadentis* and †*Ptychotrygon rostrispatula* within sclerorhynchoids (Node = 66, Bremer = 2, Bootstrap= 55, Pp = 87%) (Figs. 4.11-4.12) based on their pectoral fin anatomy with the enlargement and paddle shape of propterygium, mesopterygium and metapterygium (Char. 92) and the reduced postorbital process (Char 38) (Fig. 4.10). Most of the posterior part of the branchial skeleton of †*Ptychotrygon rostrispatula* is preserved and is very similar to that of †*Sclerorhynchus atavus* (NHMUK PV P 49546), with the presence of a well-developed second hypobranchial fused, along with the third hypobranchial, to the basibranchial (Char.26) and with no evidence of a direct articulation of any branchial element to the second hypobranchial as seen in Rajiformes (Fig. 4.10).

†*Asflapristis cristadentis* (NHMUK PV P 73925) and †*Ptychotrygon rostrispatula* (NHMUK PV P73630) possess a very similar upper part of the second hypobranchial to that seen in other sclerorhynchoids (e.g. †*Sclerorhynchus atavus*, NHMUK PV P 49546) which seems to be characteristic of the sclerorhynchoids. †*Asflapristis cristadentis* and †*Ptychotrygon rostrispatula* also present a wide and stout basihyal, a large and well-mineralised first hypobranchial that subsequently articulates with the pseudohyal. These characters along with the presence of a transversal crest differentiating the labial crown face and well-developed labial visor, place them within Ptychotrygonidae (*sensu* Kriwet *et al.,* 2009).

As with other morphological analyses, the placement of Platyrhinidae (Node = 47, Bremer = 2, Bootstrap = 69, Pp = 99%) as a sister group to electric rays (Node = 44, Bremer = 7, Bootstrap = 98, Pp = 100%) (Figs. 4.11-4.12) within the order

Torpediniformes (*sensu*, Naylor *et al.* 2012) was not recovered in the present study, despite some taxa sharing characters like an irregular shape of the antorbital cartilages (Char. 9), lateral projection of the lateral stays (Char. 53) and at some point of their oncogenic development the separation of the ventral antimeres of scapulocoracoid (Char. 85; Fig. 4.10). The Bayesian analysis recovered Platyrhinidae as part of a polytomy that compromises all modern groups with the exclusion of sclerorhynchoids (Fig. 4.11) similar to that recovered by Aschliman *et al*. (2012a; text-fig. 2). This was expected as the relations within Rhinopristiformes and Torpediniformes are problematic for morphological based analysis, mostly because of the presence of highly derived taxa like *Pristis* and electric rays complicates the identification of synapomorphies between these taxa and the more plesiomorphic ones in their respective orders.

Myliobatiformes is recovered as a monophyletic group (Node = 59, Bremer = 4, Bootstrap = 78, Pp = 100%) (Figs. 4.11-4.12) and its composition changed little to that recovered by Aschliman *et al*. (2012a) and other molecular studies (Aschliman *et al*., 2012b). This group is easily differentiated as noted by the large number of synapomorphies found in the present study (Fig. 4.10). Of special interest is the placement of *Zanobatus* (panrays) within this group, the present study found similar relations for this genus as those recovered in Aschliman *et al*. (2012a; text-fig. 3.7 and 2012b; text-fig. 2) which places them as a suborder within Myliobatiformes. Naylor *et al*. (2012; text-fig. 2.10) recovered the panrays within Rhinopristiformes but as noted by the authors this placement is model dependent and should be addressed carefully. The most current molecular phylogeny places them as part of Myliobatiformes (Naylor *et al.,* 2012; text-fig. 2.11; Last *et al*., 2016; text-fig. 2.1) however the authors do not discuss this change further. Following Fricke *et al*. (2018) classification at the ordinal level, which is based on Naylor *et al*. (2012) and Last *et al*. (2016).

Discussion

Phylogenetic analysis

Although reductive coding in some cases leads to ambiguous optimisations of the characters or logically impossible state reconstructions (i.e. situations in which a logically impossible transformation may be reconstructed, for example a change in feather colour in an ancestor with no feathers). It provides a logical hierarchical arrangement of characters, were the presence-absence of a structure is linked to whether or not changes occur in set structure (Mannion *et al*., 2013), without making assumptions on the change order of characters (polarization). This logical hierarchy of characters might be desirable for phylogenetic analysis with fossil taxa, as it could improve the information retrieved from fossils, where the fossilisation process by its nature implies the loss of character information (Sansom *et al.,* 2010; 2013).

Phylogenetic relations of Sclerorhynchoids

The phylogenetic relations recovered in the present study for sclerorhynchoids differ from those recovered by previous studies (Kriwet 2004, Claeson *et al*., 2013 and Underwood & Claeson, 2017) as the present analysis, not only included changes in the coding of some characters (e.g. Char. 6: Calcified suprascapula) but also previously unknown observations (e.g. Char. 26: Second hypobranchial fused to the basibranchial (Fig. 4.2) which place sclerorhynchoids in a close relation with rajoids (Fig. 4.10). The close relation between rajoids and sclerorhynchoids were already suggested in previous taxonomic works, that place them as part of the order Rajiformes (Cappetta, 2012). However, the definition of Rajiformes on previous works was laxer, as it corresponds to taxonomic works previous to Naylor *et al.* (2012), in which the Rajiformes were re-

structured and no longer included the guitarfishes (rhinobatoids+platyrhinoids), which are currently classified in the orders Rhinopristiformes and Torpediniformes.

Based on the present results Cappetta´s (2012) classification is kept, with Sclerorhynchoidei forming a suborder of Rajiformes (*sensu* Naylor *et al.,* 2012) However, the lower support for this affiliation recovered in the present analysis need to be taken in to account (Bremer = 1, Bootstrap = 4, Pp = 74%) and as more specimens of well-preserved sclerorhynchoids are discovered, and more characters made evident, the relation between these two groups will become clearer.

Current classification show an interesting evolutionary pattern which was previously recognized by Claeson (2010), in which within every batoid order there is a group with a 'rhinopristiform' body plan (elongate body form, robust caudal region and enlarged and well-developed rostral cartilages), suggesting that this overall body plan is possibly a primitive feature within Batoidea (Fig. 4.10, taxa labelled in red).

Conclusion.

Present results separate sclerorhynchoids from Rhinopristiformes (Cappetta & Case, 1999) and suggest that the similarities to the Pristidae are superficial and convergent. Sclerorhynchoids were recovered in a close phylogenetic relationship between sclerorhynchoids and rajoids based on similarities in their branchial skeleton (e.g. lack of articulation surface between the basibranchial and second hypobranchial). None of the sclerorhynchoids included in the present analysis showed evidence of articulation between the second hypobranchial and any other branchial element. The fact that Bayesian analysis further differentiates Sclerorhynchoidei into two groups, suggests an internal topology for the group could be recovered with further analysis (Chapter 5), and

supports the idea that a number of distinct families are present within the Sclerorhynchoidei (Kriwet *et al*., 2009a; Cappetta, 2012).

Well-preserved partial skeletons of †*Asflapristis cristadentis* and †*Ptychotrygon rostrispatula* from the Late Cretaceous of Morocco have aid in the understanding of sclerorhynchoids. These taxa present a suite of morphological characters that place them within sclerorhynchoids (e.g. enlarged proximal pectoral elements, lack of suprascapula). Both analyses differentiate †*Asflapristis cristadentis* and †*Ptychotrygon rostrispatula* from other sclerorhynchoids, placing them in a close relation as members of the Ptychotrygonidae (*sensu* Kriwet *et al*., 2009a) family. Current analysis suggests that absence of enlarged rostral denticles as previously suggested for †*Ptychotrygon* (Cappetta & Case, 1999) along with the flattened rostrum and transversal crest differentiating the labial crown face and very well-developed labial visor can be considered as characteristics Ptychotrygonidae (*sensu* Kriwet *et al*., 2009a).

The discovery of †*Asflapristis cristadentis* and †*Ptychotrygon rostrispatula*, allow the observation of previously unknown characters within sclerorhynchoids (e.g. posterior and anterior fenestra of the lateral facet of the scapulocoracoid, the dorsally directed lateral stays of the synarcual, the shape and interactions of the basihyal with the second hypobranchial) and allow their identifications in other specimens (e.g. †*Sclerorhynchus atavus* NHMUK PV P49546).

Chapter 5

Phylogenetic relations within sclerorhynchoids

Results presented in this chapter were published in:

- Eduardo Villalobos-Segura, Charlie J. Underwood & David J. Ward. 2019b. **The first skeletal record of the Cretaceous enigmatic sawfish genus *Ptychotrygon* (Chondrichthyes: Batoidea) from the Turonian (Cretaceous) of Morocco**. *Papers in Palaeontology.* (in press)

Co-authors contributions

- o E. Villalobos Segura: Description of character used. Participated in the discussion of the characters used. Phylogenetic analysis.

- o C.J. Underwood: Participated in the discussion of the characters used.

- o D.J. Ward: Participated in the discussion of the characters used.

Introduction

Currently the most view of Sclerorhynchoidei is provided by Cappetta (2012), to which later works have added information (e.g. Welten *et al*., 2015; Underwood *et al*., 2016a). The peculiar morphology of the group is characterised by the presence of a hypertrophied rostrum with canals for the superficial ophthalmic and buccopharyngeal canal with rostral denticles not embedded in the rostral cartilages along with three enlarged rostral denticle series (ventro lateral, ventro central and lateral cephalic). But also includes a very simple rectangular shaped neurocranium with no major foramina nor fenestrae except for an oval-shaped precerebral fenestra on the anterior region of neurocranium and small and laterally projected nasal capsules. The ophthalmic region presents a reduced postorbital process along with the enlarged odontoid process. As with other batoids the antorbital cartilages are attached to the distal edge of the nasal capsules. However, they do not attach directly to the propterygium. The mouth cartilages are large compared with the rest of the neurocranium and protrude beyond it laterally, although this is rather common in batoids. The palatoquadrate is thinner than Meckel´s cartilage and both seem to have been supported by the hyomandibula. The pectoral proximal elements (propterygium, mesopterygium and metapterygium) are large and form a solid structure with no pectoral radials directly articulated with the scapulocoracoid between them.

Despite what has been published about the skeletal anatomy of sclerorhynchids, most of the fossil record of sclerorhynchoids, as with other chondrichthyans, is composed of highly mineralised skeletal elements (e.g. rostral cartilages and vertebral centra), and by regularly shed body elements with enameloid layers (teeth, placoid scales, rostral denticles and tail spines). These structures are usually phylogenetically uninformative and, in most cases, lead to uncertainty in the relations of these taxa. This is the case for several the taxa within sclerorhynchoids (e.g. †*Ptychotrygon* and †*Onchopristis*), in

which the lack of direct association to rostral denticles has led to taxonomic uncertainty for the genus.

Recently several extremely well-preserved three-dimensional remains of sclerorhynchoids with previously unseen morphological details have been discovered in the region of Asfla and the "Kem Kem Beds" in the northeast of Morocco corresponding to the Late Cretaceous, allowing a restudy of the phylogenetic relations and taxonomic classification of several sclerorhynchoid taxa. Of these specimens five present a similar tooth morphology to †*Ptychotrygon* providing the first skeletal record for this genus, six present a previously unknown morphology that belongs to a new species and genus †*Asflapristis cristadentis* Villalobos *et al.* (2019a) and one presents a tooth and rostral denticle morphology that corresponds to †*Onchopristis numidus* and provides the first cranial and synarcual remains for the genus. These specimens are included in a phylogenetic analysis along with several other species to assess the phylogenetic relations within sclerorhynchoids using the TNT and PAUP programs.

The taxonomic affiliations *Ptychotrygon* have changed from group to group since its redescription, from †*Ptychodus triangularis* (von Reuss, 1844) to †*Ptychotrygon triangularis* by Jaekel (1894) based on new specimens from the Kreideformation (Turonian) in Bohemia. Mcnulty & Slaughter (1972), placed the genus within the batoids in the family Dasyatidae and suggested that the tooth morphology fits as part of the galeoid-batoid succession, along with its similarities with other sclerorhynchoids (ganopristoid). Cappetta (1973) retained the dasyatoid affiliation and based on their histological features of teeth mentioned a possible affiliation with Rajiformes. Cappetta & Case (1999) based on Cappetta's (1973) observations placed the genus as either a sclerorhynchoid or a rhinobatoid, due to the lack of direct association between rostral denticles and oral teeth (until recently rhinobatoids were placed within the order

Rajiformes). Kriwet (1999a) placed it within the Rajiformes, based on the resemblance of the of possible rostral denticles found in mixed assemblages with those of Rajidae, and also mentioned their similarity with those found in other fossil assemblages (e.g. Case 1978a). Large dermal denticles, similar to those reported by Kriwet (1999a) have been observed for †*Libanopristis hiram* (Chapter 4;text-fig.4.7) and described for †*Sclerorhynchus atavus* (Welten *et al*., 2015, Underwood *et al*., 2016a). Cappetta (2006) placed †*Ptychotrygon* within the Rajiformes with its more exclusive taxonomic affiliations uncertain, as still no direct association with rostral denticles has been found. Kriwet *et al.* (2009) based on †*Ptychotrygon* tooth morphology proposed the family Ptychotrygonidae and placed it within the order Sclerorhynchiformes (*sensu* Kriwet, 2004). Cappetta (2012) kept the family Ptychotrygonidae which included three genera †*Ptychotrygon,* †*Ptychotrygonoides* and †*Texatrygon*. However, the systematic affiliation and position of the genus and family with the sclerorhynchoids remained doubtful as no direct association between rostral denticles and teeth has been proven.

The taxonomic relations of †*Onchopristis* have changed less since Cappetta (1980b) assigned to the suborder Sclerorhynchoidei. However, its affiliation to the family Sclerorhynchidae are still debated as the presence of a pulp cavity in the rostral denticles seems to vary within the two valid species of †*Onchopristis* (†*O. dunklei* presents a large cavity whereas †*O. numidus* presents a tiny pulp cavity that expands at the base of the denticle)*.

Material

Institutional abbreviations

A: Royal College of Surgeons, London (Hunterian Museum) BRC: Birkbeck Reference Collection. BSP: Bayerishe Staatssammlung fur Paläontologie und Geologie, Munich,

Germany. NHMUK: Natural History Museum United Kingdom, London. UERJ: Universidade do Estado do Rio de Janeiro

Material examined

Extant material. *Amblyraja radiata* (BRC-*Amblyraja*). *Anoxypristis cuspidata* (A.442.6). *Pristis sp.* (BRC-*Pristis). Raja clavata* (BRC-*Raja). Rajella fyllale* (BRC-*Rajella). Rhinobatos glaucostigma* (CNPE-IBUNAM 17810). *Zapteryx brevirostris,* (UERJ 1234, 1237, 1240).

Fossil material: †*Asflapristis cristadentis* (NHMUK PV P 73925, 75428 a-e, 75429 a-d, 75431, 75432, 75433). †*Ischyrhiza mira* (Sternes & Shimada, 2018;text-fig. 2 a-I, text-fig. 4 a-f, text-fig 5 a-I; Slaughter & Steiner 1968;text-fig. 4A-C). †*Micropristis solomonis* (Cappetta 1980, pl. 1, fig. 1-4; pl. 2, fig. 1). †*Libanopristis hiram* (Cappetta, 1980, pl. 1, fig. 4; NHMUK PV P 108705, 108706, 13858, 63610, 75075). †*Onchopristis numidus* (NHMUK PV P 75502, 75503, UV 353500). †*Ptychotrygon rostrispatula* (NHMUK PV P73630, 75496, 75496, 75497, 75500). †*Sclerorhynchus atavus* (Slaughter & Steiner, 1968, text-fig. 4D; NHMUK PV P4017, 4776, 49546, 49518, 49533, 49547). †*Shizorhiza stromeri* (Smith *et al*., 2015;text-fig. 1a-l; 2a-f; NHMUK PV P 73625). †*Spathobatis bugesicus* (NHMUK P6010, 2099 (2); BSP AS I 505, 1952 I 82).

Methods

A matrix of 14 taxa (eight sclerorhynchoid taxa with relatively good skeletal remains) and 23 characters using previous observations (Aschliman *et al*., 2012; Claeson *et al.,* 2013; Underwood & Claeson, 2017; Villalobos-Segura et al. 2019) and new characters was assembled in Mesquite 3.31 (Maddison & Maddison, 2018) (Appendix 5.1). Contingent/reductive coding (Brazeau, 2011) was implemented. Because, spurious

results can arise from this coding referring to zero-length branches (ZLB) (Strong & Lipscomb, 1999). The ZLB were collapsed, this is done by default in NONA and TNT and has to be set manually in PAUP (Brazeau, 2011). Fast and slow optimisations were used to evaluate all mapping possibilities and character state changes implications.

Following the previous chapter, the outgroup included three members of Rajidae (*Amblyraja radiata, Raja clavata* and *Rajella fyllale*), a Jurassic batoid (†*Spathobatis bugesicus*) and two members of Rhinopristiformes (*Rhinobatos glaucostigma, Anoxypristis cuspidata* and *Pristis sp.*). The matrix was analysed in the phylogenetic software TNT 1.1 (Goloboff *et al.*, 2013) and PAUP 4.0 (Swofford, 2001). As TNT was conceived mostly as a tool for analysis of large data sets, its results were contrasted with those of PAUP. The characters were mapped and optimised using WINCLADA (Nixon, 2002). The use of a smaller matrix allowed the further discussion regarding the ambiguous optimisation of character produced by reductive coding.

In both, the TNT and PAUP analyses a heuristic search with unweighted characters was performed. The TNT search was performed with the menu interface and the following parameters: tree bisection and reconnection (TBR) was used as the search algorithm, 1000 random seed, 10000 replications and 10 trees saved per replication. The PAUP search used the heuristic option with TBR as search algorithm and stepwise addition with 1000 random replications. The bootstrap analysis was performed in PAUP with 1000 iterations of random stepwise addition, to evaluate the support for all the clades recovered by the heuristic analyses. The analyses kept two uninformative characters (chars. 3 and 10); due to the lack of information they currently do not provide group data, however, they may offer interesting discussion points for future works (see character discussion).

Results

Phylogenetic analysis

Character discussion and mapping optimisation hypotheses

1. Enlarged and paddle like proximal pectoral elements: (0) absent, (1) present.

All known remains of pectoral fins of sclerorhynchoids present enlarged proximal pectoral elements (propterygium, mesopterygium and metapterygium), that present a narrow base and a wide distal end. There is a process that extends anteriorly in the propterygium and posteriorly in the metapterygium.

Optimisation

Unambiguous. This type of optimisation implies that slow and fast optimisations lead to the same number of steps. No pectoral remains are known for †*Ischyrhiza,* †*Onchopristis* and †*Schizorhiza* or have been described for *Anoxypristis* (?). Under unambiguous optimisation the use of (?) creates ambiguity for the terminals as both states (0 and 1) are considered to be possible by the phylogenetic software. The current data suggesting that the enlargement and modification of proximal pectoral elements is a synapomorphy of group II (†*Libanopristis*, †*Sclerorhynchus*, †*Micropristis*, †*Asflapristis cristadentis* and †*Ptychotrygon rostrispatula*) suggesting that this state appear later in the evolutionary history of the group. However, the present results do not disprove the possible presence of this state of character in †*Ischyrhiza,* †*Onchopristis* and †*Schizorhiza;* further fossil discoveries are needed to corroborate or disprove the presence of this state in these taxa and other sclerorhynchoids.
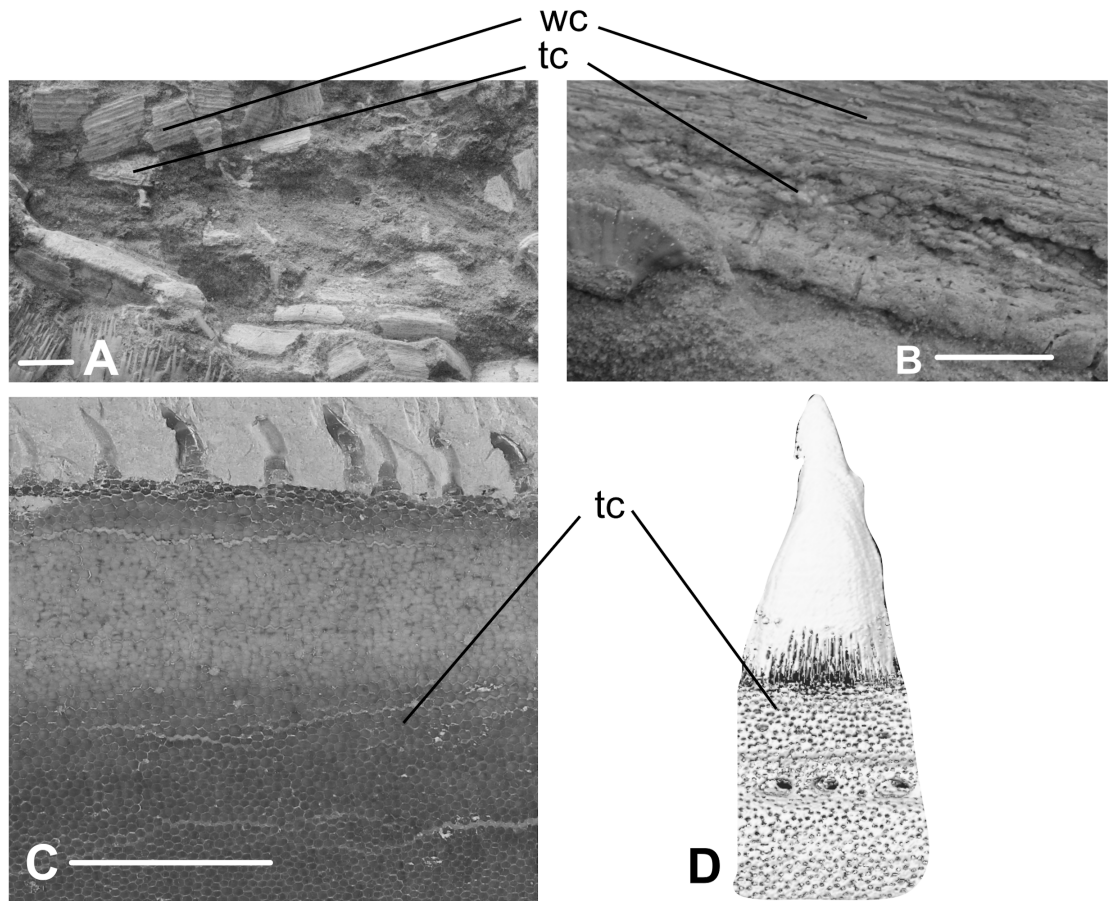
Figure 5.1. Rostrum sections of: **A**, †*Shizorhiza stromeri* NHMUK PV P 73625 (scale bar: 1cm). **B**, †*Onchopristis numidus* NHMUK PV P 75502 (scale bar: 1cm). **C**, †*Libanopristis hiram* NHMUK PV P 63610. (scale bar: 1cm). **D**, *Anoxypristis cuspidata*, A.442.6. **Abbreviations**: tc , tesserae (mosaic) cartilage; wc, wood-like cartilage.

2.   'Wood like' cartilage: (0) absent, (1) present.

†*Onchopristis*, †*Schizorhiza,* †*Ischyrhiza* and †*Asflapristis* present a peculiar type of cartilage on some regions of their chondroskeleton (Fig. 5.1A-B). This resembles wood cortex with several vertical, parallel and well mineralized ridges. Underneath this layer are columns of tesserae (Fig. 5.1C-D).

Optimisation

All three optimisations place the presence of this type of cartilage as a homoplasy between Clade IV and †*Asflapristis cristadentis*. This character was kept like this as it might suggests a tendency within sclerorhynchoids to develop this type of cartilage.

3. 'Wood-like' cartilage if present: (0) mouth, (1) rostrum.

This type of cartilage is not found in the same structures. †*Onchopristis*, †*Schizorhiza* (Kirkland & Aguillón-Martínez, 2002) and †*Ischyrhiza* presented it in the rostral cartilages and †*Asflapristis* in the mouth. Under current data, this character lacks phylogenetic information (uninformative), it was kept as it arises from the use of reductive coding (Brazeau, 2011), and because there are no other known skeletal remains to compare. The present analysis places the occurrence of this type of cartilage in the rostral cartilages (1) represents a synapomorphy for the †*Onchopristis*, †*Schizorhiza* and †*Ischyrhiza* clade, and its presence in the mouth an autapomorphy for †*Asflapristis* (0).

Optimisations

Unambiguous. The presence of 'wood like' cartilage in the rostral cartilages is a synapomorphy of †*Onchopristis*, †*Schizorhiza* and †*Ischyrhiza*. Its presence in the mouth cartilages as an autapomorphy of †*Asflapristis*. However, it is not displayed in the tree as a result of the ambiguity in the other taxa. Current phylogenetic software deal with inapplicable characters (-) in the same way as they deal with unknown character (?) placing ambiguity in those terminals coded with (- or ?) as it assumes that all states of character are possible in them.

Slow. Its appearance later in the evolutionary history of the group places its presence in the rostral cartilages (1) as a synapomorphy of †*Onchopristis*, †*Schizorhiza* and †*Ischyrhiza* with the plesiomorphic state being the presence in the mouth (0), this implies a subsequent independent loss on each terminal with the exception of †*Asflapristis*.

Fast. Recovers a similar evolution of the character. However, the presence of 'wood like' cartilage in the rostral cartilages is gained earlier in the evolution of Clade I with its subsequent loss in *Raja* and *Amblyraja*.

4. Enlarged denticle series associated to rostral cartilages and cephalic region: (0) absent, (1) present.

Several groups of chondrichthyans have developed enlarged denticle series associated to the cephalic and rostral region. However, some sclerorhynchoids are the only known batoids that present more than one series.

Optimisation

All three optimisations recovered the presence of this denticle series as a synapomorphy between sclerorhynchoids and pristioids (1) with a subsequent loss in *Raja* and *Amblyraja* (0). However, the placement as a synapomorphy for these two groups is unlikely considering the vast amount of character differences between sclerorhynchoids and pristioids.

5.   Number of denticle series associated to rostral cartilages and cephalic region: (0) one, (1) two or more.

The number of enlarged denticle series associated with the rostral region varies between sclerorhynchoids. The Moroccan fossil remains of †*Asflapristis cristadentis* and †*Ptychotrygon rostrispatula* indicate that in ptychotrygonoids only one series of enlarged denticles is present (0) the lateral cephalic. †*Ptychotrygon rostrispatula*. remains show no rostral or ventral denticle series attach to it. This suggests that the enlarged denticles recovered from mixed assemblages reported in the literature for the genus (Case 1978) correspond to the lateral anterior cephalic series. No cephalic remains of †*Schizorhiza* are known, its rostral remains present only the rostral cartilage lateral denticle series (lack the ventral denticle series). Therefore, the number of enlarged denticles series associated with the rostral cartilages and lateral anterior cephalic region is unknown. †*Sclerorhynchus* (Welten *et al.,* 2015: text-figs. 8-9; Underwood *et al.,* 2016a text-fig. 1C), †*Libanopristis* and †*Onchopristis* have four enlarged rostral denticle series (1): one on the sides of the rostrum; other the anterior lateral parts of the cephalic region; and two on the ventral side (one in the centre and other in the sides) . In †*Micropristis* at least two series of enlarged denticles (1) have been observed (lateral rostral and lateral cephalic)

this information is based in published records (no direct observation) (Cappetta 1980, plate 1, Figs. 1).

Optimisation

All three types of optimisation recovered the presence of more than one series as a synapomorphy of sclerorhynchoids and pristioids with a subsequent loss of several of these series in †*Ptychotrygon* and †*Asflapristis*. The presence of just one series of denticles should not be interpreted a synapomorphy between pristioids, †*Asflapristis* and †*Ptychotrygon* as they present different denticles series. Under current coding there us ambiguity for †*Spathobatis, Rhinobatos, Raja* and *Amblyraja* as this character is coded as inapplicable (-) for these taxa (see character 3, for discussion on the implications of this).

6. Rostral cartilages lateral denticles series: (0) absent, (1) present.

This character refers only to the lateral rostral series associated with the rostral cartilages. Its presence varies within sclerorhynchoids. No direct association between the rostral cartilages and this denticle series has been observed (0) for †*Asflapristis* and †*Ptychotrygon rostrispatula*. In the remaining taxa of sclerorhynchoids either a direct association has been observed or reported in the literature (e.g. Cappetta, 2012) (1).

Optimisation

All three types of optimisation recovered the presence of the lateral rostral cartilages as a shared characteristic of sclerorhynchoids and pristioids with a subsequent loss in †*Ptychotrygon* and †*Asflapristis*. There are other characters (e.g. Char 9 and 22) that suggest that instead of a synapomorphy the presence of this series is a homoplasy between sclerorhynchoids and pristioids. The absence of these series is recovered as a synapomorphy of †*Asflapristis* and †*Ptychotrygon*. Under current coding there is ambiguity for †*Spathobatis, Rhinobatos, Raja* and *Amblyraja* as this character is coded

as inapplicable (-) for these taxa (see character 3, for discussion on the implications of this).

7. Ventral rostral denticles series: (0) absent, (1) present.

The presence of a ventral series of denticles has been reported for †*Sclerorhynchus* (Welten *et al.* 2015: text-figs. 8-9; Underwood *et al.,* 2016a text-fig. 1C)*,* and a similar series has been observed in †*Libanopristis* (1). From the literature review this state could not be determined for †*Micropristis* (?). The specimens of †*Asflapristis*, †*Ptychotrygon* and †*Schizorhiza* (0) showed no evidence or this series. In †*Onchopristis* there seems to be a uniform cover on the ventral surface of the rostrum some of which are enlarged (1) and are similarly shaped to those reported for †*Ischyrhiza* (Sternes & Shimada 2018).

Optimisations

Unambiguous. The presence of this series is a shared characteristic between most of sclerorhynchoids. It also recovers ambiguity in †*Micropristis* due to the lack of observations and in †*Spathobatis, Rhinobatos, Raja* and *Amblyraja* as the character is coded as (-). In the case of †*Spathobatis* and *Rhinobatos* the ambiguity extends in to the ancestors of pristioids which is followed by the absence of these series in sawfishes.

Fast and *Slow* optimisations consider this trait as a shared characteristic between several sclerorhynchoids with an independent loss in pristioids, †*Asflapristis*, †*Ptychotrygon* and †*Schizorhiza.* Under current coding there us ambiguity for †*Spathobatis, Rhinobatos, Raja* and *Amblyraja* as this character is coded as inapplicable (-) for these taxa (see character 3, for discussion on the implications of this).

8. Enlarged cephalic denticle series: (0) absent (1) present.

This character refers to the presence the enlarged series on the lateral cephalic region. In †*Ptychotrygon rostrispatula* sp. nov. remains show no rostral or ventral denticles series attached to it. This suggests that the enlarge denticles recovered from mixed assemblages

reported in the literature for the genus (Case, 1978; plate 4, fig. 7a-c) correspond to the lateral anterior cephalic series. †*Onchopristis* is a similar case no direct association has been reported. However, different morphologies of denticles for this genus have been reported some of which (e.g. Stromer, 1927; plate 1, fig. 32a-b and Werner, 1989; plate 20, fig. 9) are similar to the cephalic series reported for †*Sclerorhynchus* by Welten *et al*. (2015).

Optimisations

Unambiguous. Under this optimisation the presence of this series is lost as a shared characteristic between most of sclerorhynchoids. It also recovers ambiguity in: †*Micropristis,* †*Ischyrhiza* and †*Asflapristis* due to the lack of observations (?) and for †*Spathobatis, Rhinobatos, Raja* and *Amblyraja* as the character is coded as (-). In the case of †*Spathobatis* and *Rhinobatos* the ambiguity extends into the ancestors of pristioids which is followed by the absence of this series in sawfishes.

Fast and *slow* optimisations consider the trait as a shared characteristic between several sclerorhynchoids. Under current coding there is ambiguity for †*Spathobatis, Rhinobatos, Raja* and *Amblyraja* as this character is coded as inapplicable (-) for these taxa (see character 3, for discussion of the implications of this). The ambiguity in †*Asflapristis*, †*Ischyrhiza* and †*Schizorhiza* is a result of the lack of observations to code this character (?).

9. Replacement of rostral cartilage denticles series: (0) absent (1) present.

Rostral denticles in sclerorhynchoids are shed constantly, in contrast to those found in extant and fossil pristioids that are not replaced and grow continuously.

Optimisations

Unambiguous.

The addition of denticles in the lateral series of the rostrum is a shared characteristic among sclerorhynchoids. The lack of this series in the †*Asflapristis* and †*Ptychotrygon* clade makes it inapplicable for these taxa (-). The absence of addition of rostral denticle series is shared characteristic between *Pristis* and *Anoxypristis*.

10. Addition of rostral denticles: (0) in batteries, (1) lateral similar sizes, (2) symmetric with denticles of different sizes being constantly.

This character is uninformative, it was kept as the type of replacement of rostral denticles varies among sclerorhynchoids taxa. In †*Onchopristis* (NHMUK 75502; 75503) denticles of different sizes are constantly being added (2). It is unknown whether there is a temporality in the replacement or if denticles are just added as the space in the rostrum becomes available. In †*Schizorhiza*, the denticles are arranged in batteries (0) one beneath the other (Smith *et al*., 2015). In †*Sclerorhynchus* (Welten *et al.,* 2015, text-figs. 8-9; Underwood *et al.,* 2015 text-fig. 1C)*,* †*Libanopristis,* †*Micropristis* and †*Ischyrhiza* (Sternes & Shimada, 2018 text-fig. 2A-D) similar size rostral denticles are being added (1). It is worth mentioning that †*Shizorhiza* and †*Ischyrhiza* are the only species in the present study that present rostral denticles with large roots with several lobes.

Optimisations.

All three types of optimisation recovered a similar evolutionary history for this character, in which the plesimorphic character state is type B (denticles are replaced by denticles of the same size). The ambiguity in this character arises from the use inapplicability of this character for pristioids, †*Spathobatis, Rhinobatos, Raja*, *Amblyraja,* †*Asflapristis* and †*Ptychotrygon.*

Slow. Recovers less ambiguity as places the two different types of replacement observed in †*Onchopristis* and †*Shizorhiza* as an autapomorphy.

Fast. Places the battery replacement (0) as the plesiomorphic state for the †*Onchopristis*+†*Shizorhiza* clade.
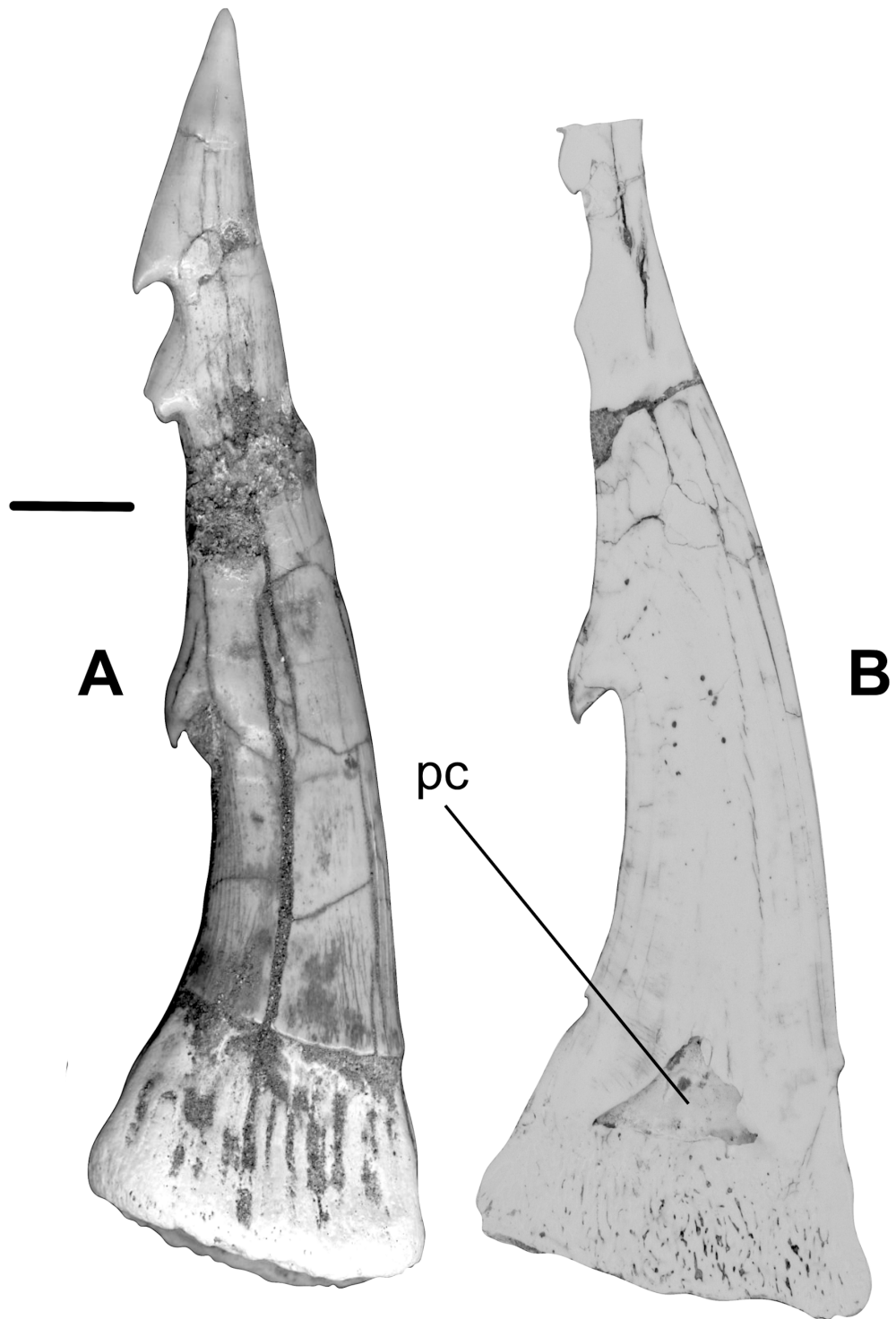
Figure 5.2 †*Onchopristis numidus*. **A**, lateral rostral denticles. **B**, section of lateral rostral denticle. **Abbreviations:** pc, pulp cavity. (scale bar: 1 cm).

11. Pulp cavities in the enlarged rostral cartilages denticles: (0) absent, (1) present.

Several species of sclerorhynchoids (†*Onchopristis* (Fig. 5.2)*;* †*Sclerorhynchus* and †*Ischyrhiza* (Slaughter & Steiner, 1968, Fig. 4 A-D) and †*Libanopristis*) present pulp cavities at base of the rostral denticles (1). While pristioids rostral denticles lack pulp cavity (0).

Optimisations

All three types of optimisation recovered a similar evolutionary history for this character, in which the presence of a pulp cavity (1) is a shared characteristic for sclerorhynchoids. The ambiguity in this character arises from the inapplicability of this character for †*Spathobatis, Rhinobatos, Raja*, *Amblyraja*, †*Asflapristis* and †*Ptychotrygon.*

Unambiguous. Does not recover the presence of a pulp cavity as a synapomorphy and adds ambiguity to the outgroup (†*Spathobatis* and *Rhinobatos*) and pristioids nodes due to the inapplicable (-) coding for them.

Slow and *Fast* optimisations recover less ambiguity as they place the presence of a pulp cavity as a synapomorphy for sclerorhynchoids. With the plesiomorphic state being the absence of cavity observed in pristioids.

12. Mesopterygium-metapterygium: (0) radials articulate between them, (1) no radials between them.

In all the known remains of sclerorhynchoids there is no evidence of direct articulation between the radials and the scapulocoracoid (1). Whether or not the lack of radials directly articulated to the scapulocoracoid is more widespread within the sclerorhynchoids is unknown as no pectoral remains of †*Ischyrhiza,* †*Onchopristis* and †*Schizorhiza* have been reported or for any of the species included the present analysis (?).

Optimisations

All three types of optimisation recovered the same topology and distribution, in which the lack of direct articulation between the radials and the scapulocoracoid is recovered as a synapomorphy for group (II). However, the present results do not disprove the possible presence of this state of character in †*Ischyrhiza,* †*Onchopristis* and †*Schizorhiza,* further

fossil discoveries are needed to corroborate or disprove whether state (1) is more widely distributed among sclerorhynchoids or an isolated feature of group (II).

13. Postorbital process: (0) reduced, (1) well-developed.

The postorbital process is reduced in †*Sclerorhynchus*, †*Libanopristis*, †*Micropristis*, †*Asflapristis* and †*Ptychotrygon* (0). †*Spathobatis, Raja, Rhinobatos, Pristis* and *Anoxypristis* present a postorbital process (1). Although this character might be present in †*Onchopristis*, †*Schizorhiza* and †*Ischyrhiza* so far under current fossil evidence it cannot be corroborated (?).

Optimisations

All three types of optimisation recovered the same topology and distribution. The reduction of the postorbital process is recovered as a synapomorphy for group (II). However, the present results do not disprove the possible presence of this character state in †*Ischyrhiza,* †*Onchopristis* and †*Schizorhiza,* further fossil discoveries are needed to corroborate or disprove whether state (1) is more widely distributed among sclerorhynchoids or an isolated feature of group (II).

14. Second hypobranchial-basibranchial: (0) articulated, (1) fused.

The lack of articulation surface between the second hypobranchial and basibranchial (1) was observed in †*Sclerorhynchus atavus* NHMUK PV P 49546 and †*Ptychotrygon rostrispatula*, its presence in both taxa could suggest that could be widely distributed within sclerorhynchoids and point of similarity between rajoids and sclerorhynchoids (Villalobos *et al.,* 2019a).

Optimisation

All three types of optimisation recovered a similar topology and distribution. The lack of articulation surface between the hypobranchial and basibranchial is recovered as a synapomorphy for the rajoid+sclerorhynchoid clade. The ambiguity within this clade

arises from the current lack of fossil evidence to code this character in †*Ischyrhiza,* †*Onchopristis*, †*Schizorhiza,* †*Libanopristis*, †*Micropristis*. The present results do not disprove the possible presence of this state for those*,* further fossil discoveries are needed to corroborate or disprove whether state (1) is more widely distributed among sclerorhynchoids. Both slow and fast optimisations recover the same character distribution.

15. Third hypobranchial-basibranchial: (0) articulated, (1) fused.

In †*Sclerorhynchus* and †*Ptychotrygon rostrispatula* sp. nov. there is no articulation surface between the third hypobranchial and basibranchial (1). The outgroup presents an articulation surface between the third hypobranchial and basibranchial (0).

Optimisations

Unambiguous. Recovers the fusion between the third hypobranchial and basibranchial (1) as a shared characteristic of †*Sclerorhynchus,* †*Libanopristis,* † *Asflapristis* and †*Ptychotrygon*. However, is not mapped due the lack of information for †*Micropristis* (?) (see character 3 for discussion on ambiguity caused by missing data)*.*

Slow. Places the state (1) as a synapomorphy of the †*Sclerorhynchus,* †*Libanopristis,* †*Asflapristis* and †*Ptychotrygon* group.

Fast. Places the state (1) as a synapomorphy of the †*Micropristis,* † *Sclerorhynchus,* †*Libanopristis,* †*Asflapristis* and †*Ptychotrygon* group.

16. Ornament on teeth: (0) absent, (1) present.

Sclerorhynchoids generally present different ornamentations (ridges and crest) in their teeth specially in the labial face.

Optimisation

All three types of optimisation recovered a similar topology and distribution, in which the presence of ridges and crests in the crown surface of the teeth is a synapomorphy for

the clade that includes †*Sclerorhynchus,* †*Libanopristis,* †*Asflapristis* and †*Ptychotrygon* (1).

17. Transverse crests on teeth: (0) absent, (1) present.

This character was proposed by Kriwet *et al*. (2009a) as one of the synapomorphies of the family Ptychotrygonidae this transverse crest strongly differentiate the labial face from the lingual one. †*Libanopristis* also present this character (1) (Cappetta, 1980, pl. 2, fig. 5). However, in †*Libanopristis* the crests are slightly more laterally directed, and its teeth are more symmetric than those of †*Ptychotrygon* species which general present more than just one crest in the labial region.

Optimisation

All three optimisations recover the presence of a transverse crest on the labial surface (1) as a synapomorphy of †*Libanopristis,* †*Asflapristis* and †*Ptychotrygon*.

18. Lingual uvula: (0) absent, (1) present.

In †*Asflapristis*, †*Onchopristis* and †*Schizorhiza* the lingual uvula is absent (0). In †*Ptychotrygon* the development of the lingual uvula variates (0 & 1) (†*Ptychotrygon gueveli* Cappetta, 2004 and †*Ptychotrygon rugosa* Case *et al.,* 2001) (0).

Optimisation

All three optimisations implied two loss events of the lingual uvula (0), one in the †*Onchopristis* and †*Schizorhiza* clade and the las one in †*Asflapristis.* Unambiguous optimisation was preferred, as both slow and fast fail to recover the uncertainty in †*Ptychotrygon* as both states were present in this taxon.

19. Enlarged denticles in body: absent (1), present (0).

In some rajoids some enlarge dermal denticles are present across the body (1). Cappetta noticed that the distribution of †*Peyeria* and †*Onchopristis* overlap and proposed the synonymy of †*Peyeria* with †*Onchopristis* (Cappetta, 2012, text-fig. 371 B-D). The same

commonality was found in the "Kem Kem Beds" supporting Cappetta's (2012) hypothesis. A similar occurrence has recently reported in the United States for the genus †*Ischyrhiza* (Sternes & Shimada, 2018) (1). In no other sclerorhynchoid species this denticles have been reported (0). Considering the relatively good fossil record of some species in group (II) this character could indicate a very peculiar trait for †*Onchopristis* and †*Ischyrhiza* (group I).

Optimisation

All three optimisations recover the presence of enlarge denticles in the body (1) as a synapomorphy of the *Raja*, *Amblyraja*, *Ischyrhiza*, †*Onchopristis* and †*Schizorhiza* clade.
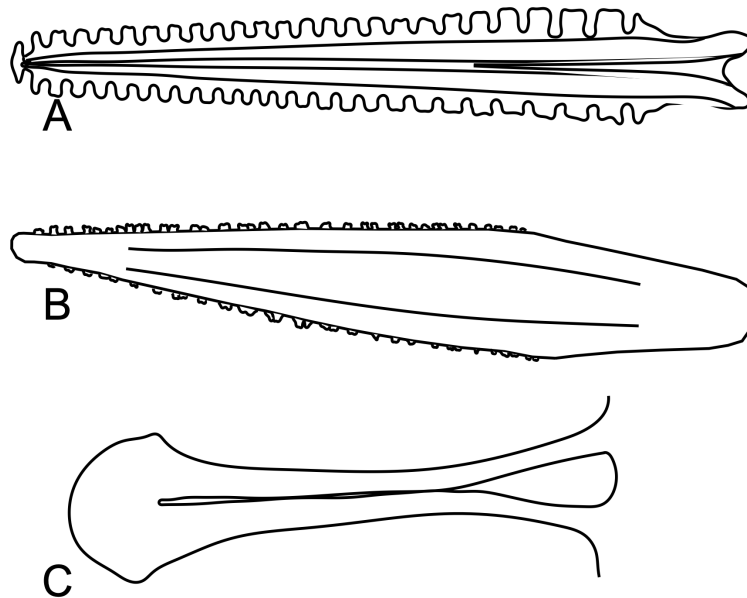
Figure 5.3. Rostrum shape of: **A,** *Pristis sp.* BRC-Pristis, **B,** †*Libanopristis hiram* NHMUK PV P 75075, **C,** *Rhinobatos glaucostigma* CNPE-IBUNAM 17810.

20.   Rostrum shape: (0) triangular reaching its maximum width at the base, (1) leaf shaped with its maximum width reached before the base of the rostrum, and (2) Triangular-Concave (spatula shaped) with a precerebral fenestra (Fig. 5.3A-C).

The codification of this character is not ideal, as it is a composite character. The presence/absence of a precerebral fenestra has been used in previous works (Brito *et al.,*

2013) and needs to be revaluated as its absence seems to be a convergent between sawfishes, sawsharks and sclerorhynchoids.

†*Libanopristis,* †*Micropristis*, †*Sclerorhynchus* and †*Ptychotrygon* (1) present a leaf shaped rostrum that reaches its maximum width beyond its base. †*Onchopristis* and †*Schizorhiza* (0) present a triangular rostrum similarly shaped to that of modern sawfishes and saw-sharks.

Optimisations

Unambiguous. Recovers the presence of a leaf shaped rostrum (1) as a synapomorphy of the Clade II. And places ambiguity regarding the transition between states (2) and (0).

Fast. Places the leaf shaped rostrum (1) as a synapomorphy for the pristids+Rajidae+sclerorhynchoids clade with a change to state (2) in Rajidae. Both unambiguous and fast optimisation fail to recover the Pristidae clade as the character is pushed backwards as a shared feature between Pristidae and clade IV.

Slow. Recovers the least ambiguity. It suggests a different topology as a later evolution of the shape of the rostrum implies that the triangular shape of the rostrum evolved two times (1): one in the †*Ischyrhiza*, †*Onchopristis* and †*Schizorhiza* and in the pristioids clades. This optimisation also suggests that the triangular-Concave rostral cartilages with a precerebral fenestra, is the most common state among batoids and evolved once.

21. Differentiated lateral uvulae on teeth: (0) absent, (1) present

This character was proposed by Claeson *et al.* (2013, char. 22) this character refers to the presence of lateral root directed projections of the crown commonly observed in several Rhinopristiformes (*sensu* Naylor *et al.,* 2012).

Optimisation

All three optimisations recover the lack of lateral uvula in the oral teeth (0) as a synapomorphy of the *Rajoids+sclerorhynchoids* clade.

22. Rostral denticles embedded in alveoli of rostral cartilage: (0) present, (1) absent. Character proposed by Kriwet (2004), rostral denticles on the known sclerorhynchoids remains are superficially attached to the rostral cartilages, supported by connective tissue and dermis. In *Pristis* the denticles are deeply embedded into deep grooves on the margins of the rostral cartilages.

Optimisations

Unambiguous. recovers the ambiguity in the ancestral state between pristioids and sclerorhynchoids.

Fast and *Slow.* Recovered the same mapping for this character and place the superficial articulation of the lateral denticles series of the rostral cartilages (1) as a synapomorphy for the sclerorhynchoids and place the deeply embed lateral series of denticles in the rostral cartilages as the ancestral state (0).

23. Calcified suprascapula: (0) absent, (1) present (Based on AMC2012, char. 6).
This character is based on Aschliman's (2012) work, the character and states were changed as the present study involves fossil species and states such as fused medially and not fused medially can be difficult to be defined in fossil taxa. Under current fossil data the absence or presence of a cartilage connecting the antimeres of the scapulocoracoid of Jurassic batoids and sclerorhynchoids cannot be proven. The lack of preservation of this cartilage in these groups could be caused by the absence of mineralization in the whole cartilage. Ontogenetic series of *Zapteryx brevirostris* show a late calcification of this cartilage which could be the case for Jurassic batoids and sclerorhynchoids in which this cartilage could be present but not calcified.

†*Libanopristis* present a cartilage that resembles the suprascapula found in *Raja*. Due to the damage observed in the specimen it was not possible to determine if this cartilage is in fact the suprascapula. Because, of this Claeson *et al*. (2013) coding was kept for this taxon.

Optimisation

All three optimisations differentiate the Jurassic batoids represented by †*Spathobatis* from other 'rhinobatoid-like' batoids. The lack of a well mineralised suprascapula is occurred twice in the present analysis one in †*Spathobatis* and in the †*Asflapristis cristadentis* and †*Ptychotrygon rostrispatula* clade. Whether this character is widely distributed within sclerorhynchoids remains unknown due to the lack of fossil evidence.

Phylogenetic analysis

Figure 5.4. A, TNT and PAUP most parsimonious tree (MPT). Roman numerals are the node numbers and below them in parenthesis are the Bootstrap values. **B,** character optimisations supporting the clades mapped in the TNT tree using WINCLADA. Non-homoplastic synapomorphies represented by filled figures. Unfilled figures are relevant characters with a consistency index < 1.00 (homoplastic synapomorphies).

TNT and PAUP phylogenetic analyses recovered a single most parsimonious tree with same topology of 33 steps and a consistency index of 0.75 and retention indices of 0.84 (Fig. 5.4A). The present analysis suggests that a phylogenetic structure can be recovered from current data for sclerorhynchoids. The topology recovered a large group the includes the sclerorhynchoid+rajoid (Clade I, Bootstrap support (Bs)= 45) similar to Villalobos *et al*. (2019a) (Chapter 4). Clade I, is supported by two unambiguous synapomorphies under the unambiguous optimisation (Uo): Char. 14, lack of articulation surface between the second hypobranchial and basibranchial and char. 21, lack of lateral uvula on teeth. Slow and Fast optimisation add six extra synapomorphies: Char. 5, more than one series of denticle series associated to rostrum and cephalic series; Char. 7, presence of ventral rostral denticle series; Char. 8, presence of cephalic enlarge denticle series; Char. 9, presence of replacement of rostral cartilage denticle series; Char. 11, presence of pulp cavity in the enlarged rostral cartilages denticle series; Char. 22, lateral rostral denticles not embedded in alveoli of rostral cartilages (Fig. 5.4B). Two monophyletic groups are recovered within Clade I: *Amblyraja, Raja,* †*Ischyrhiza,* †*Onchopristis* and †*Schizorhiza* (Clade III) and Clade II, that includes several members of Sclerorhynchidae (*sensu* Cappetta, 2012): †*Micropristis,* †*Sclerorhynchus,* †*Libanopristis,* †*Asflapristis cristadentis* and †*Ptychotrygon rostrispatula* (Fig. 6.4A).

Clade II (Bs = 57) is supported by four characters (Uo): Char. 1, the presence of enlarge and paddle like proximal pectoral elements; Char. 12, the lack of direct articulation between the pectoral radials and the scapulocoracoid; Char. 13, reduced postorbital process; and Char. 20, leaf shaped rostrum that reaches its maximum width after the base (Fig. 5.4). The fast optimisation adds an extra character: Char. 15, lack of articulation surface between the basibranchial and third hypobranchial. †*Libanopristis* is recovered as sister group (Bs = 41) of the †*Asflapristis cristadentis* and †*Ptychotrygon rostrispatula* clade and is supported by the presence of a transverse crest in the crown teeth labial face

(Char 17). The †*Asflapristis cristadentis* and †*Ptychotrygon rostrispatula* clade, presents the highest support value (Bs = 88) and is supported by one unambiguous synapomorphy: the lack of enlarged lateral series of denticles in the rostral cartilages (Char. 6) (Fig. 5.4). It is worth mentioning that this clade is also differentiated by three other characteristics in the unambiguous optimisation: presence of one series of enlarged denticles associated to rostral cartilages and cephalic region (Char. 5), the absence of ventral rostral denticles series in rostral cartilages (Char. 7) and the lack of a calcified suprascapula (Char. 23). The fast optimisation adds an extra character to this clade: Char. 18, absence of a lingual uvula. However, this character requires further review as it is polymorphic within †*Ptychotrygon* (e.g. †*P. triagularis* present a cusp while †*P. gueveli* and †*P. rugosus* lacks it). Of the specimens reviewed only †*Asflapristis cristadentis* consistently lacks a medial cusp.

Clade III was not recovered by the Bootstrap analysis, which instead recovered a polytomy between Rajidae and the eight sclerorhynchoid taxa included in the present analysis, and therefore no bootstrap value was assigned to it. Clade III includes the most peculiar fossils in the present study (†*Onchopristis*, †*Schizorhiza* and surprisingly †*Ischyrhiza*) (Fig. 5.4). This clade is supported by one unambiguous synapomorphy (Uo): Char. 19, the presence of enlarged denticles in the body. Under fast optimisation an additional synapomorphy was added: Char. 3, the presence of 'wood-like' cartilage in the rostrum. Clade IV (Bs = 46) includes †*Onchopristis*, †*Schizorhiza* and †*Ischyrhiza* and is supported by one character (Uo): Char. 2, presence of 'wood-like' cartilage. Under slow optimisation an extra character and an unambiguous synapomorphy are added: Char. 3 presence of 'wood-like' cartilage in the rostrum; Char. 20, rostral cartilages with is widest point at the base (Fig. 5.4). It is worth mentioning that the genera in group II present different types of rostral denticles replacement (Char. 10) which points towards a possible further differentiation within this clade.

Discussion

Phylogenetic analysis

Although time consuming the display and comparation of three types of optimisation, revealed further information, regarding the possible implications of character state changes and provide a richer discussion on the evolution of the group. However, special attention must be given to the type of optimisation if chosen. The unambiguous optimisation might be preferred, as fast and slow optimisation make further assumptions regarding taxa with characters states coded as inapplicable and unknown.

Phylogenetic relations within Sclerorhynchoidei

As recovered in Chapter 4 the present analysis recovered a close relation between sclerorhynchoids and rajoids. Within sclerorhynchoids two major groups were recovered by the present analysis, clade II which includes †*Micropristis,* †*Sclerorhynchus*, †*Libanopristis,* †*Asflapristis cristadentis* and† *Ptychotrygon rostrispatula* and clade IV with †*Onchopristis*, †*Schizorhiza* and surprisingly †*Ischyrhiza*. All of these clades present peculiar characteristics that suggest a taxonomic rework for the group which could be divided in to two or three subordinate groups. Most of the differences between these groups were found in the rostrum (e.g. presence of "wood-like" cartilage accompanied by the presence of a thick layer of peripheral cartilage at the sides of the rostrum) which suggest that this structure was highly plastic and might be used in different manners within these groups. As suggested by the discovery of remains described in Chapters 2 and 3.

Phylogenetic relations of Ptychotrygoninae

Whilst taxonomic and phylogenetic uncertainty will remain regarding the taxonomical hierarchy of ptychotrygonoids as the analysis in Chapter 4 suggest a family affiliation with †*Asflapristis* and †*Ptychotrygon* being placed as sister groups of †*Libanopristis* and †*Sclerorhynchus*, whereas those of the present chapter suggest a subfamily re-assignment with †*Asflapristis* and †*Ptychotrygon* being placed as group within Sclerorhynchidae (†*Micropristis*, †*Libanopristis* and †*Sclerorhynchus*). Both analyses place them as a group monophyletic group within the Sclerorhynchoidei based on the loss of the lateral and both ventral (lateral and central) series of enlarge denticles in the rostrum. However, as the present analysis includes bigger sample of sclerorhynchoid taxa †*Asflapristis cristadentis* and †*Ptychotrygon rostrispatula* are placed as part of the subfamily Ptychotrygoninae as part of the Sclerorhynchidae family.

The placement of Ptychotrygoninae within the Sclerorhynchidae family is mostly based on similarities on their tooth morphology specially with those of †*Libanopristis* which also present transverse crests in the labial apron (Cappetta, 1980b, text-fig 7 B; 2012, text-fig. 368 I), However, in general the teeth of †*Libanopristis* present more prominent cusp and the labial apron less ornamented than those of Ptychotrygoninae (Fig. 5.5). Furthermore, in †*Ptychotrygon* there is a deep central interlocking depression. Cappetta (1980) mentions a depression for some teeth of †*Libanopristis hiram* but it is not clear form the illustrations if he refers to the profile of lingual face or to a region of the lingual uvula.
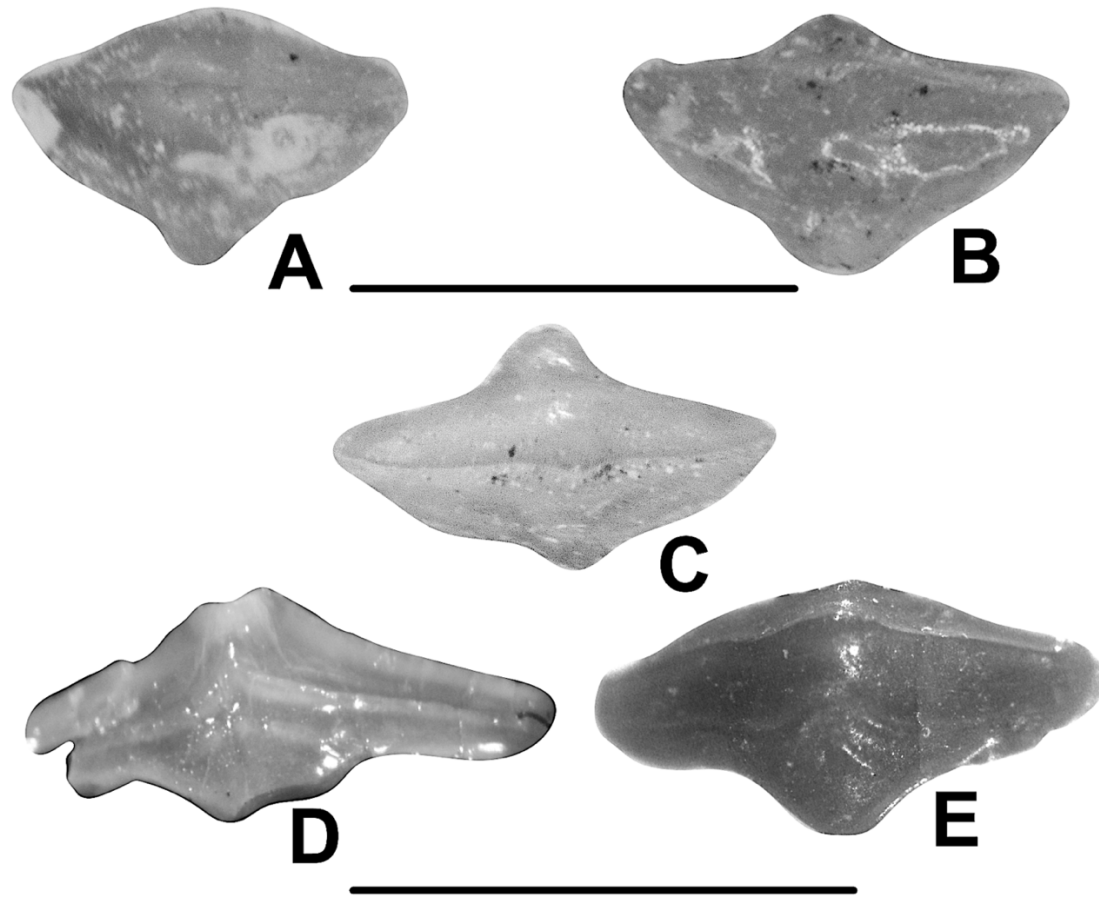
Figure 5.5. **A-C,** occlusal view of teeth of †*Libanopristis hiram* (NHMUK PV P 13858). Teeth of †*Ptychotrygon rostrispatula*. **D,** labial view and **E,** occlusal view. Scale bars: **A-C,** 1mm. **D-E**, 2mm.

Phylogenetic relations within Onchopristidae

Present analysis recovered a second clade within the Sclerorhynchoidei which includes taxa previously associated to Sclerorhynchidae (Cappetta, 2012). The Onchopristidae family is proposed to accommodate †*Ischyrhiza* and †*Onchopristis.* This new family is characterised by its very peculiar rostral morphology with a thick lateral layer of cartilage on the sides of the rostral cartilages were the enlarge denticle lateral series attach, an external layer of "wood-like" cartilage in the centre of the rostrum and enlarge denticles in the body (Sternes & Shimada, 2018).

Phylogenetic relations within †Schizorhiza

According to the present analysis the genus †*Schizorhiza* should be placed within the family Onchopristidae, as suggested by the presence of a thick lateral layer of cartilage on the sides of the rostral cartilages were the enlarge denticle lateral series attach and the external layer "wood-like" cartilage in the rostrum. However, considering that no cranial nor enlarge denticles of the body are known and the highly specialized replacement of the lateral series of the rostral enlarge denticles, its phylogenetic relations are kept as *incertae sedis*.

Conclusion

The present analysis recovered two large monophyletic groups (Sclerorhynchidae and Onchopristidae). The family Ptychotrygonidae (Kriwet *et al*., 2009a) is placed as a subfamily of Sclerorhynchidae.

The Sclerorhynchidae family can be identified by the presence of a thin and leaf-shaped rostrum that reaches its maximum width after the base. The presence of enlarged lateral rostral series of denticles does not seem to be an exclusive characteristic for this group as it is absent in the Ptychotrygoninae subfamily and is a shared characteristic with the Onchopristidae.

Present analysis recovers a close relation between ptychotrygonoids (†*Asflapristis cristadentis* and †*Ptychotrygon rostrispatula*) and †*Libanopristis* supported by the presence of a transverse crest in the crown teeth labial face in three taxa. However, in general the teeth of †*Libanopristis* presents a more prominent cusp and the occlusal surface, specially the labial apron is less ornamented and Ptychotrygoninae lacks the rostral enlarged denticle series.

†*Onchopristis*, †*Schizorhiza* and surprisingly †*Ischyrhiza* are placed with the same clade mostly due to the similarities in their rostral cartilages. However, the taxonomic relations of †*Schizorhiza* are still in doubt as no cranial remains are known and its highly specialised replacement of the lateral rostral series differentiate the genus from the other members of the Onchopristidae family. †*Onchopristis* and †*Ischyrhiza* are proposed as members of the Onchopristidae family, based on the presence of enlarged denticles in the body, 'wood-like' cartilage in the rostrum and thick cartilage on the sides of the rostrum, This classification differs from previous ones (Cappetta, 2012) in which they were placed as part of Sclerorhynchidae.

Chapter 6

Estimating the divergence time of sclerorhynchoids: a batoid time scaled phylogeny with special interest on modern groups.

This chapter is an extended version of the following publications: Eduardo Villalobos-Segura and:

Estimating the divergence time of sclerorhynchoids: A batoid time scaled phylogeny. (in review).

Co-authors contributions

- o E. Villalobos Segura: Phylogenetic and time-scaling analyses. Discussion of the results.

- o C.J. Underwood: Discussion of the results.

Introduction

Phylogenetic comparative methods are a powerful tool for understanding biological evolution. These methods reach an even greater potential when are scaled trough time (Bapst & Hopkins 2017). This allows an estimation of divergence times and node ages by combining a set of fossil calibrations that constrain the minimum age of the nodes and a phylogenetic analysis or a phylogeny that includes those taxa or groups related to them (Lloyd *et al.* 2016). There are two main approaches for time-scaling a phylogeny: Tip-dating which simultaneously infer both relationships and divergence dates for a set of taxa and *a posteriori* time-scaling (APT) which dates a pre-existing unscaled topology, given a set of stratigraphic data for the taxa involved (Lloyd *et al.*, 2016; Bapst *et al.*, 2016).

Tip-dating is a relatively new approach, commonly implemented for the analysis of molecular data by Bayesian phylogenetic software (Bapst & Hopkins, 2017) (e.g. Mr Bayes or BEAST 2). In this approach uses fossils as priors to estimate maximum and minimum divergence times and assign a stratigraphic range to the branch lengths (changes between terminals). It is differentiated from other model-based analyses in that it looks for a set of nodal depths (distance between an ancestral node to is descendants) that maximize the probability of obtaining a data set. This allows the recovery of the series of ordered evolutionary events in a group, along with estimates for the magnitude of changes within and between groups and estimates for change rates. Which are calculated by constraining the occurrence times of key evolutionary events (Benton & Donoghue, 2007). The tip-dating approach requires character and stratigraphic data to generate a probability model that describes the expected waiting times between branching

events and clock model that makes assumptions on the rates of character changes across the tree. It can be strict (rates of characters changes are the same across the tree) or relaxed (variation in the rates of character changes across branches) (Stadler, 2010; Baum & Smith, 2013; Stadler & Yang, 2013).

A posteriori time-scaling (APT) methods work independently of the phylogenetic analysis and rely solely on occurrence data (Appendix 6.2). Most APT approaches involve simple algorithms that often translate to incongruence between the phylogeny and the order of stratigraphic appearance creating zero length branches (ZLB) (polytomies). This is problematic for trait evolution as any evolutionary changes across ZLB will appear as instantaneous (Bapst, 2013). To avoid the methodological issues of ZLB several successive methods have been developed (e.g. minimum length branches, equal branch length). These approaches suffer from arbitrary choices of required variables, make strong assumptions on the quality of the fossil record without reference to that fossil record (Lloyd, 2016) and do not allow uncertainties in node ages (Bapst, 2013).

Batoids are the most diverse group of Neoselachii (*sensu* Compagno, 1977) today, with approx. 665 species (Fricke *et al.,* 2019). Phylogenetically they are considered a monophyletic group in a sister group relationship to sharks (Dunn & Morrissey, 1995; Schwartz & Maddock, 2002; Douady *et al*., 2003; Winchell *et al.,* 2004; Aschliman *et al.,* 2012b; b; Naylor *et al.,* 2012; Last *et al.,* 2016). The earliest unambiguous fossil remains of the group come from the Early Jurassic (Toarcian) (Cappetta, 2012). However, a Late Triassic-Early Jurassic origin for the group has been suggested (Aschliman *et al*., 2012b), although no unequivocal Triassic remains have been found. Fossil batoids remain a poorly studied group and are mostly studied as part of larger studies of the Neoselachii despite the large ecological differences between them and sharks. Diversity estimation

analyses for Neoselachii suggest episodic events of diversification events in the Jurassic, Cretaceous and Paleocene (Kriwet & Benton, 2004; Underwood, 2006; Guinot *et al*., 2012a). Aschliman *et al*.´s (2012b) molecular time scaled phylogeny suggests similar time for those cladogenesis events.

Based in the phylogenetic analysis of Chapter 4, the present study presents an estimated divergence time for sclerorhynchoids. The analysis included the four genera (†*Sclerorhynchus, †Libanopristis, †Ptychotrygon, †Asflapristis*) with the most complete fossil record along with their oldest known appearance in the fossil record. The remains of †*Onchopristis numidus* (Chapter 3) were not considered for the present analysis as the 70% of the characters in the matrix are postcranial and visceral skeleton features which remain unknown in †*Onchopristis* and would make it a wild-card taxon in the analysis. Along with these sclerorhynchoid taxa, Jurassic and Cretaceous fossil species and fossil representatives of modern batoids clades were included in the analysis, making it the first time-scaled phylogenetic analysis using morphological data for batoids. Because of this, the results and discussion on this chapter deepens the implications of these estimates for the other batoids even if they are not the main objective of the chapter. The phylogenetic analysis included topological constraints to account for the phylogenetic relations recovered for the fossil taxa by previous works (de Carvalho, 2004; Naylor *et al.,* 2012; Claeson *et al.,* 2013; Brito *et al.,* 2013; Last *et al.,* 2016; Underwood & Claeson, 2017; Brito *et al.,* 2019; Villalobos *et al.,* 2019a) and designation of major extant taxonomic groups (orders) (Naylor *et al.,* 2012; Last *et al.,* 2016; Fricke *et al.,* 2019).

Both time-scaling methods (tip-dating and APT) were used and compared using stratigraphic consistency indices (Sansom *et al.,* 2018). The diversity ages estimated with tip-dating obtained higher stratigraphic consistency index scores and were compared with estimated divergence ages from molecular phylogenetic analyses (Aschliman *et al.,*

2012b) and previous diversity analyses (Kriwet & Benton, 2004; Underwood, 2006; Guinot *et al.,* 2012a) along with a taxic diversity estimate and shareholder quorum subsampling analyses to determinate if the diversity ages estimated by the time-scaling analysis overlap with diversity changes in the fossil record.

Material and Methods

Institutional abbreviations

AMNH: American Museum of Natural History. BHN: Muséum d'Histoire naturelle de Boulogne-Sur-Mer. BRC: Birkbeck Reference Collection. BSP: Bayerische Staatssammlung für Paläontologie und Geologie, Munich, Germany. CNPE-IBUNAM: National Collection of Fishes, Biology Institute, Universidad Nacional Autónoma de México (UNAM). JM-SOS: Jura Museum Eichstätt, Germany. MNHN: Muséum national d'histoire naturelle, Paris. NHMUK: Natural History Museum United Kingdom, London. UERJ: Universidade do Estado do Rio de Janeiro.

Specimens used

The same matrix as chapter 4 was used, with the inclusion of the following **fossil material**: †*Asterodermus platypterus* (NHMUK P 12067, 10934; JM-SOS 3647). †*Asterotrygon maloneyi* (AMNH P 11557; FMNH PF 12914, 12989, 12990, 14069, 14097, 14098, 14567, 15166, 15180; Specimens figured in de Carvalho (2004; text-figs. 1-13)). †*Cyclobatis major* (NHMUK P 4010, 4011, 49514 63175). †*Cyclobatis radians* (NHMUK P61243). †*Cyclobatis tuberculatos* (NHMUK PV P 10436). †*Cyclobatis oligodactylus* (NHMUK PV P 601). †*Iansan beurleni* (DGM-917, 918, NHMUK P 62947). *"*†*Dasyatis" zignii* (MGP-PD 150Z/151Z; Specimen figured in Marramà *et al.* (2018; text-fig. 8)). †*Heliobatis radians* (AMNH P 19665; FMNH PF 2020; Specimens

figured in de Carvalho (2004, text-figs. 28-29)). †*Promyliobatis gazolae* (MCSNV VII.B.90). †*Raja davisi* (NHMUK PV P 4780; FMNH UF 295). †*"Rhinobatos" tenuirostris* (NHMUK 4770). †*"Rhinobatos" maronita* (MNHN 1946.17.274, NHMUK P4012, 48215, 10696, 39233, 49511). †*"Rhinobatos" latus* (NHMUK PV P4014). †*"Rhinobatos" intermedius* (NHMUK PV P 49516; MNHN-SHA 1643). †*"Rhinobatos" grandis*; NHMUK PV P 4013, 49513, 13861. †*"Rhinobatos" whitfieldi* (NHMUK P 9145, 63187, 63199, 24965). †*"Rhinobatos" hakelensis* (MNHN 1946-17-272). †*"Rhinobatos" latus* (NHMUK PV P 4014). †*Rhombopterygia rajoides* (MHMH HDJ 483). †*Stahlraja sertanensis* (UERJ-PMB 400; MPSC-P 099; Specimen figured in Brito *et al.* (2013 text-fig. 3)). †*Tethybatis selachoides* (MCSNV 515-516, 511-512). †*Tingitanius tenuimandibulus* (NHMUK PV P66857; Specimen figured in Claeson *et al.* (2013; text-figs. 2-7)). †*Titanonarke molini* (MCSNV IG. VR.67290; Specimen figured in Marramà *et al.* (2018; text-figs. 3A)). †*Tlalocbatus applegatei* (IGM 5853; Specimen figured in Brito *et al.* (2019; text-figs: 2-3)).

Phylogenetic analysis

For the analysis the same matrix used in Chapter 4 with the inclusion of 18 extra fossil genera that included the oldest known skeletal remains of at least one fossil representative of the four orders of batoids (Rajiformes, Torpediniformes, Rhinopristiformes and Myliobatiformes), along with several fossil batoids of unknown phylogenetical relations (Appendix 6.1) was used. The matrix was analysed with Mr Bayes (3.2.6) (Ronquist & Huelsenbeck, 2003) in CIPRES (Miller *et al.,* 2010). The outgroup was composed of Jurassic batoids, as such the present analysis did not deal with the origin of batoids.

Two analyses with the same topological constraints were performed: a non-timescaled analysis to produce a phylogeny to be time-scaled using "*a posteriori*" methods and a tip-dating analysis.

To evaluate the results recovered by the different time-scaling methods, indices of stratigraphic congruence, were calculated for each tree topology using the R package **strap** (Bell & Lloyd, 2015) and the function **StratPhyloCongruence** (Appendix 6.3). These indices assess different things about the relations of a cladogram and the fossil record and should be reported together. However, none of the indices proposed to date are free of biases and are affected by different factors, (e.g. tree size, percentage resolution, tree shape, mean age of tree, range of first appearances, size of the character matrix), with tree balance (shape) as one of the main causes affecting the values of stratigraphy indices (O'Connor & Wills, 2016). As the different time-scaling methods present different approaches towards polytomies which ultimately can affect tree shape, the Colless' index an estimate of the tree shape and the percentage of resolution were estimated to quantify this change. The Colless' index was estimated in the R package **apTreeshape** (Bortolussi *et al*., 2005) using the function **colles** (Appendix 6.3). The percentage of resolved nodes calculated using O'Connor & Wills (2016) formula "$r/(n-2) * 100$", where r is the number of internal nodes and n is the number of taxa.

Divergence ages by the tip-dating analysis were compared with those obtained by molecular analysis (Aschliman *et al.,* 2012b). However, the molecular analysis does not present the same sampling of groups and does not provide a raw tree with ages as such a comparison using stratigraphic indices between the different results of the analysis was impossible. As such the divergence ages estimated by the molecular and the present analyses were compared using a more empirical approach using diversity curves to evaluate if the divergence ages estimated by these phylogenies overlap with diversity shifts.

Time-scaling methods

Tow *a posteriori* time-scaling methods were implemented, both of them are available in the R package **Paleotree** (Bapst, 2012) with the **timePaleoPhy** function and specified with the type parameter (Appendix 6.3):

- Minimum branch length (MBL) (Laurin, 2004) scales all branches, so they are greater than or equal to a time variable, and subtract time added to later branches from earlier branches in order to maintain the temporal structure of events.
- Basic (Smith, 1994) is the simplest of time-scaling methods it ignores time variable and scales nodes, so they are as old as the first appearance of their oldest descendant.

Tip-dating: Currently there is no standard method for tip-dating with morphological data. The selection of parameters was based on two papers Matzke & Wright (2016) and Bapst *et al.*, (2016) (Appendix 6.4). Two models of node calibration were used to calibrate the nodes with the commands fixed and uniform. Their results were compared using their marginal likelihood which is a measurement used to assess how well a set of models adjust to given data (Xie *et al*. 2010). The marginal likelihood was calculated using the steppingstone algorithm implemented in Mr Bayes (Xie *et al*. 2010). As the uniform command requires an interval of ages (a minimum and a maximum), in the cases of extant species with no fossil record the age of the oldest fossil representative within the clade was used as a maximum limit.

The node ages of the tip dated trees were observed with the FigTree (v.1.4.3) software (http://tree.bio.ed.ac.uk/software/figtree). The node ages for the ATP methods were recovered with the **GetNodeAges** function of the R package **claddis** Lloyd (2016) (table 4) (Appendix 6.3).

Indices used

***Stratigraphic Consistency Index* (SCI)** proposed by Huelsenbeck (1994). It assesses the congruence between first appearance date in the fossil record and nodal distances from the root. It is calculated as a ratio of the number of stratigraphically consistent nodes (i.e. those which their terminals are the same age or younger than those of its sister node) to the total number of nodes excluding the root. The SCI ranges from 0.0 (maximally inconsistent) to 1.0 (maximally consistent).

Gap Excess Ratio* (GER) *and derivatives proposed by Wills (1999) is expressed as the Minimum Implied Gap (MIG) scaled between the ghost ranges of the optimal (G min) and maximally suboptimal (G max) possible topologies. Its values range from 0.0 (maximally suboptimal fit) to 1.0 (optimal fit). However, the GER can never reach the theoretical minimum or maximum on a balanced tree, as the MIG can never be equal to either Gmin or Gmax.

***Modified Manhattan Stratigraphic Measure* (MSM)** proposed by Pol & Norell (2001). Can be derived from parsimoniously optimising the first appearance of taxa as an irreversible Sankoff character on a tree and calculating the total length of the resultant phylogeny. The MSM ranges from 1.0 when the Sankoff character is optimised with the minimum possible steps (best possible fit) and tends towards 0.0 as the number of steps increases (although a value of zero is never attained).

***Relative Completeness Index* (RCI)** proposed by Benton and Storrs (1994). It operates rather differently from the other indices. Nodes are not simply consistent or inconsistent, but rather contribute to an overall measure of "inconsistency" (the total ghost range or minimum implied gap MIG) in proportion to the difference between the ages of origin of the branches (or taxa) they support. The MIG is divided by the total observed range length

or standard range length (SRL), and the complement of this value expressed as a percentage to yield the RCI. The RCI is not limited to between 0 and 100 as it can have negative values if MIG is greater than the SRL (total observed range).

Diversity analysis

Seeking to indicate which methods reflect more the changes in diversity of batoids observed through their fossil record, diversity curves were used as mean to compare the diversity ages estimated by the different time-scaling methods and the possible diversity change events in their fossil record. The study of the implications of the biotic and abiotic factors that might affect and have affected the diversity of extinct and extant batoids these goes beyond the objective of the present chapter and requires further study.

Two approaches for estimation of diversity were used. Taxonomic diversity estimate (TDE) is simplest and requires minimal information. However, it has been shown to be biased by sampling heterogeneity and other sources of error in the sedimentary rock record, and may provide inaccurate estimates of diversity (Raup, 1972; 1976; Benton *et al*., 2011). Shareholder quorum subsampling (SQS) belongs to the standardized sampling methods. SQS is different from other standardized methods, as it does not follow the idea that uniform sampling = accurate sampling. Instead it is based on the principle that fair sampling = accurate sampling (i.e. the method must sample harder instead of uniformly when richness increases), to achieve this the algorithm instead of using the number of items uses the 'coverage' of the data set. The coverage of a species is relative to the frequency of appearances of it (i.e. a proportion of occurrences that belong to the species (Alroy, 2010).

• **TDE:** Measures the number of taxa in a time interval. It attempts to overcome bias by using higher taxa and range interpolation (first and last appearance) as a proxy for

estimating diversity. This approach is subject to a number of strong biases that arise from the incomplete nature of the fossil record, the different duration of the time intervals and variation in sampling intensity on different section of the stratigraphic record. It also cannot identify gaps in the fossil record that occur prior to a taxon first and last appearance in the stratigraphic record (Smith, 1994; Smith & McGowan, 2011).

- **SQS:** Targets the frequencies of data items. To do this it treats each species as a "shareholder" and their shares are the frequency of appearances which is given in respect to their proportion of occurrences. Because many taxa remain unknown a coverage of an entire frequency distribution is highly unlikely, therefore the quora are used which represent a certain amount of coverage, at which the majority of taxa could be sampled (Alroy, 2010). A variable of the code described in Alroy (2010) was used (http://strata.uga.edu/8370/rtips/shareholderQuorumSubsampling.html) with 100 subsampling trials for batoid occurrence data were performed, and the mean diversity was reported (Appendix 6.5).

Data used in the diversity estimates

For the TDE a database with the genus name and the first and last appearance in the fossil record was assembled. The dates assigned to the genera were based on a bibliographic review (Guinot *et al*., 2012a; Cappetta 2006; 2012). To assess the validity of the genera Cappetta (2006; 2012) taxonomic classification was used. For the SQS analysis a 2060 occurrence database (https://doi.org/10.5281/zenodo.3362508) was downloaded from Paleobiology Database. The level of classification within the occurrence database was used as exclusion criteria and records with no genus level taxonomic affiliation were removed leaving a 1934 occurrence data frame, from which the occurrences of the genus in the geological age were counted and the coverage estimated (https://doi.org/10.5281/zenodo.3362508).

Results

Time-scaling

Two models of node calibration were tested by the tip dated analysis: fixed and uniform. Between them it was the uniform age model that recovered the better marginal likelihood (-1177.45) compared to the fixed (-1182.44). Therefore, it was the model used.

Following O'Connor and Wills (2016) the stratigraphic indices estimated for each scaling method were compared along with their Colless' index and percentage of resolution (Table 6.1). All trees yield Colless' values lower than 0.5, suggesting that in all cases the topologies are balanced along with relatively high percentage of resolution. This last one (percentage of resolution) probably due to the use of only highly preserved specimens in the present analysis.

	SCI	RCI	GER	MSM	Colless' index	% resolution
Tip-dating	0.690	66.99	0.91	0.25	0.159	81.13
Basic	0.692	62.25	0.89	0.22	0.150	75.47
MLB	0.692	62.25	0.89	0.22	0.173	75.41

Table 6.1. Stratigraphic indices values, Colless' index and percentage of resolution estimated for the different time-scaling methods topologies. **Abbreviations:** SCI, Stratigraphic Consistency Index. RCI, Relative Completeness Index. GER, Gap Excess Ratio. MSM, Modified Manhattan Stratigraphic Measure.

Overall the tip-dating analysis recovered a better score in the values of GER and MSM and its topology implies fewer gaps in the fossil record (RCI ~ 67%) (table 6.1). Because of this and as tip-dating is the only method that implies possible changes in the phylogenetic relations of the groups during the time-scaling, its topology will be

compared to that of the non-timescaled tree used in the MBL and basic. Followed by a second comparison for the age nodes estimated with this analysis and those proposed by previous phylogenetic studies and in diversity analysis for the neoselachian group, (Underwood, 2006; Guinot *et al.,* 2012a; Aschliman *et al.,* 2012b).

Node	Tip-dating			MBL	Basic	FDA*
	95% L HPD	Mean	95% U HPD			
Jurassic (root)	157.34	166.04	176.20	178.7	177.7	177.7
Jur+Cret	145.57	159.49	173.60	177.6	175.6	175.6
Rajiformes+other batoids	109.93	128.77	147.47	120	113	113
Torpediniformes+ other batoids	99.80	99.74	132.60	120	113	113
Torpediniformes	86.64	106.04	126.61	99	93.9	93.9
Modern electric skates	38.19	49.97	67.46	62.7	58.7	58.7
Myliobatiformes	61.77	73.53	101.13	70.5	65.5	65.5
Sclerorhynchoidei-Rajiformes	98.56	115.54	133.78	116	113	113
Cyclobatis-Rajiformes	85.44	101.54	117.17	100.6	99.6	99.6
Rajoids	67.10	80.16	93.48	71.6	70.6	70.6
Rhinopristiformes	93.92	107.10	120.22	117	113	113
Modern rhinopristoids	32.24	47.86	65.58	58.8	55.8	55.8
Rhino+mylio	97.97	114.26	130.93	118	113	113

Table 6.2. Ages of the selected nodes recovered by the different time-scaling methods. **Abbreviation**: HPD, high posterior density interval. FDA*, first date appearance on the fossil record of the oldest taxon in the clade.

The different time-scaling methods used in the present analysis recovered discrepancies in the age nodes (table 6.2). Their variation in respect to the age of node estimates probably reflects the use of time data by the tip-dating analysis as part of the phylogenetic analysis, leading to slightly different topologies and percentage of resolution, than MBL and basic methods that do not solve polytomies. These modifications might push further back or forwards the age of a clade (e.g. the Rajiformes clade is more resolved in the tip-dating analysis as a result the rajoid clade (†*Raja davisi* + *Raja* and *Bathyraja*) is placed further back in time in the tip-dating analysis (10 Ma. more) than the other methods (Table. 6.2).

Phylogenetic analysis
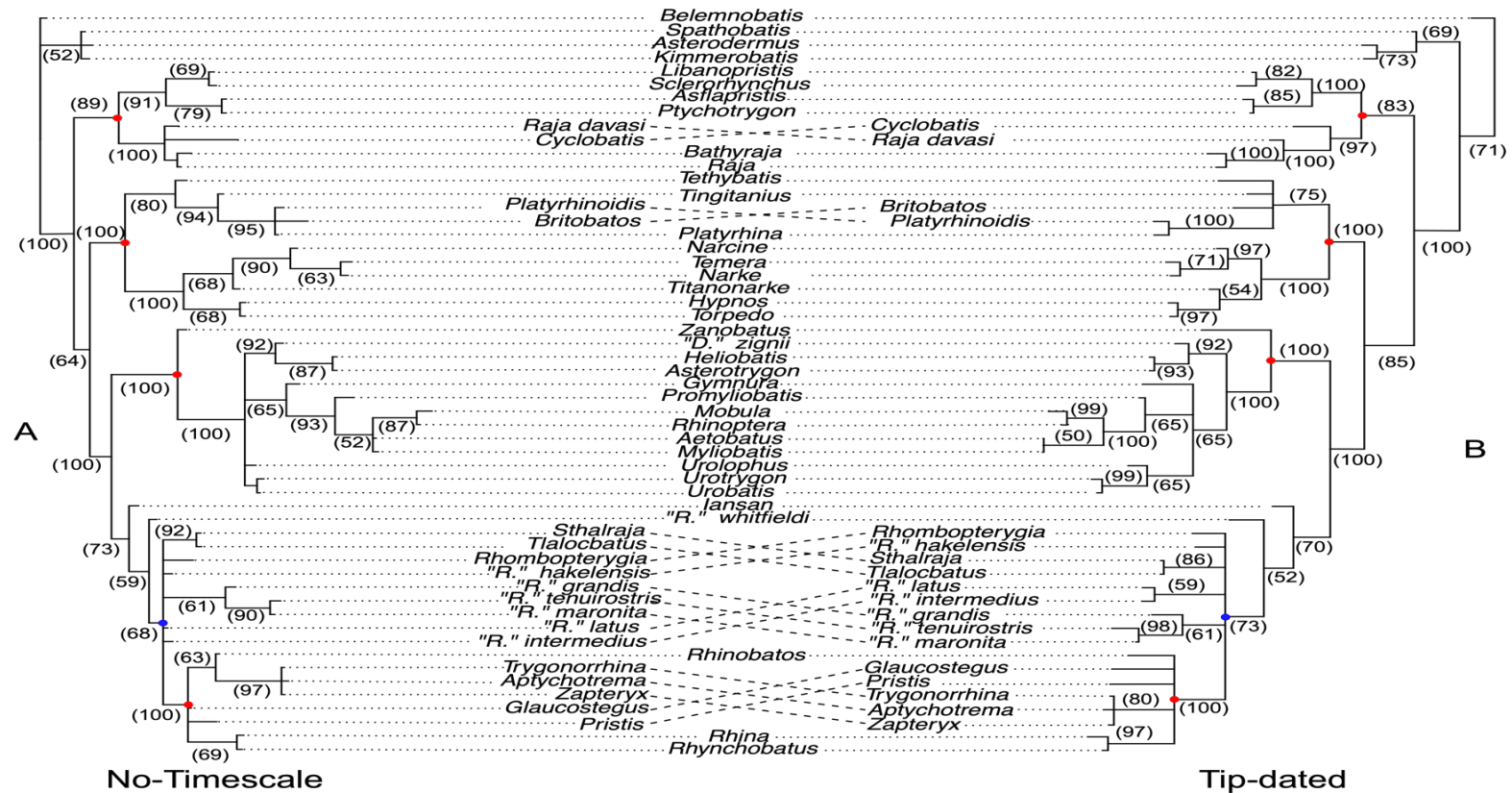
Figure 6.1. Phylogram resulted from the analyses; clade credibility is placed beneath the clades. **A,** Non-timescaled and **B,** Tip-dating. Orders mark with a red dot. Rhinopristiformes+Cretaceous batoids politomy mark with a blue dot.

Both analyses (non-timescaled and tip-dated) recovered four large monophyletic groups which represent the four recognized orders of batoids (Fricke *et al.,* 2019) marked in red (Fig. 6.1), with a similar arrangement of these groups (orders) as that recovered by molecular analyses (Douady *et al*., 2003; Aschliman *et al.,* 2012b; Naylor *et al.,* 2012; Last *et al.,* 2016) (Fig. 6.1). The present topology is characterized by a large polytomy that includes several Cretaceous batoids (†*"Rhinobatos" grandis,* †*"R." latus,* †*"R." intermedius,* †*"R." hakelesis,* †*"R." tenuirostris,* † *"R" marinota,* †*Rhombopterygia,* †*Stahlraja* and †*Tlalocbatus*) which were placed as part of "comb" (Fig. 6.1 marked in blue), that includes the Rhinopristiformes (Posterior probability (Pp) = 68%; Fig. 6.1A, Pp = 73; Fig. 6.1B). This group was produced as a result of a topological constraint that included Myliobatiformes and modern Rhinopristiformes trying to reduce the comparison available for these fossil taxa and information from previous works (e.g. Claeson *et al.,* 2013; Georges 2016; Underwood & Claeson, 2017; Brito *et al.,* 2019). However, both analyses (No-Timescale and Tip dated) failed to regain the relations found by those previous analyses for these fossil taxa. No apparent further affiliation than a close relation to Rhinopristiformes for these fossil taxa was recovered by both analyses.

In both analyses the Jurassic batoids are no longer recovered in a close relation to any member of Rhinopristiformes, this contrast with previous works (Claeson *et al*., 2013; Underwood & Claeson, 2017) regardless of their morphological similarities. The non-timescaled analysis placed †*Belemnobatis* at the base of a polytomy within a monophyletic group composed of the remaining Jurassic batoids (Pp =100%; Fig 6.1A). The tip dated analysis recovers †*Belemnobatis* diverging next to the remaining Jurassic taxa (†*Spathobatis,* †*Kimmerobatis* and †*Asterodermus*) with a posterior probability = 71% (Fig 6.1B). The Jurassic taxa are placed in a monophyletic group (Pp = 69) and as a sister group to all remaining batoids (Pp = 100%; Fig 6.1B).

Rajiformes (Sclerorhynchoidei+rajoids) is placed close to the Jurassic batoids as the following group to diverge and in both analysis (time-scaled and not scaled) is placed in a sister group relation to the remaining batoids (Pp = 89%; Fig. 6.1A, Pp = 83%; Fig. 6.1B) this relation was previously recovered in Chapter 4. Both analyses placed †*Cyclobatis* as a sister and within Rajiformes as suggested by Claeson (2010) (Pp = 100% Fig. 6.1A, Pp = 97%; Fig. 6.1B). The tip dated analysis further places †*Raja davisi* as a sister group to modern rajoids as suggested by Georges (2016) (Pp = 73%; Fig. 6.1B).

Following the phylogenetic relations proposed by molecular data (Naylor *et al*., 2012; Last *et al*., 2016) and the uncertainty with morphological data (Chapter 4 and Aschliman *et al.* 2012a), a topological constraint was used for Torpediniformes to include Platyrhinidae. In general, the non-scaled analysis recovered a more resolved topology, which places †*Tethybatis* (Pp = 80%; Fig. 6.1A) as a sister group for the remaining platyrhinoids (†*Tingitanius,* †*Britobatos, Platyrhina* and *Platyrhinoidis*).

 †*Tingitanius* is the next taxa to diverge (Pp = 94%; Fig. 6.1A) followed by the polytomy that includes †*Britobatos* and modern platyrhinoids (Pp = 95%; Fig. 6.1A). The placement of these fossil taxa within Platyrhinidae was suggested by De Carvalho (2004); Claeson *et al*. (2013) and Brito *et al.* (2013). Whereas the tip dated analysis places the fossil taxa along with modern platyrhinoids in a polytomy (Pp = 75%; Fig. 6.1B). Similar topologies are recovered for the electric skates by both analyses, with the only difference being the placement of †*Titanonarke,* which is recovered as a sister taxa to the *Narcine, Narke* and *Temera* clade (Pp = 68%) by the non-timescaled analysis and as a sister taxa to the *Hypnos* and *Torpedo* clade (Pp = 54%).

Both analyses recovered a similar arrangement for Myliobatiformes to that proposed by molecular analysis (Aschliman *et al.,* 2012b; Naylor *et al.,* 2012). The panrays (*Zanobatus*) are recovered as a sister group for the remaining myliobatoids (Pp = 100%;

Fig. 6.1A-B). The placement of the monophyletic group that includes the fossil myliobatoids (†*Heliobatis*, †*Asterotrygon*, †*"Dasyatis" zignii* and †*Promyliobatis*) changes between both analyses (Pp = 92; Fig, 6.1A-B). The tip-dating analysis recovers a more resolved topology, placing the fossil myliobatoids as a sister group for the remaining Myliobatiformes with the exception of *Zanobatus* (Pp = 100%; Fig. 6.1B). Whereas the non-times scaled analysis place the fossil clade as part of a polytomy (Pp = 100%; Fig. 6.1A) that includes all of the remaining myliobatoids in a slightly similar position is to that recovered by De Carvalho *et al.* (2004) at least for †*Heliobatis* and †*Asterotrygon* as †*"Dasyatis" zignii* was not included in that study.

†*Promyliobatis* is recovered in a close relation to (Myliobatinae, *Rhinoptera* and *Mobula*) (Pp = 93%; Fig. 6.1A, Pp = 65%; Fig. 6.1B). This relation was expected as the fossil remains suggest a clear kinship with Myliobatinae.

All modern Rhinopristiformes are placed in a polytomy by both analyses, with includes two monophyletic groups: Trygonorrhinidae (Pp = 97; Fig. 6.1A, Pp = 80; Fig. 6.1B) and *Rhina+Rhynchobatus* (Pp = 69; Fig. 6.1A, Pp = 97; Fig. 6.1B). Both of these clades have been recovered previously by molecular data (Aschliman *et al.,* 2012b; Naylor *et al.,* 2012; Last *et al.,* 2016).

Tip dated analysis

In general, the tip-dating analysis recovered a topology with long internal branches. This pattern could indicate a rapid radiation after an extended period of slow diversification. However, it could also reflect the incompleteness of skeletal remains in the fossil record of batoids (Rees, 2002; Underwood & Rees, 2002). The means of the intervals estimated by the present analysis should be considered as a minimum boundary as the clades recovered were already well-established and differentiated from each other by those

times. Of more interest are the upper values of the high posterior density interval (HPD) proposed by the tip-dating which in most cases moves further back from the known fossil records the possible origin of the clades and groups.

The present analyses (tip-dating and APT) did not deal with the possible origin of batoids, as the fossils record from the Late Triassic-Early Jurassic is mostly composed of teeth and therefore were not included in the analysis. However, molecular analyses place the origin of batoids in the Late Triassic-Early Jurassic (approx. 230 and 200 (Ma.) million years ago) (Delsate & Candoni, 2001; Aschliman *et al*., 2012b). Suggesting an origination time preceding the first appearance of any extant shark groups and hence indicate an origin within the Triassic neoselachians. Currently there are no unequivocal batoid remains form the Late Triassic, however, based on histological similarities (lack of a multiple enameloid layer on teeth) it is hypothesised that some neoselachian remains from the late Triassic (e.g. †*Doratodus,* †*Vallisia* and †*Pseudodalatias*) could be in fact early representatives of batoids (Cuny & Benton, 1999; Botella *et al.,* 2009).

The oldest unambiguous batoid remains come from open marine environments of the Toarcian (Lower Jurassic, approx. 182.7 to 174.1 Ma), period characterized as a rapid cladogenesis episode for neoselachians probably driven by the colonization of new habitats as a consequence of transgression (Underwood, 2006). The fossil remains of this period are mostly fragmentary and dominated by teeth of genera like †*Toarcibatis* and †*Cristabatis* (Cappetta, 2012) with rarer occurrences of †*Belemnobatis* and †*Spathobatis* (Delsate & Candoni, 2001). The Mid-Late Jurassic (Bathonian to Tithonian) neoselachian faunas have been described several times (Martill, 1991; Kriwet, 2003; Kriwet & Klug, 2004; Underwood, 2006; Tennant *et al*., 2017) and batoid diversity remains represented by just two genera (†*Spathobatis* and †*Belemnobatis*). This apparent homogenization of batoids diversity could be attributed to the reduced diversification and extinction rates of

neoselachian product of the absence of barriers in the seas (Kriwet *et al.*, 2009b). However, there seems to be an important biasing factor in sampling as all Jurassic batoids collected are from near-shore marine sediments and therefore unlikely that it represents a full census of the batoid diversity and at that time.

The present analysis included the only four Jurassic genera (†*Asterodermus, †Belemnobatis, †Kimmerobatis* and †*Spathobatis*) known from skeletal remains, which by no means should be considered basal groups as they share several synapomorphies with extant species (e.g. synarcual product of the of lateral expansion of vertebral centra. presence of antorbital cartilages and aplesodic pectoral fins) and suggest that by the Late-Middle Jurassic batoids where already a well-differentiated monophyletic group and that the overall morphology of batoids has changed little since that time supporting an even earlier appearance in time as suggested by the molecular data (Aschliman *et al.,* 2012b). The node age for the divergence between Jurassic taxa and the clade leading to Cretaceous+modern (Clade 1) is estimated between 145.57-173.60 Ma. (Fig. 6.3A) with a mean of 159.49 Ma. (Oxfordian) (Fig. 6.2). †*Spathobatis* is recovered as a sister group to the remaining Jurassic taxa, the node age for clade 9 is estimated between 138.43-168.22 Ma. (Fig. 6.3I) with a mean of 153.07 Ma. (Kimmeridgian) (Fig. 6.2).
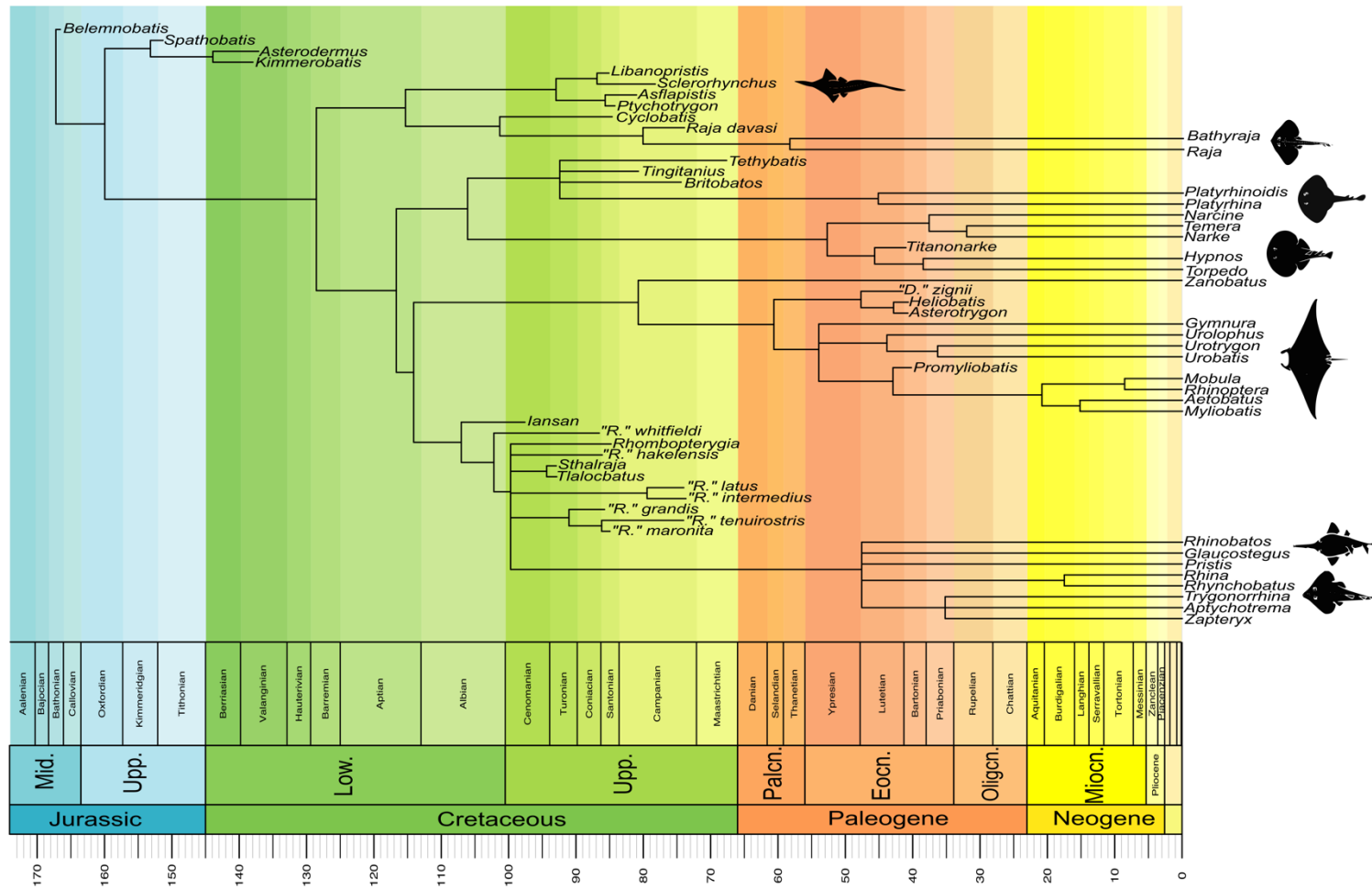
Figure 6.2. Phylogenetic tree recovered from the tip-dated analysis.

188
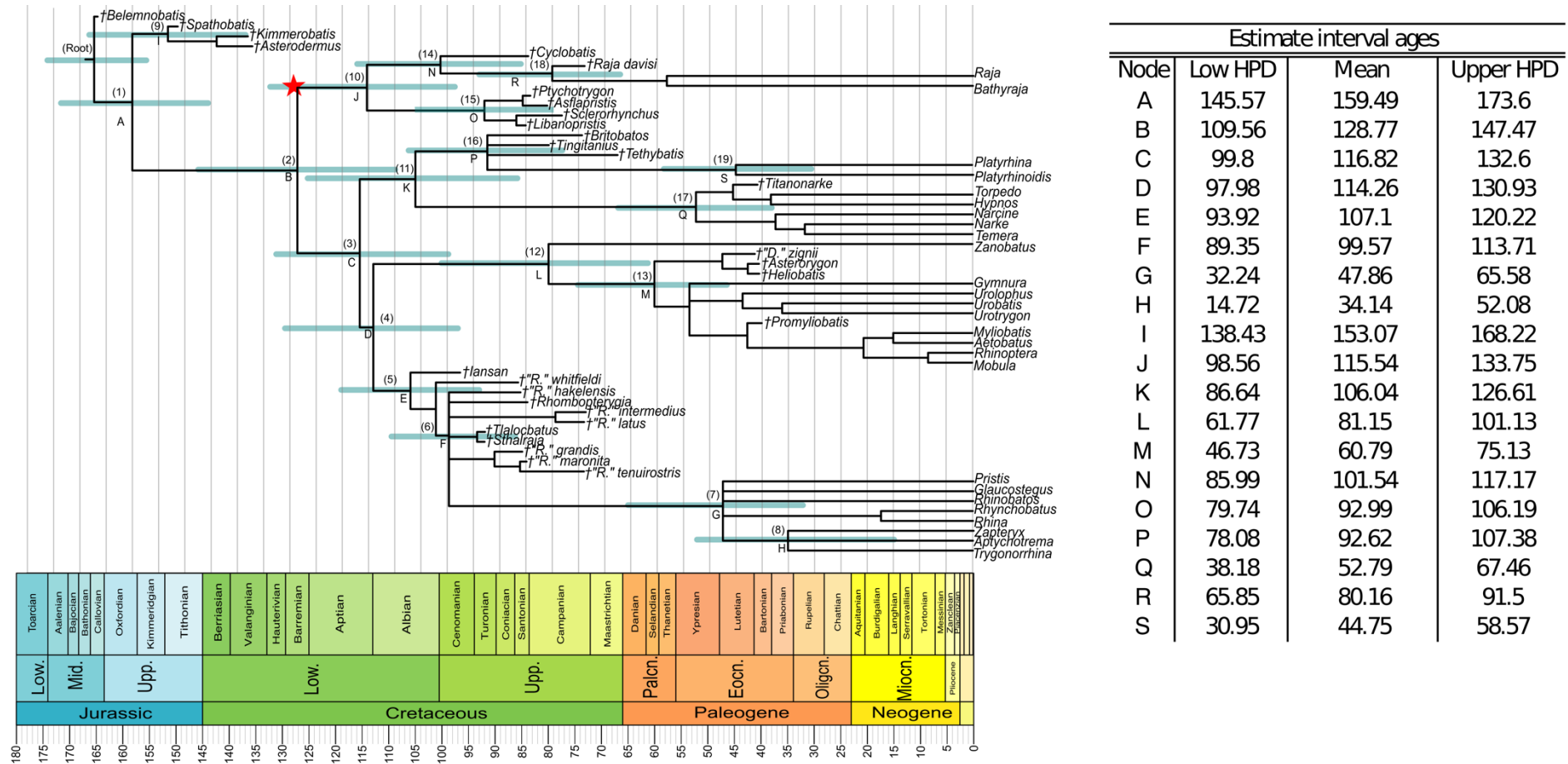
Figure 6.3. Tip-dated tree with estimated divergence ages marked in blue for the relevant clades. Letters refer to the estimated ages. Number in prarenthesis refer to the nodes. Age of the oldest fossil record of sclerorhinchoids mark with a red poin.

The following node to be differentiated contains all the remaining batoids (Clade 2) is divergence time is estimated between 109.56-147.47 Ma. (Fig. 6.3B) with a mean of 128.77 Ma. (Barremian) (Fig. 6.2). This time estimation suggests an important diversification event for batoids during the Late Jurassic-Early Cretaceous. The Late Jurassic represents the earliest time period from which both boreal and Tethyan neoselachian faunas are well known (Underwood, 2006) and is characterised by a combination of short-term catastrophic events, produced from fragmentation of Pangaea (Scotese, 1991; Nürnberg & Müller, 1991; Monger *et al*., 1994; Shephard *et al.,* 2013). Episodes of transgression and regression of sea level, shifts of circulatory regimes and nutrient flux (Danelian & Kenneth, 2001; Cuny & Benton, 1999) decimated reef environments leading to dramatic faunal and ecological turnovers in the sea between shallow shelf-dwelling faunas, to more mobile and ecologically plastic groups, which favour neoselachian diversification (Kriwet, 2003; Rees, 2005).

Diversity estimation analysis suggest a steady increase of neoselachian diversity thought the Late Jurassic-Early Cretaceous. With its lowest point in the J/K (Jurassic-Cretaceous) boundary, as a result of decreased origination rates and heightened extinction rates (Kriwet & Klug, 2008; Kriwet *et al*., 2009b) and reaching its peak at the Late Cretaceous (Underwood, 2006; Guinot *et al.,* 2012a). Present results suggest that this increase in diversity might not been as gradual, and that Early Cretaceous diversity might be significantly higher. Several divergence events are placed in the Early Cretaceous and suggest an active cladogenetic period, that lead to the Late Cretaceous high diversity.

- Clade 10 includes Rajoids+sclerorhynchoids and is placed as sister group of the remaining batoids. This has been already stablished by molecular analyses (Aschliman *et al.,* 2012b; Naylor *et al.,* 2012; Last *et al.,* 2016). Within this clade two monophyletic groups are found one that includes all rajoid associated taxa (†*Cyclobatis* and †*Raja*

davisi) and other including all sclerorhynchoid taxa. The node age estimated for this clade is between 98.56 and 133.75 Ma. (Fig. 6.3J) and a mean of 115.54 Ma. This result suggest that Rajiformes were already a well-stablish monophyletic group in the Aptian (Fig. 6.2). The upper limit of the high posterior density interval (HPD) suggests a split between these two groups as late as the Valanginian (132.9-139.8 Ma).

• Torpediniformes, Rhinopristiformes (along with several Cretaceous taxa) and Myliobatiformes node age is estimated between 99.80-132.60 Ma. (Clade 3; Fig. 6.3C) with a mean of 116.82 Ma. (Aptian) (Fig. 6.2).

• Within the Torpediniformes two monophyletic groups are recovered (Clade 11) one that includes †*Tethybatis*, †*Britobatos*, †*Tingitanius* and extant platyrhinoids as suggested by De Carvalho (2004) and Claeson *et al*. (2013) and other including all electric skate taxa as suggested by molecular analysis Naylor *et al.* (2012) and Last *et al.* (2016). The divergence age for the clade is estimated between 86.64-126.61 Ma. (Fig. 6.3H) and a mean of 106.04 Ma. (Albian) (Fig. 6.2) with a split leading to both groups as late as the Barremian. and constrains this fossil taxa within Torpediniformes (*sensu* Naylor *et al.,* 2012).

• Clade 4 includes Rhinopristiformes (along with several Cretaceous taxa) and Myliobatiformes. Its divergence age is estimated between 97.98-130.93 Ma. (Fig. 6.3D) with a mean of 114.26 Ma. (Aptian) (Fig. 6.2).

• Within the Rhinopristiformes several fossil taxa are recovered as a sister group to modern rhinopristiforms with †*Iansan* at the base of clade 5. The divergence time estimated for this clade is between 93.92-120.22 Ma. (Fig. 6.3E) and a mean of 107.10 Ma (Fig. 6.2). Present results place Rhinopristiformes as a monophyletic group in the Albian with a divergence time as late as the Aptian.

These cladogenetic events suggest changes in the dynamic of this diversity increase and that the steady increase in diversity recovered by diversity analyses (Underwood, 2006;

Guinot *et al.,* 2012a) is a product of the transition between a period with poor fossil record to one more complete (e.g. not a single marine neoselachian fauna has been described for the Berriasian and the only three neoselachian species are known from the brackish facies (Underwood 2006)). Current standardization methods cannot adjust time intervals with zero diversity. Therefore, any diversity changes from an unsampled time bin to a sampled one will be an artefact of sampling.

Regardless of the cause, all diversity curves studies reviewed (Underwood, 2006; Kriwet *et al.,* 2009b; Guinot *et al.,* 2012a), suggest that Late Cretaceous standing diversity was substantially higher than Late Jurassic. This high stand in diversity is often correlated to the substantial rise of global sea level during the Cretaceous, caused by the spreading of the Atlantic and the rise of temperature that reached its highest point in the Turonian-Cenomanian (Miller *et al.,* 2005; Tennant *et al.,* 2017).

Neoselachian diversity presents an episodic increase in diversity during the Late Cretaceous (Underwood 2006; Kriwet *et al.,* 2009b; Guinot *et al.,* 2012a). The increasing tendency for the group is kept until the Cenomanian-Turonian anoxic event, in which there is a sudden drop in the number of taxa, followed by a steady recovery in diversity throughout the Coniacian/Santonian. During the Santonian/Campanian there is another decrease in diversity, which has also been found in other marine organism diversity curves (Lloyd *et al.,* 2012) but has not been attributed to a specific geological event. Finally, neoselachian diversity reaches its maximum during the Campanian-Maastrichtian (approx. 83.6-66 Ma) (Underwood, 2006; Guinot *et al.,* 2012a).

Present analyses place several Late cretaceous fossil taxa as sister groups of the extant clades of batoids. Of the extant batoids, the rajoids (Clade 14) extend the furthest back in this period. Within this clade a †*Cyclobatis* is placed as a sister group of the remaining rajoids (as suggested by Claeson, 2010), with a divergence time estimated between 85.99-

117.17 Ma. (Fig. 6.3N) with a mean of 101.54 Ma. (Albian) (Fig. 6.2), the upper value of the HPD suggest a divergence time in the Aptian. †*Cyclobatis* is a rather interesting taxon morphologically similar to rajoids (e.g. pelvic fin divided in to two lobes anterior and posterior) and sting rays (e.g. reduced antorbital cartilages). Clade 18 recovers †"*Raja*" *davisi* as sister group to modern rajoids as previously suggested by Georges (2016) with a divergence time estimate between 65.85-91.50 Ma. (Fig. 6.3R) and a mean of 80.16 Ma. This result suggests "rajoid-like" taxa were well established as a monophyletic group in the Campanian (Fig. 6.2), with a divergence time as late as the Early Cenomanian.

Clade 16 includes the ancestors of extant platyrhinoids (De Carvalho, 2004; Claeson *et al*., 2013) The divergence time estimated places the split of the group leading to modern groups between 78.08-107.38 Ma. (Fig. 6.3P) and a mean of 92.62 Ma. This result suggests a that platyrhinoids were a well-defined monophyletic group before the Turonian (Fig. 6.2).

Clade 12 includes †*Heliobatis*, †*Asterotrygon,* †*"Dasyatis" zignii* and †*Promyliobatis* which are recovered as part of the Myliobatiformes, with *Zanobatus* being placed at the base of the group in a similar arrangement to that proposed by molecular analysis (Naylor *et al.,* 2012; Last *et al*., 2016). The divergence time for the clade is estimate between 61.77-101.13 Ma. (Fig. 5.3L) and a mean of 81.15 Ma, which suggest that Myliobatiformes were already a well-establish monophyletic group in the Campanian, with an earliest estimated divergence time in the Early Cenomanian.

Clade 6 includes several "rhinobatid like" fossils (†*"Rhinobatos" grandis,* †*"R." whitfieldi*, †*"R." hakelensis,* †*"R." tenuirostris,* †*"R." latus,* †*"R." intermedius* †*"R." maronita,* † *Rhombopterygia*, †*Tlalocbatus* and †*Stahlraja*) taxa previously classified within Rajiformes within the suborder Rhinobatoidei (*sensu* Cappetta, 2012). Present results place these fossil taxa as a sister group to Rhinopristiformes (*sensu* Naylor *et al.,*

2012). This affiliation was previously proposed for some of the fossil taxa within this group (e.g. *Tlalocbatus*) (Brito *et al*., 2019). The divergence time for the clade is estimated between 89.35-113.71 Ma. (Fig. 6.3F) and a mean of 81.15 Ma. This result suggests that Rhinopristiformes were already a monophyletic group in the Cenomanian (Fig. 6.2), with an earliest estimated divergence time in the Aptian.

The K/Pg boundary is a complex period for batoids as extinctions seem to affect unevenly depending on the taxonomic level analysed (family, genus, species). More exclusive taxonomic levels (species and genera) seem to be more affected by these extinctions (Kriwet & Benson, 2004). This reflects the problems of dealing with higher systematic groups when addressing biodiversity and extinction patterns. But also shows problems with the allocation of fossil species into higher taxonomic units specially in batoids (e.g. under current taxonomic classification (Cappetta, 2012) families like Rhinobatidae extend form the Lower Jurassic till present and no order has become extinct since the origin of the subclass Batoidea).

After the K/Pg boundary and through the Paleogene there is a rapid recovery in neoselachian diversity (Underwood, 2006; Guinot *et al.,* 2012a). Thoughout this period there are shifts in global climate, from a warm earth with the high sea levels during the Eocene (Miller *et al.,* 2005) to a colder climate with glaciation in the Oligocene. This reduction on earth's temperature, is a result of continental drift (Ehrmann & Mackensen, 1992). (e.g. Northward drift of Australia and India, the opening of the Drake Passage and the Circum-Antarctic current is established leading to the thermal isolation of Antarctica). These climatic cooling events occurred in a series of threshold events with the transition between events marked by rapid cooling that caused a decrease in the sea level and possible an inverse effect to the Cretaceous warm. The cooling of the sea also had an effect in primary production in the seas which causes stress in higher up in the food chain

leading to changes in the diversity (Corliss *et al*., 1984). This is supported by the present analysis, which place the radiation of all modern batoids clades in the Early-Middle Paleogene period.

- Clade 19 is composed by the *Platyrhina* and *Platyrhinoidis* with an estimated divergence time between 30.95-58.57 Ma. (Fig. 6.3S) and a mean of 44.75 Ma. (Lutetian) (Fig. 6.2).

- Clade 17 recovered †*Titanonarke* within the electric skates with an estimated divergence time between 38.19-67.46 Ma. (Fig. 6.3Q) and a mean of 52.79 Ma. (Ypresian) (Fig. 6.2)

- Clade 13 recovered †*Heliobatis*, †*Asterotrygon*, †*"Dasyatis" zignii* as a sister group to more derived myliobatoids the divergence time estimated for is between 46.73-75.13 Ma. (Fig. 6.3M) with a mean of 60.79 Ma. (Selandian) (Fig. 6.2)

- Clade 7 which includes al modern genera of Rhinopristiformes also underwent an important radiation event during the Palaeocene with an estimated divergence time between 32.24-65.58 Ma. (Fig. 6.3G) and a mean of 47.86 Ma. (Lutetian) (Fig. 6.2). Unfortunately, the present topology for the group is less resolved than that recovered by molecular analysis (Aschliman *et al.,* 2012b; Naylor *et al.,* 2012; Last *et al.,* 2016). Trygonorrhinidae (Clade 8) is recovered as a monophyletic group within this polytomy and the present analysis estimates its divergence time between 14.72-52.08 Ma. (Fig. 6.3H) and a mean of 34.14 Ma. (Priabonian) (Fig. 6.2).

Discussion

Comparison between time-scaled analyses

Tip-dating recovered larger discrepancies in its node ages estimations when compared with the fossil record and the other time-scaling methods (Table 6.2). This is probably

caused by the adjustment to the nodal depths that the tip-dating analysis does in order to maximize the probability of obtaining a data set. Overall tip-dating obtained better stratigraphic indices that the other time-scaling methods. However, this comparison might be unfair considering the simplistic approach the of the basic and minimum length branch methods.

Recently a stochastic APT method using more complex algorithms was developed, the three-rate calibrated time-scaling cal3 method (Bapst, 2013) is based in the node-dating approach of Hedman (2010) and is incorporated in the R package **Paleotree**. A comparation between tip-dating and cal 3 could be more proper. However, the current non-time scaled tree topology (Fig 6.1A) with large polytomies (more than 3 taxa) (e.g. Rhinopristiformes+Cretaceous batoids clade) could be problematic because, Cal3 assigns node ages using a zipper movement in which descendant nodes cannot occur before ancestral nodes (Bapst 2013), similar to the consistent nodes of the SCI (Siddall, 1996,1998). Larger polytomies will result in such nodes presenting short or no time intervals, resulting in similar ages as those recovered by the basic method, which could also affect nearby clades giving the a much earlier or later age. This can be prevented by randomly solving the polytomies before time-scaling the tree or by using the ages of the taxa. However, the clades produced will not be derived from a character analysis and because of this it was not used.

Divergence of sclerorhynchoids

Two events in sclerorhynchoid evolution are recovered in the present analysis: the divergence of sclerorhynchoids and rajoids and the divergence of Ptychotrygoninae (see Chapter 6) from other sclerorhynchoids.

- **Divergence of sclerorhynchoids and rajoids** (Clade 10)**:** For the results present in this chapter only the first and last appearance of †*Libanopristis*, †*Sclerorhynchus*, †*Asflapristis* and †*Ptychotrygon* were used. The estimated ages for this event was 98.56-133.75 Ma. (Fig. 6.3J) with a mean of 115.54 Ma (Aptian) (Fig. 6.2). A second analysis (Appendix 6.7-8) using the oldest known record for the suborder (Barremian; Kriwet & Kussius, 2001) estimated divergence age for this event where the oldest record was 103.82-139.45 with a mean of 121.11 Ma. The higher limit of both estimate ages places the possible origin of sclerorhynchoids earlier than is oldest fossil record within the Valanginian (132.9-139.8) (Figs. 6.2 and 6.3J).

- **Divergence of Ptychotrygoninae (see Chapter 6) from other sclerorhynchoids (Clade 15):** The estimated ages (79-106.19 with a mean of 92.98 Ma.) (Fig. 6.3O) for this event in the present study suggest a possible origin of Ptychotrygoninae within the oldest period reported for the group (Albian; Kriwet, 1999a; Kriwet *et al*., 2009a; Kriwet & Kussius, 2001) (Figs. 6.2 and 6.3O).

Node	Present study			Aschliman *et al.* 2012b Bayesian		
	95% L HPD	Mean	95% U HPD	95% L HPD	Mean	95% U HPD
(a) Jurassic	157.34	166.04	176.20	173.8	187.8	203.5
Jur+Cret	145.57	159.49	173.60			
Rajiformes+other batoids	109.93	128.77	147.47			
(b) Torpediniformes+ other batoids	99.80	99.74	132.60	164.9	177.6	191.9
Torpediniformes	86.64	106.04	126.61	150.2	164.2	179.7
Modern electric skates	38.19	49.97	67.46	64.6	72.8	93.7
Myliobatiformes	61.77	73.53	101.13	134.5	142.2	151.3
Sclerorhynchoidei-Rajiformes	98.56	115.54	133.78			
Cyclobatis-Rajiformes	85.44	101.54	117.17			
Rajoids (Rajidae-Bathyrajidae)	67.10	80.16	93.48	64.6	78.4	93.7
Rhinopristiformes	93.92	107.10	120.22			
Modern rhinopristoids	32.24	47.86	65.58			
(c) Rhino+mylio	97.97	114.26	130.93	148.5	158.9	170.4

Table 6.3. Comparison between the estimated divergence ages by the present study and Aschliman *et al.* (2012b).

Overall, the results of the present analysis recovered later divergence time intervals when compared to the ages estimated by molecular analysis (Aschliman *et al*., 2012b; text-fig. 4) (i.e. molecular analysis gives a longer evolution time for the batoids clades). Aschliman *et al*. (2012b) propose an Early-Middle Jurassic age for the divergence leading to the major groups of batoids (rajoids, torpedinoids, myliobatoids and rhinopristoids) with additional divergence within those groups during the Late Cretaceous-Early Paleocene. Whereas the present analysis places all major divergence events leading to all extant orders of batoids in the Late Jurassic-Early Cretaceous with subsequent divergences within these clades during the Late Cretaceous and Early-Mid Paleocene (Table 6.3).

There are several methodological differences regarding the use of fossil dates between both methods. The node calibration is more complex and inform in molecular analysis by the use of evolutive models. However, one of the differences between the present analysis and Aschliman *et al*., 2012b could be the inclusion of †*"Dasyatis" speetonensis* Underwood *et al*., 1999. In the molecular analysis †*"D." speetonensis* is used as the calibration lineage for the analysis, which is the lineage with the greatest proportion of its true temporal range captured by the fossil record. The age of the oldest fossil of this lineage provides the best minimum age constraint for calibrating the phylogeny (Marshall, 2008). If this fossil is considered a myliobatiform, it pushed the known age of the group by 30 Ma. leaping from the Cenomanian (possible Albian) to the Hauteruvian (Underwood *et al*. 1999) and being the calibration lineage it subsequentially moves back all the remaining clades. †*"D." speetonensis* was not include in the present analysis as the fossil species is only known from tooth remains and could not be coded as a terminal for a matrix based on skeletal characters and also due to the taxonomic uncertainties associated with the taxon (Cappetta, 2012). The time interval estimated for Myliobatiformes in the present analysis places the radiation of the group as late as the Albian which approximates to the oldest unambiguous fossil record for the order

†*Enantiobatis tarrantensis* Cappetta & Case, 1999 (Cenomanian). However, the divergence age estimated between Rhinopristiformes and Myliobatiformes falls within the time range of † *"Dasyatis" speetonensis* and could suggest that some representatives of Myliobatiformes were present at that time.

The divergence between rajoids and other batoids is another major difference between both studies, mostly because they work under different definitions of the order Rajiformes. Aschliman *et al.* (2012b) present a broader delimitation of the order in which the Jurassic batoids were considered members of the Rajiformes (*sensu* Cappetta, 2012). Following the phylogenetic results of the present study (Chapter 4 and 6) which place the Jurassic batoids in a clade separated from Rajiformes and are considered separate groups. This taxonomic discrepancy pushes further back the subsequent clades radiating from Rajiformes (Aschliman *et al*., 2012b; text-fig. 4). The estimate of the divergence of Rajoids with other batoids of the molecular analysis is compared with the divergence estimate between the Jurassic batoids and the remaining batoids recovered by the present study.

The divergence ages estimated by the present analysis overlay better with the diversity shifts observed of the known fossil record and present a smoother succession of cladogenetic events, with the divergence leading to all extant order of batoids overlaying with the diversity recovered after the J/K extinction event and rise of diversity through the Cretaceous (Fig. 6.4A-D) (Guinot *et al*., 2012a). Aschliman *et al.,* 2012b estimated divergences events in the Early-Middle Jurassic with subsequent ones leading to the major groups (rajoids, torpedinoids, myliobatoids and rhinopristoids) in the Middle-Late Jurassic contrast with the relative static diversity of neoselachian in that period (Kriwet *et al.,* 2009b) and diversity curves (Fig. 6.4A-D). The similarities between the divergence ages estimated in this analysis and the fossil record, should be noted. However, caution

must be kept as whether this shifts actually reflect diversity changes or are produced by sampling bias. Although, methods less susceptible to sampling bias are available such as subsampling methods (e.g. (SQS) shareholder quorum subsampling), in view of the extremely uneven sampling at periods some (e.g. Jurassic only 38 records of eight genera compared to the Maastrichtian 503 records of 48 genera) (https://doi.org/10.5281/zenodo.3362508) subsampling methods might still be affected by sampling. Also considering the poverty of the fossil record for batoids remains in some stages it is possible that representatives of the Torpediniformes were present in the Jurassic as suggested by Aschliman's *et al.* (2012b) divergence estimates but have not been recognized or collected (e.g. all known Jurassic batoids come from near shore marine sediments and therefore is unlikely that they represent a full census of batoid diversity at that time (Underwood *et al.*, 2016b).
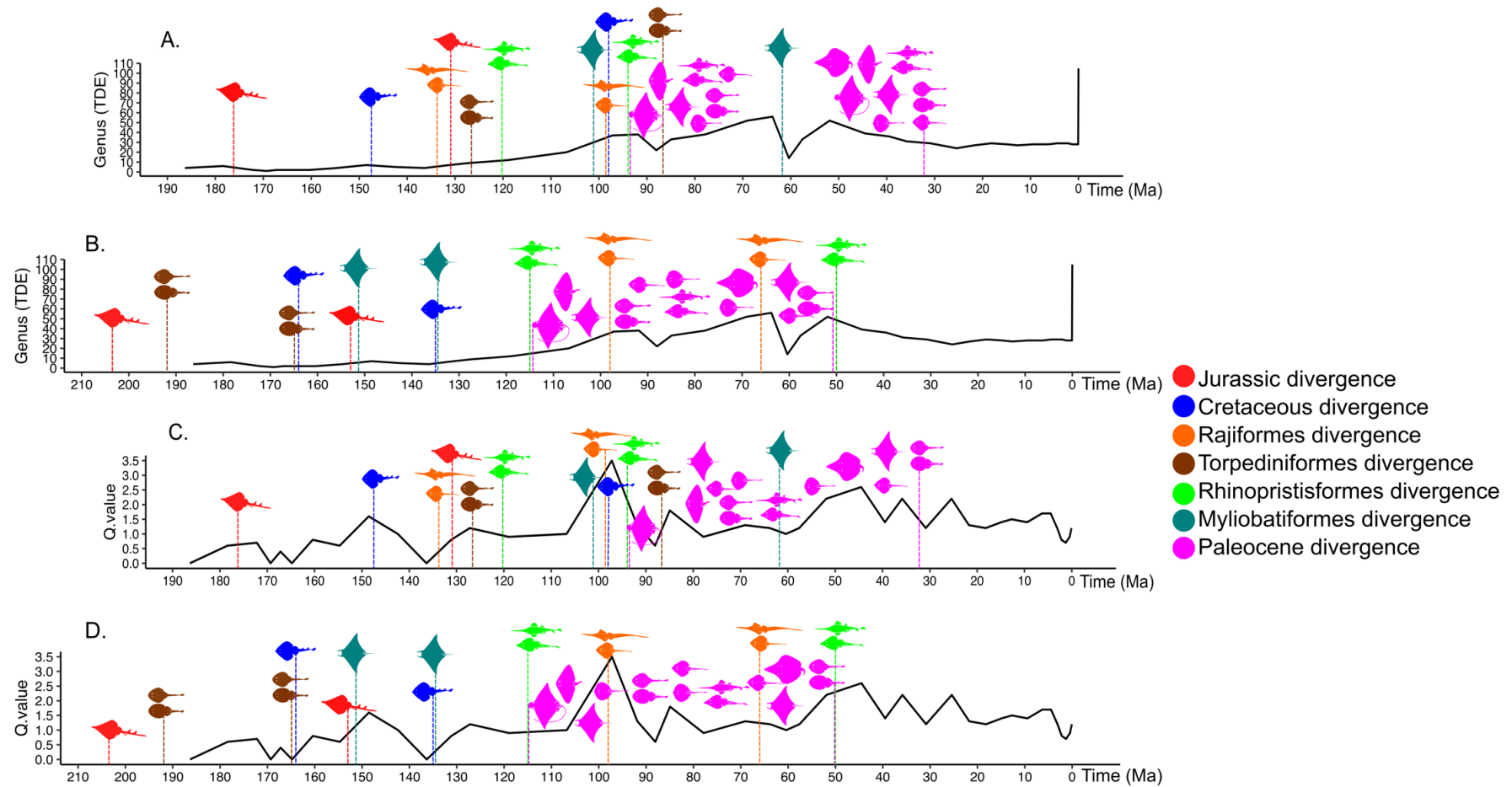
Figure 6.4. Diversity curves estimated for batoids: **A,** Taxonomic diversity estimate (TDE) curve overlay with the estimated divergence events recovered by the present analysis. **B,** TDE overlie curve overlie with the estimated divergence events recovered by Aschliman *et al.* (2012b). **C,** Shareholder quorum subsampling curve of batoids (Quorum 4) (SQS) overlie with the estimated divergence events recovered by the present analysis. **D,** SQS curve overlie with the estimated divergence events recovered by Aschliman *et al*. (2012b).

Conclusion

In general, tip-dating obtained better stratigraphic indices that the other time-scaling methods, especially in the GER and MSM indices which suggest a better fit with the known fossil record, also its topology implies fewer gaps in the fossil record (RCI ~ 67%). The tip-dating analysis placed the possible divergence time of the sclerorhynchoid+rajoid clade, between the Valanginian and Cenomanian with a mean in the Aptian. Both the mean and lower limit (Cenomanian) fall within the known fossil record of the group (Table 6.). However, the upper limit Valanginian falls well beyond the oldest known record of the group (Barremian, Kriwet *et al*., 2009a). Considering that this oldest record belongs to †*Onchopristis numidus* which shares several characteristics with later taxa (e.g. †*Ischyrhiza* and †*Schizorhiza*), it is possible that the upper limit of the divergence age estimate is accurate. The estimated age for the divergence between Ptychotrygoninae from other sclerorhynchoids is between 79.74-106.19 with a mean of 92.98 Ma falling within the oldest period reported for the group (Albian; Kriwet, 1999a; Kriwet *et al*., 2009a Kriwet & Kussius, 2001).

As expected from previous comparisons among morphological and molecular phylogenies of Neoselachii and the fossil record (Maisey, 2004; Underwood, 2006), the present analysis recovered later divergence time intervals than those estimated by the molecular analysis (Aschliman *et al*., 2012b; text-fig. 4). Molecular analysis gives longer evolution times for the batoids, proposing cladogenetic events in the Early-Middle Jurassic with subsequent ones leading to the appearance of major groups (rajoids, torpedinoids, myliobatoids and rhinopristoids) in the Middle-Late Jurassic, with additional radiation events within those groups in the Late Cretaceous-Early Paleocene. Whereas the present analysis places all major divergence events leading to all extant

orders of batoids in the Late Jurassic-Early Cretaceous with subsequent divergences within these clades during the Late Cretaceous and Early-Mid Paleocene. When compared with the fossil record, the estimated ages recovered by the present analysis overlay better with the diversity shifts observed in the fossil record. The present analysis shows a smoother succession of cladogenesis events, with the divergence leading to all extant orders of batoids overlaying with the increase of diversity after the J/K extinction event and through the Cretaceous. Molecular divergences age estimates for all extant orders of batoids in the Middle-Late Jurassic contrast with the relatively static diversity of neoselachians and batoids in that period (Kriwet *et al.,* 2009b) (Fig. 6.4).

It is unknown whether the similarities between the fossil records and the present study could represent actual shifts in diversity changes or are produced by sampling bias needs further study. A method less susceptible to sampling bias was used (SQS), however, considering how intermittent the sampling of the fossil record is (e.g. In the Jurassic period there are only 38 records of eight genera, whereas stages like the Maastrichtian are extremely well sampled with 503 records of 48 genera) (https://doi.org/10.5281/zenodo.3362508) subsampling methods and current divergence age estimates might be affected by sampling.

Chapter 7

Taxonomic review of the Sclerorhynchoidei Cappetta (1980a)

Introduction

Sclerorhynchoidei (*sensu* Cappetta, 2012) is one of the most diverse group of extinct batoids, partly because they are easily recognised by their large rostral denticles. They are a common element of shallow marine nearshore and non-marine Cretaceous assemblages of the Tethyan realm and the Western Interior Seaway (Becker *et al.,* 2006). Some rarer forms such as †*Ganopristis*, seem to have inhabited more Boreal and deeper waters (Underwood, 2006). The group is restricted to the Cretaceous with its oldest fossil record corresponding to the genus †*Onchopristis* from the Early Cretaceous (Barremian) of Spain (Kriwet, 1999b). Some records of the Late Jurassic (Curtis & Padian, 1999) are known. However, those remains seem to have been reworked records (Kriwet & Kussius, 2009; Cappetta, 2012) Based on their overall shape it has been hypothesised that sclerorhynchoids occupied an ecological niche equivalent to that presently filled by sawfishes and sawsharks (Welton & Farish, 1993).

The group has been largely collected in localities of North America (Canada, USA, Mexico), Europe, Africa and the Near East. Some of these localities have provided some beautifully well-preserved rostral blades and articulated skeletons (e.g. Cappetta, 1980b; Sternes & Shimada, 2018). However, most of the fossil record of sclerorhynchoids, as with other chondrichthyans, is composed of highly mineralised skeletal fragmented elements (e.g. rostral cartilages and vertebral centra), and by regularly shed body

elements with enameloid layers (teeth, placoid scales, rostral denticles). Although, these elements are taxonomically informative and allow the association of the taxa to a group. Their phylogenetic relevance remains uncertain.

Two previous works are considered as background for the present chapter:

• Kriwet & Kussius (2001) explore the palaeobiogeographical aspects of sclerorhynchoids and provide a very complete account of the known diversity of the group till that time. According, to their bibliographical review the group comprises a total of 16 valid genera and at least 40 species. It reaches is maximum diversity during the Cenomanian while the Late Campanian-Maastrichtian marks the peak of their distribution, both of which coincides with a period of high seal level (Miller *et al.,* 2005). The study also proposes the Tethys area of Middle Europe as the centre of origin and recognises †*Ischyrhiza* as the most successful sclerorhynchoid and recovers North America as the area with the greatest diversity followed by Africa.

• Cappetta (2012) presents a large taxonomical recount of several fossil Chondrichthyan taxa which includes the sclerorhynchoids. The study places them within the order Rajiformes in the suborder Sclerorhynchoidei that comprises two possible families (Sclerorhynchidae and Ptychotrygonidae) as the relations between Ptychotrygonidae and Sclerorhynchoidei are considered dubious by the author. Between both species a total of 55 valid species, 25 genera are reached. The bibliographical review assigns 12 species to †*Ptychotrygon* and nine to †*Ischyrhiza*, making †*Ptychotrygon* the most diverse genus among the sclerorhynchoids.

The present chapter presents an update on the taxonomic relations within the sclerorhynchoids based on the results recovered in previous chapters 4 and 5 and a bibliographic review, that comprises approx. 200 publications (Appendix 7.1).

Methods

Overall Cappetta's (2012;2006) taxonomic framework is followed. However, in cases where species were not included in that work and no account of synonymy or re-assignment made for previously described species, the record was considered valid. A brief description of genera based on their known remains and their descriptions is presented. Names of the skeletal components and teeth structures in the descriptions follow (Nishida, 1990; Cappetta, 2006; 2012; Underwood *et al.,* 2016a).

Only records reaching the genus level or below were considered in the present study, the number of species and genera are compared and cumulative curves of the known valid species and genera for Sclerorhynchoidei are presented with special interest in the decade between 1970 and 1980 during which bulk sampling and sieving became widely used or a common practice (Underwood *et al.*, 2016b). Comparison between the present bibliography and those of Kriwet & Kussius (2001) are compared at the genus level which was the taxonomic unit used in their study and plotted on maps using the R package **ggplot2**.

Results

Bibliographic review

The present review found a total of 30 valid genera and 72 valid species for the suborder Sclerorhynchoidei making it one of the most if not the most diverse group of extinct batoids. According to the analysis in Chapter 5, two major groups are recognized in the suborder: Sclerorhynchidae and Onchopristidae. Seven genera were placed as indeterminate family. †*Ptychotrygon* (19), †*Ischyrhiza* (8) and †*Texatrygon* (5) are the most diverse sclerorhynchoid genera (Fig. 7.1)
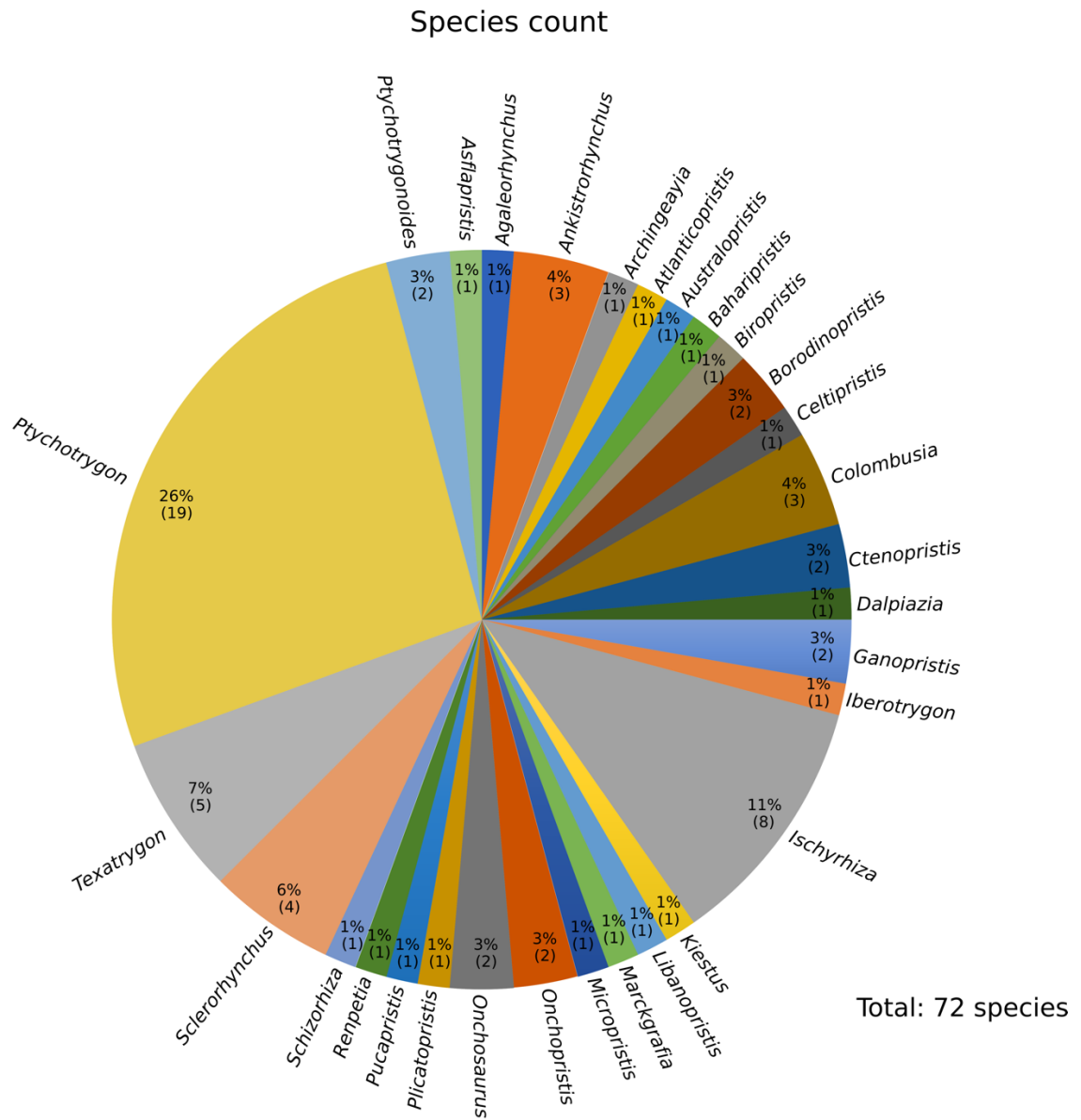
Figure 7.1. Number of species per Genera of Sclerorhynchoidei found in the present review. Species within the genus in parenthesis.

Systematic palaeontology

Class **Chondrichthyes** Huxley, 1880.

Superorder **Batomorphii** Cappetta, 1980b.

Order **Rajiformes** *sensu Naylor et al.*, 2012.

Suborder **Sclerorhynchoidei** Cappetta 1980b.

Family: **Sclerorhynchidae** Cappetta, 1974

†*Agaleorhynchus* Guinot *et al*., 2012b

Oral teeth wider than long. Crown is small and on occlusal view has an oval to sub-triangular outline with a well-developed, lingually oriented medial cusp that presents several well-marked and thick labial folds that originate at its base and radiate over the whole labial face reaching the small apron. The lingual face has a concave profile with a small and very broad uvula. Root is small and flat on basal view with a slightly flared outline (Guinot *et al.,* 2012b).

The oral teeth of the genus are extremely similar to those of †*Sclerorhynchus* and †*Ganopristis*. However, they can be differentiated from them by small crown and root, less developed apron and uvula and ornamented lingual face. The rostral denticles differ by the presence of ridges in the lower anterior edge of the cap. Oral teeth ornamentation resemblances those †*Borodinopristis,* but overall tooth morphology is different. †*Ptychotrygonoides* also presents similar ornamentation however, this taxon possesses stronger folds that delimitate the depressed and smooth lingual region of the occlusal face from the ornamented labial region where a well-developed apron is present (Guinot *et al.,* 2012b).

- **Type species:** †*Agaleorhynchus britannicus* Guinot *et al.,* 2012b: fig. 8 F-P. Santonian-Campanian. Europe: Berkshire, Winterbourne. Buckinghamshire, Taplow. West Sussex, England.

†*Ankistrorhynchus* Casier, 1964

Genus known only by rostral denticles which are bent backwards, their cap is longer than the peduncle and its anterior edge is smooth with two sharp ridges in the posterior face.

The peduncle is very sinuous, and reaches into the cap in the posterior face. The peduncle base presents many radiating folds.

Type species: †*Ankistrorhynchus lonzeensis* Casier, 1964: text-fig. 357. Santonian. Europe: Lonzée, Belgium.

- †*A. major* Cappetta & Case, 1975a:plate 9, Fig 26-26'. Maastrichtian. North America: Hop Brook, New Jersey. USA.

- †*A. washakiensis* Case, 1987a:text-fig. 10. Campanian. North America: Mesaverde Formation, east of Worland, Washakie County, Wyoming. USA.

†*Baharipristis* Werner, 1989

Description of the genus based on rostral denticles and oral teeth. Rostral denticles are small, sturdy and compressed in a lateral view. The cap is longer than the peduncle and presents several ridges that expand from its base towards the tip. Posteriorly, the cusp presents several lateral cutting edges and a median cutting edge with a short barb at its base. The peduncle reaches in to the cap in the posterior face.

Teeth small, on occlusal view the crown is larger than the root and present lateral projections with triangular corners and a well-developed posteriorly directed and acute medial cusp. Labial contour is convex with well-developed ridges that converge at the mid and a distally expanded apron that protrudes anteriorly. Lingual contour is concave with a flat but well-develop uvula. The root is expanded laterally and has lateral-lingual foramina. Root vascularisation is holaulacorhize type with a well-developed root canal that divides the root into in two lobes.

- **Type species:** †*Baharipristis bastetiae* Werner 1989:text-fig. 19-23, plates 24-30. Cenomanian. Africa: Gebel District, Bahariya Oasis, Egypt.

†*Biropristis* Suarez & Cappetta, 2004

Oral teeth present a rhomboidal outline on ocular view, with rounded lateral corners. The occlusal view of the labial side of the crown has several small irregular ridges that radiate from the middle and cover almost its entire dorsal surface of the apron but fail to reach the sturdy and posteriorly directed medial cusp. The labial contour of the crown is convex with the apron extending anteriorly. The lingual contour is smooth and concave with a moderately salient uvula that reaches into the root. The root surpasses the cusp laterally in occlusal view. Root vascularisation is holaulacorhize, with two broad, flat lobes separated by a deep furrow.

- **Type species:** †*Biropristis landbecki* Suarez & Cappetta, 2004: plate 1-2. Maastrichtian. South America: Algarrobo locality, Quiriquina Formation, Chile.

†*Borodinopristis* Case, 1987b

Rostral denticles small and delicate with the peduncle longer than the cap. The cap is pointed, smooth and presents two-three posteriorly directed barbs on its posterior edge which bases reach the mid of the denticle. The peduncle is divided into two lobes separated by a deep groove. In a posterior view, the peduncle reaches slightly into the cap.

Teeth small, on occlusal view the crown presents strong radiating ridges that begin at the apex of the medial cusp and extend at the base of the labial face. The medial cusp is board, high and posteriorly directed. The lingual contour is convex with a well-developed lingual uvula. Labial contour is concave, with a well-developed apron projected anteriorly. Root surpasses the crown laterally. Root vascularisation holaulacorhize with two flat lobes separated by a deep medial groove.

- **Type species**: †*Borodinopristis schwimmeri* Case, 1987b: figs. 1 A-F, 2 A-I, 3 A-C, 4 G, 5 A-F, 6 A-H. Santonian-Campanian. North America: Blufftown Formation. North bank of Hannahatchee Creek, Stewart County, Georgia. USA.

- †*B. ackermani* Case *et al.,* 2001: pate 2 fig. 23-31. Santonian. USA: Upatoi Creek, Chattahoochee County, Georgia, USA.

†*Celtipristis* Kriwet, 1999b

Oral teeth present a tall, broad and laterally expanded crown, with a blunt and posteriorly placed medial cusp with lateral rounded expansions. On lateral view, the labial surface presents a well-developed apron that protrudes anteriorly; and the lingual surface has a meandric profile with a little uvula that reaches into the root. The crown is generally larger than the root. The basal surface of the root is flat to slightly oblique with a pair of large lateral-lingual foramina. Root with holaulacorhized vascularisation with a narrow basal groove with and additional foramina at the basal canal.

- **Type species:** †*Celtipristis herreroi* Kriwet, 1999b: Plate 4 fig. 1-4. Barremian. Europe: Alcaine, Teruel, Spain.

The species has also been reported in the of the upper Blesa Formation (upper Barremian), Oliete sub-basin, Spain, Europe (Kriwet *et al.,* 2009).

†*Colombusia* Case *et al.,* 2001

Re-assigned by Cappetta (2012)

Teeth are small, broader than long with a slender and sharp central cusp and long lateral heels. Crown lateral shoulders reduced with an acute tall median cusp similar to those of *Squatina*, but differentiated by the presence of a slender, long and narrow apron that

extends well-beyond margin of root and a holaulacorhize type root. On the ligual face the uvula is long and rounded and does not overhang the lingual notch of the root. The root is smaller than the crown but exceeds it laterally on both sides in occlusal view and presents a deep medial furrow. Root lobes are flat on the whole except along the margins of the furrow where a kind of crest develops.

The genus was previously assigned to the Orectolobiformes by Case *et al.,* (2001a) and subsequently Cappetta (2006). However, Cappetta (2012) and Kirkland *et al.,* 2013 consider the genus close to some sclerorhynchoids on the basis of the root morphology, particularly the distinctly marked axial furrow, and of the general design of the teeth. Teeth of this genus are also similar to those of †*Onchopristis.* However, the remains of †*Colombusia* have not been associated to any enlarged rostral denticles and present a smaller root and a slenderer labial apron than those associated to †*Onchopristis.* †*Colombusia* remains occur much later in the fossil record (Campanian) than those of †*Onchopristis* (Albian-Cenomanian).

- **Type species:** †*Colombusia fragilis* Case *et al.,* 2001: pl. 2, figs. 32–36. Santonian. North America: Eutaw Formation of Georgia, USA.
- †*C. roessingi* (Case, 1987a: plate 7, figs.1–4). Campanian. North America: Mesaverde Formation, Bighorn Basin, Wyoming, USA. Originally described as †*Squatirhina roessingi* and was later redescribed as part of the genus †*Colombusia* by Cappetta (2012).
- †*C. deblieuxi* (Rowe *et al.,* 1992:text-fig. 3 D). Campanian. North America: Aguja Formation, Trans-Pecos, Texas. Wahweap Formation, Paunsaugunt Plateau, Bryce Canyon National Park, Utah, USA. Kirkland *et al.,* 2013 fig. 9.19A-O. Originally

described as †*Onchopristis dunklei* (Rowe *et al.,* 1992) it was redescribed as †*Colombusia deblieuxi* by Kirkland *et al.* (2013) based on Cappetta (2012).

†*Ctenopristis* Arambourg, 1940

Rostral spines long and strongly directed backwards and depressed. Its posterior cutting-edge is concave and anterior edge is convex. Apical view of the cusp of denticles has a diamond-like outline, with sharp anterolateral margins. The basal bulge pronounced. The peduncle is small and flattened with a rectangular contour. The basal face is flat and has a large elliptic foramen in the posterior half.

Teeth wider than long. Crown wider than the root with rounded lateral expansions. The occlusal face presents a wide, tall and posteriorly directed medial cusp with transversal ridges that converge at the labial cutting edge in the middle of the crown. The labial contour is convex and presents a well-developed and anteriorly directed apron that surpasses the root basal plate. Lingual surface has a meningeal profile with a small uvula that into the root. The root vascularisation is holaulacorhize with a well-developed central groove separating it into two flat lobes.

- **Type species:** †*Ctenopristis nougareti* Arambourg, 1940:text-fig. 11-12, plate 2, fig. 4-5, 7. Maastrichtian. Africa: Ouled Abdoun basin, Morocco.

The type species has also been reported for the Maastrichtian of Africa: Angola, Cabinda; Republic of Zaire, Egypt and Middle East: Iraq, Israel, Syria (Kriwet & Kussius, 2001).

- †*C. jordanicus* Mustafa *et al.,* 2002: text-fig. 8 1-8. Santonian. Jordan: Wadi Umm Ghudran formation, Wadi Falqa, AI-Husseinia, Karak District.

The genus has also been reported for the Coniacian of Africa: Morocco; Campanian of Middle East: Irak (Signeux, 1959), Jordan (Cappetta *et al.,* 2000), Israel (Lewy & Cappetta 1989); Africa: Egypt (Cappetta, 1991a), the Democratic Republic of Congo and Enclave of Cabinda (Dartevelle & Casier, 1959) and Maastrichtian of East: Syria (Bardet *et al.,* 2000)

†*Dalpiazia* Checchia-Rispoli, 1933

Rostral denticles large, their peduncle is greater than the cap. The cap is narrow pointed with well-developed cutting edges. The anterior cutting edge is rectilinear and presents a well-developed hook that projects into the peduncle. The posterior cutting edge is shorter and presents a bulge at the base. Peduncle widens towards the basal region and contains a large pulp cavity.

Teeth crown slender and tall; the root surpasses the crown laterally and posteriorly. The apron is small but stands out from the contour of the labial surface. In some teeth several well-marked thick ridges are present the labial side. The medial crest is tall, slender, acute and bent backwards. The lingual face has a concave profile with no uvula. The root vascularisation is holaulacorhize with a central groove dividing it into two board lobes.

- **Type species:** †*Dalpiazia stromeri* Checchia-Rispoli, 1933:text-fig. 363. Maastrichtian. Africa: Tripolitania, Libya.

Cappetta (2012) reports a second species for this genus †*D. indica* (Chiplonkar & Ghare, 1977) described from the Cenomanian-Turonian of India. However, there is no record of the species in Cappetta (2006) or in PBDB. The original description was not found. Because of this the species was not considered in the present analysis.

The genus has also been reported in the Maastrichtian of Africa: Morocco (Arambourg, 1935; 1952; Noubhani & Cappetta, 1997), Egypt (Cappetta, 1991a), Niger (Cappetta, 1972), Democratic Republic of Congo (Dartevelle & Casier, 1943), Angola (Auntunes & Cappetta, 2004); Europe: Spain (Cappetta & Corral, 1999) and Middle East: Jordan (Cappetta *et al.,* 2000) and Syria (Bardet *et al.,* 2000).

†*Ganopristis* Arambourg, 1935

Rostral denticles tall and slender. The cap is flat and larger than peduncle with two cutting edges. The anterior cutting edge is slightly convex at the base; the posterior cutting edge is concave at the base and ends into the peduncle and presents several oblique folds. The peduncle is short and wide. The basal face depressed in the axial region and has two lobes.

Teeth wider than long; the crown is smaller than the root laterally. On occlusal view the labial side presents several thick folds covering most of the apron and converging towards the cusp but failing to reach its tip. The lingual face has a concave profile with a small uvula that reaches into the root. The root vascularisation is holaulacorhize with two broad lobes.

- **Type species:** †*Ganopristis leptodon* Arambourg, 1935: plate 4, fig. 1. Maastrichtian of Africa: Ouled Abdoun basin, Morocco.

The type species was also described as:†*Problematicum* (Quaas, 1902:plate. 28, fig. 15); †*Dalpiazia stromeri* (Checchia-Rispoli, 1933:plate. 1 and Cappetta, 1987: fig. 125); †*Onchosaurus maroccanus* (Arambourg, 1935:plate. 19, fig. 8) and †*Onchosaurus manzadinensis* (Dartevelle & Casier, 1943:plate 14, fig. 1-8, text-fig. 55).

The type species has also been reported in the Maastrichtian of Africa: Tunisia (Arambourg, 1952); Europe: Netherlands (Albers & Weiler, 1964), Spain (Cappetta &

Corral, 1999); Middle East: Iraq (Signeux, 1959) and North America: Canada (Hessin *et al.,* 2007).

- †*G. karakensis* Mustafa *et al.,* 2002. Santonian: text-fig. 9 1-5. East: Wadi Umm Ghudran formation, Wadi Falqa, AI-Husseinia, Karak District, Jordan.

The genus has also been reported in the Maastrichtian of East: Syria (Bardet *et al.,* 2000) and Africa: Angola (Auntunes & Cappetta, 2002).

†*Kiestus* (Cappetta & Case, 1975b)

Re-assigned by Cappetta (2006)

Oral teeth wider than long with a high, acute and lingually directed medial cusp. Labial face presents a sharp anterior edge that extends from the tip of the medial cusp and fails to reach the apron. On lateral view the labial profile is convex and the narrow apron projects anteriorly. The lingual surface is smooth and concave with a wide round uvula. The lateral projections of the crown present are triangularly shaped and present a sharp edge on occlusal view. Root surpass the crown laterally; its posterior face carries a pair of lateral internal foramina and presents holaulacorhize vascularisation.

- **Type species:** †*Kiestus texana* (Cappetta & Case, 1975b:text-fig 6 A-E). Turonian- Coniacian. North America: Kiest Boulevard, Dallas County, Texas. First described as †*Ischyrhiza texana* but later reassigned to the genus †*Kiestus* by Cappetta & Case (1999: plate 23, fig. 1-8).

The species was also described as †*Ptychotrygon triangularis* (McNulty & Slaughter 1972: plate 1, fig. 16-17) and †*Ptychotrygon ritchei* (Meyer, 1974: fig. 37A)

†*Libanopristis* (Hay, 1903)

Rostral blade wide, reaches its maximum width in front of the base. Rostral spines directed backwards with a sigmoid profile. The cap is large, smooth and blade shaped. The peduncle is small and broad and has a rectangular shape. The basal face is depressed, divided into two lobes with a central foramen.

The nasal capsules are small and posteriorly directed, their posterior edge articulates with the smooth triangular-shaped antorbital cartilages. Palatoquadrate and Meckel's cartilage are narrow and curved. Teeth are small, wider than long, with a clear, sharp transverse cusp and with on labially directed transverse ridges and other lingually at crown. The apron is narrow and anteriorly directed. The lingual has a small uvula that reaches in to the root. On occlusal view the root surpasses the crown.

Postorbital process present but not well-developed. The synarcual cartilage surpasses the pectoral girdle and presents a well-developed medial crest. The pectoral pterygia are well developed and form a rigid structure. Propterygium and metapterygium are triangular shaped and present a large distal edge; the propterygium is anteriorly directed and doesn't reach the nasal capsules; the metapterygium extends backwards. The mesopterygium is long and rectangular shaped.

- **Type species:** †*Libanopristis hiram* (Hay, 1903: plate 26, fig 1). Cenomanian. East; Hadjula, Lebanon. First described as †*Sclerorhynchus hiram* it was later assigned to its current genus by Cappetta (1980b, Plate. 2, fig. 2-8 and text-fig. 3, 5, 6, 7) species is also figured in Cappetta (2012, text-fig. 367-368A-N).

The species was also described as †*Rhinobatus eretes* (Hay, 1903, plate. 24, fig. 2) and †*Ganopristis hiram* (Arambourg, 1940).

†*Marckgrafia* Weiler, 1935

Rostral denticles cap wide shorter than the peduncle and with cutting edges. The base of the cap has many parallel short ridges around its circumference with a poorly developed bulge. The peduncle is massive and has a broad base, with a narrow but deep medial-posterior notch. The anterior profile of the peduncle is convex under the cap, concave in its lower half; the posterior profile is convex and at its base presents a profound and narrow depression. The upper and bottom faces of the peduncle are moderately concave and have dull, alternating vertical grooves. The basal face is deeply depressed and funnel-shaped.

Tooth crown of triangular contour in lingual view. On occlusal view the well-developed cusp presents a median crest restricted to its basal part which sometimes has small irregular protuberances. Transversely the labial face is convex with a prominent apron that protrudes labial outline. The lingual face is concave with a large, rounded uvula. The root surpasses anteriorly and posteriorly crown in lingual view. Root vascularization is holaulacorhize with two triangular-shaped lobes.

- **Type species:** †*Marckgrafia libyca* Weiler, 1935: plate 1, and plate 2. Cenomanian. Africa: Bahariya, Egypt.

Species is also figured in Werner (1989: plate 31, Fig.1-7, plate 32, Fig.1-4, plate 33, Fig.1-5) and Cappetta (2012:text-fig. 3680-R).

The species was also described as Cfr. †*Onchopristis numidus* by Stromer (1927: plate 1, fig. 4 a-b).

†*Micropristis* (Hay, 1903)

Re-described by Cappetta 1980b

Rostrum broad, short and presents small rostral spines, very closely spaced. Rostral spines have a wide cap shorter than the peduncle. The basal bulge is very marked, rounded at the front and back with sharp edges in its posterior-lateral regions. The sharp edges do not reach the bulge. The anterior face of the spine has several parallel, small folds. The peduncle is massive, and it is funnel-shaped. The basal surface is cut out by some deep indentations.

The nasal capsules are large and elliptical, perpendicular to the body axis. The antorbital cartilages present a smooth triangular shape; their proximal section articulates to the nasal capsules and its distal section does not reach the propterygium. The supra-orbital crest has a slightly concave edge. The mandibles are laterally expanded; the palatoquadrate is narrow and the Meckel's cartilage is wide. The teeth are small, cuspidate, expanded laterally and with high and sharp shoulders with a cutting edge. The cusp is not bent lingually, the ornamentation consists of a longitudinal centre-labial ridge. The root is smaller than the cap. The root vascularization is holaulacorhize the two lobes are basally flat basal. Pectoral pterygia are separated. The propterygium has a triangular shape with a long, straight distal edge and a concave, small proximal edge. The mesopterygium is broad and rectangular shaped. The metapterygium and the propterygium are similar shaped.

- **Type species:** †*Micropristis solomonis* (Hay, 1903: plate. 25). Cenomanian. East; Hadjula, Lebanon. The species is first described a member of †*Sclerorhynchus*, and it

was later assigned to its current genus by Cappetta (1980b, plate. 1 and 2, fig. 1 and text-fig. 8-9).

The species was also described as: †*Ganopristis senta* by Arambourg (1940), †*Ischyrhiza cf. avonicola* by Casier (1964, text-fig. 3-5 and plate 2, fig. 3-5). †*Ischyrhiza germaniae* by Alberts and Weiler (1964, p. 18, p. 24, fig. 31-32).

The type species has also been described in the Santonian and Campanian of Europe: Belgium (Casier 1964) and Germany (Albers & Weiler 1964).

- †*M. truyolsi* Bernárdez 2002: plate 77, fig. 1. Cenomanian. Europe: Soto de Dueñas, Spain. The species is described in a PhD thesis and has no publish data. However, Cappetta (2012) considers it as a valid record for the genus.

†*Plicatopristis* Cappetta, 1991a

Rostral denticles present a triangular cap which is smaller than the peduncle. The posterior face of the cap presents several well-developed ridges that end in bulges at the level of the intersection with the peduncle. The peduncle expands towards the proximal edge and near the base is divided into two lobes.

Tooth crown with a tall triangular cusp and rounded shoulders with sharp edges. Cusp triangular and robust on the labial side presents a longitudinal ridge that fails to reach the tip of the cusp and bifurcates at the apron. On lateral view the lateral profile is convex with a well-developed apron that extends anteriorly, and the lingual profile is concave, with no uvula. The root protrudes laterally. Basal face of the root is flat, and its vascularization is holaulacorhize with two lobes which have a triangular contour.

- **Type species:** †*Plicatopristis strougoi* Cappetta 1991a: plate 5-6. Maastrichtian. Africa: Mine A, Bed 1, near Wadi Teban, Hamrawein area, Egypt. Species figured in Cappetta (2012, text-fig. 373 A-H).

The type species has also been described for the Maastrichtian of East: Palmyrides Chain, Syria (Bardet *et al.,* 2000).

†*Renpetia* Werner, 1989

Re-assigned by Cappetta 2006

Teeth small. Crown present a wide cusp lingually directed with sharp heels. On labial view the apron presents several vertical ridges directed towards the central cusp. On lateral view the labial profile is convex with an apron that projects anteriorly; the lingual profile is concave with a wide almost incipient uvula. Root surpasses the crown laterally and presents holaulacorhized vascularization with two triangular lobes; on its lingual side of the root presents three foramina.

- **Type species:** †*Renpetia labiicarinata* Werner, 1989: plate 39-40. Cenomanian. Africa: Gebel Distrit, Bahariya Oasis, Egypt.

†*Sclerorhynchus* Woodward (1889b)

Hypertrophied rostrum with a rostral blade that reaches is maximum width after the base. Presents four distinct series of denticles, one on the lateral margins of the rostrum another extending caudally on the sides of the head and finally two ventral one on the side of the rostrum and other in the middle (Smith *et al.,* 2012). Lateral rostral denticles are flat and tall with a slender cap, slightly longer than the peduncle, with anterior and posterior cutting edges. There is a clear and sharp basal bulge. The peduncle is rather squat and

222

clearly bilobed in its posterior basal region its anterior edge is rectilinear. The basal edges of the peduncle are straight and very slightly undulating. The basal face is depressed. Cephalic denticles smaller those of the lateral rostral series, are more strongly curved, with a small crown, short pedestal and a distinctive large, flaring, sinusoidal base. Both series of ventral denticles present a similar shape to the lateral series but are smaller (Welten *et al*., 2015).

 Neurocranium square-shaped reaching is maximum width at the nasal capsules that are laterally expanded and lack of anterior process. Antorbital cartilages smooth triangular shaped and articulated to the posterolateral margin of the nasal capsules. Palatoquadrate slender and becomes wide towards the articulation its distal end. Teeth small and cuspidate. The labial visor is well united to the crown's labial contour and juts well out over the root's labial face. The labial face of the crown has many folds converging toward the apex; these folds are joined, above the visor, by an irregular but sharp crest; the lingual face is smooth, and the uvula is long, with a rounded extremity and broad base. The root is large and extends laterally beyond the crown. The basal face of the lobes is broad and flat, with a subtriangular contour and not very marked angles. In the young individuals, the folds of the labial face can disappear.

Pectoral pterygia large, paddle like and slightly more separated than in other species all pectoral radials articulate to them. The pelvic girdle is narrow and slightly arched toward the front with short a prepubic lateral processes.

- **Type species:** †*Sclerorhynchus atavus* Woodward, 1889b: plate 3, fig. 1. Santonian. East: Sahel Alma, Lebanon.

The type species has also been described as †*Sclerorhynchus setus* (Hay, 1903) and as †*Squatina crassidens* (Woodward, 1889a).

- †*S. fanninensis* Cappetta & Case, 1999: plate 21, fig. 1-5. Campanian. North America: North Sulphur River, Fannin County, Texas, USA.

- †*S. pettersi* Case & Cappetta, 1997: text-fig. 8, plate 12, figs 5-6. Maastrichtian. North America: Kemp Clay Formation, Commerce, Hunt County, Texas, USA.

- †*S. priscus* Cappetta & Case, 1999: plate 22, fig. 4-10. Coniacian-Turonian. North America: Eagle Ford Shale, Austin Chalk, Dallas, Texas, USA.

Subfamily: Ptychotrygoninae

Re-assigned from Kriwet *et al.* (2009a)

Cappetta & Case (1999) place ptychotrygonoids as a member of either Sclerorhynchoidei or *Rhinobatos*. However, despite all arguments, the tooth morphology of †*Ptychotrygon* identifies them as Sclerorhynchoidei. Numerous species oral teeth have been described but none directly associated to rostral spines (small possible rostral spines have been found associated with †*Ptychotrygon*, but only in mixed assemblages), which are thought to be characteristic of Sclerorhynchiformes. Kriwet (1999b) tentatively assigned enlarged placoid scales similar to those found in the ligamentous band between rostrum and skull of Sclerorhynchiformes (Kriwet, 1999b) as possible rostral spines to †*Ptychotrygon*. Welten *et al.* (2015) described such placoid scales as one of the series of rostral spines in †*Sclerorhynchus atavus* this based on the histological similarities with the spines located in the rostrum. Recently several specimens from Morocco have been collected with similar teeth morphologies to those of Ptychotrygonidae (sensu Kriwet *et al.,* 2009a) which seem to corroborate the hypothesis that this group belongs within Sclerorhynchoidei. Although Underwood (2006) considers †*Celtipristis*, †*Kiestus* and †*Ptychotrygon* to represent additional, separately evolving, clades with no close relationships to Sclerorhynchiformes.

The subfamily can be differentiated from all other sclerorhynchoids by the following combination of two diagnostic dental characters (transversal crests differentiating the labial crown face and very well-developed and ornamented labial visor with several ridges and smaller crests) and the lack of lateral and ventral enlarged rostral denticles series in the rostral cartilages.

†*Asflapristis* Villalobos *et al.,* 2019 (Chapter 1)

Rostrum of uncertain length but robust and apparently lacking enlarged rostral denticles and 'wood-like' cartilage. Neurocranium (posterior to nasal capsules) of similar length and width with flattened roof with an anterior fontanelle and the level of the nasal capsules. Palatoquadrate and Meckel's cartilages are wide and stout and with a thin outer layer of 'wood-like' perichondrium. Dentition relatively homodont, teeth oval in occlusal view and lacking a medial cusp but present a medial crest and a secondary crest with small branching ridges between them and on the apron. The lingual face presents also a secondary crest but no branching ridges and a well-developed uvula. Transverse sectioning revealed a large pulp cavity. Root smaller than cusp and with holaulacorhized vascularization. Second hypobranchial without an anterior process. Synarcual long with well-developed medial crest and dorsally directed lateral stays but does not directly connect to the pectoral girdle. Synarcual lip large and fits within the chondrocranium. Vertebral centra fail to reach the middle of the synarcual. Lateral facet of scapulocoracoid thick and compact and articulate to the pectoral elements. Propterygium, mesopterygium and metapterygium expand distally and paddle-shaped.

- **Type species:** †*Asflapristis cristadentis* Villalobos *et al.,* 2019: text-fig. 1-10. Turonian. Africa: Akrabou Formation, Morocco.

†*Ptychotrygon* (Jaekel, 1894)

Re-assigned by Kriwet *et al.* (2009b)

sensu Villalobos *et al.,* 2019b

Hypertrophied rostrum with no enlarged lateral nor ventral denticle series attached to it. On ventral view two parallel ventral canals one on each side of the rostrum. Palatoquadrate and Meckel's cartilages slim. Second and third hypobranchials well-developed close to each other and with no articulation surface with the basibranchial. Teeth are small and oval-shaped, with a sharped and strong enamelled pyramidal crown and transverse crests (in some cases short transverse ridges are also present on the labial crown face). On labial view the apron variably developed and in some cases with a straight sagittal ridge on the upper part. On lateral view labial face is sigmoidal with projecting anteriorly apron; the lingual uvula is short and broad with a weak central interlocking depression. Root vascularization holaulacorhize type with a single pair of margino-lingual foramina.

- **Type Species:** †*Ptychotrygon triangularis* (von Reuss, 1844:plate 2, Fig. 14-19). Turonian. Europe: Kosstitz and Borzen, near Bilin, Bohemia, Czech Republic. The genus was first described as *Ptychodus* and later assigned to †*Ptychotrygon* by Jaekel (1894) based on revision of new specimens from the Kreide formation (Turonian) in Bohemia.

- †*P. agujaensis* McNulty & Slaughter 1972: plate. 1, Fig. 11-15. Campanian. North America: Aguja Formation, Texas. USA.

- †*P. blainensis* Case 1978: text-fig. 16, plate 4, figs. 7 a-c, 8 a-d. Campanian. North America: Judith River Formation, Montana, USA.

- †*P. boothi* Case 1987a: plate 13, fig. 4, plate 14, fig. 2. Campanian. North America: Mesaverde formation, Wyoming, USA.

- †*P. chattahoocheensis* Case *et al.* 2001: plate 5, fig. 105-109). Santonian. North America. Eutaw formation. Georgia. USA.

- †*P. cuspidata* Cappetta & Case 1975a: text-fig. 11 A-D, plate 4, fig. 19-22). Maastrichtian. North America: Willow Brook, New Jersey. USA.

- †*P. ellae* Case 1987a: plate 14, fig.1, 3. Campanian. North America: Mesaverde formation, Wyoming, USA.

- †*P. eutawensis* Case *et al.* 2001: text-fig. 6, plate 5, fig. 110, plate 6, fig. 111-113, 116-117. Santonian. Eutaw formation. Georgia. USA.

- †*P. geyeri* Kriwet 1999b: text-fig. 3-23. Albian. Europe: Utrillas Formation, Teruel Spain

- †*P. gueveli* Cappetta 2004: figs. 2-7. Turonian. Europe: Saint-Michel-sur-Loire, Indre-et-Loire, France.

- †*P. henkeli* Werner 1989: text-fig. 26, plate 34, fig. 1-7. Cenomanian. Africa: Bahariya, Egypt.

- †*P. ledouxi* Cappetta, 1973:plate 2, fig. 7-17, plate 3, fig. 8-9. Turonian. North America: Carlile Shale formation. Dakota. USA.

- †*P. pustulata* Kriwet *et al.,* 2009b: text-fig. 9Q–X, 10A–H. Albian-Cenomanian. Europe: Mosqueruela and Utrillas formations, Aliaga. Spain.

- †*P. rostrispatula* Villalobos *et al.,* 2019b. Turonian. Africa: Akrabou Formation. Morocco.

- †*P. rugosa* (Case *et al.,* 2001: plate 5, fig. 100-104). Santonian. North America: Eutaw formation, Georgia. USA. The species was first described within the genus †*Erguitaia*, but later assigned to the genus †*Ptychotrygon* by Cappetta (2006; 2012).

- †*P. slaughteri* Cappetta & Case, 1975b: text-fig. 5 a-d. Cenomanian. North America. Woodbine formation. Texas. USA.

- †*P. striata* Kriwet *et al*., 2009b: text-fig. 11 A-P. Cenomanian. Europe: Mosqueruela Formation, Spain.

- †*P. vermiculata* Cappetta, 1975b: text-fig. 1 A-D. Maastrichtian. North America: Willow Brook, New Jersey, USA.

- †*P. winni* Case & Cappetta, 1997: plate 13, fig. 1-3. Maastrichtian. North America: Kemp Clay formation. Texas. USA

The genus has been described for the Cenomanian of Europe: Spain (Bernardez, 2002); Turonian of North America, Texas, U.S.A (Cappetta & Case, 1999); Coniacian of North America, U.S.A, Texas, (Cappetta & Case, 1999) and New Mexico (Johnson & Lucas, 2003); Santonian of North America, Texas, U.S. (Cappetta & Case, 1999) and France, Europe (Cappetta, 1981); Campanian of North America, Texas, U.S.A. (Cappetta & Case, 1999) and Alberta Canada (Beavan & Russell, 1999); Maastrichtian of North America, Texas U.S.A. (Cappetta & Case, 1997: 1999) and Africa Morocco (Cappetta, 1987, Noubhani & Cappetta, 1997 and Egypt Cappetta, 1991a).

†*Ptychotrygonoides* Landemaine, 1991

Possible synonym of †*Ptychotrygon* Kriwet *et al.* (2009a)

Re-assigned by Kriwet *et al.* (2009a)

Teeth broader than long, strongly cuspidate with a distinct and sharp transverse keel. Labial face is convex and bears a median crest bend towards the margin of the face and with radiating irregular folds stopping above that margin. A sort secondary crest (incipient) differentiates along the margin and reaches the marginal angles in some lateral

teeth. Small lingual uvula with horizontal crest on its both sides. The lingual face bears narrow vertical ridges located on its median part on some teeth. The genus differentiates from †*Ptychotrygon* by is cusp directed lingually with a little high root and a very little marked lingual uvula.

The root surpasses the crown in occlusal view and presents holaulacorhize vascularization. There is a pair of large margino-lingual foramina and a pair of foramina open on the labial face of the root.

- **Type species:** †*Ptychotrygonoides pouiti* Landemaine, 1991: plate 14, fig. 1-6. Cenomanian. Europe: Les Renardieres, near Lussant, Charente-Maritime, southwestern France.

- †*Ptychotrygonoides sabatieri* Guinot *et al.,* 2012b:text-fig. Fig. 9 I–Q. Turonian. Europe: Justine-Herbigny, Ardennes, France.

Bernardez (2002) describes three more species for the genus two in Cenomanian (†*P. herreroae* and †*P. lamoldoi*) and one for the Turonian (†*P. hermani*) of Europe: Manjota, Cabaña y Las Tercias formations, Spain. The species are described in a PhD thesis with no published data. However, Cappetta (2012) considers them as valid record for the genus.

The genus is considered a synonym of †*Ptychotrygon* according to Kriwet *et al.* (2009a).

†*Texatrygon* Cappetta & Case, 1999

Re-assigned by Kriwet *et al.* (2009a)

Teeth with a smooth crown or with numerous short vertical labial folds. Oval shaped with a very prominent apron in occlusal view. The crown is high, sharp and cuspidate. Lingual face shows a broad and salient uvula and a very little marked articular hollow surmounted by a pustule or a short transverse crest. Root is slightly broader than the crown in occlusal view and presents holaulacorhize vascularization. *Texatrygon* can be differentiated thanks to the lack of ornamentation in the central region of the tooth crown lacking transverse crests or radiating folds (e.g. †*Ptychotrygonoides*) and the little marked lingual bulge surmounted by a very short transverse crest. In some cases, the tooth presents a series of ridges on the labial facet.

- **Type species:** †*Texatrygon hooveri* (McNulty & Slaughter, 1972: plate 1, fig. 6-10). Cenomanian-Turonian. North America: Eagle Ford Formation, Dallas, Texas, USA. The species was first described as †*Ptychotrygon hooveri*, it was assigned to a new genus by Cappetta & Case (1999).

The species has also been described as †*Ptychotrygon greybullensis* Case 1987b: plate 14, fig. 4-5.

- †*T. avonicola* (Estes, 1964: text-fig. 6). Maastrichtian. North America. Lance Formation, Wyoming, USA. The species was first described as †*Onchopristis*, then reassigned to †*Ischyrhiza* by Slaughter & Steiner (1968), and later was assigned to †*Texatrygon* by Kirkland *et al.* (2013).

This species has also been described for the Turonian of North America: Eagle Ford Formation, Texas (Slaughter & Steiner, 1968) and Cenomanian-Turonian of North America Greenhorn Cyclothem, Arizona (Williamson *et al.,* 1993). The species has also been described as †*I. basinensis* Case (1987).

- †*T. benningensis* (Case *et al.,* 2001: plate 5, fig. 90-99). Santonian. North America: Eutaw Formation, Georgia. USA. The species was first described within the genus †*Erguitaia*, but later assigned to the genus †*Ptychotrygon* by Cappetta (2006, 2012). The species is currently considered as a member of †*Texatrygon* (Cicimurri *et al*. 2014).

- †*T. copei* Cappetta & Case, 1999: plate. 27, fig. 5. Campanian. North America: Taylor Marl Formation, Texas.

- †*T. stouti* (Bourdon *et al.,* 2011: text-fig. 21 A-F). Santonian. North America: Hosta Tongue, New Mexico, USA.

- †*T. brycensis* Kirkland *et al.*, 2013. Campanian. North America: Wahweap Formation, Bryce Canyon National Park, Utah, USA.

The genus has also been reported Turonian of North America, Texas, U.S.A.(Cappetta & Case, 1997). Campanian of North America, Texas U.S.A. (Cappetta & Case, 1999).

Family: **Onchopristidae**

The family can be differentiated from other sclerorhynchoids groups by the following combination of characters: Presence of "wood-like" cartilage in their rostral cartilages, the development of thick reinforcements on the side of the rostral cartilages were the lateral series of enlarge rostral denticles attach and the presence of enlarge denticles in the body.

Within this family there seem to be to different types of arrangement of rostral denticles. In both genera rostral denticles are a constantly added. However, in †*Onchopristis* denticles of different smaller size are added as the space in the rostrum becomes available an develop though time. The presence of small denticles in a vertical functional position

suggest a vertical movement of this movement. In †*Ischyrhiza* similar sized rostral are added and denticles seem to lay as they grow and gradually gain a vertical functional position(Sternes & Shimada, 2018 text-fig. 2 A-D).

†*Ischyrhiza* Leidy, 1856a

Rostrum compressed dorso-ventrally. On both dorsal and ventral sides presents two parallel grooves that run longitudinally through the entire length of the rostrum, to fit the ophthalmic and the positions of bucco-pharyngeal nerves. The rostrum consists of tessellated cartilage formed by a layer of small of prismatic calcified cartilage blocks, with a thin layer of fibrous cartilage 'wood-like cartilage' (Kirkland & Aguillón-Martínez, 2002; Maisey, 2013). Evidence of the association between rostrum and rostral denticles was recently published (Sternes & Shimada, 2018). Rostral denticles placed on the lateral sides of the rostrum with a diastema between the two adjacent 'functional' denticles. Rostral denticles cap larger than the peduncle; the cap is thick and narrowly pointed with two sharp edges. The peduncle thick and spreads outwards towards its base; anterior and posterior edges are convex; the basal face of the peduncle presents a deep depression that separates it into two by a transverse ridge.

Tooth with a wide crown that presents a blunt and posteriorly directed cusp. The on lateral view the labial contour is convex with a well-developed apron projecting anteriorly the lingual face presents a large uvula that reaches into the root. The root vascularisation is holaulacorhize and extends laterally beyond the crown. The two lobes separated are sub-triangular in shape and have a flat basal face.

 Enlarged body denticles have been collected recently and associated to this species similar to those of †*Onchopristis*. Denticles are compressed, cone-shaped and bent backwards with several ridges on the base that extend apically and converge at the tip of the denticle. The base is flat or slightly concave.

- **Type species:** † *Ischyrhiza mira* Leidy, 1856b.There is no precise type locality of the USA where the species was fist collected.

 The type species has also been collected in the Turonian-Maastrichtian of North America of the Eagle Ford formation, the Austin Chalk and the Taylor Formation Texas, USA (Slaughter & Steiner, 1968); Turonian of Atarque Sandstone, Socorro County, New Mexico (Spielmann *et al.,* 2009) and Carlile Shale, Kansas (Bice & Shimada, 2016); Santonian of Mississippi: Eutaw Formation (Cicimurri *et al., 2014*); Maastrichtian of New Jersey, U.S.A (Cappetta & Case, 1975a, Case & Cappetta, 2004), Peedee Formation of North Carolina (Case, 1979), Arkadelphia Formation of Arkansas (Becker *et al*., 2006); Maastrichtian-Campanian of Delaware: Merchantville, Marshalltown and Mount Laurel formations (Lauginiger & Hartstein, 1983) and Alabama and Tennessee: Ripley Formation (Sternes & Shimada, 2018); Campanian of Georgia: Blufftown Formation (Case & Schwimmer, 1988). Campanian of Canada: Dinosaur Park Formation (Beavan & Russell, 1999; Peng *et al.,* 2001).

- †*I. chilensis* (Philippi, 1887: plate 55, fig. 8). Maastrichtian. South America: Quiriquina Formation Chile (Suarez & Cappetta 2004). First described as a *Plesiosaurus* remain was reassigned to the genus *Ischyrhiza* by Wetzel (1930*).*

- †*I. georgiensis* Case *et al.,* 2001: plate 6, fig. 120-125. Santonian. North America: Eutaw formation, Georgia, USA.

- †*I. hartenbergeri* Cappetta, 1975a:text-fig. 2-3. Maastrichtian. South America: El Molino formation, Bolivia.

- †*I. monasterica* Case & Cappetta, 1997: plate 11, fig. 5. Maastrichtian. North America: Kemp Clay formation. Texas. USA.

- †*I. nigeriensis* (Tabaste, 1963: plate 10, fig. 1-4). Maastrichtian. Africa: Mont Igdaman, Niger. First described as †*Marckgrafia nigeriensis* the species is reassigned by Cappetta (1972).

- †*I. serra* Nessov, 1997: plate 56, fig. 2. Coniacian. Middle East: Bissekty formation, Uzbekistan.

- †*I. viaudi* Cappetta, 1981: plate 1, fig. 1-2. Santonian. Europe: Notre-Dame-de-Riez, Vendee, France.

†*Onchopristis* (Haug, 1905)

Re-described by Stromer, 1917

Rostrum thick and with reinforcements. Triangular shaped rostrum that consists of tessellated cartilage formed by a layer of small of prismatic calcified cartilage blocks, with a thin layer of fibrous cartilage 'wood-like cartilage' covering the grooves of the ophthalmic nerves and adding solidity of the rostrum. Rostral denticles on the lateral series of the rostrum are slender their caps are bigger than the peduncle and its apical posterior region has one or more hook-like protuberance (barbs). Underneath the barbs converging at its base are numerous well marked ridges that extend and cover most the denticle posterior surface. The anterior face of the denticles is also ornamented with smaller ridges that are restricted to the lower third of the cap. The basal bulge is well marked. The peduncle is small with flat and strongly grooved lateral faces. The denticles on the lateral cephalic series do not present barbs and are smaller and wider that the rostrum series. Their anterior profile face is concave on smaller denticles and sigmoidal on larger ones.

Neurocranium square-shaped, with a small precerebral fenestra at the level of the nasal capsules. The supra orbital crest well-developed; post-orbital process small and

triangular, both orbital structures stand out from the level of the remaining cranial elements. The posterior end presents a deep indentation for the insertion odontoid process (synarcual lip) at the sides of the indentation de neurocranium projects laterally to form wide articulation surface for the large lateral process of the synarcual. The palatoquadrate is thin and straight while the Meckel's cartilage is wider. Tooth crown with a large medial cusp and laterally expanded by the shar lateral shoulders. The thick cusp is triangular-shaped bent lingually. On lateral view the labial profile is convex and the long apron projects anteriorly and surpasses the root. The lingual profile is concave with an almost incipient uvula. The root is bigger that the cap and protrudes the crown laterally and its vascularization is holaulacorhize. Only the anterior portion of the neurocranium is preserved presents a large odontoid process and large antero lateral condyles. The medial crest is well-developed and thin.

Recently a case for the association between the large dermal denticles of †*Peyeria libyca* Weiler, 1935 and †*Onchopristis* was made (Cappetta, 2012). This overlapping of the remains is also observed in the "Kem Kem Beds" (Morocco) and supports synonymising both species. The enlarged body denticles of †*Onchopristis* are compressed and conical shaped, with ridges in all its periphery that converge in the apex of the denticle. The Moroccan specimens present an enameloid layer in its anterior edge, that has not been reported for the Egyptian specimens.

The description of the genus was based on rostral denticles from the Cenomanian of Egypt and was made by Stromer (1917, plate 1-25). The oral teeth of the genus were first described as †*Squatina aegyptica* (Stromer, 1927, plate 1, fig. 4 a, b). Slaughter & Thurmond (1974) were the first to suggest and association to †*Onchopristis* and associated some fragments of dorsal fin spines and cephalic spines with †*Onchopristis*,

which belong to a hybodont. Werner (1989) assigned the oral teeth of †*Onchopristis* to the genus †*Sechmetia*.

- **Type species:** †*Onchopristis numidus* (Haug, 1905: plate 17, fig. 9-13). Albian. Africa: Djoua, Algeria. The species was described as the species *Gigantichthys*.

The species has also been reported for the Cenomanian of Africa: Egypt by Werner (1989: plate 19-20, 23, 35-38) and Morocco by Cappetta (1980b) and the present study.

The species has also been described as †*Squatina aegyptica* (Stromer, 1927: plate 1, fig. 4 a, b) and †*Peyeria libyca* (Weiler, 1935: plate 1, Fig.35-41 and plate 2, Fig.3; Werner, 1989, plate 4).

- †*Onchopristis dunklei* McNulty & Slaughter, 1962: text-fig. 1. Cenomanian. North America: Woodbine Formation, Texas, U.S.A The species bears three to five barbs on the posterior margin of the cap of the rostral teeth. However, multi-barbed denticles have been reported from Morocco (Stromer, 1917, plate 1, fig. 9,11) and Egypt (Werner, 1989, plate 20, fig. 1, 3, 5-7), that cast doubt in the utility of this character to distinguish these two species. †*Onchopristis dunklei* rostral denticles present larger pulp cavities than those of †*O. numidus*.

This genus has also been reported for the Barremian of Europe: Alcaine, Teruel, Spain (Kriwet, 1999b: plate 4, Fig. 5); Albian of North America: Walnut Formation, Texas, U.S.A (Welton & Farris, 1993); Albian-Cenomanian of Brazil Pereira and Medeiros (2007).

Indeterminate family

†*Archingeayia* Vullo *et al.,* 2007

Genus described based only on oral teeth with no association with rostral denticles. However, the overall tooth morphology suggests a possible association with Sclerorhynchoidei. Reported in association with species of †*Ptychotrygonoides* and †*Ptychotrygon* and its morphology of teeth resembles that of a member of the family Ptychotrygonidae with a high, triangular, and clearly cuspidate crown. †*Archingeayia* differentiated from other Ptychotrygonidae taxa by the lack of ornamentation labially, with no secondary crest and transversal ridges with only a medial vertical labial fold, that bifurcates downward into the well-developed apron. The lingual face is steeper from a lateral view and presents one or two pairs of oblique folds which not reach the apex. The uvula above the root notch is rather well differentiated and bears a weak interlocking hollow. The root is relatively low (half to third as high as the crown), slightly narrower than the crown. The root lobes from a basal view are triangular.

- **Type species:** †*Archingeayia sistaci* Vullo *et al.,* 2007: text-fig. 6 A-C. Cenomanian. Europe: Font-de-Benon quarry, Archingeay-Les Nouillers, Charente-Maritime, France.

†*Atlanticopristis* Pereira & Medeiros, 2008

Rostral denticles bear similarities to those of †*Onchopristis* in both being compressed, long and slightly recurved posteriorly and with multiple barbs in the apical posterior edge of the cap. What differentiates †*Atlanticopristis* from *Onchopristis* and other Sclerorhynchoidei is the presence of two series of barbs in its rostral denticles (four on the anterior margin and five in the posterior margin).

On the lateral faces the denticles present nearly straight ridges at the base of the cap that diverge apically and spread apically specially the central ridges that are almost parallel and the longest. The peduncle is smaller than the cap, irregularly grooved.

- **Type species:** †*Atlanticopristis equatorialis* Pereira & Medeiros, 2008, text- fig. 3 A-F. Albian-Cenomanian. South America: Falésia do Sismito, Cajual Island, Alcântara. Itapecuru Group, Northern Maranhão State, Brazil.

†*Australopristis* Martill & Ibrahim, 2012

Description of the genus based only in a few rostral denticles, that are similar to those of †*Onchopristis.* Rostral denticles are elongate terminating in sharp cap in smaller specimens and becoming slightly blunt in larger individuals. Cap larger than the peduncle its posterior margin presents two barbs similar to those described for †*O. numidus* and †*O. dunklei*. Root small and with smooth margins that according to Martill and Ibrahim (2012) are the key feature to distinguish the genus along with small size of the denticles (8mm-20mm in length), the different age of the denticles and the geographic isolation of the taxon.

- **Type species:** †*Australopristis wiffeni* Martill & Ibrahim, 2012: text-fig. fig. 7 A-D. Campanian-Maastrichtian. New Zealand: Mangahouanga Stream, North Island. East Wing. Marlborough.

Previously described as a subspecies of †*O. dunklei* as synonym of †*Onchopristis dunklei praecursor* Thurmond, 1971: Keyes 1977, Figs. 1–15.

†*Iberotrygon* Kriwet *et al*., 2009a

Teeth small, with a bulky 'cross-like crown' in occlusal view. Cusp bulky, well-developed, lingually inclined and well-detached from the short crown shoulders. The apron is broad, with a rounded extremity that is bent basally and is detached from the labial contour. On labial face the median crest presents short vertical ridges with no transversal labial ridges and short knob-like ridges along the labial edge. Median vertical labial crest, which sometimes bifurcates basally delimiting the apron. The lingual face is fairly steep, and has a well-developed vertical directed uvula, above which is a well-marked central depression. Lingual depression present, dorsally bordered by short transversal crest. Root is low and narrow, with two lobes separated by a deep central groove.

- **Type species** †*Iberotrygon plagiolophus* Kriwet *et al.,* 2009a: text-fig. 11 Q-X. Cenomanian. Europe: Mosqueruela formation, Spain.

†*Pucapristis* Schaeffer, 1963

Rostral denticles long and slender, with a cap longer than the peduncle. The cap posterior side presents a downwards directed barb. Anterior edge presents curvature at the same level of the posterior barb. Both posterior and anterior edges present several ridges that converge towards the base. The peduncle is broad at its base and has a rectangular profile.

Teeth present well-developed cusp. On labial face the apron is board and rounded with several ridges that converge towards the medial cusp and seem to extend till its apex. On lateral view the labial profile is convex with an apron that extends anteriorly; the lingual profile is concave with a rounded uvula. The root surpasses laterally the crown and has

holaulacorhize vascularization; the margin-lingual faces of the root present a pair of foramina.

- **Type species:** †*Pucapristis branisi* Schaeffer, 1963: text-figs. 1 A-D; 2, 3, 4 A-B. Maastrichtian. South America: El Molino formation, Bolivia. Oral teeth figured in Cappetta (1975a:text-fig. 1 A-G).

Onchosaurus Gervais, 1852

Rostral denticles long and pointed, with an asymmetrical cap shorter than the peduncle. On lateral view the anterior edge presents a downward directed barb, some specimens present second barb on the posterior edge. The peduncle is large with a broad base and a rectangular contour. Its base is flat but has a rather broad, shallow axial depression with slightly raised edges and many marked folds covering the basal half of the lateral faces; an anterior and posterior notch cut into the basal face.

- **Type species:** †*Onchosaurus radicalis* Gervais, 1852: plate 59, fig. 26. Campanian. Europe: †*Belemnitella mucronata* chalk, Meudon, Paris basin, France. The species was first described as a †*Mosasaurus*.

- †*O. pharo* (Dames, 1887: text-fig. 4, plate 3). Santonian. Africa: 10 km west of pyramids of Gizeh, Egypt. The species was first described as †*Titanichthys pharaoh*. As †*Titanichthys* Newberry, 1885, was assigned to a placoderm fish, the species was moved to †*Gigantichthys* (Dames, 1887) and the later was synonymized with †*Onchosaurus* by Priem (1914), a view confirmed by Arambourg (1940).

This species has also been reported for the Turonian of Africa: Iembe, Cuanza Basin, Angola (Antunes & Cappetta, 2002), South America: Magdalena, Colombia (Paramo-

Fonseca, 1997); Conacian of South America: Celedin Formation, Peru (Kriwet & Klug, 2012); Cenomanian-Turonian of Africa: Damergou Niger (Arambourg & Joleaud, 1943); Santonian of Africa: Bulu-Zambi, Democratic Republic of Congo (Dartevelle & Casier, 1943), Japan: Iwaki, (Uyeno & Hasegawa, 1986); Campanian of North America: Presidio County, Texas, USA (Lehman, 1989).

 The genus has also been descried for the Turonian of South America: Napo, Ecuador (Dunkley 1951, text-fig. 1 A-C); Coniacian of North America: Bernalillo County, New Mexico, USA (Spielmann & Lucas 2006), Europe: Barrio Panizares, Burgos, Spain (Corral *et al*. 2012).

†*Schizorhiza* Weiler, 1930

Rostrum is triangular shaped, the rostral spines are attached to its sides in batteries suggesting a regular replacement, this patter is unique among sclerorhynchids (Kirkland & Aguillón- Martínez, 2002). Rostral cartilage consists of tessellated cartilage formed by a layer of small of prismatic calcified cartilage blocks, with a thin layer of fibrous 'wood-like cartilage'.

Rostral denticles small, with a cap shorter than the peduncle. The cap is flat and triangular, with rectilinear cutting edges; the boundary of the enameloid is well marked and convex toward the base. The peduncle is long and presents two strongly divergent lobes. Each lobe is flat and becomes broader towards its base, where it bears marked irregular indentations corresponding to folds covering the basal part of each face.

Teeth small, higher than broad with a triangular, tall and acute cusp with well-marked cutting edges that extend its entire length. Cusp bent lingually with short folds at its base. On lateral view the labial profile is convex and does not present an apron; the lingual

profile concave and does not presents uvula. The root is heart-shaped and with anaulacorhize vascularization, the median groove begins to open on the lingual side but remains closed in the labial.

- **Type species:** †*Schizorhiza stromeri* Weiler, 1930: plate 39-40. Maastrichtian. Africa: Wadi Hammame, Egypt. Species rostral denticles and oral teeth figured in Cappetta (2012, text-fig. 377 A-L), rostrum and rostral denticles figured in Kirkland & Aguillon-Martinez (2002, text-fig. 2, 4 and 6).

Type species is synonym of †*Schizorhiza weileri* (Serra, 1933:text-figs. 1-7) and †*Schizorhiza cf. weileri* (Dunkle, 1948:text-fig. 2) and as part of the genus †*Scymnus* (Wetzel, 1930).

This species has also been reported for the Campanian of North America: Difunta group, Coahuila, Mexico (Kirkland & Aguillón-Martinez, 2002), Arkansas: (Becker *et al.,* 2006); Maastrichtian of Africa: Morocco (Arambourg, 1940;1952), Egypt (Stromer & Weiler, 1930; Cappetta, 1991a), Libya (Serra, 1933), Nigeria (White, 1934; Cappetta, 1972), Democratic Republic of Congo and Angola (Dartevelle & Casier, 1943), Middle East: Jordan (Cappetta *et al.,* 2000), Syria and Iraq (Signeux 1959; Bardet et al. 2000), South America; Bolivia (Cappetta, 1975a; 1991b; Gayet *et al.,* 1993) Chile (Wetzel, 1930) and North America, Maverick County, Texas, USA (Welton & Farish, 1993).

Discussion

Previous classifications (Cappetta, 2012) only recognised the family Sclerorhynchidae within Sclerorhynchoidei and placed Ptychotrygonidae (*sensu* Kriwet *et al*., 2009a) as a group with uncertain affiliations. The present taxonomic classification places the suborder Sclerorhynchoidei as part of a more restricted Rajiformes (*sensu* Naylor et al.,

2012) which no longer includes the Rhinopristiformes. Within this suborder two families (Sclerorhynchidae and Onchopristidae) are proposed which comprehend 30 valid genera and 72 valid species. Furthermore, within Sclerorhynchidae the subfamily Ptychotrygoninae is proposed which includes the newly described genus †*Asflapristis* (Chapter 2) and the genera †*Ptychotrygon*, †*Ptychotrygonoides* and †*Texatrygon* previously classified within Ptychotrygonidae (Cappetta, 2012). Of the 21 genera Sclerorhynchidae only four were given a subfamily classification. However, considering the size of the group and the variability observed within the group it is likely that more subgroups could be founded within the family.

Most of the fossil record for the sclerorhynchoids correspond to the Late Cretaceous (100-66 Ma) with only a few collections (7) in to the Early Cretaceous (129.4-100.5) (Fig. 7.5). The oldest records of sclerorhynchoids are those of †*Onchopristis* and †*Celtipristis* from the Barremian of Spain (Kriwet, 1999b) followed by those of †*Atlanticopristis* from the Albian-Cenomanian (Pereira & Medeiros, 2008), †*Onchopristis* from the Albian (Welton & Farris, 1993) of the American continent and †*Ptychotrygon* (†*P. pustulata,* †*P. geyeri*) from the Albian of Europe (Kriwet, 1999b: Kriwet *et al.*, 2009a) (Fig. 7.2).

The Barremian findings might indicate that the possible center of origin and diversification of the group is located somewhere in the Tethys realm, as mentioned in previous works (Kriwet & Kussius, 2001). However, considering that one of those Barremian records correspond to †*Onchopristis* a group that shares several characteristics with Late Cretaceous groups (e.g. †*Ischyrhiza*), the Barremian and Tethys realm hypothesis as possible center origin requires further information, considering that the sclerorhynchids group within the realm at that stage were a well-established monophyletic group. The presence of sclerorhynchoids records in the American (North

and South) and European continents and the Middle East regions during the Albian suggest that by the Upper part of the Early Cretaceous the group presented a cosmopolitan distribution. Overall sclerorhynchoid distribution follows the coast lines and shallow seas (Fig. 7.2A), this could suggest a relation with this kind of environments as proposed by previous works (e.g. Welton & Farris, 1987). However, most of the outcrops correspond to these environments (Vajda & Bercovici, 2014) and so the collection bias cannot be disregarded.
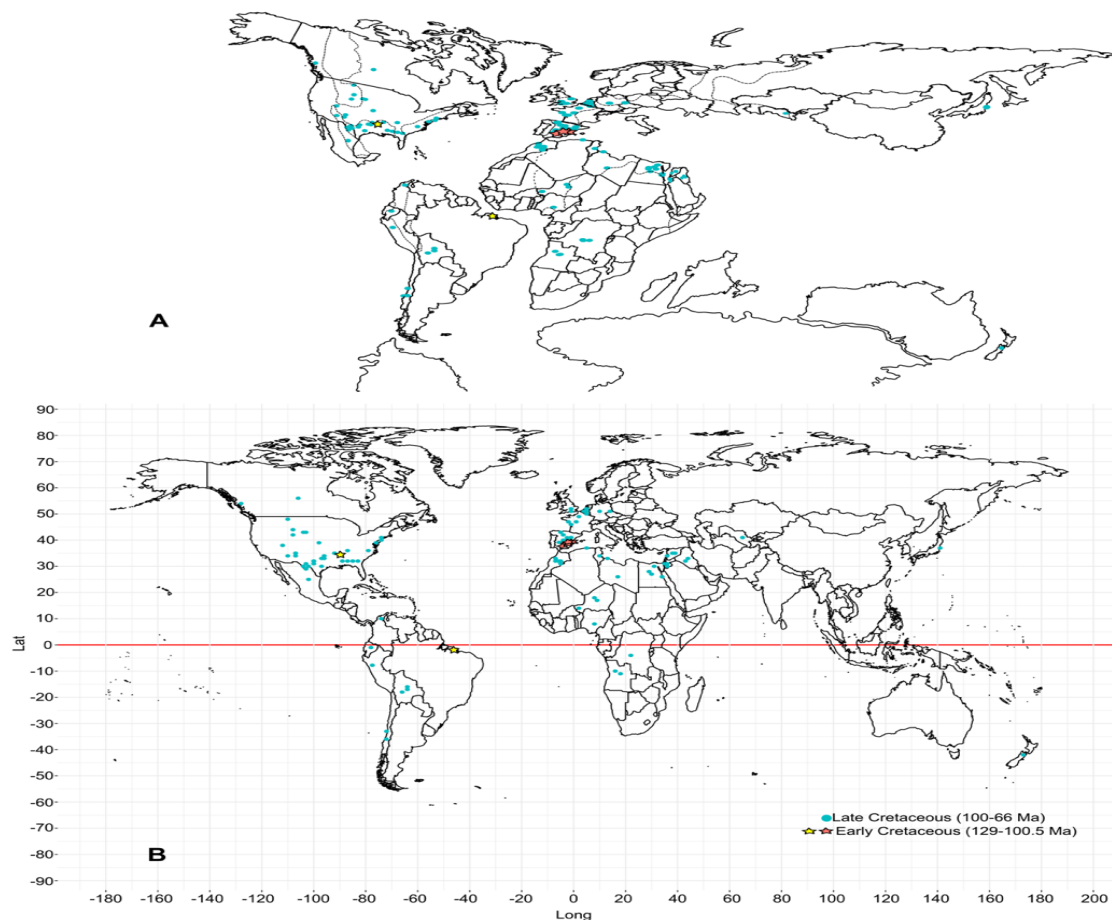
Figure 7.2. Sclerorhynchoid occurrences mapped. A. reconstruction of the continents during the Cenomanian (100 Ma). The map was generated using software available at Fossilworks (Alroy, 2013). Dashed lines represent submerged parts. B. Map of the collections of Sclerorhynchoids found in the bibliographic review. Red line: Equator. Red star: Europe Early Cretaceous. Yellow star: American Early Cretaceous.

At a family level Sclerorhynchidae is the most diverse group with 21 genera. Both Sclerorhynchidae (Fig. 7.3) and Onchopristidae (Fig. 7.4) present a cosmopolitan distribution. However, in both cases the northern hemisphere presents a lager diversity

record. Within Sclerorhynchidae, eight genera present a Gondwanian distribution (Table. 7.1), mostly located in Africa and the Middle East (Fig. 7.3).

Within Sclerorhynchidae, of the 29 locality points corresponding to Ptychotrygoninae 17 correspond to the genus †*Ptychotrygon* 12 of which are placed in North America along with †*Texatrygon* five species and eight known localities all of which are located in North America (Fig. 7.3), give this subfamily a larger Laurasian distribution with only two genera and three species with Gondwanian affinities (†*Asflapristis cristadentis,* †*Ptychotrygon rostrispatula* and †*P. henkeli*). Of the remaining genera within Sclerorhynchidae*, Sclerorhynchus* is the more diverse with five species most of which are distributed in North America. However, †*Dalpiazia* (9), †*Ganopristis* (9), †*Ctenopristis* (7) present most of the collection point, many of which are distributed in Africa and the Middle East (Appendix 7.4).

Onchopristidae presents a tendency to a Laurasian distribution. With †*Ischyrhiza* being the more dominating genera (Fig. 7.4). Most of the distribution of this genus is located in North America with 13 of its 18 known locations in this area. †*Onchopristis* presents a more equilibrated distribution with 6 known localities, three of which correspond to the species †*Onchopristis dunklei* in Laurasia and three to the species †*O. numidus* in Gondwana.

Of the seven genera with uncertain family affiliations, †*Onchosaurus* and †*Shizorhiza* are de dominant genera with 27 of the 33 locality points corresponding to these taxa. Both of these genera present a Cosmopolitan distribution with Gondwanian tendencies (12 locality points for †*Shizorhiza* and five for †*Onchosaurus* corresponding to this zoogeographical zone) (Fig, 7.5).
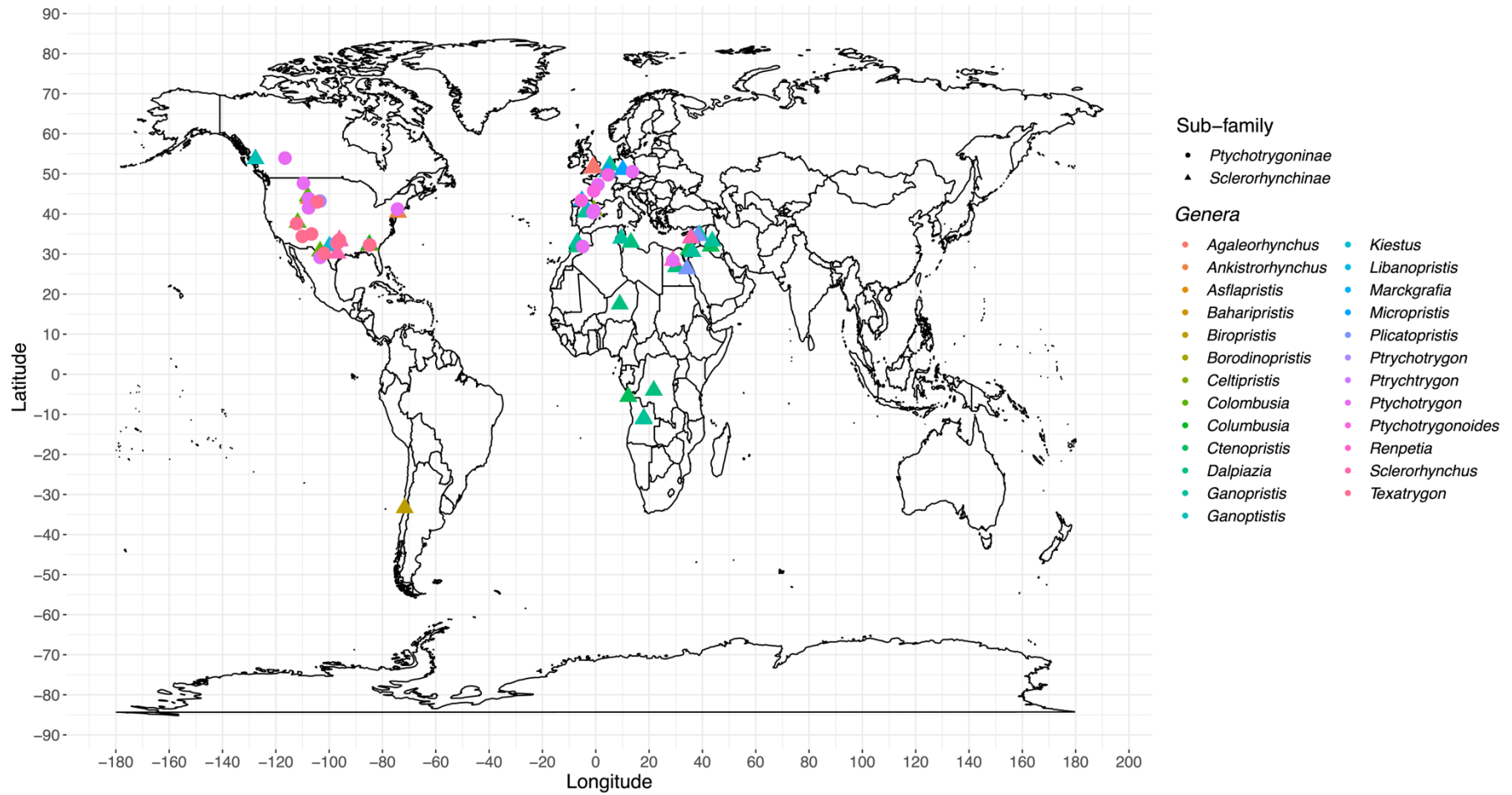
Figure 7.3. Map with the current continental configuration showing the locations of collection of the genera within the family Sclerorhynchidae. Data in Appendix (7.4).
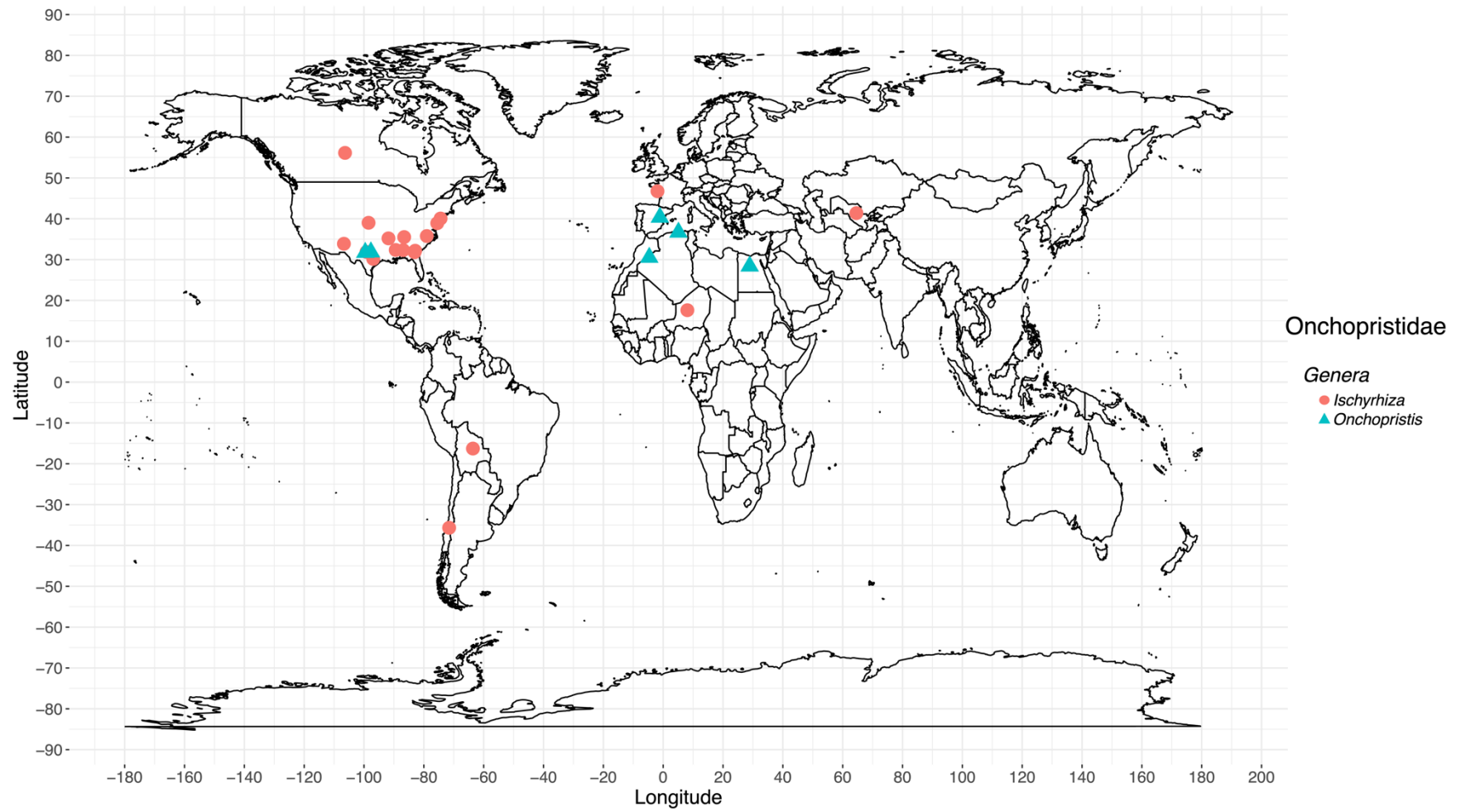
Figure 7.4. Map with the current continental configuration showing the locations of collection of the two genera in Onchopristidae. Data in Appendix (7.4).
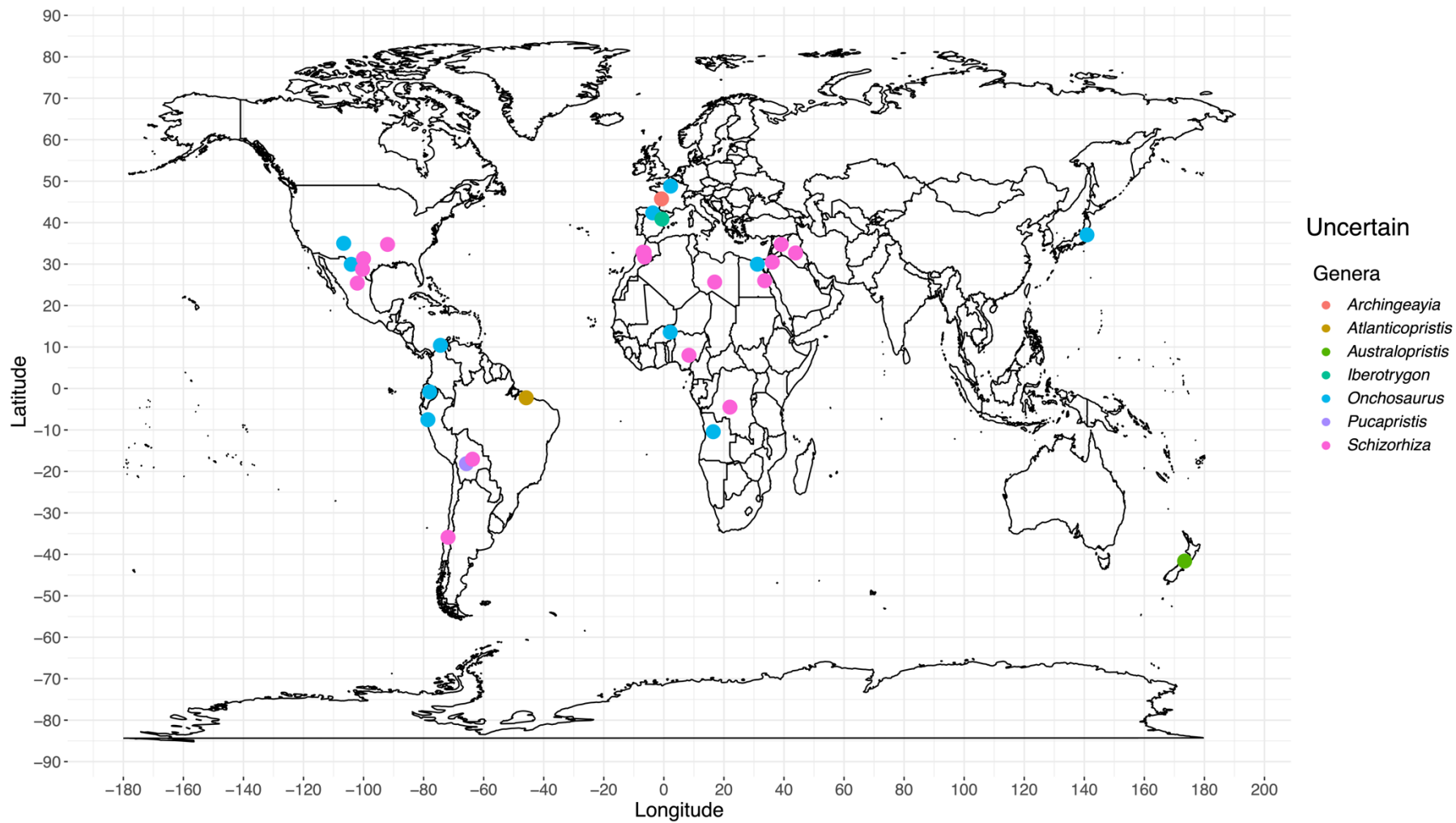
Figure 7.5. Map with the current continental configuration showing the locations of collection of the genera with uncertain family associations. Data in Appendix (7.4).

In order to compare the present bibliographic review with previous ones (Kriwet & Kussius, 2001), two zoogeographical zones (Laurasia and Gondwana) were recognized. Most of the sclerorhynchoids species are exclusive to Laurasian, of the 72 valid species found in the present review 44 are in this zone (36 species are North American) whereas 22 were exclusive to the Gondwana region (Fig. 7.6) (Appendix 7.2).
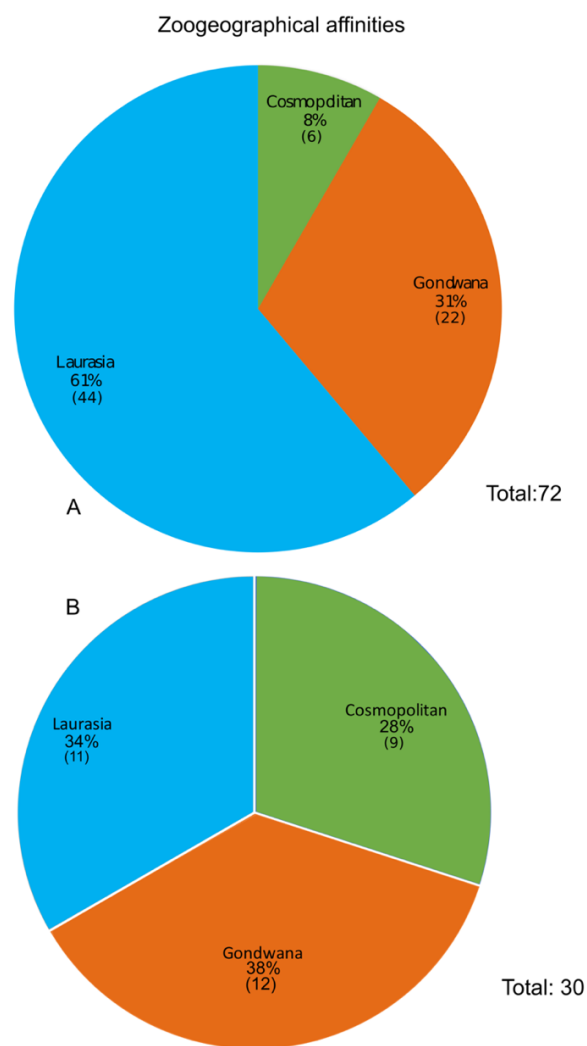
Figure 7.6. Total sclerorhynchoids found in each zoogeographical zone. **A,** Species. **B,** Genera. Number in parenthesis is the total of taxa for the zone.

The comparison between the present work and Kriwet & Kussius (2001) were done at a genus level as it was the taxonomic unit in their study (Table 7.1) (Appendix 7.3).

249

Gondwana genera	Laurasia genera	Cosmopolitan genera
(S;P)†*Asflapristis*	**(S)†*Agaleorhynchus***	(S)†*Dalpiazia***
(I)†*Atlanticopristis*	(S)†*Ankistrorhynchus***	(S)†*Ganopristis***
(I)†*Australopristis*	(S)†*Borodinopristis***	(O)†*Ischyrhiza***
(S)†*Baharipristis***	(S)†*Celtipristis*	(S)†*Micropristis*
(S)†*Biropristis*	(S)†*Colombusia* ⊛	(O)†*Onchopristis***
(S)†*Ctenopristis***	**(I)†*Iberotrygon***	(I)†*Onchosaurus***
(S)†*Libanopristis***	(S)†*Kiestus* ⊛	(S;P)†*Ptychotrygon* ⊛
(S)†*Marckgrafia***	(S;P)†*Ptychotrygonoides* ⊛	(I)†*Schizorhiza***
(S)†*Plicatopristis***	(S;P)†*Texatrygon* ⊛	(S)†*Sclerorhynchus***
(I)†*Pucapristis***	**(I)†*Archingeayia***	
(S)† *Renpetia* ⊛		

Table 7.1. Zoogeographical affinities of the sclerorhynchoid genera. Marked with (**) are the genera previously identified by Kriwet & Kussius, 2001 in those zoogeographical zones. In bold are the genera that where described after Kriwet & Kussius, 2001. Marked with (⊛) are genera that were re-assigned later than (2001) to the Sclerorhynchoidei. **Abbreviations**: (S), Sclerorhynchidae. (S;P), Sclerorhynchidae; Ptychotrygoninae. (O), Onchopristidae. (I) Uncertain taxonomic affiliations.

At the genus level both studies recovered Gondwana as the most diverse zoogeographical region at the genus level (Fig. 7.6), with six of the gondwanian genera proposed Kriwet and Kussius (2001) (†*Ganopristis*, †*Ischyrhiza*, †*Onchopristis*, †*Onchosaurus* and †*Schizorhiza*) recovered as part of the 12 exclusive gondwanian genus of the present study. The exclusive Laurasian genera also increased to ten genera, from two proposed in the (2001) previous work. Finally, there was an increase in the cosmopolitan genera (present in both Laurasia and Gondwana regions) from seven previously proposed by Kriwet & Kussius (2001) to nine (Table 7.1).

Most of the differences between the present study and Kriwet & Kussius (2001) correspond to the description of new genera, with seven genera described between 2001-2019. The genera re-assigned to Sclerorhynchoidei by subsequent studies are slightly less with only six (Table. 7.1). Among the genera re-assigned to Sclerorhynchoidei the present study includes all the known member of Ptychotrygonidae.
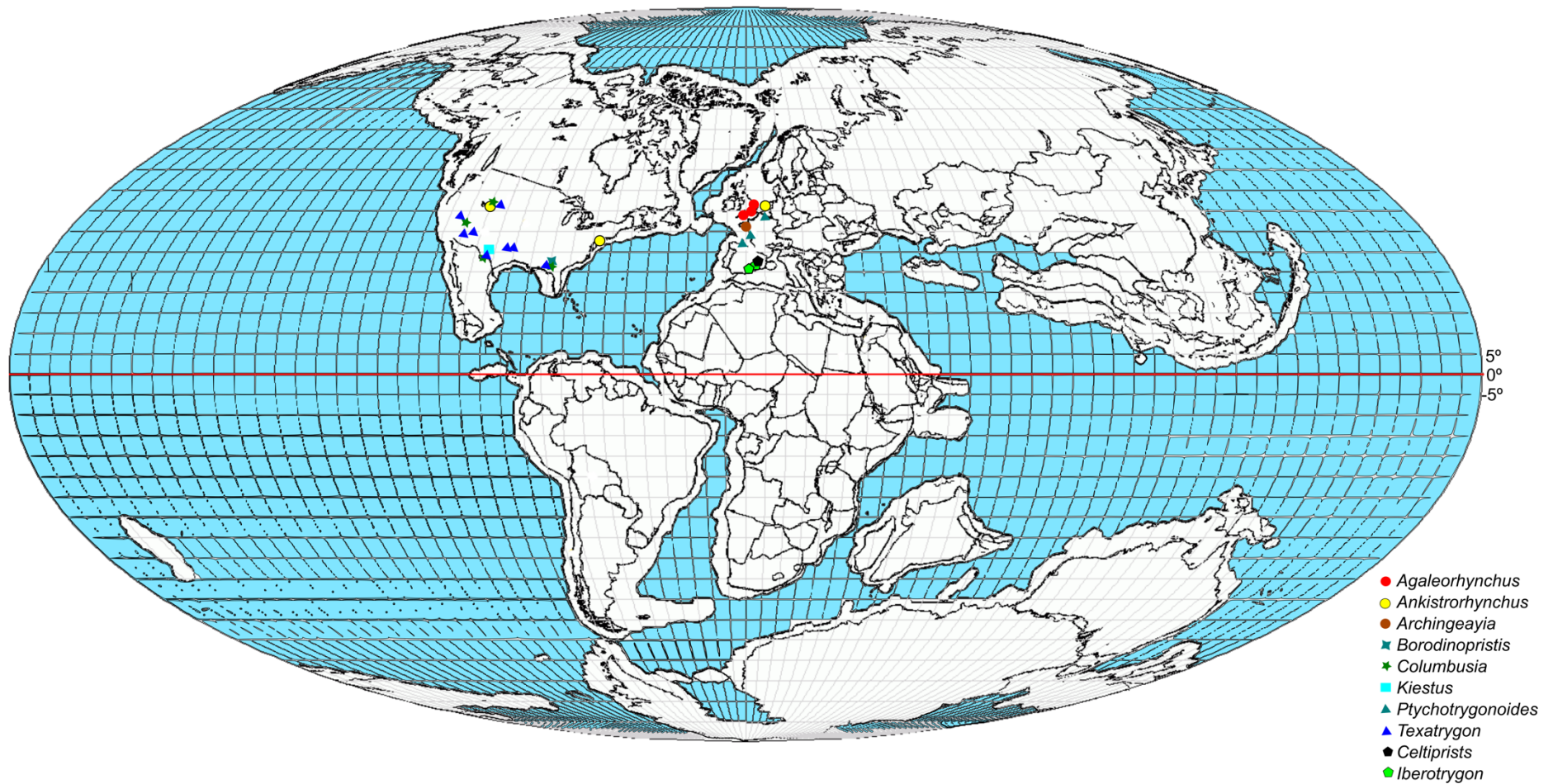
Figure 7.7. Palaeogeographical map of the Late Cretaceous (100 Ma) showing the localities of the ten genera with Laurasia affiliations. The map was generated using software available at Fossilworks (Alroy, 2013). Red line: Equator. Blue outline. Sea. Continental cuts and Cretaceous costal line white. Data in Appendix (7.4).
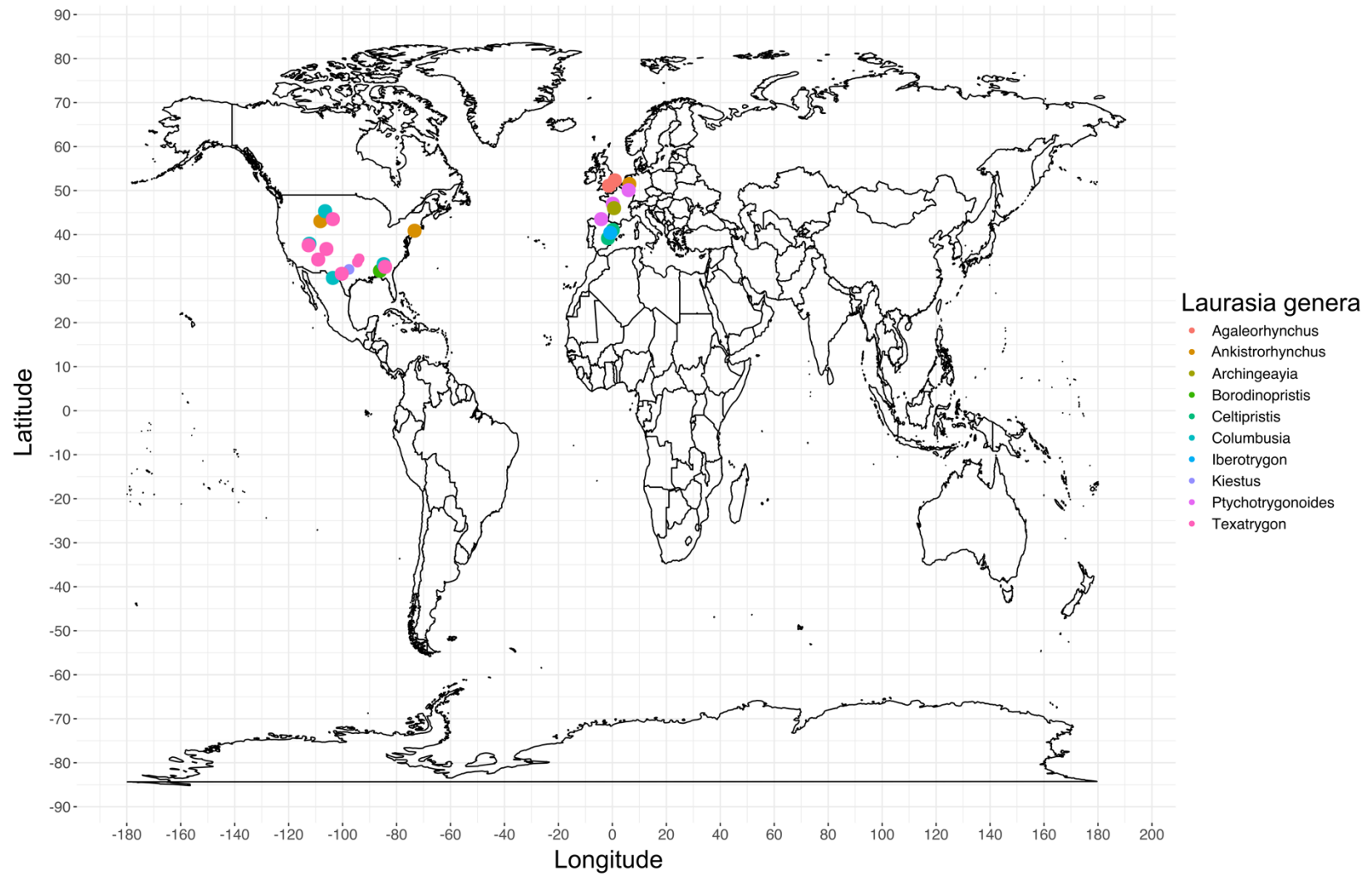
Figure 7.8. Map with the current continental distribution showing the localities were the ten genera with Laurasian affiliations have been collected. Data in Appendix (7.4).
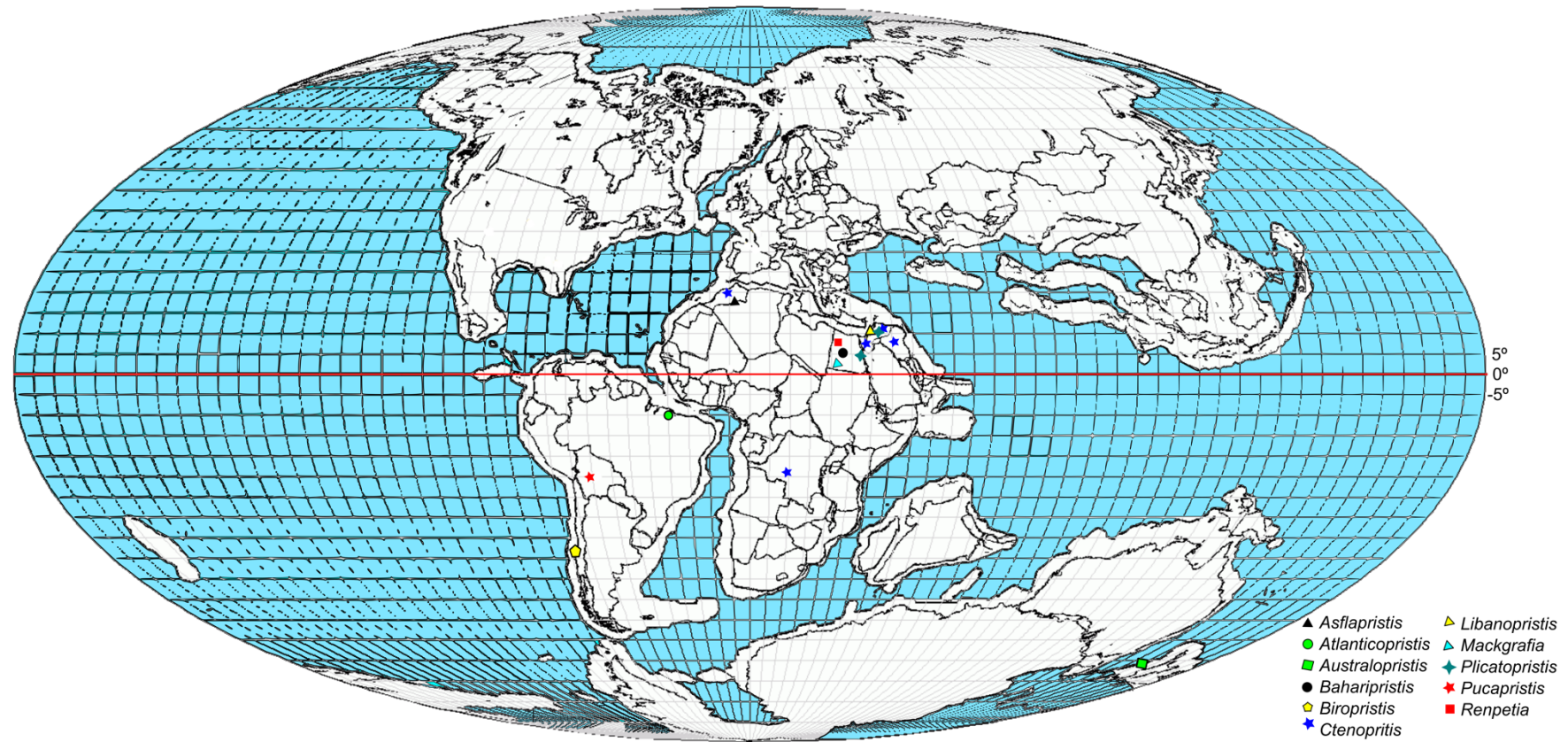
Figure 7.9. Palaeogeographical map of the Late Cretaceous (100 Ma) showing the localities of the 11 genera with Gondwanan affiliations. The map was generated using software available at Fossilworks (Alroy, 2013). Red line: Equator. Blue outline. Sea. Continental cuts and Cretaceous costal line white. Data in Appendix (7.4).
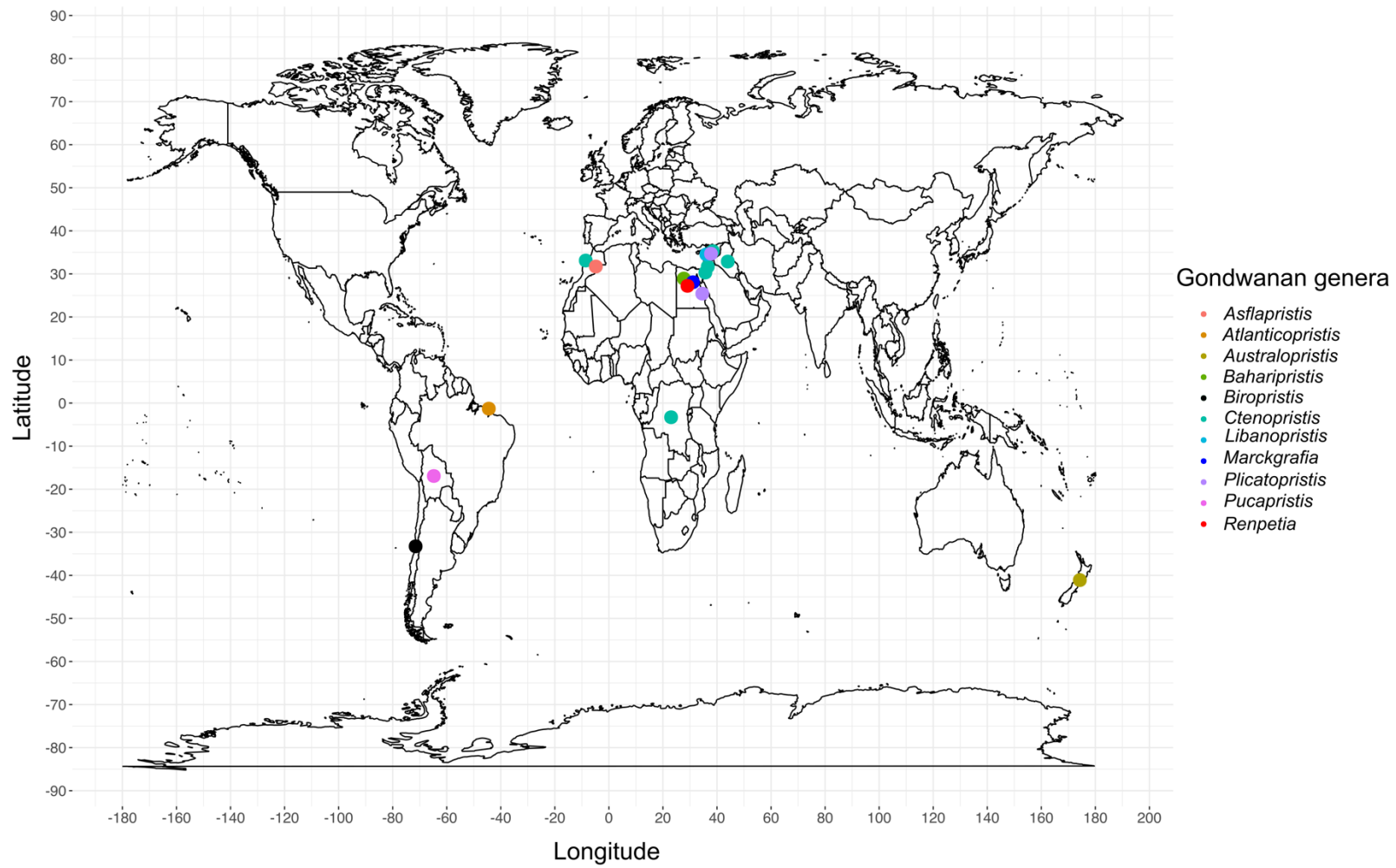
Figure 7.10. Map with the current continental distribution showing the localities were the 11 genera with Gondwanan affiliations have been collected. Data in Appendix (7.4).
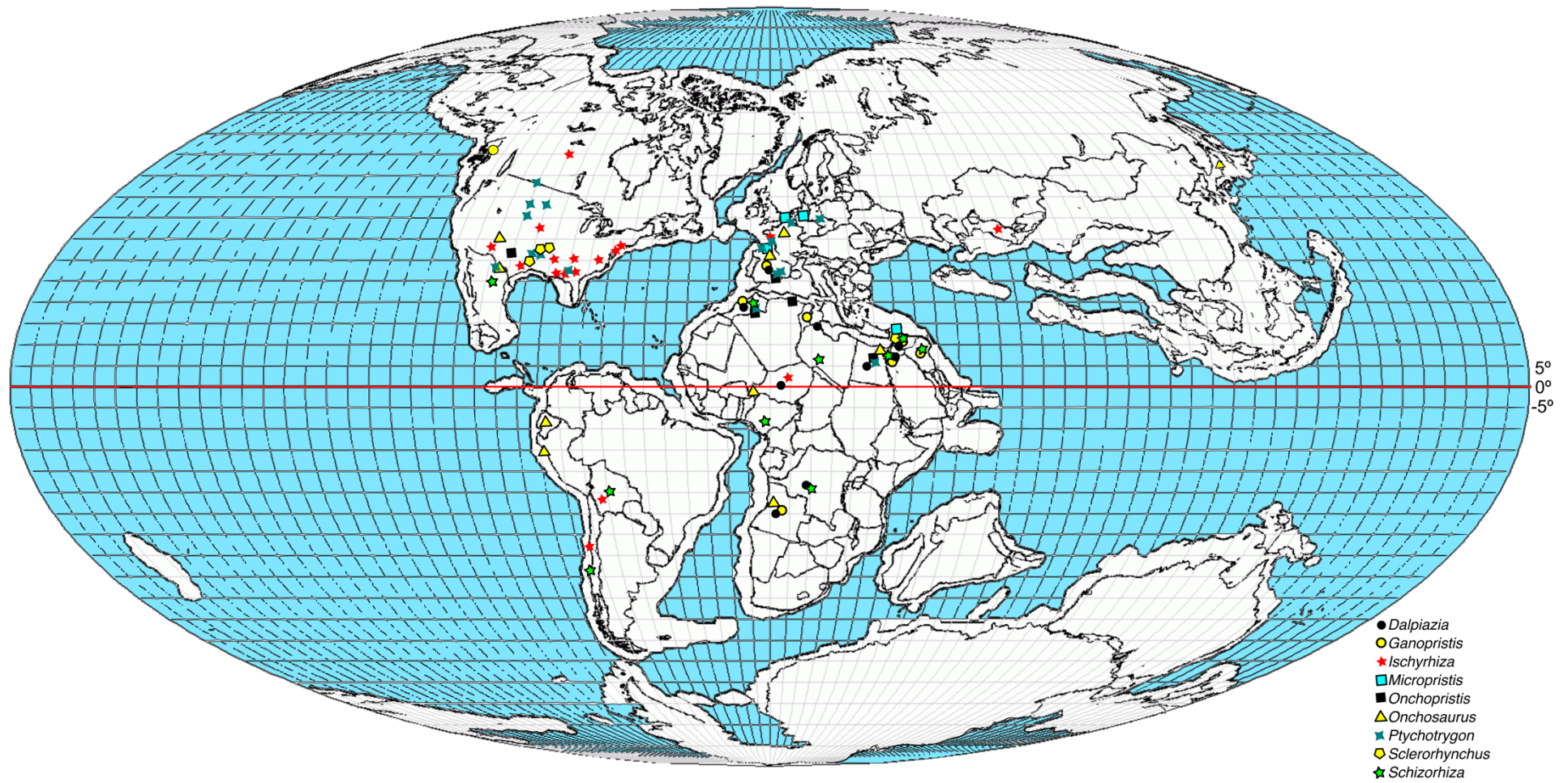
Figure 7.11. Palaeogeographical map of the Late Cretaceous (100 Ma) showing the localities of the nine genera with Cosmopolitan affiliations. The map was generated using software available at Fossilworks (Alroy, 2013). Red line: Equator. Blue outline. Sea. Continental cuts and Cretaceous costal line white. Data in Appendix (7.4).
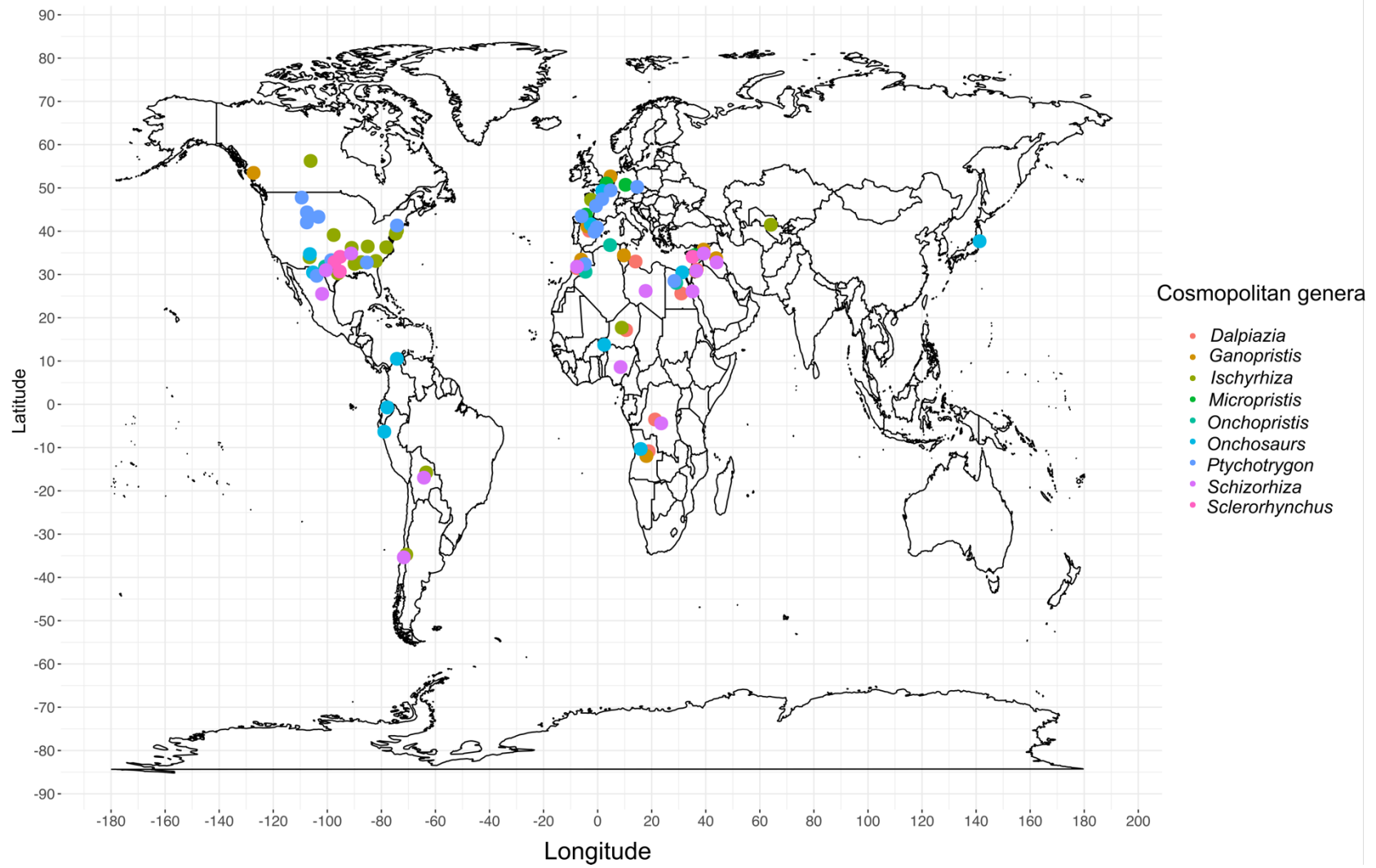
Figure 7.12. Map with the current continental distribution showing the localities were the of the nine genera with Cosmopolitan affinities have been collected. Data in Appendix (7.4).

†*Texatrygon* is the Laurasia-exclusive genus with the most species (five) and records (eight), followed by †*Colombusia* and †*Ankistrorhynchus* with three species and records each. Among them †*Ankistrorhynchus* is the only one present in both continents (American and Europe). Europe present the more diversity of Laurasian genera with six, closely followed by America with five. However, America presents a major number of collections with 16 against 12 in Europe which include the oldest record for the group (Figs. 7.7-7.8 and Table 7.1).

†*Ctenopristis* is the Gondwana genus with the most species (two) and records (five). The rest of the gondwanan genera are singletons (one record and one species) (Figs. 7.9-7.10). Africa is the more diverse among the Gondwana localities with five genera and seven records. Followed by the Middle East with three species and four records. South America presents three genus and three records which include the oldest for the Gondwana genera (Figs. 7.9-7.10).

†*Ptychotrygon* is the cosmopolitan genus with the most species (19) and collections in three continents (America, Europe and Africa). †*Ischyrhiza* presents eight species and the most extended distribution of all Sclerorhynchoid genera with collections in America (North and South) Europe, Asia and Africa (Figs. 7.11-7.12).

Like many other chondrichthyans, many sclerorhynchoids species are mostly known from small fossil remains (e.g. rostral spines, teeth, placoid scales), only eight of the 30 valid genera present a known skeletal record. Most of the skeletal record is associated to sites of Africa and the Middle East, with few records in America (Fig. 7.13).
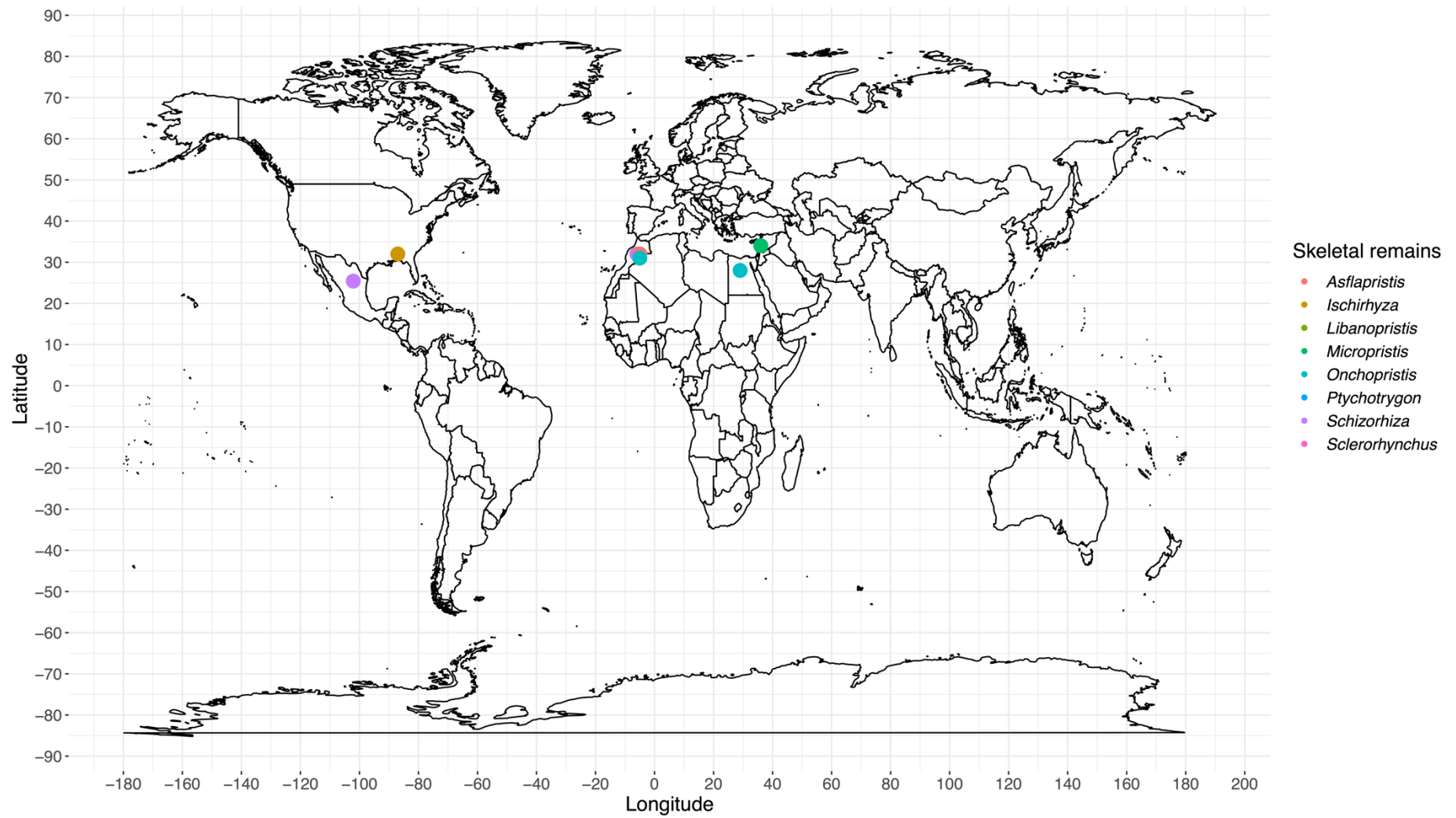
Figure 7.13. Location of the published skeletal records of Sclerorhynchoidei found in the present review. Data in Appendix (7.4).

Most of the early fossil collections (1855-1950) (Fig. 7.14A) of the sclerorhynchoids is characterized by a general lack of small remains, with most of it composed by large specimens or robust rostral spines showing an early focus on large specimens. Many of these early finds probably come from quarries and probably were collected by quarry workers as a means of income, similar to the phosphorite quarries of northern Morocco today (Underwood *et al.,* 2016b). It is therefore likely that there was a preselection of taxa collected based on their possible selling price. In most of these cases after this early preselection on taxa based on size, there has been a later description or redescription of smaller remains associated to them.
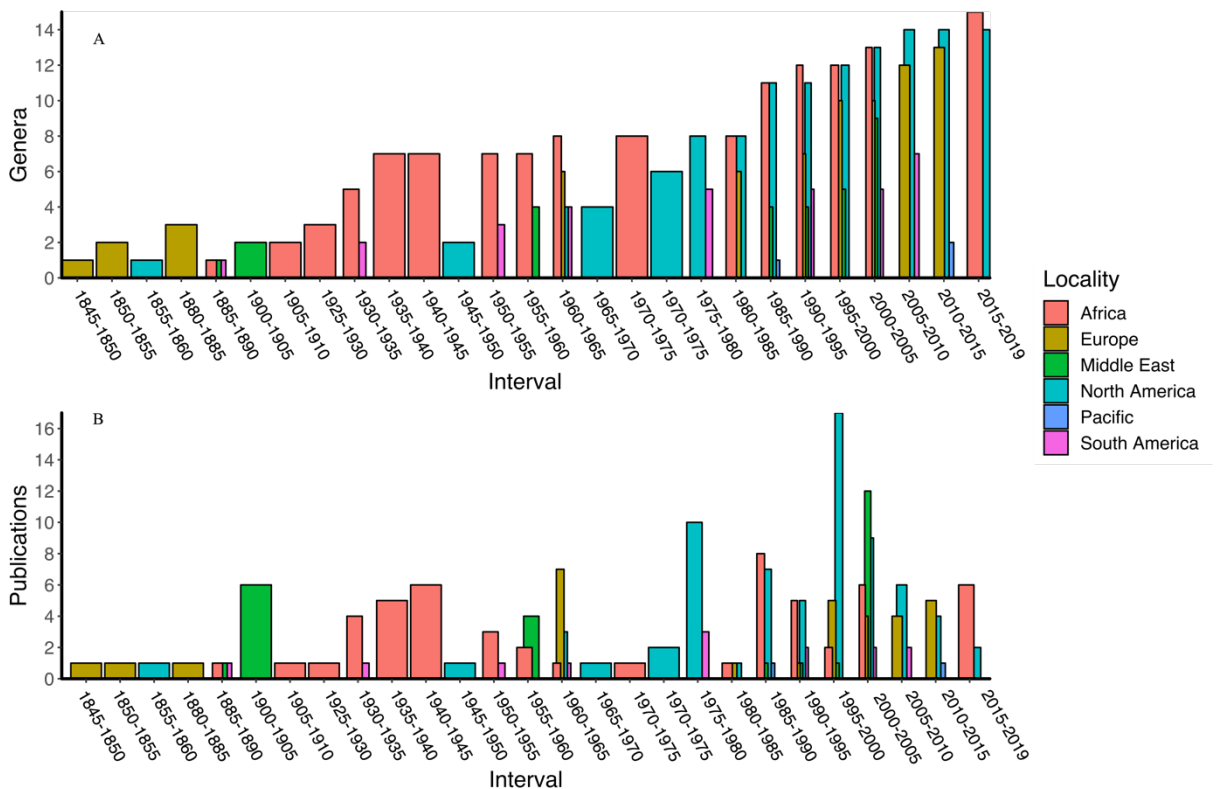
Figure 7.14. Number of species described: **A,** By intervals of ten years and separated by locality of finding. Data in Appendix (7.6). **B,** Total number of species described in the different localities. Data in Appendix (7.1).

Smaller remains become more common in 1970-2015 period, with most of the publications being focused in North America during the 1995-2000 period (Fig. 7.14B).

259

As a result, the Northern Hemisphere (Europe and North America) presents a bigger publication record (99) compared to the (92) of the Southern Hemisphere which could be interpreted as an equal sampling effort. However, in a smaller scale differences in study effort appear (e.g. 32 publications in North America in the last 24 years, compared to the six publications of South America in the same number of years) (Appendix 7.1), which coincide which what has been reported for other chondrichthyan groups (Underwood *et al.*, 2016b).
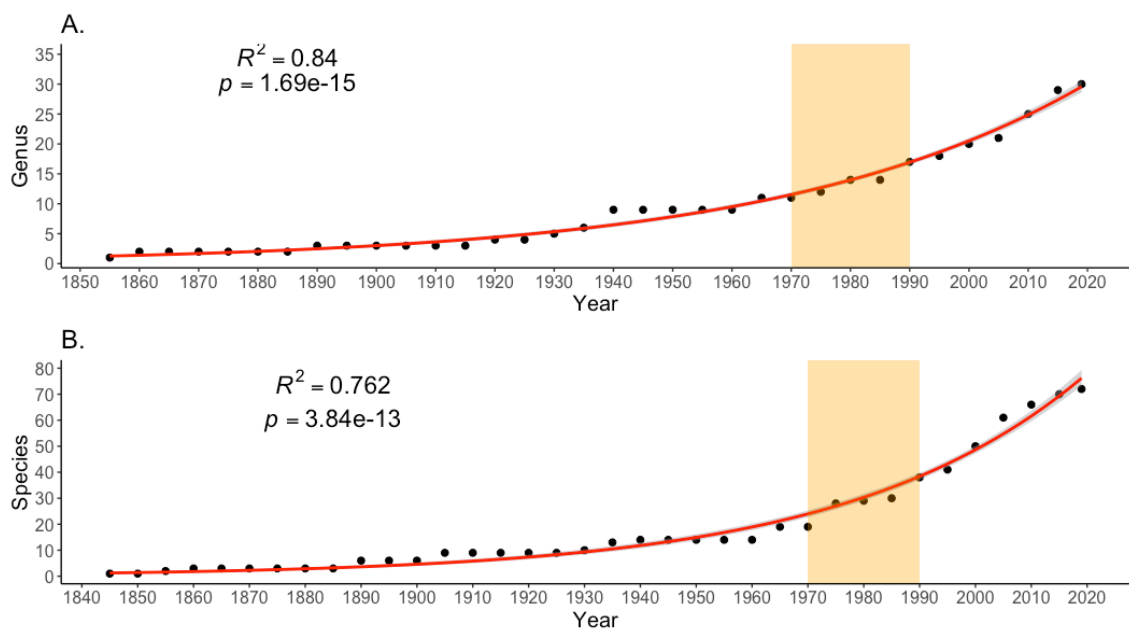
Figure 7.15. Cumulative curve of valid taxa of Sclerorhynchoidei. **A,** Genus Data in Appendix (7.7). **B,** Species Data in Appendix (7.8). Line in red is the best fit curve. Grey shadow is the standard deviation and the orange shadow area is the approximated period in which sieving and bulk sampling started.

The period between the years 1970 to 2019 presents a rapid increase in the number of descriptions of species and genera. In the case of the species the number of described taxa almost quadruple from 19 in 1970 to 72 in 2019 (Fig. 7.15) this tendency becomes more abrupt in the 1990-2015 period in which the implementation of collection techniques of microfossils spreads. While the slightly slower increase species description in the 1970-1990 period coincides with the introduction of techniques such as bulk sampling (Underwood 2006). As these techniques become a common practice a more systematic attempt to study fossil faunas became possible, focussing in isolated small teeth and in

the increase of collection effort in different parts of the globe, (Fig. 7.15). Similar result has been reported for the group (Kriwet & Kussius, 2001) and other chondrichthyan groups (Underwood *et al.,* 2016b; Guinot *et al.,* 2012a).

At both taxonomic levels (species (five), and genera (three)) the period between the years 2015-2019 presents a reduction in the description of new taxa. This slowing tendency in the description and redescription of taxa in recent years could the result of a saturation in the diversity of the group, which could be argued from the genus level considering how close the number of exclusive genera among the zoogeographical regions in the present study are (Gondwana: 12, Laurasia: 11, Cosmopolitan: 9) and the similarities in the publication records between regions (e.g. Laurasia: 100. Gondwana: 93). However, a closer look these records shows that most of the publication effort has been done in some regions (e.g. North America (60) and Africa (53)) while other regions remain largely un-studied (South America (13)). This slowing tendency observed in recent years in the description of species rather than be attributed to a normalization in the number of know taxa, could represents a shift in palaeontological interest as taxonomic focused studies become scarce. A quick search using ISI web knowledge (https://apps.webofknowledge.com) with different combinations of the key words revealed an increase in the number of publications towards 2000-2015 (Fig. 7.16A-C). This rise coincides with the results recovered by the literature review for sclerorhynchoids (Fig. 7.16A), which seems to be part of a systematic effort to describe fossil faunas in different parts of the word. In the years leading to 2019 there seems to be a reduction in the number of publications (Fig. 7.16A-D) which could be the result of a shift of interest in the field. These sources of bias such as oversampled areas and geological periods, need to be addressed before focusing in less taxonomic studies.
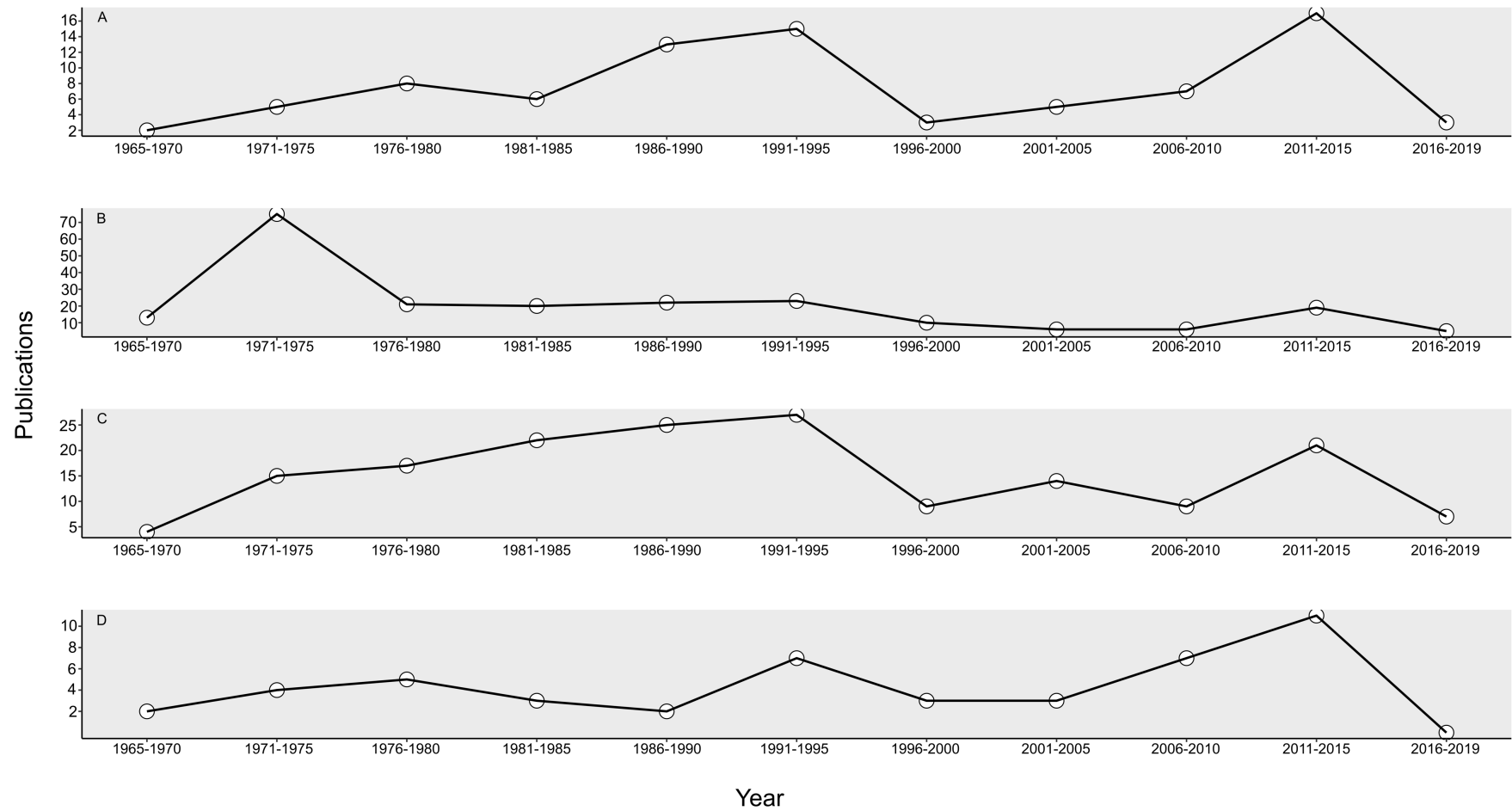
Figure 7.16. Publication numbers five-year using different key words: **A,** Title: fossil assemblage or fossil fauna, Topic: Taxonomy, description, vertebrates. **B,** Title: description and fossil assemblage or fossil fauna, Topic: Taxonomy. **C,** Title: Fossil assemblage or fossil fauna. Topic: Taxonomy, description. **D,** Title: Fossil assemblage or fossil fauna, Topic: Taxonomy, description, Chondrichthyes. Data in Appendix (7.5).

Conclusion

The sclerorhynchoids remain as a sub-order of the Rajiformes order as proposed by Cappetta (2012). However, the taxonomic identity of the order Rajiformes in the present study is restricted since guitarfishes (Rhinopristoidei) and saw fishes (Pristoidei) are excluded from it (Chapter 4). This division is also recovered in molecular analysis (Naylor *et al*., 2012; Last *et al*., 2016).

The Sclerorhynchoidei currently includes two families: Sclerorhynchidae and Onchopristidae. Sclerorhynchidae is the most diverse and widely distributed group with 21 genera and 45 species. Ptychotrygonoids are placed as a members of the sub-order Sclerorhynchoidei as part of the family Sclerorhynchidae in the sub-family Ptychotrygoninae, as suggested in Chapters 4 and. This family comprehends four genera (†*Ptychotrygon*, † *Ptychotrygonoides*, †*Asflapristis* and †*Texatrygon*). The subfamily and the genus †*Ptychotrygon* show a clearly Laurasian affinity with 12 of those species being described in North America. †*Ptychotrygon* represents the most diverse Genus of sclerorhynchoids with 19 valid species. The diversity of genera known since 2001 specially in the Laurasia genera as a result of an increase in the collection efforts in North America in the years 2000-2015, leading to a total of 12 exclusive Gondwana: genera, 11 in Laurasian and nine Cosmopolitan. These results suggest that sclerorhynchoids in general presented a wider distribution.

In recent years this increase tendency in the description of new fossil species has slowed, considering the similarities in the number of genera between the regions (Gondwana: 12, Laurasia: 11, Cosmopolitan: 9) and the similarities in the publication records between regions (e.g. Laurasia: 100. Gondwana: 93). This slowing tendency could the result of a saturation in the diversity of the group. However, the bibliographic review revealed

important differences in the study effort among the different regions of these zoogeographical regions (e.g. the present study found a total of 60 publications describing fossil faunas in North America, 53 in Africa and 13 in South America 13), suggest that this in fact is a saturation of diversity at some areas whereas others remain largely unstudied and sclerorhynchoid and batoid diversity could be significantly larger than what is assumed. The present results suggest that oversampling is not only restricted to geological periods, but to geological areas. These sources of bias need to be addressed before focusing in less taxonomic studies.

Chapter 8

General Discussion

This project started as a description of specimens collected in a very peculiar taphonomic environment in Morocco in which three-dimensional fossil remains of batoids were previously discovered (Claeson *et al.,* 2013). The preparation of the pectoral region of the specimen NHMUK PV P75433 (†*Asflapristis cristadentis*), revealed they were sclerorhynchids. The preparation of the mouthpiece of the specimen NHMUK PV P73630 (†*Ptychotrygon rostrispatula*), revealed a well-differentiated tooth morphology, along with slender jaws. The preparation of the specimen NHMUK PV P75498 and NHMUK PV P75496 (†*Ptychotrygon rostrispatula*) revealed a more gracile synarcual cartilage. When compared to the stout and almost rectangular synarcual cartilage and wide mouth cartilage of specimen NHMUK PV P75431 and NHMUK PV P75433, suggested the presence of two sclerorhynchoid species (†*Asflapristis cristadentis* and †*Ptychotrygon rostrispatula*) which represent the first know skeletal remains of the family Ptychotrygonidae.

The extremely well-reserved specimens collected in Asfla allowed a restudy of the phylogenetic relations of the group. The analyses (Chapters 4 and 5) used reductive coding, as an alternative to the unordered multistate commonly used in phylogenetic analysis of fossil batoids (e.g. Brito *et al*., 2013;2019; Claeson *et al*; 2013; Underwood & Claeson, 2017). A discussion on the changes in character coding and characters used is provided for each of the analyses, trying to provide further insight on why changes were made from previous works.

Both Chapters 4 and 5 place sclerorhynchoids within Rajiformes, this placement differs from previous phylogenetic analyses (e.g. Brito *et al*., 2013;2019; Claeson *et al*; 2013; Underwood & Claeson, 2017). However, the resulting classification is not, as this relation was already establish in previous taxonomic works (Cappetta, 2012). However, what differentiates the placement of sclerorhynchoids as suborder (Sclerorhynchoidei) of Rajiformes proposed here, is that the definition of Rajiformes is much more specific and no longer includes groups with unclear relations (e.g. Jurassic Batoids, guitarfishes (Rhinobatoidei) and Pristoidei). The close relation between sclerorhynchoids and rajoids recovered here is supported by similarities on the branchial skeleton (lack of articulation surface between second hypobranchial and basibranchial) observed in members of the family Sclerorhynchidae (†*Sclerorhynchus atavus* and †*Ptychotrygon rostrispatula*). Whether this character is more widely distributed in the suborder Sclerorhynchoidei remains unknown under current palaeontological evidence. This first analysis of the thesis was also used to compare the results recovered by the two phylogenetic estimation methods used (parsimony and Bayesian inference). This comparison aim was not to point the merits of each phylogenetic inference approach, but as way to cross-validate the groups recovered with each analysis. The contrast between the results reached by these methods might be more informative, especially when studying a group with poor phylogenetic background. In general composition of the crown groups retrieved by both methods was the same, giving reliability to the existence of these groups. However, different cladogenesis events leading to these groups were recovered by both methods suggesting that further analysis is needed. It is possible using just skeletal characters might not be enough to solve this issue, fortunately the fossil record offers other sources of information (e.g. tooth microstructure) that might help solve these issues.

The hypothesis that smaller clades within the Sclerorhynchoidei could be recognised with the current skeletal fossil evidence was boosted by the discovery of the first cranial

remains of †*Onchopristis numidus* in the "Kem Kem Beds" and results of the Bayesian analysis of Chapter 4 which suggested that a phylogenetic hypothesis could be formulated within the suborder. With this aim a more focused analysis was proposed. Using parsimony (heuristic search), several taxa were excluded in this analysis as Chapter 4, suggested no close relation with sclerorhynchoids (e.g. myliobatiforms and torpediniforms). The character pool was also modified for this analysis, as some of the species included in the analysis are only know from rostral fragments or neurocranium (†*Schizorhiza* and †*Onchopristis*). Because of this, the analysis in Chapter 5 focused on rostral, tooth and cranial character with just a few post-cranial features. Chapter 5 analysis recovered two large groups, one that includes †*Libanopristis*, †*Micropristis,* †*Sclerorhynchus,* †*Asflapristis cristadentis* and †*Ptychotrygon rostrispatula* and a second with †*Ischyrhiza,* †*Schizorhiza* and †*Onchopristis*. Most of the differences between these groups were found in the rostrum (e.g. presence of robust rostrum, with "wood-like" cartilage accompanied by the presence of a thick layer of peripheral cartilage at the sides of the rostrum; or a thin rostrum with similar size lateral rostral denticles, along with series of enlarge denticles in the ventral portion of the rostrum; or a thin rostrum lacking of enlarge rostral denticle series) which suggest that this structure was highly plastic and might be used in different manners within these groups.

The topological arrangement of Chapter 5 contrasts with previous classifications which only recognized the family Sclerorhynchidae within the sclerorhynchoids (Cappetta, 2012). Furthermore, within the first group †*Asflapristis cristadentis* and †*Ptychotrygon rostrispatula* were placed as a monophyletic group which was later classified as the subfamily Ptychotrygoninae.

With a smaller matrix some issues that arise from the use of reductive coding were explored in this second analysis. Reductive coding provides a sort of logical order for the

characters and provides grouping that might be overlooked by the unordered multistate (Brazeau, 2011; Mannion *et al*., 2013). However, current phylogenetic software deal with inapplicable characters (-) in the same way as they deal with unknown character (?) placing ambiguity in those terminals coded with (- or ?) as it assumes that all states of character are possible which brings issues with the assignation of ancestral states and results in ambiguous optimisation of characters (Brazeau, 2011). To provide further insight in this in the analysis of Chapter 5 several types of optimisation (fast, unambiguous and slow) were compared and although time consuming this approach might be more beneficial as it further deepens the discussion of the characters used and their possible evolutionary implications.

The general composition of the crown groups retrieved by the phylogenetic analysis in Chapter 4 also very similar to the proposed by phylogenetic analysis with molecular data (Aschliman *et al.,* 2012b; Naylor *et al.,* 2012) at least at the order level. A time-scaled analysis was proposed, with the aim of estimating a divergence age for the suborder Sclerorhynchoidei and also for the major clades (orders) of batoids. Two approaches were used: Tip-dating, which allows the extinct taxa to be included as terminals with phylogenetic inference and divergence time estimation occurring simultaneously and "*a posteriori*" which dates a pre-existing unscaled topology, given a set of stratigraphic data for the taxa involved. Stratigraphic indices were calculated to compare the divergence ages estimated by the different methods. The tip-dating approach obtained a more resolved topology and slightly better stratigraphic index scores than the other methods (Table 5.1). The tip-dating analysis placed the possible divergence time of the sclerorhynchoid+rajoid clade, in the Valanginian with a mean in the Aptian, the mean and lower limit (Cenomanian) fall within the know fossil record of the group (Table 5.2). However, the Valanginian falls well beyond the oldest know record of the group (Barremian, Kriwet *et al*., 2009a). Considering that this oldest record belongs to

†*Onchopristis numidus* which shares several characteristics with more latter taxa (e.g. †*Ischyrhiza* and †*Schizorhiza*), it is possible that the upper limit of the divergence age estimate is accurate.

There has been only one other study to time scale a batoid phylogeny (Aschliman *et al.,* 2012b). This study used molecular data and did not include fossils as terminals but just as calibration points for the node ages. As expected from previous comparison among morphological and molecular phylogenies of Neoselachii and the fossil record (Maisey, 2004; Underwood, 2006) the present analysis recovered later divergence time intervals than those estimated by the molecular analysis. To evaluate the differences on the estimated ages, both analyses (tip-dating and Aschliman´s *et al*. (2012)) were compared against the known fossil record using diversity curves. With this aim a taxonomic diversity estimate (TDE) and a shareholder quorum subsampling curve (SQS) were estimated. The divergence dates recovered by the present analysis overlay better with the diversity shifts observed in the fossil record and present a smoother succession of cladogenesis events with the divergence leading to all extant order of batoids overlaying with the diversity recoveree after the J/K extinction event and rise of diversity through the Cretaceous and Paleogene. Aschliman *et al.,* (2012b) estimated divergences events in the Early-Middle Jurassic with subsequent ones leading to the major groups (rajoids, torpedinoids, myliobatoids and rhinopristoids) in the Middle-Late Jurassic, contrast with the relative static diversity of neoselachian during that period (Kriwet *et al.,* 2009b). However, this overlapping between the present study and the fossil record could be a result of the taxa sampled for the time scaled analysis, with fewer taxa in the Jurassic than in the Cretaceous and subsequent periods which could ultimately reflect the sporadic nature of the fossil record of batoids. Where periods with a better fossil records (e.g. In the Jurassic period there are only 38 records of eight genera, whereas stages like the Maastrichtian are extremely well sampled with 503 records of 48 genera) will have a

more complete skeletal record. It is possible that representatives of the Torpediniformes were present in the Jurassic as suggested by Aschliman *et al.* (2012b) divergence estimates, but have not been recognized or identifies considering how poor is fossil record for batoids remains in some stages (e.g. not a single marine neoselachian fauna has been described for the Berriasian and the only three neoselachian species are known from the brackish facies (Underwood 2006)). This uneven sampling issue could have several causes (e.g. lack of fossil bearing formations or lack sampling). Currently there no studies addressing diversity estimations for batoids.

In the last part of the present study an update on the taxonomic arrangement of Sclerorhynchoids is presented, following the results of Chapters 2-5 and a bibliographic revision. This arrangement presents two families within the suborder Sclerorhynchoidei (Sclerorhynchidae and Onchopristidae) that differs from previous classifications which recognised one family Sclerorhynchidae (Cappetta, 2012).

The two families proposed comprise a total of 30 valid genera and 72 valid species, of which 21 genera are classified within Sclerorhynchidae, two are included within Onchopristidae and seven are placed as indeterminate family. †*Ptychotrygon* is the most diverse genus of the suborder with 19 valid species, followed by †*Ischyrhiza* with 8 and *Texatrygon* with 5.

Following results of Chapter 5, Ptychotrygonidae (*sensu* Kriwet *et al.*, 2009a) previously classified as a group with uncertain affiliations (Cappetta, 2012) is placed within Sclerorhynchidae as the subfamily Ptychotrygoninae which includes the newly described genus †*Asflapristis* (Chapter 2) and the genera previously classified within it (†*Ptychotrygon*, †*Ptychotrygonoides* and †*Texatrygon*). Only one subfamily was recognised within Sclerorhynchidae. However, considering the size of the group and the

variability observed within it, is likely that more subgroups could be founded within the family.

With the bibliographical revision data, the geographical distribution of the description of the Sclerorhynchoidei taxa was used to compare with previous works that explored palaeobiogeographical aspects of the group. The present study found that most of the sclerorhynchoid species are exclusive to Laurasia, with 44 in this zone (36 of which are found in North American). Gondwana presented 22 species and only six were cosmopolitan. At a genus level both studies recovered Gondwana as the most diverse zoogeographical region at the genus level. With six of the Gondwanan genera proposed Kriwet and Kussius (2001) (†*Ganopristis*, †*Ischyrhiza*, †*Onchopristis*, †*Onchosaurus* and †*Schizorhiza*) recovered as part of the 12 exclusive Gondwanan genera of the present study. However, the marked difference in diversity between Gondwana and Laurasia previously found (Kriwet & Kussius, 2001) was reduced dramatically and the Laurasian genera increased to ten genera. Finally, there was an increase in the cosmopolitan genera (present in both Laurasia and Gondwana regions) from those found by Kriwet & Kussius (2001) to six of the nine were previously.

North America (USA), Europe Africa and the Middle East are the localities with the most extensive record of collections. Whereas large parts of the globe remain poorly sampled (e.g. South America) suggesting that the number of known species for the group could dramatically change with the eventual shift of sampling effort to these zones. The description of batoid fossils faunas seems to have reached its peak 1980-2000 period which coincided with the collection techniques of microfossils becoming a common practice. However, in recent years there has been a slowing down in the number of taxonomic publications for the sclerorhynchoids and other extinct batoids. This shift suggests a change of focus in palaeontology. This issue is briefly considered in Chapter

6, were diversity curves are estimated a mean of comparison divergence estimate ages recovered by phylogenetic analysis the present study. Considering the discrepancies in occurrences between geological periods and regions one might consider that although methods less susceptible to sampling biases are available, they might represent part of the answer to establish an adequate approximation to the diversity of the group, with the other part being the refocus of the sampling effort.

General conclusion

Based on the revision of the material recently collected in Morocco (Africa), the suborder Sclerorhynchoidei is placed within Rajiformes (sensu Naylor *et al.,* 2012) as suggested by the similarities in their branchial skeleton (e.g. no articulation surface between the second hypobranchial and basibranchial). This suborder is one the most successful group of fossils batoids with 30 valid general and 72 valid species and is restricted to the Cretaceous with its divergence time from Rajiformes estimated as late as the Valanginian (132 Ma). The suborder probably appears in some part the Tethyan realm during the Early Cretaceous, as suggested by its oldest fossil record corresponds to the Barremian (129.4-125) of Spain.

Based on skeletal fossil records, two large groups are recognised within the Sclerorhynchoidei (Sclerorhynchidae and Onchopristidae). These two groups are recognized by their rostral cartilage anatomy. Onchopristidae presents a sturdier rostrum with different types of cartilage and thickening of the peripheral cartilage of the rostrum which might be indicative of a more active use in this structure. Sclerorhynchidae present a more thin and fragile rostral structure and within this group the subfamily Ptychotrygoninae is recognised based on the lack of enlarged rostral denticle series associated to the rostral cartilages which includes the genera †*Ptychotrygon,*

†*Ptychotrygonoides*, †*Texatrygon* and the newly described †*Asflapristis*. This anatomical difference suggests the rostrum was used in different manners by these groups.

The revision of the fossil record of the suborder is mostly restricted to the Late Cretaceous and is mainly composed of fragments of teeth and rostral spines. However, beautifully preserved skeletal remains form localities of North America (Alabama) Middle East (Lebanon) and Africa (Morocco) are known. The present analysis places †*Ptychotrygon* as the most diverse genus with 19 species, followed by †*Ischyrhiza* eight species. Most of these species been described in North America (Texas), making Laurasia the most diverse region at a species level. However, at a genus and family level the Sclerorhynchoidei present a wide distribution that could be indicative of the success this group had in the Cretaceous. Although, there seems to be an equilibrium in the number of genus between regions (Laurasia and Gondwana) which coincides with a slowing tendency in the description and redescription of taxa in the last years (2015-2019) and suggest a saturation in the diversity of the group. However, in closer look these records shows that most of the publication effort has been done in some regions (e.g. North America (60) and Africa (53)) while other regions remain largely un-studied (South America (13)) and that this slowing tendency in the description of species rather than a normalization in the number of known taxa, could represents a shift in palaeontological interest as taxonomic focused studies become scarce.

Summary

Chapter 2

In chapter 2 I prepared and described specimens collected from the Asfla region North-west Africa. Six of these specimens present tooth morphologies that correspond to a new genus and species, which were described as †*Asflapristis cristadentis* and five correspond

to a new species †*Ptychotrygon rostrispatula*. These specimens are Turonian in age and represent the first skeletal record for the sub-family Ptychotrygoninae. Previously unknown skeletal structures are reported for the first time (e.g. branchial skeleton and basal portion of the claspers).

From these remains a description of the paleoenvironment is provided, which suggest that the Asfla region corresponds to a specialised biotic association that indicate an environment with not the 'normal' open carbonate shelf, in which the rarity of benthic shelly fossils may be an indication of a hostile seafloor inhibiting nectobenthic taxa

Chapter 3

In Chapter 3 I present a comparison between †*Onchopristis numidus* and †*O. dunklei*, based on the description of material collected from the "Kem-Kem Beds" area of Morocco, which teeth and rostral denticles morphology are similar to that of †*O. numidus*. From this material the first description of cranial mouth and synarcual cartilages of †*O. numidus* is presented along with a description of the rostral anatomy for the genus which resembles that of †*Shizorhiza* and †*Ischyrhiza* with a medial section with wood-like cartilage and a thick peripherical layer of cartilage to which the enlarge rostral denticles are attached. The "Kem-Kem Beds" peculiar neurocranium anatomy with an anterior oval-shaped anterior fenestra at the base of the rostrum and rostral similarities with †*Ischyrhiza* confirm Cappetta (2012) classification of the group within the Sclerorhynchoidei. However, the genus affiliation with the family Sclerorhynchidae is doubtful. Its rostral anatomy; replacement and arrange of the enlarge rostral denticle series are different from other members of the group (e.g. †*Sclerorhynchus* and †*Libanopristis*).

Chapter 4

In Chapter 4, I present a phylogenetic analysis using Bayesian and parsimony methods to place the sclerorhynchoids within batoids and in close relation Rajiformes (*sensu* Naylor *et al.,* 2012), based on similarities in their branchial skeleton. This analysis incorporates new observations form the skeletal remains of †*Asflapristis cristadentis* and †*Ptychotrygon rostrispatula* along with the re-description of several previously proposed characters (Aschliman *et al*., 2012a; Claeson *et al.*, 2013; Brito *et al.,* 2013 and Underwood & Claeson, 2017). Present results suggest no relation between sclerorhynchoids and Rhinopristiformes and suggest that similarities with Pristidae as proposed in previous studies (Kriwet, 2004 and Underwood & Claeson, 2017) are convergent. Bayesian analysis further differentiates separates Sclerorhynchoidei into two groups and supports the idea that a number of distinct families can be identified within the Sclerorhynchoidei (Kriwet *et al*., 2009a; Cappetta, 2012).

Chapter 5

In Chapter 5 following the results of Chapter 4 I present a phylogenetical analysis within sclerorhynchoids, based on observations made in the Asfla and "Kem-Kem" specimens. The analyses were kept separate as some of the species included in Chapter 5 analysis are represented only by fragments (e.g. †*Schizorhiza* which is only know from rostral remains, rostral denticles and possible some teeth), the use of a larger matrix using several parts of the anatomy of batoids would imply that taxa like †*Schizorhiza* would become wild cards jumping from clade to clade. These wild card taxa would lower the resolution of the analysis just as a result of missing data. Because of this the analyses (Chapter 4 and 5) were kept separate and the matrix in Chapter 5 focused on rostral and cranial characters. This analysis implied the restudy of several specimens housed in the NHM

and the report of previously unstudied structures in them (e.g. branchial skeleton of †*Sclerorhynchus atavus*). The present analysis proposes the presence of two large clades within the suborder (which in chapter 7 where given the family level): Clade II (†*Libanopristis,* †*Micropristis,* †*Sclerorhynchus,* †*Asflapristis* and †*Ptychotrygon*) and other and Clade IV (†*Ischyrhiza,* †*Schizorhiza* and †*Onchopristis*). While proposing synapomorphies for each clade, in this chapter the possible ambiguous character optimisations produced by the use of reductive coding are discussed by comparing three types of optimisations of characters are used (fast, unambiguous and slow) and the synapomorphies suggested by each type of optimisations are compared.

Chapter 6

In Chapter 6, I present a time-scaled analysis based on the matrix used in Chapter 4, trying to establish the node age of sclerorhynchoids and other batoids clades. Minimum branch length, equal branch length and tip-dating methods are compared using stratigraphic indices which suggest that tip-dating outperforms the other time-scaling methods. Compared with molecular analysis, the divergence time retrieved from the tip-dating analysis suggest more recent time origin for all the clades. Overall divergence times estimated by the present analysis coincide with several relevant geological events. However, they imply shorter times for the evolution of the batoid clades and suggest periods of rapid morphological change followed by large periods of stasis which might only be reflecting the sporadic nature of the skeletal fossil record

Chapter 7

In chapter 7, a taxonomic arrangement for sclerorhynchoids that recapitulates the results of previous chapters in proposed. Sclerorhynchoids are placed as the suborder Sclerorhynchoidei within the Rajiformes. Within this suborder, two families

(Onchopristidae and Sclerorhynchidae) and the Ptychotrygonidae family *sensu* Kriwet *et al*., (2009a) is placed within the family Sclerorhynchidae as a subfamily (Ptychotrygoninae) following the results of Chapters 5.

As part of this analysis, descriptive statics are used to represent the results from the bibliographic review along with a comparison with previous paleozoogeographical accounts (Kriwet & Kussius, 2001). The bibliographic review revealed a rapid increase in known diversity of sclerorhynchoids from 1970 forward as a result of sieving and bulk sampling methods that allowed a more systematic sampling of fossil outcrops. Overall the known sclerorhynchoid fossil record presents a slightly larger sampling record in the Norther hemisphere and is largely restricted towards the Late Cretaceous.

Bibliography

Albers, H., and Weiler, W. 1964. Eine Fischfauna aus der oberen-Kreide von Aachen und neuere Funde von Fischresten aus dem Maestricht des angrenzenden belgisch-hollandischen Raumes. *Neues Jahrbuch für Geologie und Paläontologie Abhandlungen*. **120:**1-33.

Alfonso, A.F., and Gallo, V. 2001. Study of the scapulocoracoid and cervico-thoracic synarcual cartilage of Rhinoptera brasiliensis Müller & Henle and Rhinoptera bonasus (Mitchill) (Elasmobranchii, Rhinopteridae. *Revista Brasileira de Zoología*, **18**(2), 319-331.

Alroy, J. 2010. Fair sampling of taxonomic richness and unbiased estimation of origination and extinction rates. *The Paleontological Society Papers.* **16**:55-80.

Alroy J. 2013. *Online paleogeographic map generator*. Available from: http://fossilworks.org/?a=mapForm.

Andreev, P., Coates, M.I., Karatajūtė-Talimaa, V., Shelton, R.M., Cooper, P.R., Wang, N., and Sansom, I.J. 2016. The systematics of the Mongolepidida (Chondrichthyes) and the Ordovician origins of the clade. *PeerJ* 4:e1850 https://doi.org/10.7717/peerj.1850

Aschliman, N.C., Claeson K.M., and McEachran J.D. 2012a. Phylogeny of Batoidea. *In*: Carrier, J. C., Musick, J. A. & Heithaus, M. R. (eds.). *Biology of Sharks and Their Relatives*. Second edition. Florida: CRC Press, Boca Raton, 57-95.

Aschliman, N.C., Nishida, M., Miya, M., Inoue, J.G., Rosana, K.M., and Naylor, G.J. 2012b. Body plan convergence in the evolution of skates and rays (Chondrichthyes: Batoidea). *Molecular Phylogenetics and Evolution*, **63** (1), 28-42.

Arambourg, C. 1940. Le groupe des ganopristinés. *Bulletin de la Société géologique de France.* **10**(5):127–147.

Arambourg, C. 1935. Note preliminaire sur les vertebres fossiles des phosphates du Maroc. *Bulletin of the Geological Society.* France. **5**(5): 413-439.

Arambourg, C. 1952. Les vertebres fossiles des gisements de phosphates (Maroc-Aigerie-Tunisie). *Notes et Memoires Service Géologique.* Maroc, **92**: 1-372.

Arambourg, C., and Joleaud, L. 1943. Vertebres fossiles du Bassin du Niger. Bull. Dir. Mines, Afr. Occident. France. **7**:27-84.

Antunes, M. T., and Cappetta, H. 2002. Selaciens du Cretace (Albien-Maastrichtien) d' Angola. *Palaeontographica Abteilung A.* **264**(5-6):85-146.

Bapst, D.W. 2012. Paleotree: an R package for paleontological and phylogenetic analyses of evolution. *Methods in Ecology and Evolution.* **3**(5):803-807.

Bapst DW. 2013. A stochastic rate-calibrated method for time-scaling phylogenies of fossil taxa. *Methods in Ecology and Evolution.* **4**(8), 724–733.

Bapst, D.W., and Hopkins, M.J. 2017. Comparing cal3 and other a posteriori time-scaling approaches in a case study with the Pterocephaliid trilobites. *Paleobiology.* **43:** 49–67.

Bapst, D.W., Wright, A.M., Matzke, N.J., and Lloyd, G.T. 2016. Topology, divergence dates, and macroevolutionary inferences vary between different tip-dating

approaches applied to fossil theropods (Dinosauria). *Biology Letters*. **12**: http://dx.doi.org/10.1098/rsbl.2016.0237.

Bardet, N., Cappetta, H., Pereda Suberbiola, X., Mouty, M., Almaleh, A K., Ahmad, A M., Khrata, O., and Gannoum, N. 2000. The marine vertebrate faunas from the Late Cretaceous Phosphates of Syria. *Geological Magazine.* **137**(3): 269-290.

Bardet, N., Suberbiola, X., and Jalil, N. 2003a. A new mosasauroid (Squamata) from the Late Cretaceous (Turonian) of Morocco. *Comptes Rendus Palevol*, **2**(8):607–616.

Bardet, N., Suberbiola, X., and Jalil, N. 2003b. A new polycotylid plesiosaur from the Late Cretaceous (Turonian) of Morocco. *Comptes Rendus Palevol*, **2**(5):307–315.

Baum, D.A., and Smith, S.D. 2013. *Tree thinking: an introduction to phylogenetic biology*. Roberts and Company Publishers, Greenwood Village. 476 pp.

Beavan, N.R., and Russell, A.P. 1999. An elasmobranch assemblage from the terrestrial-marine transitional lethrbridge coal zone (dinosaur park formation: Upper Campanian), Alberta, Canada. *Journal of Paleontology*. **73**(3):494–503

Becker, M.A., Chamberlain, J., and Wolf, G. 2006. Chondrichthyans from the Arkadelphia Formation (Upper Cretaceous: Upper Maastrichtian) of Hot Spring County, Arkansas. *Journal of Paleontology*. **80**(4):700–716.

Bell, M.A., and Lloyd, G.T. 2015. strap: an R package for plotting phylogenies against stratigraphy and assessing their stratigraphic congruence. *Palaeontology*. **58**(2)**:**379-389.

Belverde, M., Nour-Eddine, J., Breda, A., Gattolin,G., Bourget H., Khaldoune, F., and Dyke, G. J. 2013. Vertebrate footprints from the Kem Kem Beds (Morocco): A novel

ichnological approach to faunal reconstruction. *Palaeogeography, Palaeoclimatology, Palaeoecology*. **383** (2013): 52-58

Benton, M.J., and Donoghue, P.C.J. 2007. Paleontological Evidence to Date the Tree of Life. *Molecular Biology and Evolution*. **24**(1): 26–53.

Benton, M.J., and Storrs, G.W. 1994. Testing the quality of the fossil record: paleontological knowledge is improving. *Geology.* **22**(2):111-114.

Benton, M.J., Dunhill, A.M., Lloyd, G.T., and Marx, F.G. 2011. Assessing the quality of the fossil record: insights from vertebrates. *In*: McGowan, A.J. and Smith, A.B., (Eds.), *Comparing the Geological and Fossil Records: Implications for Biodiversity Studies*. Geological Society of London Special Publications. **358**(1):63-94.

Bernardez, E. 2002. *Los dientes de seláceos del Cretácico de la Depresión Central Asturiana*. PhD Thesis, University of Oviedo. 476 pp.

Bice, K.N., and Shimada, K. 2016. Fossil marine vertebrates from the Codell Sandstone Member (middle Turonian) of the Upper Cretaceous Carlile Shale in Jewell County, Kansas, USA. *Cretaceous Research*. **65**:72–198.

Bonaparte, C.L. 1838. Synopsis vertebratorum systematis. *Nuovi Annali delle Scienze Naturali.* Bologna (2):105–133.

Bortolussi, N., Durand, E., Blum, M., and François, O. 2005. apTreeshape: Statistical Analysis of Phylogenetic tree shape. *Bioinformatics*. **22**(3):363-364.

Botella, H., Plasencia, P., Marquez-Aliaga, A., Cuny, G., and Dorka, M. 2009. *Pseudodalatias henarejensis* nov. sp. a New Pseudodalatiid (Elasmobranchii) from the Middle Triassic of Spain. *Journal of Vertebrate Paleontology, 29*(4), 1006-1012.

Bourdon, J., Wright, K., Lucas, S.G., Spielmann, J. A., and Pence, R. 2011. Selachians from the Upper Cretaceous (Santonian) Hosta Tongue of the Point Lookout Sandstone, central New Mexico. *Bulletin of New Mexico Museum of Natural History Sciences*. **52**:1-54.

Brazeau, M.D. 2011. Problematic character coding methods in morphology and their effects. *Biological Journal of the Linnean Society.* **104**(3): 489–498.

Brito, P., and Seret, B. 1996. The new genus *Iansan* (Chondrichthyes, Rhinobatoidea) from the Early Cretaceous of Brazil and its phylogenetic relationships. In: Arritia, G., and Gunther, V. *Mesozoic fishes-systematics and paleoecology*. Verlag Dr. Friedrich Pfeil. Munich. **1**: 47–62.

Brito, P., and Dutheil, D.B. 2004. A preliminary systematic analysis of Cretaceous guitarfishes from Lebanon. *In*: Arriatia, G., and Tintori A. (esd.). *Mesozoic fishes Systematics Paleoenvironments and Biodiversity*. Verlag Dr. Friedrich Pfeil. München, **3**:101–109.

Brito, P., Leal, M., and Gallo, V. 2013. A new lower Cretaceous guitarfish (Chondrichthyes, Batoidea) from the Santana formation, Northeastern Brazil. *Boletim do Museu Nacional, Geologia*, **75**:1–13.

Brito, P., Villalobos-Segura, E., and Alvarado-Ortega, J. 2019. A new early cretaceous guitarfish (chondrichthyes, batoidea) from the Tlayúa Formation, Puebla, Mexico. *Journal of South American Earth Sciences*. **90**:155-161.

Buchy, M., Métayer, F., and Frey, E. 2005. Osteology of *Manemergus anguirostris* n. gen. et sp., a new plesiosaur (Reptilia, Sauropterygia) from the Upper Cretaceous of Morocco. *Palaeontographica Abteilung A*. 97–120.

Cappetta, H. 1972. Les poissons cretaces et tertiaires du bassin des Iullemmeden (Republique du Niger). *Palaeovertebrata*, **5**(5): 179-251.

Cappetta, H. 1973. Selachians from the Carlile Shale (Turonian) of South Dakota. *Journal of Paleontology*. **47** (3): 504-514.

Cappetta, H. 1974. Sclerorhynchidae nov. fam., Pristidae et Pristiophoridae: un example de parallélisme chez les Sélaciens. Comptes rendus de l'Académie des Sciences. Paris, 225-228.

Cappetta, H. 1975a. Sur quelques selaciens nouveaux du Cretace superieur de Bolivie (Amerique du Sud). *Geobios*, **8**(1):5-24.

Cappetta, H. 1975b. *Ptychotrygon vermiculata* nov.sp., sélacien nouveau de Campanien du New Jersey (USA). C.R. somm. Soc. géol. France, (5): 164-166.

Cappetta, H. 1980a. Les sélaciens du Crétacé supérieur du Liban. I: Requins. *Palaeontographica Abteilung A.*, 69-148.

Cappetta, H. 1980b. Les Selaciens du Cretace superieur du Liban. II. Batoïdes *Palaeontographica, Abteilung. A.* **168**(5-6):149–229.

Cappetta, H. 1981. Sur la découverte des genres *Ischyrhiza* et *Ptychotrygon* (Selachii, Batomorphii) dans le Crétacé supérieur de Vendée (France). *Geobios.* **14**(6):807–813.

Cappetta, H., 1987. Chondrichthyes II: Mesozoic and Cenozoic Elasmobranchii, volume 2. G. Fischer Verlag. 193pp.

Cappetta, H. 1991a. Découverte de nouvelles faunes de sélaciens (Neoselachii) dans les phosphates maastrichtiens de la Mer Rouge, Egypte. *Münchner geowissenschaftliche Abhandlungen. Geologie und Paläontologie*, 19: 17-56.

Cappetta, H. 1991b**.** Late Cretaceous selachian faunas from Bolivia: new data and summary. *In*: Suarez Soruco R. (ed.). *Fosiles y Facies de Bolivia; Vol. I: Vertebrados. Rev. Teen*. Yacirnientos Petroliferos Fiscales Bolivianos. **12**(3-4):435-439.

Cappetta, H. 2004. A new species of *Ptychotrygon* (Neoselachii: Rajiformes) from the Upper Turonian of Touraine (France). *Neues Jahrbuch fur Geologie und Palaontologie-Monatshefte*, (1):41–52.

Cappetta, H. 2006. Fossilium Catalogus, I: Animalia. *Backhuys Publishers*, Leiden, Netherlands. 472 pp.

Cappetta, H. 2012. Chondrichthyes: Mesozoic and Cenozoic Elasmobrachii: Teeth. *Gustav Fischer Verlag*. München, **3**:512pp.

Cappetta, H., and Case, G.R. 1975a. Contribution à l'étude des Sélaciens du groupe Monmouth (Campanien-Maestrichtien) du New Jersey. *Palaeontographica Abteilung A*. **151** (1-3): 1-46.

Cappetta, H., and Case, G. R. 1975b. Sélaciens nouveaux du Crétacé du Texas. *Geobios*, **8:** 303–307.

Cappetta, H., and Case, G. 1997. A new selachian fauna from the Late Maastrichtian of Texas (Upper Cretaceous/Navarroan; Kemp Formation). Münchner Geowissenschaftliche Abhandlungen, 34: 131-189

Cappetta, H., and Case, G. 1999. Additions aux faunes de sélaciens du Crétacé du Texas (Albien Supérieur-Campanien. *Palaeo Ichthyologica*, **9**: 5–111.

Cappetta, H., and Corral, J. 1999. Upper Maastrichtian selachians from the Condado de Trevifio (Basque Cantabrian region, Iberian Peninsula). *Estudios del Museo de Ciencias naturales de Alava*. **14**(1):339- 372.

Cappetta, H., Pfeil, F., and Schmidt-Kittler, N. 2000. New biostratigraphical data on the marine Upper Cretaceous and Palaeogene of Jordan. *Newsletters on Stratigraphy.* **38** (1):81-95.

Carroll, R.L. 1988. Vertebrate paleontology and evolution. W.H. Freeman and Company. USA. 698 pp.

Case, G.R. 1978**.** A new selachian fauna from the Judith River Formation (Campanian) of Montana. *Palaeontographica Abteilung A*. **160** (1-6), 176-205.

Case, G. R. 1979. Cretaceous selachians from the Peedee Formation (Late Maastrichtian) of Duplin County, North Carolina. *Brimleyana*, **2:**77-89.

Case, G.R. 1987a. A new selachian fauna from the Late Campanian of Wyoming (teapot sandstone member, Mesaverde formation, Big Horn basin. *Palaeontographica Abteilung A*. **197** (1-3):1-37.

Case, G.R. 1987b. *Borodinopristis schwimmeri*, a new ganopristine sawfish from the Upper Blufftown formation (Campanian) of the Upper Cretaceous of Georgia. *Bulletin of the New Jersey Academy of Sciences*. **32**(1): 25–33.

Case, G. R., and Cappetta, H. 1997. A new selachian fauna from the Late Maastrichtian of Texas (upper Cretaceous/Navarroan; Kemp formation). *Münchner Geowissenschaftliche Abhandlungen A.* **34**, 131–189.

Case, G.R., and Cappetta, H. 2004. Additions to the elasmobranch fauna from the late Cretaceous of New Jersey (middle Maastrichtian, Navesink Formation). *Palaeovertebrata.* **33**(1-4):1-16.

Case, G.R., and Schwimmer, D.R. 1988. Late Cretaceous fish from the Blufftown Formation (Campanian) in western Georgia. *Journal of Paleontology.* **62**:290–301.

Case, G.R., Schwimmer, D.R., Borodin, P.D., and Leggett, J.J. 2001. A new selachian fauna from the Eutaw formation (Upper Cretaceous/early to middle Santonian) of Chattahoochee county, Georgia. *Palaeontographica Abteilung A.* **261**(4-6):83–102.

Casier, E. 1964. Contributions à l'étude des poissons fossiles de la Belgique. XIII. Présence de ganopristinés dans la Glauconie de Lonzée et le Tuffeau de Maestricht. *Bulletin de l'Institut Royal des Sciences Naturelles de Belgique.* **40**(11):1–25.

Cavin, L. 1995. *Goulmimichthys arambourgi* ng, n. sp., un Pachyrhizodontidae (Actinopterygii, Teleostei) d'une nouvelle localité à nodules fossilifères du Turonien inférieur marocain. Comptes rendus de l'Académie des sciences. Série 2. *Sciences de la terre et des planètes*, **321**(11):1049–1054.

Cavin, L., and Dutheil, D. 1999. A new Cenomanian ichthyofauna from Southeastern Morocco and its relationships with other early late Cretaceous Moroccan faunas. *Geologie en Mijnbouw*, **78**(3-4):261–266.

Cavin, L. 2001. Osteology and phylogenetic relationships of the teleost *Goulmimichthys arambourgi* Cavin, 1995, from the upper Cretaceous of Goulmima, Morocco. *Eclogae Geologicae Helvetiae*, **94**(3):509–536

Cavin, L., and Forey, L. P. 2004. New mawsoniid coelacanth (Sarcopterygii: Actinistia) remains from the Cretaceous of the Kem Kem Beds, Southern Morocco. *In*: Arriatia, G.,

and Tintori A. (esd.). *Mesozoic fishes Systematics Paleoenvironments and Biodiversity*. Verlag Dr. Friedrich Pfeil. München, **3**:101–109.

Cavin, L., Tong, H., Boudad, L., Meister, C., Piuz, A., Tabouelle, J., Aarab, M., Amiot, R., Buffetaut, E., and Dyke, G. 2010. Vertebrate assemblages from the Early-Late Cretaceous of southeastern Morocco: an overview. *Journal of African Earth Sciences*, **57**(5):391–412.

Checchia-Rispoli, G. 1933. Di un nuovo genere di" Pristidae" del Cretaceo superiore della Tripolitania. *Coll.Memorie della Classe di Scienze Fisiche, Matematiche e Naturali*, **1**(4):1-6.

Chiplonkar, G.W., and Ghare, H.A. 1977. Palaeontology of the Bagh Beds. Part 6. *Pisces. Publ. Centr. adv. Stud. Geol., Panjab Univ.* **11**:130-138.

Cicimurri, D.J, Ciampaglio, C.N., and Runyon, K.E. 2014. Late Cretaceous elasmobranchs from the Eutaw formation at Luxapalila Creek, Lowndes County, Mississippi. *PalArch's Journal of Vertebrate Paleontology*. **11**(2):1–36.

Claeson, K.M. 2010. Trends in evolutionary morphology: a case study in the relationships of angel sharks and batoid fishes. PhD thesis, The University of Texas at Austin. 254 pp.

Claeson, K.M., and Hilger, A. 2011. Morphology of the anterior vertebral region in elasmobranchs: special focus, Squatiniformes. *Fossil Record*. **14**(2): 129-140.

Claeson, K.M., Underwood, C.J., and Ward, D. 2013. †*Tingitanius tenuimandibulus*, a new platyrhinid batoid from the Turonian (Cretaceous) of Morocco and the Cretaceous radiation of the Platyrhinidae. *Journal of Vertebrate Palaeontology*, **33**(5):1019–1036.

Claeson, K.M. 2014. The impacts of comparative anatomy of electric rays (Batoidea: Torpediniformes) on their systematic hypotheses. *Journal of Morphology*. **275:** 597–612.

Coates, M.I., Gess, R.W., Finarelli, J.A., Criswell, K.E., and Tietjen, K. 2017. A symmoriiform chondrichthyan braincase and the origin of chimaeroid fishes. *Nature*, 541(7636), 208.

Coates, M.I., Finarelli, J.A., Sansom, I.J., Andreev, P.S., Criswell, K.E., Tietjen, K., Rivers, M.L., and La Riviere, P.J. 2018 An early chondrichthyan and the evolutionary assembly of a shark body plan. *Proceedings of the Royal Society B: Biological Sciences*. 285: 20172418. http://dx.doi.org/10.1098/rspb.2017.2418

Compagno L.J. 1973. Interrelationships of living elasmobranchs. *Zoological Journal of the Linnean Society*. (53):15–61.

Compagno, L.J. 1977. Phyletic relationships of living sharks and rays. *American zoologist*. 17(2), 303-322.

Corliss, B.H., Aubry, M.P., Berggren, W.A., Fenner, J.M, Keigwin Jr, L.D., and Keller, G. 1984. The Eocene-Oligocene boundary event in the deep sea. *Science.* **226** (4676):806-810.

Corral, J.C., Bardet, N., Pereda-Suberbiola, X., and Cappetta, H. 2012. First occurrence of the sawfish Onchosaurus from the Late Cretaceous of Spain. *Journal of Vertebrate Paleontology*. **32**(1):212-218.

Cuny, C., and Benton, M.J. 1999. Early radiation of the Neoselachian sharks in Western Europe. [Premiere radiation adaptative des requins néosélaciens en Europe de l'Ouest]. *GEOBIOS*. **32**(2):193-204.

Curtis, K., and Padian, K. 1999. An Early Jurassic microvertebrate fauna from the Kayenta Formation of northeastern Arizona: microfaunal change across the Triassic–Jurassic boundary. *PaleoBios*. **19**(2):19-37.

Da Silva, J.P.C., and De Carvalho, M.R. 2015. Morphology and phylogenetic significance of the pectoral articular region in elasmobranchs (Chondrichthyes). *Zoological Journal of the Linnean Society.* **175**(3), 525-568.

Dames, W. 1887. Ueber Titanichthys pharao novo gen., novo sp., aus der Kreideformation Aegyptens. Sitzungsberichte der Gesellschaft Naturforschender Freunde zu Berlin, **1887**:69-72.

Danelian, T., and Kenneth, G.J. 2001. Patterns of biotic change in middle Jurassic to early Cretaceous Tethyan Radiolaria. *Marine Micropalentology*. **43**(3-4):239–260.

Dartevelle, E., and Casier, E. 1943. Les poissons fossiles du Bas-Congo et des regions voisines. *Ann. Musee Congo Belge, Ser. A (Miner., Geol., Paleontol.)*. **2**(l): 1-200.

De Carvalho, M.R. 1996. Higher-level elasmobranch phylogeny, basal squaleans, and paraphyly. *In*: Stiassny, M. L., Parenti, L. R. & Johnson, G. D. (eds.). Interrelationships of fishes. New York: Atlantic Press. **3**:35-62.

De Carvalho, M., Maisey, J. C., and Grande, L. 2004. Freshwater stingrays of the Green river formation of Wyoming (early Eocene), with the description of a new genus and species and an analysis of its phylogenetic relationships (Chondrichthyes: Myliobatiformes). *Bulletin of the American Museum of Natural History*, 284: 1–136.

De Carvalho, M. 2004. A Late Cretaceous thornback ray from southern Italy, with a phylogenetic reappraisal of the Platyrhinidae (Chondrichthyes: Batoidea). *In*: Arriatia,

G., and Tintori A. (esd.). *Mesozoic fishes Systematics Paleoenvironments and Biodiversity*. Verlag Dr. Friedrich Pfeil. München, **3**:75–99.

Dembo, M., Matzke, N.J., Mooers, A.Ø., and Collard, M. 2015. Bayesian analysis of a morphological supermatrix sheds light on controversial fossil hominin relationships. *Proceedings of the Royal Society B: Biological Sciences.* **282**(1812): https://doi.org/10.1098/rspb.2015.0943.

Delsate, D., and Candoni, L.W. 2001. Description de nouveaux morphotypes dentaires de Batomorphii toarciens (Jurassique inférieur) du Bassin de Paris: Archaeobatidae nov fam. *Bulletin de la Société des naturalistes luxembourgeois.* **102**:131-144.

Domínguez, H.M.M., and González-Isáis, M. 2007. Contribution to the knowledge of anatomy of species of genus Mobula Rafinesque 1810 (Chondricthyes: Mobulinae). *The Anatomical Record: Advances in Integrative Anatomy and Evolutionary Biology*. **290**(7): 920-931.

Douady, C.J., Dosay, M., Shivji, M.S., and Stanhope, M.J. 2003. Molecular phylogenetic evidence refuting the hypothesis of Batoidea (rays and skates) as derived sharks. *Molecular phylogenetics and evolution*. **26** (2): 215-221.

Dunkle, D.H. 1948. On two previously unreported selachians for the Upper Cretaceous of North America. *Journal of the Washington Academy of Sciences*. **38**(5):173-176.

Dunn, K.A., and Morrissey, J.F. 1995. Molecular phylogeny of elasmobranchs. *Copeia*. **1995**, 526-531.

Dutheil, B.D. 1999. An overview of the freshwater fish fauna from the Kem Kem Beds (Late Cretaceous: Cenomanian) of Southeastern Morocco. *In*: Arratia, G. and Schultze

H.P. (eds.) *Mesozoic Fishes Systematics and Fossil Record*. Verlag Dr. Friedrich Pfeil, München, **2**: 553-563,

Ehrmann, W.U., and Mackensen, A. 1992. Sedimentological evidence for the formation of an East Antarctic ice sheet in Eocene/Oligocene time. *Palaeogeography, Palaeoclimatology, Palaeoecology.* **93**(1-2):85–112.

Ettachfini, E.M., and Andreu, B. 2004. Le cénomanien et le turonien de la plateforme préafricaine du Maroc. *Cretaceous Research*, **25**(2):277–302.

Estes, R. 1964. Fossil vertebrates from the Late Cretaceous Lance Formation, Eastern Wyoming. *University California Publications in Geological Sciences.* **49**:1-180.

Fricke, R., Eschmeyer, W.N., and Fong, J.D. 2019 Species by Family/Subfamily. http://researcharchive.calacademy.org/research/ichthyology/catalog/SpeciesByFamily.a sp 09/Feb/2019

Gayet, M., Sempre, T., Cappetta, H., Jaillard, E., and Lévy, A. 1993. La présence de fossiles marins dans le Crétacé terminal des Andes centrales et ses conséquences paléogéographiques. *Palaeogeography, Palaeoclimatology, Palaeoecology.* **102**(3-4): 283-319.

Georges, K. 2016*. Revision of the fossil batomorphs from the Cretaceous of Lebanon, and their impact on our understanding of the early step of the evolution of the clade*. PhD thesis. Université Libanaise. 217pp.

Gervais, P. 1852. *Zoologie et paléontologie françaises (animaux vertébrés): Ou nouvelles recherches sur les animaux vivants et fossiles de la France*. Paris. 271 pp.

Guinot, G., Adnet, S., and Cappetta, H. 2012a. An analytical approach for estimating fossil record and diversification events in sharks, skates and rays. *PLoS One*. **7**(9): https://doi.org/10.1371/journal.pone.0044632.

Guinot, G., Cappetta, H., Underwood C.J., and Ward, D.J. 2012b. Batoids (Elasmobranchii: Batomorphii) from the British and French Late Cretaceous. *Journal of Systematic Palaeontology*. **10**(3): 445–474.

Goodrich, E.S. 1909. Cyclostomes and Fishes. *In*: Lancaster, E.R. (ed.). *A Treatise on Zoology*, Vol. 9. London: A and C Black.

Goloboff, P.A. 2003. Parsimony, likelihood, and simplicity. *Cladistics*: **19**(2): 91-103.

Goloboff, P.A., Farris, J.S., Källersjö, M., Oxelman, B., Ramírez, M.J., and Szumik, C.A. 2003. Improvements to resampling measures of group support. *Cladistics*. **19**(4): 324-332.

Goloboff, P.A., Farris, J., and Nixon, K. 2013. TNT: Tree Analysis Using New Technology. Updated at: http:// www.lillo.org.ar/phylogeny/tnt/, accessed 12 January2019.

Goloboff, P.A. 2014. Extended implied weighting. *Cladistics*. **30**(3): 260-272.

Haug, E. 1905. Paleontologie. Documents scientifiques de la mission saharielme (mission Foureau-Lamy). - Publ. Soc. Geogr., p. 751-832.

Hay, O.P. 1902.Bibliogrphy and catalogue of the fossil Vertebrata of North America. Bulletin of the United State Geological Survey. 179: 1-868.

Hay, O.P. 1903. On a collection of upper Cretaceous fishes from Mount Lebanon, Syria, with descriptions of four new genera and nineteen new species. *Bulletin of the American Museum of Natural History*. **19**(10):395- 452.

Hedman, M. 2010. Constraints on clade ages from fossil outgroups. *Paleobiology*. **36**(1):16–31.

Hessin, W.A, Morrison, K., and Bowen, D. 2007. *Pictorial guide to the fossil shark teeth from the Upper Cretaceous of Hornby Island, British Columbia, Canada*. Digital Production. W.A Hessin, 35pp.

Huelsenbeck, J.P. 1994. Comparing the stratigraphic record to estimates of phylogeny. *Paleobiology*. **20**(4):470-483.

Huxley, T.H. 1880. On the application of the laws of evolution to the arrangement of the Vertebrata and more particularly of the Mammalia. *Proceedings of the Zoological Society of London. Zoological Society of London*. 649–662 pp.

Jaekel, O. 1894. Die eocänen Selachier vom Monte Bolca: ein Beitrag zur Morphogenie er Wirbelthiere / von Otto Jaekel. Berlin: J. Springer. 228pp

Johanson, Z., Trinajstic, K., Carr, R., and Ritchie, A. 2013. Evolution and development of the synarcual in early vertebrates. *Zoomorphology*, 132(1), 95-110.

Johnson, S.C., and Lucas, S.G. 2003. Selachian fauna from the Upper Cretaceous Dalton Sandstone, middle Rio Puerco Valley, New Mexico. *New Mexico Geological Society Guidebook*. 54:353-358.

Kennedy, W., and Juignet, P. 1981. Upper Cenomanian Ammonites from the environs of saumur, and the provenance of the types of *Ammonites vibrayeanus* and *Ammonites geslinianus*. *Cretaceous Research*, **2**(1):19–49.

Kennedy, W., Gale, A., Ward, D.J., and Underwood, C.J. 2008. Lower Turonian ammonites from Goulmima, Southern Morocco. *Bulletin de l'Institut Royal des Sciences de Belgique, Sciences de la Terre*, **78**:149–177.

Keyes, I.W. 1977. Records of the northern hemisphere Cretaceous Sawfish genus Onchopristis (order Batoidea) from New Zealand. *New Zealand Journal of Geology and Geophysics.* **20**(2):263-272.

Kilian, C. 1931. Des principaux complexes continentaux du Sahara. *Comptes Rendus Sommaires de la Société Géologique de France.* **9**: 109–111.

Kirkland, J., and Aguillón-Martínez, M. 2002. *Schizorhiza*: a unique sawfish paradigm from the Difunta group, Coahuila, México. *Revista Mexicana de Ciencias Geológicas*, **19**(1):16-24.

Kirkland, J.I, Eaton, J.G., and Brinkman, D.B. 2013. Elasmobranchs from upper Cretaceous freshwater facies in Southern Utah. *In*: Titus, A. L., and Loewen, M. A. (eds.). *At the top of the Grand Staircase: The Late Cretaceous of southern Utah.* Indiana University Press.153–194.

Kriwet, J. 1999a. *Ptychotrygon geyeri* n. sp. Chondrichthyes, Rajiformes from the Utrillas Formation (upper Albian) of the central lberian Ranges (east-Spain). *Profil*. **16**: 337-346.

Kriwet, J. 1999b. Neoselachier (Pisces, Elasmobranchii) aus der Unterkreide (unteres Barremium) von Galve und Alcaine (Spanien, Provinz Teruel). *Paleo Ichthyologica*, 9: 113-142.

Kriwet, J. 2003. Neoselachian remains (Chondrichthyes; Elasmobranchii) from the middle Jurassic of SW Germany and NW Poland. *Acta Paleontologica Polonica*, 48(4): 583–594.

Kriwet, J. 2004. The systematic position of the Cretaceous sclerorhynchid sawfishes (Elasmobranchii, Pristiorajea). *In*: Arratia, G. & Tintori, A. (eds.). *Mesozoic fishes Systematics Paleoenvironments and Biodiversity.*: Verlag Dr. Friedrich Pfeil. Munich. **3**: 57-73.

Kriwet, J., and Benton, M.J. 2004. Neoselachian (Chondrichthyes, Elasmobranchii) diversity across the Cretaceous–tertiary boundary. *Palaeogeography, Palaeoclimatology, Palaeoecology,* **214**(3), 181-194.

Kriwet, J., Kiessling, W., and Klug, S. 2009b. Diversification trajectories and evolutionary life-history traits in early sharks and batoids. *Proceedings of the Royal Society of London B: Biological Sciences*. **276**(1658):945–951.

Kriwet, J., Nunn, E.V., and Klug, S. 2009a. Neoselachians (Chondrichthyes, Elasmobranchii) from the Lower and lower Upper Cretaceous of north-eastern Spain. *Zoological Journal of the Linnean Society*. **155** (2), 316-347.

Kriwet, J., and Klug, S. 2004. Late Jurassic selchians (Chondrichthyes, Elasmobranchii) from Southern Germany: Re-evaluation on taxonomy and diversity. *Zitteliana*. **44**: 67-95.

Kriwet, J., and Klug, S. 2008. Diversity and biogeography patterns of Late Jurassic Neoselachians (Chondrichthyes: Elasmobranchii). *Geological Society, London, Special Publications.* **295**(1):55–70.

Kriwet, J., and Klug, S. 2012. Presence of the extinct sawfish, *Onchosaurus* (Neoselachii, Sclerorhynchiformes) in the Late Cretaceous of Peru with a review of the genus. *Journal of South American Earth Sciences.* 39 (2012):52-58.

Kriwet, J., and Kussius, K., 2001. Paleobiology and paleobiogeography of sclerorhynchid sawfishes (Chondrichthyes: Batomorphii). *Revista Española de Paleontología*, 16:35– 46.

Landemaine, O. 1991. Selaciens nouveaux du Cretace superieur du Sud-Ouest de la France. Quelques apports à la systematique des elasmobranches. *Saga*, **1**:1-45.

Läng, E., Boudad, L., Maio, L., Samankassou, E., Tabouelle, J., Tong, H., and Cavin, L. 2013. Unbalanced food web in a Late Cretaceous dinosaur assemblage. *Palaeogeography, Palaeoclimatology, Palaeoecology*. **381**(2013): 26-32.

Last, P., Naylor, G., Bernard, S., White, W., De Carvalho M.R., and Stehmann, M. 2016. *Rays of the World*. Csiro Publishing. 790 pp.

Lauginiger, E.M., and Hartstein, E.F. 1983. *A guide to fossil sharks, skates, and rays from the Chesapeake and Delaware Canal area, Delaware*. Delaware Geological Survey Open File Rep. **21**:1–64.

Laurin, M. 2004. The evolution of body size, Cope's Rule and the origin of amniotes. *Systematic Biology.* **53**(4):594-622.

Lehman, T.M. 1989. Giant Cretaceous sawfish (*Onchosaurus*) from Texas. *Journal of Paleontology*. **63**(4):533-535.

Leidy, J. 1856a. *Notice of some remains of fishes discovered by Dr. John E. Evans.* Proceedings of the Academy of Natural Science of Philadelphia, **8**: 256–257.

Leidy, J. 1856b. Notices of remains of extinct vertebrate animals of New Jersey collected by Cook of the State Geological Survey under the direction of Dr. W. Kitchell. *Proceedings of the Academy of Natural Sciences of Philadelphia.* **8**(6):220-221.

Leriche, M. 1940. Le synchronisme des formations Eocenes marines des cotes de I' Atlantique, d 'apres leur faune ichthyologique. *Comptes rendus de l'Académie des Sciences*, **210:** 589-592.

Lewis, P.O. 2001. Phylogenetic systematics turns over a new leaf. *Trends in Ecology and Evolution*. **16**:30–37.

Lewy, Z., and Cappetta, H. (1989). Senonian Elasmobranch teeth from Israel. Biostratigraphic and paleoenvironmental implications. *Neues Jahrbuch für Geologie und Paläontologie, Monatshefte.* **1989**(4):212-222.

Lezin, C., Andreu, B., Ettachfini, E.M., Wallez, M., Lebedel, V., and Meister, C. 2012. The upper Cenomanian–lower Turonian of the preafrican trough, Morocco. *Sedimentary Geology*, **245**:1–16.

Lloyd, G.T. 2016. Estimating morphological diversity and tempo with discrete character-taxon matrices: implementation, challenges, progress, and future directions. *Biological Journal of the Linnean Society*. **118** (1): 131-151.

Lloyd, G.T., Bapst, D.W., Friedman, M., and Davis, K.E. 2016. Probabilistic divergence time estimation without branch lengths: dating the origins of dinosaurs, avian flight and crown birds. Biology Letters. **12**(11): http://dx.doi.org/10.1098/rsbl.2016.0609.

Lloyd, G.T., Pearson, P.N., Young, J.R., and Smith, A.B. 2012. Sampling bias and the fossil record of planktonic foraminifera on land and in the deep sea. *Paleobiology*. 38(4):569–584.

Lovejoy, N.R. 1996. Systematics of myliobatoid elasmobranchs: with emphasis on the phylogeny and historical biogeography of neotropical freshwater stingrays (Potamotrygonidae: Rajiformes). *Zoological Journal of the Linnean Society*. **117**(3): 207-257.

Maddison, W.P., and Maddison, D.R. 2018. Mesquite: A Modular System for Evolutionary Analysis. Version 3.51 http://mesquiteproject.org, accessed 4 May 2018.

Maisey, J.G. 1978. Growth and form of finspines in hybodont sharks. *Palaeontology*. **21**(3): 657-666.

Maisey, J.G. 1984. Chondrichthyan phylogeny: A look at the evidence. *Journal of Vertebrate Palaeontology*. (4):359–371

Maisey, J.G. 2012. What is an 'elasmobranch'? The impact of palaeontology in understanding elasmobranch phylogeny and evolution. *Journal of Fish Biology*, *80*(5), 918-951.

Maisey, J.G. 2013. The diversity of tessellated calcification in modern and extinct chondrichthyans. *Revue de Paléobiologie*. **32**:355–371.

Maisey, J.G., and Moody, J. 2001. A review of the problematic extinct teleost fish Araripichthys, with a description of a new species from the lower Cretaceous of Venezuela. *American Museum Novitates,* 1–27.

Maisey, J.G., Naylor, G.J., and Ward, D.J. 2004. Mesozoic elasmobranchs, neoselachian phylogeny and the rise of modern elasmobranch diversity. *In*: Arriatia, G., and Tintori A. (esd.). *Mesozoic fishes Systematics Paleoenvironments and Biodiversity.* Verlag Dr. Friedrich Pfeil. München. **3**:17-56.

Maisey, J., Janvier, P., Pradel, A., Denton, J., Bronson, A., Miller, R., and Burrow, C. 2019. *Doliodus* and Pucapampellids: Contrasting Perspectives on Stem Chondrichthyan Morphology. In Z. Johanson, C. Underwood, & M. Richter (Eds.), Evolution and Development of Fishes (pp. 87-109). Cambridge: Cambridge University Press. doi:10.1017/9781316832172.006

Mannion, P. D., and Barrett, P. M. 2013. Additions to the sauropod dinosaur fauna of the Cenomanian (early Late Cretaceous) Kem Kem Beds of Morocco: Palaeobiogeographical implications of the mid-Cretaceous African sauropod fossil record. *Cretaceous Research*. **45** (2013): 49-59

Mannion, P.D., Upchurch, P., Barnes, R.N., and Mateus, O. 2013. Osteology of the Late Jurassic Portuguese sauropod dinosaur *Lusotitan atalaiensis* (Macronaria) and the evolutionary history of basal Titanosauriforms. *Zoological Journal of the Linnean Society*. **168:** 98–206.

Marramà, G., Carnevale, G., Engelbrecht, A., Claeson, K., Zorzin, R., Fornasiero, M., and Kriwet, J., 2018. A synoptic review of the Eocene (Ypresian) cartilaginous fishes (Chondrichthyes: Holocephali, Elasmobranchii) of the Bolca konservat lagerstätte, Italy. *Paläontologische Zeitschrift*, **92**:283–313.

Marshall, C.R. 2008. A simple method for bracketing absolute divergence times on molecular phylogenies using multiple fossil calibration points. *The American Naturalist.* **171**(6):726-742.

Martill, D.M. 1988. Preservation of fish the Cretaceous Santana formation of Brazil. *Palaeontology*, 31:1–18.

Martill, D.M. 1991. Fish. *In*: Martill D.M. and Hudson J. D. (Eds.). *Fossils of the Oxford Clay*. Field guides to fossils, Vol. 4. Palaeontological Association, London. 197–225.

Martill, D.M., and Ibrahim, N. 2012. Aberrant rostral teeth of the sawfish *Onchopristis numidus* from the Kem Kem Beds (? early Late Cretaceous) of Morocco and a reappraisal of *Onchopristis* in New Zeland. *Journal of African Earth Sciences*: **64**, 71–76.

Matzke, N.J., and Wright, A. 2016. Inferring node dates from tip dates in fossil Canidae: the importance of tree priors. *Biology letters.* **12**(8): https://doi.org/10.1098/rsbl.2016.0328.

McEachran, J.D., Dunn, K.A., and Miyake, T. 1996. Interrelationships of the batoid fishes (Chondrichthyes: Batoidea). *In*: Stiassny, M. L., Parenti, L.R. & Johnson, G.D. (eds.). *Interrelationships of fishes*. New York: Atlantic Press. 63-84.

McEachran, J.D., and Dunn, K.A. 1998. Phylogenetic analysis of skates, a morphologically conservative clade of elasmobranchs (Chondrichthyes: Rajidae). *Copeia*. **1998:** 271-290.

McEachran, J.D., and Aschliman, N. 2004. Phylogeny of Batoidea. *In:* Carrier, J.C., Musick, J.A., and Heithaus, M. R. (eds.). *Biology of sharks and their relatives*. Florida: CRC Press, Boca Raton, 79–113.

McNulty, C.L., and Slaughter, B.H. 1962. A new sawfish from the Woodbine Formation (Cretaceous) of Texas. *Copeia*, **1962** (4), p. 775-777.

McNulty, C.L., and Slaughter, B.H. 1972. The Cretaceous selachian genus, *Ptychotrygon* Jaekel, 1894. *Eclogae Geologicae Helvetiae*. **65** (3), 647-656.

Meyer, R.L. 1974. Late Cretaceous elasmobranchs from the Mississippi and East Texas embayments of the Gulf Coastal Plain. Unpublish PhD, Southern Methodist University. Arlington, Texas. 419 p

Miller, K.G., Kominz, M.A., Browning, J.V., Wright, J.D., Mountain, G.S., Katz, M.E., Sugarman, P.J., Cramer, B.S., Christie-Blick, N., and Pekar, S.F. 2005. The Phanerozoic record of global sea–level change. *Science.* 310(5752):1293-1298.

Miller, M.A., Pfeiffer, W., and Schwartz, T. 2010. Creating the CIPRES Science Gateway for inference of large phylogenetic trees. *In:* Proceedings of the Gateway Computing Environments Workshop (GCE), 14 Nov. 2010, New Orleans, LA.**1**;8.

Miyake, T., and McEachran, J.D. 1991. The morphology and evolution of the ventral gill arch skeleton in batoid fishes (Chondrichthyes: Batoidea). *Zoological Journal of the Linnean Society.* **102**(1), 75-100.

Miyake, T., McEachran, J.D., Walton, P.J., and Hall, B.K. 1992. Development and morphology of rostral cartilages in batoid fishes (Chondrichthyes: Batoidea), with comments on homology within vertebrates. *Biological Journal of the Linnean Society*, *46*(3), 259-298.

Monger, J.W.H., Heyden, P., Journeay, M.J., Evenchick, C.A., and Mahoney, J.B. 1994. Jurassic-Cretaceous basins along the Canadian coast belt: Their bearing on premid-Cretaceous sinistral displacements. *Geology.* **22**(2):175–178.

Mustafa, H.A., Case, G.R., and Zalmout, I. 2002. A new selachian fauna from the Wadi Umm Ghudran formation (Late Cretaceous) central Jordan. *Neues Jahrbuch fur Geologie und Palaontologie-bhandlungen.* **226**(3):419–444.

Müller, J., and Henle, J. 1841. Systematische beschreibung der Plagiostomen. *Verlag Von Veit und Comp.* Berlin, **3**: 345pp

Naylor, G.J., Caira, J.N., Jensen, K., Rosana, K.A., Straube, N., and Lakner, C. 2012. Elasmobranch phylogeny: A mitochondrial estimate based on 595 species. *In:* Carrier, J. C., Musick, J. A. & Heithaus, M. R. (eds.). *Biology of Sharks and Their Relatives*. Second edition. Florida: CRC Press, Boca Raton, 31-56.

Nelson, J.S., Grande, T.C., and Wilson, M.V. 2016. *Fishes of the World*. John Wiley & Sons. USA, 752 pp

Nessov, L.A. 1997 Cretaceous non marine vertebrates of Northern Eurasia. *In*: Golovnevu, B. and Verianov, A.O.A. *Institute of Earth Crust Posthumous Edition*. Saint Petersburg. Univ. Saint Petersburg, Inst. Earth Crust. 1-218.

Newberry, J.S. 1885. Descriptions of some gigantic placoderm fishes recently discovered in the Devonian of Ohio. *Transactions of the New York Academy of Sciences*. **5**:25-28.

Nishida, K. 1990. Phylogeny of the suborder Myliobatidoidei. *Memoirs of the faculty of fisheries Hokkaido University*. **37** (1-2), 1-108.

Nixon, K.C. 2002. WinClada. Version 1.0000. Published by the author, Ithaca, NY, USA.

Noubhani, A., and Cappetta, H. 1997. Les Orectolobiformes, Carcharhiniformes et Myliobatiformes (Elasmobranchii, Neoselachiil des bassins à phosphate du Maroc

(Maastrichtien-Lutetien basal). Systematique, biostratigraphie, evolution et dynamique des faunes. *Palaeo Ichthyologica*. **8**:1-327.

Nürnberg, D., and Müller, B. 1991. The tectonic evolution of the South Atlantic from Late Jurassic to present. *Tectonophysics*. **191**(1-2): 27–53.

O'Connor A., and Wills, M.A. 2016 Measuring stratigraphic congruence across trees, higher taxa, and time. *Systematic Biology*. **65**(5):792-811.

O'Reilly, J.E., Puttick, M.N., Parry, L., Tanner, A.R., Tarver, J.E., Fleming, J., Pisani, D., and Donoghue, P.C. 2016. Bayesian methods outperform parsimony but at the expense of precision in the estimation of phylogeny from discrete morphological data. *Biology Letters*: **12**(4): 1-5.

O'Reilly, J.E., Puttick, M. N., Pisani, D., and Donoghue, P. C. 2018. Probabilistic methods surpass parsimony when assessing clade support in phylogenetic analyses of discrete morphological data. *Palaeontology*: **61**(1): 105-118.

Paramo-Fonseca, M.E. 1997. *Les vertébrés marins du turonien de la vallée supérieure du Magdalena, Colombie-Systématique, paléoécologie, paléobiogéographie*. PhD dissertation. 174pp.

Pereira, A.A., and Medeiros, M.A. 2008. A new Sclerorhynchiform (Elasmobranchii) from the middle Cretaceous of Brazil. *Revista Brasileira de Paleontologia*. **11**:207–212.

Peng, J., Russell, A.P., and Brinkman, D.B. 2001. *Vertebrate microsite assemblages (exclusive of mammals) from the Foremost and Oldman Formations of the Judith River Group (Campanian) of southeastern Alberta: an illustrated guide*. Alberta Community Development, Provincial Museum of Alberta, Curatorial Section. **25**:1–54.

Philippi, R.A. 1887. *Die tertiären und quartären Versteinerungen Chiles*. Leipzig. 266 pp.

Pol, D., and Norell, N.A. 2001. Comments on the Manhattan stratigraphic measure. *Cladistics*. **17**(3):285–289.

Pradel, A., Tafforeau, P., Maisey, J.G., and Janvier, P. 2011. A new Paleozoic Symmoriiformes (Chondrichthyes) from the Late Carboniferous of Kansas (USA) and cladistic analysis of early chondrichthyans. *Plos one*. 6(9), e24938.

Priem, F. 1914. Sur des vertebres du Cretace et de l'Eocene d'Egypte. *Bulletin Société Géologique du France.* **4**(14):366- 382.

Quaas, A. 1902. Beitrag zur Kenntniss der Fauna der obersten Kreidebildungen in der libyschen Wiiste (Overwegischichten und Blatterthone). *Palaeontographica.* **30**(2):153-336.

Rage, J.D., and Dutheil, D.B. 2008. Amphibians and squamates from the cretaceous (Cenomanian) of Morocco. A preliminary study, with description of a new genus of pipid frog. *Palaeontographica Abteilung A*. (2008): 1-22.

Raup, D.M. 1972. Taxonomic diversity during the Phanerozoic. *Science*, **177**(4054), 1065-1071.

Raup, D.M. 1976. Species diversity in the Phanerozoic: an interpretation. *Paleobiology*. **2**(4):289-297.

Regan, C.T. 1906. A classification of the selachian fishes. Proceedings of the Zoological Society London 1906:722–758.

Rees, J. 2002. Shark fauna and depositional environment of the earliest Cretaceous Vitabäck Clays at Eriksdal, southern Sweden. *Transactions of the Royal Society of Edinburgh (Earth Sciences).* 93(1):59–71.

Rees, J. 2005. Neoselachain shark and ray teeth from the Valanginian, Lower Cretaceous of Wawal, Central Poland. *Palaeontology.* **48**(2):209–221.

Ronquist, F., and Huelsenbeck, J. P. 2003. Mrbayes 3: Bayesian phylogenetic inference under mixed models. *Bioinformatics.* **19**: 1572–1574.

Rowe, T., Cifelli, K L., Lehman, T. M., and Well, A. 1992. The Campanian Terlingua local fauna, with a summary of other vertebrates from the Aguja Formation, Trans-Pecos Texas. *Journal of Vertebrate Paleontology.* **12**(4):472-493.

Sansom, R.S., Gabbott, S.E., and Purnell, M.A. 2010. Non-random decay of chordate characters causes bias in fossil interpretation. *Nature*, **463**:(7282), 797.

Sansom, R.S., Gabbott, S.E., and Purnell, M.A. 2013. Atlas of vertebrate decay: a visual and taphonomic guide to fossil interpretation. *Palaeontology.* **56**(3): 457-474.

Sansom, R.S., Choate, P.G., Keating, J.N., and Randle, E. 2018. Parsimony, not Bayesian analysis, recovers more stratigraphically congruent phylogenetic trees. *Biology letters.* **14**(6): https://doi.org/10.1098/rsbl.2018.0263

Schaeffer, B. 1963. Cretaceous fishes from Bolivia, with comments on pristid evolution. *American Museum Novitates.* **2159**: 20 p.

Schaefer, J.T., and Summers, A.P. 2005. Batoid wing skeletal structure: novel morphologies, mechanical implications, and phylogenetic patterns. *Journal of Morphology*, **264**: 298–313.

Schwartz, F.J., and Maddock, M. B. 2002. Cytogenetics of the elasmobranchs: genome evolution and phylogenetic implications. *Marine and freshwater research.* **53** (2), 491-502.

Scotese, R.C. 1991. Jurassic and Cretaceous plate tectonic reconstructions. *Paleogeography, Paleoclimatology, Paleoecology.* **87**(1-4):493–501.

Serra, G. 1933. Di una nuova specie di *Schizorhiza* del Maestrichtiano della Tripolitania. *Italian Riveria Paleontology*, **39**:103-107.

Sereno, P.C., Dutheil, D.B., Iarochène, M., Larsson, H.C.E., Lyon, G.H., Magwene, P.M., Sidor, C.A., Varricchio, D.J., and Wilson, J.A. 1996. Predatory Dinosaurs from the Sahara and Late Cretaceous Faunal Differentiation. *Science.* **272:** 986–991.

Signeux, J. 1959. Contributions a la stratigraphie et la paleontologie du Cretace et du Nummulitique de la marge NW de la Peninsule Arabique. b: Poissons et reptiles du Maestrichtien et de l'Eocene inferieur des environs de Rutbah (Irak). *In*: Arambourg, C.,

Dubertret, L., Signeux, J., and Sornay, J. *Contributions a la stratigraphie et it la paleontologie du Cretace et du Nummulitique de la marge NW de la Peninsule arabique.* Notes Mem. Moyen-Orient. **7**:235-24l.

Siddall, M.E. 1996. Stratigraphic consistency and the shape of things. *Systematic Biology.* **45**(1):111-115.

Siddall, M.E. 1998. Stratigraphic fit to phylogenies: a proposed solution. *Cladistics.* **14**(2):201-208.

Shephard, G.E., Müller, D.R., and Seton, M. 2013. The tectonic evolution of the Arctic since Pangea breakup: Integrating constraints from surface geology and geophysics with mantle structure. *Earth-Science Reviews*. **124**:148–183.

Shirai, S. 1992. Phylogenetic relationships of the angel sharks, with comments on elasmobranch phylogeny (Chondrichthyes, Squatinidae). *Copeia*. **1992**, 505-518

Shirai, S. 1996. Phylogenetic interrelationships of neoselachians (Chondrichthyes: Euselachii). *In:* Stiassny, M. L., Parenti, L. R. and Johnson, G. D. (eds.). *Interrelationships of fishes*. New York: Atlantic Press. 9-34.

Slaughter, B.H., and Steiner, M. 1968. Notes on Rostral Teeth of Ganopristine Sawfishes, with Special Reference to Texas Material. *Journal of Paleontology*, **42** (1), 233–239.

Slaughter, B.H., and Thurmond, J.T. 1974. A Lower Cenomanian (Cretaceous) ichthyofauna from the Bahariya Formation of Egypt. *Annals of the Geological Society. Egypt*. **4**: 25-40.

Smith, A.B. 1994. *Systematics and the fossil record: documenting evolutionary patterns*. Blackwell, London. 218pp.

Smith, M.M., Riley, A., Fraser, G.J., Underwood, C.J., Welten, M., Kriwet, J., Pfaff, C., and Johanson, Z. 2015. Early development of rostrum saw-teeth in a fossil ray tests classical theory of the evolution of vertebrate dentitions. *Proceedings of the Royal Society B: Biological Sciences*, *282*(1816): https://doi.org/10.1098/rspb.2015.1628.

Spielmann, J.A., and Lucas, S.G. 2006. Late Cretaceous marine reptiles (Mosasauridae and Plesiosauria) from New Mexico and their biostratigraphic distribution. *New Mexico Museum of Natural History and Science Bulletin*. **35**:217- 221

Suarez, M.E., and Cappetta, H. 2004. Sclerorhynchid teeth (Neoselachii, Sclerorhynchidae) from the Late Cretaceous of the Quiriquina formation, central Chile. *Andean Geology*. **31**(1): 89-103.

Stadler, T. 2010. Sampling-through-time in birth–death trees. *Journal of theoretical biology.* **267**(3): 396–404.

Stadler, T., and Yang, Z. 2013. Dating phylogenies with sequentially sampled tips. *Systematic biology*. **62** (5): 674–688.

Sternes, P.C., and Shimada, K. 2018. Paleobiology of the Late Cretaceous sclerorhynchid sawfish, *Ischyrhiza mira* (Elasmobranchii: Rajiformes), from North America based on new anatomical data. *Historical Biology.* (2018): 1-8.

Stromer, E. 1917. Ergebnisse der Forschungsreisen Prof. E. Stromers in den Wiisten Agyptens. 11. Wirbeltier-Reste der Baharije-Stufe (Unterstes Cenoman). 4: Die Sage des Pristiden *Onchopristis. Abhandlungen der Bayerischen Akademie der Wissenschaften, Mathematisch-naturewissenshaftliche Abteilung, Neue Folge.* **28** (8),21 p.

Stromer, E. 1927. Ergebnisse der Forschungsreisen Prof. E. Stromers in den Wiisten Agyptens. 11. Wirbeltier-Reste der Baharije-Stufe (Unterstes Cenoman). 9. Die Plagiostomen mit einem Anhangiiber kano und mesozoische Riickenflossenstacheln von Elasmobranchiern. *Abhandlungen der Bayerischen Akademie der Wissenschaften, Mathematisch-naturewissenshaftliche Abteilung, Neue Folge.* **31** (5),1-64 pp.

Stromer, E., and Weiler, W. 1930. Ergebnisse der Forschungsreisen Prof. E. Stromers in den Wiisten Agyptens. VI. Beschreibung von Wirbeltier-Resten aus dem nubischen Sandsteine Oberagyptens und aus agyptischen Phosphaten nebst Bemerkungeniiber die Geologie der Umgegend von Mahamid in Oberagypten. *Abhandlungen der Bayerischen*

Akademie der Wissenschaften, Mathematisch-naturewissenshaftliche Abteilung, Neue Folge. **7**: 1-42.

Strong, E.E., and Lipscomb, D. 1999. Character coding and inapplicable data. *Cladistics.* **15**(4):363-371.

Swofford, D.L. 2001. PAUP*. Phylogenetic Analysis Using Parsimony (*and Other Methods). Version 4b10. Sinauer Associates, Sunderland, MA.

Tabaste, N. 1963. Étude de restes de poissons du Crétacé saharien. *Mémoire IFAN, Mélanges Ichthyologiques.* **68**:437–485.

Tennant, J.P., Mannion, P.D., Upchurch, P., Sutton, M.D., and Price, G.D. 2017. Biotic and environmental dynamics through the Late Jurassic-Early Cretaceous transition: evidence for protracted faunal and ecological turnover. *Biological Reviews*. **92** (2):776–814.

Thurmond, J.T. 1971. Cartilaginous fishes of the Trinity Group and related rocks (lower Cretaceous) of north central Texas. *Southeastern Geology.* **13**: 207–227.

Underwood, C.J. 2006. Diversification of the Neoselachii (Chondrichthyes) during the Jurassic and Cretaceous. *Paleobiology*. **32**(2):215–235.

Underwood, C.J., Claeson, K.M., and Ward, D. 2009. Batoids from the Turonian of SE Morocco. In 1st International Congress on North African Vertebrate Palaeontology. *Program & Abstracts.* Marrakech, pages 25–27.

Underwood, C.J., and Claeson, K.M. 2017. The late Jurassic ray *Kimmerobatis etchesi* gen. et sp. nov. and the Jurassic radiation of the Batoidea. *Proceedings of the Geologists Association.* http://dx.doi.org/10.1016/j.pgeola.2017.06.009

Underwood, C. J., and Cumbaa, S. L. 2010. Chondrichthyans from a Cenomanian (Late Cretaceous) bonebed, Saskatchewan, Canada. *Palaeontology*. **53**(4):903-944.

Underwood, C.J., Mitchell, S.F., and Veltcamp, K.J. 1999. Shark and ray teeth from the Hauterivian (Lower Cretaceous) of north-east England. *Palaeontology*. **42**(2):287-302.

Underwood, C.J., and Rees, J. 2002. Selachian faunas from the earliest Cretaceous Purbeck Group of Dorset, southern England. *Special Papers in Palaeontology*. **68**:83–102.

Underwood, C.J., Smith, M.M., and Johanson, Z. 2016a*. Sclerorhynchus atavus* and the convergent evolution of rostrum-bearing chondrichthyans. *Geological Society, London, Special Publications*, **430**, 129-136.

Underwood, C.J., Ward, D.J., and Guinot, G. 2016b. Development of understanding of the Mesozoic and Cenozoic chondrichthyan fossil record. *Geological Society, London, Special Publications*. 430(1):155–164.

Uyeno, T., and Hasegawa, Y. 1986. A new Cretaceous Ganopristoid sawfish of the genus *Ischyrhiza* from Japan. *Bulletin of the National Science Museum*. Series C. **12**(2):67-72.

Vajda, V., and Bercovici, A. 2014. The global vegetation pattern across the Cretaceous–Paleogene mass extinction interval: A template for other extinction events. *Global and Planetary Change*, **122**, 29-49.

von Reuss, A.E. 1844. Geognistische Skizzen aus Böhmen. Part II. Prague, 304 p. (1845): *Die Versteinerungen der böhmischen Kreideformalion*. Stuttgart. 58 p., 13 pis.

Villalobos-Segura, E., Underwood, C.J., Ward, D.J., and Claeson K.M. 2019a. The first three-dimensional fossils of Cretaceous sclerorhynchid sawfish: *Asflapristis cristadentis* gen. et sp. nov., and implications for the phylogenetic relations of the Sclerorhynchoidei (Chondrichthyes). *Journal of Systematic Palaeontology*. https://doi.org/10.1080/14772019.2019.1578832.

Villalobos-Segura, E., Underwood, C.J., and Ward, D.J. 2019b. The first skeletal record of the Cretaceous enigmatic sawfish genus *Ptychotrygon* (Chondrichthyes: Batoidea) from the Turonian (Cretaceous) of Morocco. *Papers in Palaeontology.* doi:10.1002/spp2.1287.

Vullo, R., Cappetta, H., and Néraudeau, D. 2007. New sharks and rays from the Cenomanian and Turonian of Charentes, France. *Acta Palaeontologica Polonica*, 52(1): 99-116.

Wagner, P.J., and Marcot, J.D. 2010. Probabilistic phylogenetic inference in the fossil record: current and future applications. *The Paleontological Society Papers.* **16:**189-211.

Weiler, W. 1930. Fischreste aus dem nubischen sandstein von mohamid und edfu und aus den phosphaten oberagyptens und der oase baharije. *Abhandlungen Bayerische Akademie des Wissenschaften, Mathematische-Naturnkun-Stliche. Abteilung Neues Fortschrifte*, **7**: 12–36.

Weiler, W. 1935. Ergebnisse der Forschungsreisen Prof. E. Stromer's in den Wiisten Agyptens. II. Wirbeltierreste der BaharijeStufe (unterstes Cenoman). Neue Untersuchungen an den Fischresten. *Abhandlungen der Bayerischen Akademie der Wissenschaften Mathematisch-naturwissenschaftliche Abteilung Neue Folge*. **16**:1–57.

Welton, B.J., and Farish, R.F. 1993. The collector's guide to fossil sharks and rays from the Cretaceous of Texas. *Before Time*. USA. 204pp

Welten, M., Smith, M., Underwood, C.J., and Johanson, Z. 2015. Teeth outside the mouth? evolution and development of the sawfish and sawshark rostral dentitions (Elasmobranchii; Chondrichthyes). *Royal Society Open Science*. **2**:2–19.

Werner, C. 1989. Die Elasmobranchier-Fauna des Gebel Dist Member der Bahariya Formation (Obercenoman) der Oase Bahariya, Agypten. *Palaeo Ichthyologica*. **5:** 1-112.

Wetzel, W. 1930. Die Quiriquina-Schichten als Sediment und palaontologisches Archiv. *Palaeontographica, Abt. A*. **73**:49-106.

White, E.L. 1934. Fossil fishes of Sokoto province. *Bulletin of the Geological Survey. Nigeria*. **14**:1-78.

Wignall, P.B. 1994. Black shales. *Oxford University Press*. USA, **30**: 127pp

Wilga, C.A. 2008. Evolutionary divergence in the feeding mechanism of fishes. *Acta Geologica Polonica*, **58** (2), 113-120.

Williamson, T.E., Kirkland, J., and Lucas, S.G. 1993. Selachians from the Greenhorn cyclothem ("Middle" Cretaceous: Cenomanian-Turonian), Black Mesa, Arizona, and the paleogeographic distribution of late Cretaceous selachians. *Journal of Paleontology*. **67**(3):447-474.

Wills, M.A. 1999. Congruence between phylogeny and stratigraphy: randomization tests and the gap excess ratio. *Systematic Biology*. **48**(3): 559-580.

Winchell, C.J., Martin, A.P., and Mallatt, J. 2004. Phylogeny of elasmobranchs based on LSU and SSU ribosomal RNA genes. *Molecular phylogenetics and evolution*, **31**(1): 214-224.

Woodward, A.S. 1895. Catalogue of the fossil fishes in the British Museum (Natural History). *British Museum*. London, **3**: 728 pp.

Woodward, A. 1889a. Catalogue of the fossil fishes in the British Museum, Part 1. *British Museum (Natural History).* London, 76-77.

Woodward, A. 1889b. *Sclerorhynchus atavus* remarks. *In:* Remarks. *Proceedings of the Zoological Society*. London: 449–451.

Wright, A.M., and Hillis, D.M. 2014. Bayesian Analysis Using a Simple Likelihood Model Outperforms Parsimony for Estimation of Phylogeny from Discrete Morphological Data. PLoS ONE 9(10): e109210. doi:10.1371/journal.pone.0109210

Wueringer, B., Squire, L., and Collin, S. 2009. The biology of extinct and extant sawfish (Batoidea: Sclerorhynchidae and Pristidae). *Reviews in Fish Biology and Fisheries*, **19**(4):445.

Wueringer, B.E., Peverell, S.C., Seymour, J., Squire Jr, L., Kajiura, S.M., and Collin, S.P. 2011. Sensory systems in sawfishes. 2. the lateral line. *Brain, Behaviour and Evolution.* **78**:150–161.

Xie, W., Lewis, P.O., Fan, Y., Kuo, L., and Chen, M.H. 2010. Improving marginal likelihood estimation for Bayesian phylogenetic model selection. *Systematic biology*. **60**(2):150-160.

Appendix 4.1

Matrix used to determine the phylogenetic relations between sclerorhynchoids and other batoids (Part 1)

```
#NEXUS
BEGIN TAXA;
      TITLE Taxa;
      DIMENSIONS NTAX=37;
      TAXLABELS
            Chimaeridae Hexanchidae Raja Bathyraja Torpedo Hypnos Narcine Narke Temera Britobatos Platyrhina Platyrhinoidis Kimmerobatis Asterodermus
Spathobatis Belemnobatis Pristis Rhynchobatus Glaucostegus Rhina Rhinobatos Zapteryx Aptychotrema Trygonorrhina Zanobatus Urolophus Urobatis Urotrygon
Gymnura Myliobatis Aetobatus Rhinoptera Mobula Ptychotrygon_rostrispatula Sclerorhynchus_atavus Libanopristis_hiram Asflapristis_cristadentis
      ;
END;

BEGIN CHARACTERS;
      TITLE  Character_Matrix;
      DIMENSIONS  NCHAR=95;
      FORMAT DATATYPE = STANDARD GAP = - MISSING = ? SYMBOLS = "  0 1 2 3 4";

      MATRIX
      Chimaeridae            00000000?0?01000??0000?0021?0?-00001?00000000001?0?0??01000000000000100000000000-000??000?0000
      Hexanchidae            0000-0-0?0?00010??0000?00(0 2)1000-00000000000000001110?-??0000000000000000????0000000-000?0000?0000
      Raja            1111111100?00011000010001100110000000000001000111210100011100100102110011000000002000001?0?0001
      Bathyraja            1111111100?00011100000?00111011000000000000100011121010001111010010211001100000002000001?0?0001
```

```
Torpedo        1111111100?000000?0000?0020--0-00101?1??0001100011011001000000000010100010?00010102001401?0?0011
Hypnos         1111111100?000000?0000?0020--0-00101?1??0001100011011001000000010100???00010102001401?0?0011
Narcine        1111111110?000000?0000?0021000?00101?1??0000000110110010000000001010010000101110200(0 1)401?0?0011
Narke          1111111110?000000?0000?0021100-00101?1??0000000100110010000000010100100?01011101000401?0?0011
Temera         1111111110?000000?0000?0020--0-00111?1??0000000100110010000000010100100?0101110?00?401?0?0011
Britobatos     ?111111110??00100?0???????100???000?00000001?????11??0101011000010?0?????0??????111041??0?0000
Platyrhina     1111111110?000100?000110021100-10000000000000011111100001011(0 1)0001010100000000011211(0 1)11010?0000
Platyrhinoidis 1111111110?000100?000110021100-100000000000?00011111100001011000010100000000011011(0 1)11010?0000
Kimmerobatis   ?101101100???010?0?????????1??1?00010?000?0010????0?1??000?000000010001?0000?????00000?00?0?0100
Asterodermus   ?1?1101100??00100?????????101100?0?0?000000?0??110?1??000?0100001000??????????00000?00?0?0100
Spathobatis    ?111101100??10100??????02101100?010?000000?0??110?1??0?0?000000010001??0?0?????00000?00?0?0100
Belemnobatis   ?111101100??10100??????021011?0?0?00000000?0??111????0?0?0000000100010??0?????00000?00?0?0100
Pristis        1111111100?000100?000100021010?000000000001000111110100011000100101011???0000010200011??100000
Rhynchobatus   1111111100?000100?000100210110000000000000000011110000011000100011?01????0000000110011010?0000
Glaucostegus   1111111100?000100?000??0021011000000000000000?111110000011000100101?????0?0???0100011010?0000
Rhina          1111111100?000100?0000?0021011000000000000000011110?000110001001??01????0000000110011010?0000
Rhinobatos     1111111100?000100?000100210110000000000000000011110000011001001010100000000000100011010?0000
Zapteryx       1111111100?000100?000110021011000000000000001000111100000111001001010100000000011000210100?0000
Aptychotrema   1111111100?000100?00011?021011000000000000?0??1111100000111001001010100010???00000120002101010?0000
Trygonorrhina  1111111100?000100?000110021011000000000000?000111110000011001001010100000000011000210100?0000
Zanobatus      1111111120?000100?000110020?00?000000000000?01011110000013111010110010200000010200030100?0000
Urolophus      1111111120?001000?1000?11?0?00?0010002100001011111310010012111000111001020000101020000301?0?0000
Urobatis       1111111120?10100??1010?11?0?00?001000200001010111310010112111000111001020000101020000301?0?0000
Urotrygon      1111111120?101000?1010?11?0?00?001000200001010011310010112111000111001020000101020000301?0?0000
Gymnura        1111111120?011000?1100?11?0?00?001000200001000111310010013111011111001020100?0102000301?0?0000
Myliobatis     1111111121001100111200?11?0?00?001001201111101100131001011311101112100102010010102000301?0?0000
Aetobatus      1111111121001100111200?11?0?00?001001211111101100131001011311101112100102010?0102000301?0?0000
```

315

```
Rhinoptera                  1111111121101100111200?11?0?00?0111012111111011001310010113111010121001020101 10102000301?0?0000
Mobula                      1111111121101100??1200?11?0?00?0111012111011001001310010113111000 12100????101?0102000301?0?0000
Ptychotrygon_rostrispatula ?111101100????100???????011000?0?01?????000?0??111????0??1000000010?0?????0?????0?000??1?0?1000
Sclerorhynchus_atavus   ?1111?1100??0?100???????011000?0?000?1??000?0??111?10?00010000000 1010????0?????0?000?01?11100?
Libanopristis_hiram     ?111111100??00100?????????1000?0?010?10000010??11?210?0001000000001010????0?????0?000001?111000
Asflapristis_cristadentis ?111101100????100?????????1????0?010?10000010??11??1010001000000????????????????02?00?01?0?100?
```

;
END;
BEGIN ASSUMPTIONS;
      TYPESET * UNTITLED = unord: 1- 95;

END;

Appendix 4.2

Script used for the Bayesian analysis

```
[insert matrix: In this case Appendix A.1]
begin mrbayes;
lset applyto=(all) rates=gamma;
      prset applyto=(all) ratepr=fixed;
      mcmc  ngen=500000  samplefreq=1000  printfr=1000  diagnfreq=2000  nruns=4  nchain=4  temp=0.2  relburnin=yes  burninfrac=0.25
savebrlens=yes;
      sumt relburnin=yes burninfrac=0.25;
      sump relburnin=yes burninfrac=0.25;
end;
```
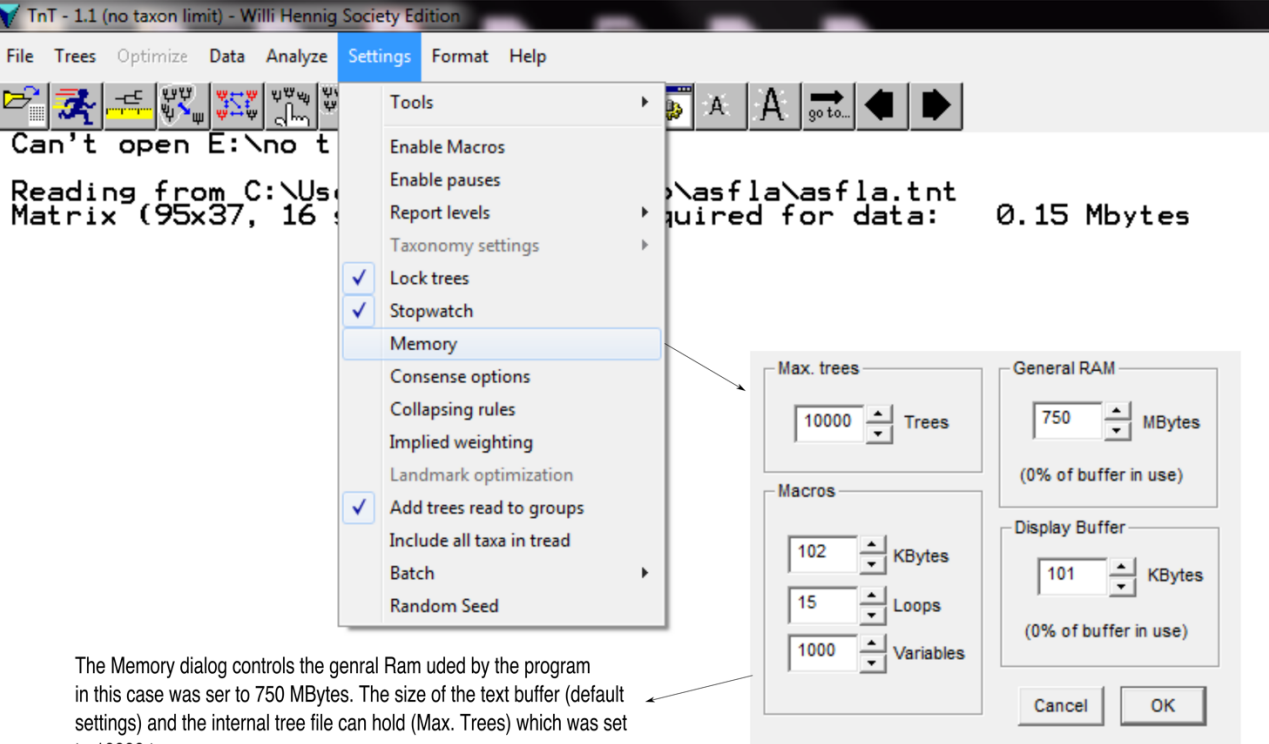
Appendix 4.3

Instructions for the TNT analysis with the menu interface

The Memory dialog controls the genral Ram uded by the program
in this case was ser to 750 MBytes. The size of the text buffer (default
settings) and the internal tree file can hold (Max. Trees) which was set
to 10000 trees.

2
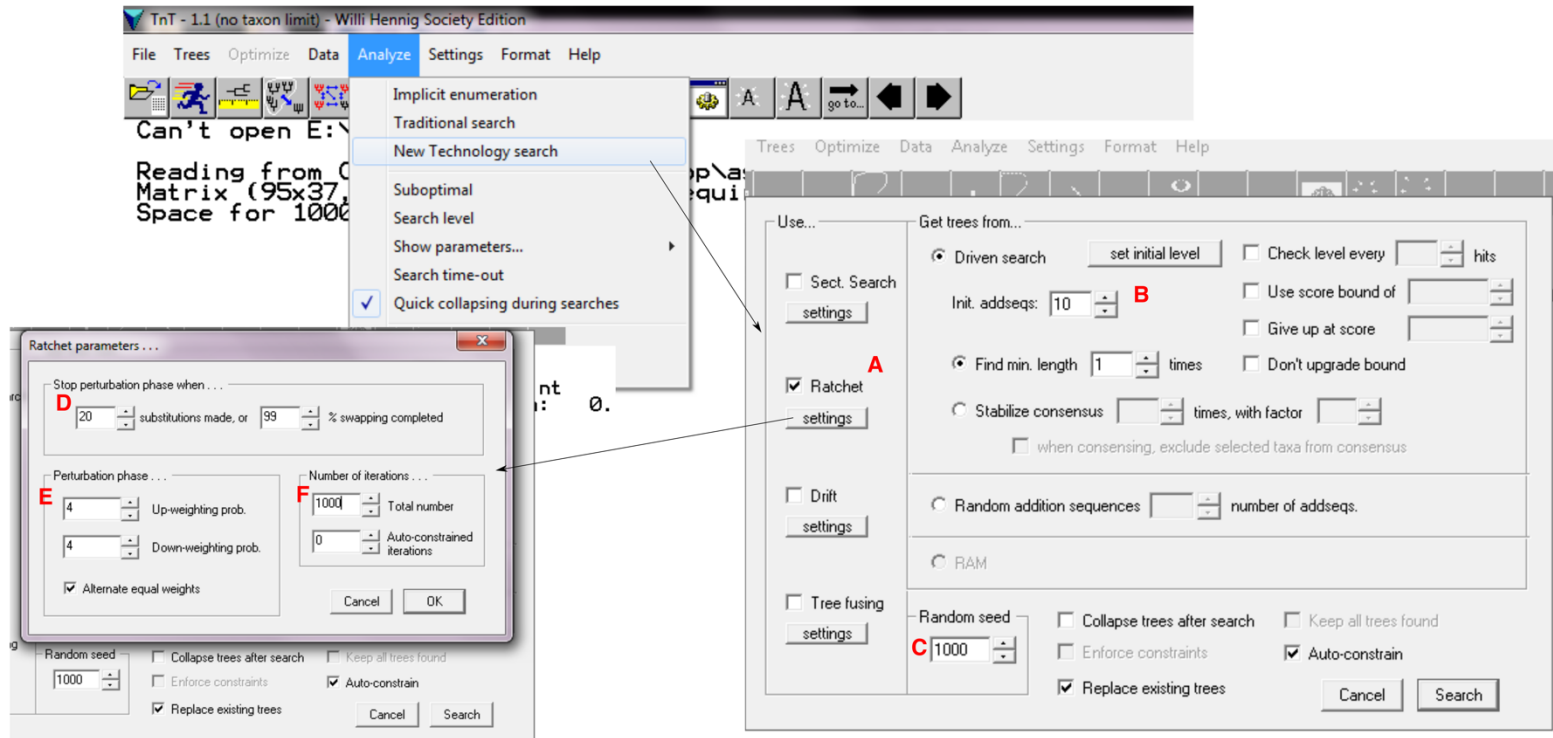
What ratchet does is alternates phases of perturbation and search. Perturbation is done by duplicating character weights, or deleting characters.
 D. Sets the number of substitutions or swappings (rearrangements) done in the anlysis: 20 sustitution or 99% of swapping completed. (Default was kept)
E. Probabitly of a character to have its weight duplicated (up weight phase) or be deleted (down weight phase). These probabilities are independent: 4 each (Default was kept)
 F. Number or iterations of the preturbation phase: 1000 (default is 0)

A. Specifies the type of new Tech searches used: Ratchet
B. Number of replications done by the analysis: 10 (default is 5) also implies that 10 Wagner trees will be constructed
C. Random seed: Defines different sequences of addition of terminals during the construction of the Wagner trees: 1000 (default is 1). For this analysis we will have 1000 different points of start.

3

Second search carried with the Traditional seach methods.
A. Uses the trees in memoriy: In this case those found with Ratchet
B. Set the number of times you want the program to randomize the order of the taxa
, create a cladogram, and submits it to branch-swapping : 1000

Appendix 5.1

Matrix used to determine the phylogenetic relations within sclerorhynchoids

```
DIMENSIONS  NTAX=14 NCHAR=23;
FORMAT DATATYPE = STANDARD GAP = - MISSING = ? SYMBOLS = "  0 1 2";
CHARSTATELABELS

MATRIX
Spathobatis     00?0???????0100001021?0
Raja            00?0???????0110001120?1
Amblyraja       00?0???????0110001120?1
Asflapristis    1101000????10??1100?0?0
Ptychotrygon    10?10001???101111{0 1}010?0
Sclerorhynchus  10?1111111101110110101?
Micropristis    10?111?111?10??0010101?
Libanopristis   10?1111111110??11101011
Onchopristis    ?1111111121????0001001?
Schizorhiza     ?111?10?101????000?001?
Ischyrhiza      ?111111?111????00011001?
Pristis         00?101000?0010000100101
Anoxipristis    ?0?101000?0?1??00100{0 1}0?
Rhinobatos      00?0???????0100001021?1
```

Appendix 6.1

Matrix used to estimate the divergence time of sclerorhynchoids (Part 1)

```
#NEXUS
BEGIN DATA;
      DIMENSIONS  NTAX=55 NCHAR=95;
      FORMAT DATATYPE = STANDARD GAP = - MISSING = ? SYMBOLS = "  0 1 2 3 4";
      MATRIX
      Raja            1111111100?0001110000100011001100000000000010001112101000111001001021100110000000002000001?0?0001
      Bathyraja       1111111100?00011100000?00111011000000000000010001112101000111101001021100110000000002000001?0?0001
      Torpedo         1111111100?000000?0000?0020--0-00101?1??0001100011011001000000000010100010?00010102001301?0?0011
      Hypnos          1111111100?000000?0000?0020--0-00101?1??0001100011011001010000000010100????00010102001301?0?0011
      Narcine         1111111110?000000?0000?0021000?00101?1??00000001101100100000000010100010000101110200(0 1)301?0?0011
      Narke           1111111110?000000?0000?0021100-00101?1??0000000010011001000000000101001 00?01011101000301?0?0011
      Temera          1111111110?000000?0000?0020--0-00111?1??0000000010011001000000000101001 00?0101110?00?301?0?0011
      Britobatos      ?111111110??00100?0???????100????000?00000001?????11??0101011000010?0?????0?????111031??0?0000
      Platyrhina      1111111110?000100?000110021100-10000000000000011111100001011(0 1)0001010100000000011211(0 1)11010?0000
      Platyrhinoidis  1111111110?000100?000110021100-100000000000?00011111100001011000101000000000011011(0 1)11010?0000
      Kimmerobatis    ?101101100??010?????????1??1?00010?000?0010????0?1??000?000000010001?0000?????00000?00?0?0100
      Asterodermus    ?1?1101100??00100?????????101100?0?0?000000?0??110?1??000?01000001000?????????00000?00?0?0100
      Spathobatis     ?111101100??10100??????02101100?010?000000?0??110?1??0?0?000000010001??0?0?????00000?00?0?0100
      Belemnobatis    ?111101100??10100??????021011?0?0?00000000?0??111????0?0?0000001000 10?0?????00000?00?0?0100
      Pristis         1111111100?000100?000100021010?000000000000 10001111101000110001001010 1?0?0000010200011??100000
      Rhynchobatus    1111111100?000100?000100021011000000000000000001111100000110001001 1?01????0000000110011010?0000
      Glaucostegus    1111111100?000100?000??0021011000000000000000?1111100000110010010101????0?0???0100011010?0000
      Rhina           1111111100?000100?0000?0021011000000000000000111110?000110001001??01????0000000110011010?0000
      Rhinobatos      1111111100?000100?000100021011000000000000001111100000111001001010000000000100011010?0000
      Zapteryx        1111111100?000100?000110021011000000000000001000111100000111001001010000000000 1100011010?0000
      Aptychotrema    1111111100?000100?00011?021011000000000000?0??111110000011100100101 01????0000001200011010?0000
      Trygonorrhina   1111111100?000100?000110021011000000000000?0001111100000111001001010100000000 01100011010?0000
```

```
Zanobatus       1111111120?000100?000110020?00?000000000000?0101111000001311101011100102000000102000301?0?0000
Urolophus       1111111120?001000?1000?11?0?00?001000210000101111131001001213100011100102000010102000201?0?0000
Urobatis        1111111120?10100??1010?11?0?00?001000200000101011131001011213100011100102000010102000201?0?0000
Urotrygon        1111111120?101000?1010?11?0?00?001000200000101001131001011213100011100102000010102000201?0?0000
Gymnura         1111111120?011000?1100?11?0?00?001000200000100011131001001313101111001020100?0102000201?0?0000
Myliobatis      1111111121001100111200?11?0?00?001001201111101100131001011313101112100102010010102000201?0?0000
Aetobatus       1111111121001100111200?11?0?00?001001211111101100131001011313101112100102010?0102000201?0?0000
Rhinoptera      1111111121101100111200?11?0?00?011101211111101100131001011311101021001020101101020000201?0?0000
Mobula          1111111121101100??1200?11?0?00?011101211101100100131001011311100121000????101?0102000201?0?0000
Ptychotrygon    ?111101100????100???????011000?0?01????000?0??111????0??1000000010?0?????0?????0?000??1?0?1000
Sclerorhynchus  ?1111?1100??0?100???????011000?0?000?1??000?0??111?10?000100000001010?????0?????0?000?01?11100?
Libanopristis   ?111111100??00100?????????1000?0?010?10000010??11?210?000100000001010?????0?????0?000001?111000
Asflapristis    ?111101100????100?????????1????0?010?10000010??11??10100010000000??????????????02?00?01?0?100?
Tingitanius     ?1?1111100???0100?????????1100?0?000?00000?10?????11100001????0???0????????????0211011??0???00
Tethybatis      ?1?11111?0??0010?????????1100???0?0?00000??0?????1???000?211?00?10??1?000??????0?00?????0?0000
G__intermedius  ?111111100??0010?????????101110?010?0?000?00?????1???000?100000?10??1??????????0?10?????0?0000
G__latus        ?111111100??0010??????????10???0?000?00000??0?????1???0000?100000?1010?????????0?10?????0?0000
G__maronita     ?111111100??0010???????021?1110?000?0?000?00??11111?0000?001000010101000000?????02200??100?0000
G__tenuirostris ?111111100???0?0??????????101110?010?0?0???0??????1??0000?00100001?????????????0?20?????0?0000
G__hakelensis   ?111111100???0?00?????????101110?000?0?000000???1111?0000?101001010?????????????0100?1???0?0000
Rhombopterygia  ?111111100??0010?????????101110?010?0?000000????11100000?101001120?????????????0110??1??0?0000
G__grandis      ?111111100???0100?????????101110?000?0?000000??1?11100000?101000010001?000?????0210?????0?0000
Cyclobatis      ?111111100??101010???????0?1000?0?100?2??00011??1?121??000021310001021010?1??????000?00???0?0001
Raja_davisi     ?111111100??1011?????????101110?000?000?0010?0??1?121??000?100?0001021??????????0?0000???0?000?
Tlalocbatus     ?111111100??0010?????????101110?000?000?00?0???????1?00???100?1001010????0?????1?10?????0?0000
Sthalraja       ?111111100??0010?????????101110?000?000000?0??1?111000000100?10010?0???????????1?10011??0?0000
G__whitfieldi   ?111111100??00100???????021000?0?000?0?000000??11111?0000?100000010101?????????01000????0?0000
Iansan          ?111111100??0100?????????100110?000?00000010??1?111000000000000010?????????????0100011??0?0000
Titanonarke     ?111111110??0000???????021??0?0?1?1?1--00011??0?00110010?00000001010?????0?????020013???0?00?1
Asterotrygon    ?11111?100??1110????????1?1000?0?1?0?200100?0??11?????00??21310001?100?0???????0?000????0?0000
Heliobatis      ?1?111?100??1110?????????1000?0?1?0?200100???1?????0???21310001?100?0???????0?000????0?0000
G__zignii       ?1?11??120??1110????????????00?0?1?0?????1?0???????????0?1?22131??010??????????0?000????0?0000
Promyliobatis   ?1?11??1210?11?0??????????0000?0?1?0????????????????????1?1?01????010??????????0?000????0?0000
;
END;
```
322

Appendix 6.2

Time data

	FAD	LAD		FAD	LAD		FAD	LAD
Raja	70.6	0	G__intermedius	85.8	83.6	Rhinobatos	55.8	0
Bathyraja	70.6	0	G__latus	86.3	83.6	Zapteryx	55.8	0
Asflapristis	93.9	89.8	G__maronita	100.5	93.9	Trygonorrhina	55.8	0
Sclerorhynchus	93.9	59.2	G__tenuirostris	86.3	83.6	G__zignii	56	47.8
Libanopristis	99.6	93.5	G__hakelensis	100.5	93.5	Promyliobatis	56	47.8
Ptychotrygon	113	89.8	G__grandis	100.5	93.5	Kimmerobatis	152.1	145
Cyclobatis	99.6	93.5	Tlalocbatus	113	100.5	Asterodermus	150.8	145.5
Raja_davisi	86.3	83.6	Sthalraja	113	100.5	Spathobatis	175.6	125
Torpedo	58.7	0	G__whitfieldi	100.5	93.5	Belemnobatis	177.7	125
Hypnos	58.7	0	Iansan	113	100.5			
Narcine	58.7	0	Aptychotrema	55.8	0			
Narke	58.7	0	Rhombopterygia	99.6	93.5			
Temera	58.7	0	Zanobatus	65.5	0			
Titanonarke	55.8	48.6	Urolophus	56	0			
Platyrhina	56	0	Urobatis	56	0			
Platyrhinoidis	56	0	Urotrygon	65.5	0			
Tingitanius	93.9	89.8	Gymnura	58.7	0			
Tethybatis	83.6	72.1	Myliobatis	65.5	0			
Britobatos	86	84.9	Aetobatus	58.7	0			
Pristis	55.8	0	Rhinoptera	58.7	0			
Rhynchobatus	55.8	0	Mobula	33.9	0			
Glaucostegus	55.8	0	Asterotrygon	56	47.8			
Rhina	23	0	Heliobatis	56	47.8			

Appendix 6.3

Script used time-scaling in paleotree and calculate stratigraphic consistency indices

```
#Set work directory
setwd("path_to_data_files")

#Install packages
install.packages(ape)
install.packages ("paleotree")
install.packages ("strap")
install.packages ("apTreeshape")
install.packages ("phylotools")
install.packages ("Claddis")
install.packages ("phytools")

#Load packages
require("ape") #tree managment, root, reading nexus etc...
require("paleotree") #time-scaling
require("strap") #plotting trees
require("apTreeshape") #evaluate tree shape
require("phylotools") #plotting tree
require("Claddis") #GetNodeAges function
require("phytools")#Compare trees

#load tree
tree <- read.nexus("tree_file.nex")

#load taxa ages file for time-scaling the trees in this case data from Appendix B.2
ages <- read.csv("age_table.csv", header = T, row.names = 1)
```

```
#select root for tree in this case the oldest taxon
tree <- root(tree_file, outgroup = "outgroup_taxon", resolve.root = T)

#plot tree and ladderize it
plot(ladderize(tree_file))

#time scale the tree using mlb and bassic methods
mlb.tree <- timePaleoPhy(tree = tree, timeData = ages, type = "mbl", plot = T, vartime = 1)
basic.tree <- timePaleoPhy(tree, ages, "basic", plot = T)


#getting ages for the nodes in bassic and mbl trees
mlb.tree.nodeages <- GetNodeAges(mlb.tree)
basic.tree.nodeages <- GetNodeAges(basic.tree)

#check node numbers to compare with the ages
plot(mlb.tree)+ nodelabels()

########Scrip used to evaluate the shape of the trees
#load tree
Bayesian.tree <- read.nexus("tipdatedtree.tree")

#plot tree and ladderize it
plot(ladderize(Bayesian.tree))

#calculate srtatigraphic congruence metrics
scitipdated <- StratPhyloCongruence(Bayesian.tree,ages = ages ,method = "basic",randomly.sample.ages=FALSE)
scibasic <- StratPhyloCongruence(basic.tree,ages = ages, method = "basic",randomly.sample.ages=FALSE)
scimlb <- StratPhyloCongruence(mlb.tree,ages = ages, method = "basic", randomly.sample.ages=FALSE)

#stratigraphic index for the rest of trees
tipdaeted <- scitipdated$input.tree.results [,1:4]
basic <- scibasic$input.tree.results [,1:4]
mlb <- scimlb$input.tree.results [,1:4]
```

```
#showing results
tipdaeted
basic
mlb

#breaking polytomies
basictreepol <- multi2di(basic.tree)
mlbtreepol <- multi2di(mlb.tree)
Bayesiantreepol <- multi2di(Bayesian.tree)

#trees as shapes
shapebasictree <- as.treeshape(basictreepol)
shapemlbtree <- as.treeshape(mlbtreepol)
shapeBayesiantree <- as.treeshape(Bayesiantreepol)

# Create a pectinate tree with 55 tips to scale the Colless index
pectinate.tree <- stree(n = 55, type = "right"); plot(pectinate.tree)

# phylo object to treeshape object:
pectinate.tree <- as.treeshape(pectinate.tree)

# Create a maximally balanced tree with 55 tips to scale the Colless index
balanced.tree <- rtreeshape(n = 1, tip.number = 55, p = 0.5, model = "biased"); plot.treeshape(balanced.tree[[1]])

# Maximum Colless (this is going to be a completely pectinate tree):
colless.pect <- colless(pectinate.tree)

# Minimum Colless (this is going to be the maximally balanced tree):
colless.bal <- colless(balanced.tree[[1]])

#colles index for the rest of trees
#so 0 is maximally balanced and 1 is pectinate then a tree with an Ic = 344 is well balanced (scaled Colless = ~0.2)
basiccolless <- colless(shapebasictree)
mlbcolless <- colless(shapemlbtree)
Bayesiancolless <- colless(shapeBayesiantree)
```

```
#scaled colless
scaled.basiccolless <- 1 - (colless.pect - basiccolless)/(colless.pect - colless.bal)
scaled.mlbcolless <- 1 - (colless.pect - mlbcolless)/(colless.pect - colless.bal)
scaled.Bayesiancolless <- 1 - (colless.pect - Bayesiancolless)/(colless.pect - colless.bal)

#porcentaje of completeness for the remainig nodes
Bayesian.tree$Nnode/(55-2)*100
mlb.tree$Nnode/(55-2)*100
basic.tree$Nnode/(55-2)*100

#####plotting tip dated tree
Bayesian.tree$root.time <- max(diag(vcv(Bayesian.tree)))
geoscalePhylo(tree = ladderize(Bayesian.tree), label.offset = 0.2, cex.tip = 0.6, quat.rm = T, cex.age = 0.6, cex.ts = 0.6)
```

Appendix 6.4

Script used for the Bayesian analysis

```
begin mrbayes;
lset applyto=(all) rates=gamma Coding=variable;
prset applyto = ( all ) ratepr = fixed;

[Topological constrains]
      outgroup Belemnobatis;
      constraint root =  Belemnobatis;
      constraint torpedinforms = Torpedo Hypnos Narcine Narke Temera
Britobatos Titanonarke Tethybatis Tingitanius Platyrhina Platyrhinoidis;
      constraint rhinopristismylio = Pristis Rhynchobatus Glaucostegus
Aptychotrema Rhina Rhinobatos Zapteryx Trygonorrhina G__grandis G__intermedius
G__latus G__maronita G__tenuirostris G__hakelensis Iansan Tlalocbatus
Sthalraja Zanobatus Urolophus Urobatis Urotrygon Gymnura Myliobatis Aetobatus
Rhinoptera Mobula Asterotrygon Heliobatis G__zignii Promyliobatis
Rhombopterygia G__whitfieldi;
constraint rhinopristis = Pristis Rhynchobatus Glaucostegus Aptychotrema Rhina
Rhinobatos Zapteryx Trygonorrhina;

[Time data: Last appearance date, Fist appearance date]
Calibrate Raja = uniform(0,70.6);
Calibrate Bathyraja = uniform(0, 70.6);
Calibrate Torpedo =uniform(0,58.7);
Calibrate Hypnos =uniform(0,58.7);
Calibrate Narcine =uniform(0,58.7);
Calibrate Narke =uniform(0,58.7);
Calibrate Temera =uniform(0,58.7);
Calibrate Titanonarke = uniform(48.6,55.8);
Calibrate Platyrhina =uniform(0,56);
Calibrate Platyrhinoidis = uniform(0,56);
Calibrate Zanobatus =uniform(0,65.5);
Calibrate Urolophus =uniform(0,56);
Calibrate Urobatis =uniform(0,56);
Calibrate Urotrygon =uniform(0,65.5);
Calibrate Gymnura =uniform(0,58.7);
Calibrate Myliobatis =uniform(0,65.5);
Calibrate Aetobatus =uniform(0,58.7);
Calibrate Rhinoptera =uniform(0,58.7);
Calibrate Mobula =uniform(0,33.9);
Calibrate Pristis =uniform(0,55.8);
Calibrate Rhynchobatus =uniform(0,55.8);
Calibrate Glaucostegus =uniform(0,55.8);
Calibrate Rhina =uniform(0,23);
Calibrate Rhinobatos =uniform(0,55.8);
Calibrate Zapteryx =uniform(0,55.8);
Calibrate Trygonorrhina =uniform(0,55.8);
Calibrate Asflapristis = uniform(89.8,93.9);
Calibrate Sclerorhynchus = uniform(59.2,93.9);
Calibrate Libanopristis = uniform(93.5,99.6);
Calibrate Ptychotrygon = uniform(89.8,113);
Calibrate Tingitanius = uniform(89.8,93.9);
Calibrate Tethybatis = uniform(72.1,83.6);
Calibrate G__intermedius = uniform(83.6,85.8);
```

```
Calibrate G__latus = uniform(83.6,86.3);
Calibrate G__maronita = uniform(93.9,100.5);
Calibrate G__tenuirostris = uniform(83.6,86.3);
Calibrate G__hakelensis = uniform(93.5,100.5);
Calibrate Rhombopterygia = uniform(93.5,99.6);
Calibrate G__grandis = uniform(93.5,100.5);
Calibrate Cyclobatis = uniform(93.5,99.6);
Calibrate Raja_davisi = uniform(83.6,86.3);
Calibrate Tlalocbatus = uniform(100.5,113);
Calibrate Sthalraja = uniform(100.5,113);
Calibrate G__whitfieldi = uniform(93.5,100.5);
Calibrate Britobatos = uniform(84.9,86);
Calibrate Kimmerobatis = uniform(145,152.1);
Calibrate Asterodermus = uniform(145.5,150.8);
Calibrate Spathobatis = uniform(125,175.6);
Calibrate Belemnobatis = fixed(177.7);
Calibrate Iansan = uniform(100.5,113);
Calibrate Aptychotrema =uniform(0,55.8);
Calibrate Asterotrygon = uniform(47.8,56);
Calibrate Heliobatis = uniform(47.8,56);
Calibrate G__zignii = uniform(47.8,56);
Calibrate Promyliobatis = uniform(47.8,56);

[Time parameters]
prset clockvarpr=igr;
PRSET brlenspr=clock:fossilization;
        PRSET nodeagepr = calibrated;[terminals are not of the same age]
        PRSET igrvarpr=uniform(0.0001, 200); [vague priot Mazke and Wright,
2016. It enforces a relaxed clock for the analysis]
prset samplestrat = random;
prset speciationpr = uniform(0,10) ; [Bapst et al., 2016]
prset extinctionpr = beta(1,1); [default, flat, extinction is relative, Bapst
et al., 2016]
[to speciation thus between 0-1]
prset fossilizationpr = beta(1,1); [default, flat, sampling is psi/(mu+psi),
0-1, Bapst et al., 2016]
prset clockratepr = normal(0.0025,0.1); [flat, Clock Rate Prior, Mazke &
Wright, 2016 and Bapst et al., 2016]

[Bayesian analysis]
PRSET topologypr = constraints ( root , torpedinforms , rhinopristismylio,
rhinopristis );
mcmc ngen = 8000000 samplefreq = 1000 printfr = 1000 diagnfreq = 2000 nruns =
4 nchain = 4 temp = 0.2 relburnin = yes burninfrac = 0.25 savebrlens = yes;
sumt relburnin = yes burninfrac = 0.25;
[sump relburnin = yes burninfrac = 0.25;]

[Steppingstone]
[ss ngen=100000000 samplefreq=1000 printfreq=1000 nchain=4 relburnin=yes
burninfrac=0.25 savebrlens=yes
                alpha=0.4 burninss=-1 nsteps=50;]
sumss allruns=yes relburnin=yes burninfrac=0.25 discardfrac=0.80 nruns=4
askmore=no;
[sump burninfrac=0.25;]

END;
```

Appendix 6.5

Script used for the diversity estimate analysis (TDE and SQS) and its plotting against the divergence

age estimated

```
# Load packages (these must be installed first):
require(paleotree)#estimate the taxonomic diversity state
require(ggplot2)#plotting results
require(ggpubr)#plotting results together

#Load function for the sqs analysis available at (http://strata.uga.edu/8370/rtips/shareholderQuorumSubsampling.html)
sqs <-function(abundance, quota=0.9, trials=100, ignore.singletons=FALSE, exclude.dominant=FALSE) {
  # abundance is a vector of integers representing the abundance of every species

  if ((quota <= 0 || quota >= 1)) {
    stop('The SQS quota must be greater than 0.0 and less than 1.0')}

  # compute basic statistics
  specimens <- sum(abundance)
  numTaxa <- length(abundance)
  singletons <- sum(abundance==1)
  doubletons <- sum(abundance==2)
  highest <- max(abundance)
  mostFrequent <- which(abundance==highest)[1]

  if (exclude.dominant == FALSE) {
```

```r
  highest <- 0
  mostFrequent <- 0}

# compute Good's u
u <- 0
if (exclude.dominant == TRUE) {
  u <- 1 - singletons / (specimens - highest)} else {u <- 1 - singletons / specimens}

if (u == 0) {stop('Coverage is zero because all taxa are singletons')}

# re-compute taxon frequencies for SQS
frequencyInitial <- abundance - (singletons + doubletons / 2) / numTaxa
frequency <- frequencyInitial / (specimens - highest)

# return if the quorum target is higher than estimated coverage
if ((quota > sum(frequency)) || (quota >= sum(abundance))) {
  stop('SQS quota is too large, relative to the estimated coverage')}

# create a list, length equal to total number of specimens,
# each value is the index of that species in the abundance array
ids <- unlist(mapply(rep, 1:numTaxa, abundance))

# subsampling trial loop
richness <- rep(0, trials) # subsampled taxon richness
for (trial in 1:trials) {pool <- ids # pool from which specimens will be sampled
  specimensRemaining <- length(pool) # number of specimens remaining to be sampled
  seen <- rep(0, numTaxa) # keeps track of whether taxa have been sampled
  subsampledFrequency <- rep(0, numTaxa) # subsampled frequencies of the taxa
  coverage <- 0

  while (coverage < quota) {
    # draw a specimen
    drawnSpecimen <- sample(1:specimensRemaining, size=1)
    drawnTaxon <- pool[drawnSpecimen]
```

```
      # increment frequency for this taxon
      subsampledFrequency[drawnTaxon] <- subsampledFrequency[drawnTaxon] + 1

      # if taxon has not yet been found, increment the coverage
      if (seen[drawnTaxon] == 0) {
        if (drawnTaxon != mostFrequent && (ignore.singletons == 0 || abundance[drawnTaxon] > 1)) {
          coverage <- coverage + frequency[drawnTaxon]}
        seen[drawnTaxon] <- 1

        # increment the richness if the quota hasn't been exceeded,
        # and randomly throw back some draws that put the coverage over quota
        if (coverage < quota || runif(1) <= frequency[drawnTaxon]) {
          richness[trial] <- richness[trial] + 1} else {
          subsampledFrequency[drawnTaxon] <- subsampledFrequency[drawnTaxon] - 1}}

      # decrease pool of specimens not yet drawn
      pool[drawnSpecimen] <- pool[specimensRemaining]
      specimensRemaining <- specimensRemaining - 1}}

  # compute subsampled richness
  s2 <- richness[richness>0]
  subsampledRichness <- exp(mean(log(s2))) * length(s2)/length(richness)
  return(round(subsampledRichness, 1))}

#vector number of occurrences per period raw data available at (https://doi.org/10.5281/zenodo.3362508)
Holocene <-c(1)
U_Pleistocene <-c(4,5,6,1,4,1,1,3)
M_Pleistocene<-c(4,2,2,1)
Calabrian <-c(9,5,2,2,1)
Gelasian <-c(4,14,1,3,1)
Piacenzian <-c(1,4,5,7,1,1,2,3,2)
Zanclean <-c(8,2,4,5,2,2,1,2,14,3,5,5,4,5,2,2,2)
Messinian <-c(10,2,1,10,1,3,1,2,19,3,9,4,8,2,11,3,2,3,1)
Tortonian <-c(8,1,13,1,1,4,23,1,3,14,10,1,14,3,3,1,3)
Serravallian <-c(16,15,1,1,2,3,18,2,1,8,2,4,2,14,2,1)
```

```
Langhian <-c(16,1,14,3,1,3,18,2,1,11,3,7,1,12,2,1)
Burdigalian<-c(10,1,10,1,1,1,3,16,1,1,7,1,2,1,1,9,6,1)
Aquitanian <-c(1,6,1,1,3,15,2,1,2,2,7,2,2,1)
Chattian <-c(1,4,1,1,1,5,2,1,2,1,2,2,1)
Rupelian<-c(3,1,6,2,10,2,2,2,1,4,3)
Priabonian <-c(11,16,4,16,9,9,1,2,7,3,1,1,2,41,7,5,7,1,8,2,2,31,13,1,7,24,11,3)
Bartonian <-c(14,1,16,5,3,3,4,1,3,1,29,1,2,17,7,2,5,6,5,1)
Lutetian<-c(10,1,7,7,2,13,12,16,1,1,1,1,5,1,1,3,1,3,2,1,30,4,2,2,1,2,20,1,8,2,16,12,14,1,1)
Ypresian <-c(7,1,2,5,1,4,6,18,1,2,1,1,1,1,4,4,1,1,2,26,2,1,2,2,8,1,1,2,13,7,3,4,1,1,1,1)
Thanetian <-c(1,1,2,5,1,1,1,1,1,20,1,3,1,1)
Selandian <-c(3,1,14,1,1)
Danian <-c(5,4,1,1,2,1,13,1,1,1,1,1,1)
Maastrictian <-c(1,1,1,1,1,1,5,1,6,8,1,4,1,1,5,3,2,1,11,95,1,188,4,4,9,7,1,1,1,19,4,1,30,2,2,24,1,26,11,7,1,1,1,3,1,1,1)
Campanian <-c(1,1,1,1,1,2,4,1,3,4,2,2,4,76,1,100,1,4,8,5,1,21,7,1,33,1,24,21,5,5,1,5)
Santonian<-c(1,1,1,1,1,1,1,1,12,1,1,6,1,1,2,4,6,1,3,1,2,1,2)
Coniacian<-c(1,10,5,1,1,1)
Turonian <-c(1,1,10,1,2,5,3,2,3,2)
Cenomanian <-c(1,1,1,2,3,1,1,1,1,1,1,3,1,8,1,1,1,1,2,10,5,1,3,1,1,1,7,2,1,1,2)
Albian <-c(1,1,20,1,8,3,5,1,1,1)
Aptian <-c(2,1,1)
Barremian<-c(1,1,1,2)
Hauterivian<-c(1,2,1)
Valanginian<-c(1)
Berriasian<-c(4)
Tithonian <-c(1,2,1,1,1)
Kimmeridgian<-c(3,1,3)
Oxfordian <-c(2,1)
Callovian <-c(1,1)
Bathonian <-c(2,2)
Aalenian<-c(2,1)
Toarcian<-c(1,4,2,7)

# Set desired quorum levels:
quorum.levels <- setNames(c(0.1,0.2,0.3,0.4,0.5,0.6,0.7,0.8,0.9), c("Quorum_0.1", "Quorum_0.2", "Quorum_0.3", "Quorum_0.4",
"Quorum_0.5", "Quorum_0.6", "Quorum_0.7", "Quorum_0.8","Quorum_0.9"))
```

```
# Create output vector for results (Holocene):
Holocene.abundace <- vector()
# For each quorum level:
for (q in 1:length(quorum.levels)) {
  # Calculate sqs diversity:
  Holocene.abundace[[q]] <- sqs(abundance = Holocene, quota = 0.2)}

# Create output vector for results:
U_Pleistocene.abundace<- vector()
# For each quorum level:
for (q in 1:length(quorum.levels)) {
  # Calculate sqs diversity:
  U_Pleistocene.abundace[[q]] <- sqs(abundance = U_Pleistocene, quota  = 0.2)}

# Create output vector for results:
M_Pleistocene.abundance<- vector()
# For each quorum level:
for (q in 1:length(quorum.levels)) {
  # Calculate sqs diversity:
  M_Pleistocene.abundance[[q]] <- sqs(abundance = M_Pleistocene, quota  = 0.2)}


# Create output vector for results:
Calabrian.abundace<- vector()
# For each quorum level:
for (q in 1:length(quorum.levels)) {
  # Calculate sqs diversity:
  Calabrian.abundace[[q]] <- sqs(abundance = Calabrian, quota  = 0.2)}

# Create output vector for results:
Gelasian.abundace<- vector()
# For each quorum level:
for (q in 1:length(quorum.levels)) {
  # Calculate sqs diversity:
```

```
  Gelasian.abundace[[q]] <- sqs(abundance = Gelasian, quota  = 0.2)}


# Create output vector for results:
Piacenzian.abundace<- vector()
# For each quorum level:
for (q in 1:length(quorum.levels)) {
  # Calculate sqs diversity:
  Piacenzian.abundace[[q]] <- sqs(abundance = Piacenzian, quota  = 0.2)}


# Create output vector for results:
Zanclean.abundace<- vector()
# For each quorum level:
for (q in 1:length(quorum.levels)) {
  # Calculate sqs diversity:
  Zanclean.abundace[[q]] <- sqs(abundance = Zanclean, quota  = 0.2)}


# Create output vector for results:
Messinian.abundace<- vector()
# For each quorum level:
for (q in 1:length(quorum.levels)) {
  # Calculate sqs diversity:
  Messinian.abundace[[q]] <- sqs(abundance = Messinian, quota  = 0.2)}


# Create output vector for results:
Tortonian.abundace<- vector()
# For each quorum level:
for (q in 1:length(quorum.levels)) {
  # Calculate sqs diversity:
  Tortonian.abundace[[q]] <- sqs(abundance = Tortonian, quota  = 0.2)}


# Create output vector for results:
Serravallian.abundace<- vector()
# For each quorum level:
for (q in 1:length(quorum.levels)) {
  # Calculate sqs diversity:
```

```
    Serravallian.abundace[[q]] <- sqs(abundance = Serravallian, quota  = 0.2)}

# Create output vector for results:
Langhian.abundace<- vector()
# For each quorum level:
for (q in 1:length(quorum.levels)) {
  # Calculate sqs diversity:
  Langhian.abundace[[q]] <- sqs(abundance = Langhian, quota  = 0.2)}

# Create output vector for results:
Burdigalian.abundace<- vector()
# For each quorum level:
for (q in 1:length(quorum.levels)) {
  # Calculate sqs diversity:
  Burdigalian.abundace[[q]] <- sqs(abundance = Burdigalian, quota  = 0.2)}

# Create output vector for results:
Aquitanian.abundace<- vector()
# For each quorum level:
for (q in 1:length(quorum.levels)) {
  # Calculate sqs diversity:
  Aquitanian.abundace[[q]] <- sqs(abundance = Aquitanian, quota  = 0.2)}

# Create output vector for results:
Chattian.abundace<- vector()
# For each quorum level:
for (q in 1:length(quorum.levels)) {
  # Calculate sqs diversity:
  Chattian.abundace[[q]] <- sqs(abundance = Chattian, quota  = 0.2)}

# Create output vector for results:
Rupelian.abundace<- vector()
# For each quorum level:
for (q in 1:length(quorum.levels)) {
  # Calculate sqs diversity:
```

```
  Rupelian.abundace[[q]] <- sqs(abundance = Rupelian, quota  = 0.2)}

# Create output vector for results:
Priabonian.abundace<- vector()
# For each quorum level:
for (q in 1:length(quorum.levels)) {
  # Calculate sqs diversity:
  Priabonian.abundace[[q]] <- sqs(abundance = Priabonian, quota  = 0.2)}

# Create output vector for results:
Bartonian.abundace<- vector()
# For each quorum level:
for (q in 1:length(quorum.levels)) {
  # Calculate sqs diversity:
  Bartonian.abundace[[q]] <- sqs(abundance = Bartonian, quota  = 0.2)}

# Create output vector for results:
Lutetian.abundace<- vector()
# For each quorum level:
for (q in 1:length(quorum.levels)) {
  # Calculate sqs diversity:
  Lutetian.abundace[[q]] <- sqs(abundance = Lutetian, quota = 0.2)}

# Create output vector for results:
Ypresian.abundace<- vector()
# For each quorum level:
for (q in 1:length(quorum.levels)) {
  # Calculate sqs diversity:
  Ypresian.abundace[[q]] <- sqs(abundance = Ypresian, quota  = 0.2)}

# Create output vector for results:
Thanetian.abundace<- vector()
# For each quorum level:
for (q in 1:length(quorum.levels)) {
  # Calculate sqs diversity:
```

```
  Thanetian.abundace[[q]] <- sqs(abundance = Thanetian, quota  = 0.2)}

# Create output vector for results:
Selandian.abundace<- vector()
# For each quorum level:
for (q in 1:length(quorum.levels)) {
  # Calculate sqs diversity:
  Selandian.abundace[[q]] <- sqs(abundance = Selandian, quota  = 0.2)}

# Create output vector for results:
Danian.abundace<- vector()
# For each quorum level:
for (q in 1:length(quorum.levels)) {
  # Calculate sqs diversity:
  Danian.abundace[[q]] <- sqs(abundance = Danian, quota  = 0.2)}

# Create output vector for results:
Maastrictian.abundace<- vector()
# For each quorum level:
for (q in 1:length(quorum.levels)) {
  # Calculate sqs diversity:
  Maastrictian.abundace[[q]] <- sqs(abundance = Maastrictian, quota  = 0.2)}

# Create output vector for results:
Campanian.abundace<- vector()
# For each quorum level:
for (q in 1:length(quorum.levels)) {
  # Calculate sqs diversity:
  Campanian.abundace[[q]] <- sqs(abundance = Campanian, quota  = 0.2)}

# Create output vector for results:
Santonian.abundace<- vector()
# For each quorum level:
for (q in 1:length(quorum.levels)) {
  # Calculate sqs diversity:
```
338

```
  Santonian.abundace[[q]] <- sqs(abundance = Santonian, quota  = 0.2)}

# Create output vector for results:
Coniacian.abundace<- vector()
# For each quorum level:
for (q in 1:length(quorum.levels)) {
  # Calculate sqs diversity:
  Coniacian.abundace[[q]] <- sqs(abundance = Coniacian, quota  = 0.2)}

# Create output vector for results:
Turonian.abundace<- vector()
# For each quorum level:
for (q in 1:length(quorum.levels)) {
  # Calculate sqs diversity:
  Turonian.abundace[[q]] <- sqs(abundance = Turonian, quota  = 0.2)}

# Create output vector for results:
Cenomanian.abundace<- vector()
# For each quorum level:
for (q in 1:length(quorum.levels)) {
  # Calculate sqs diversity:
  Cenomanian.abundace[[q]] <- sqs(abundance = Cenomanian, quota  = 0.2)}

# Create output vector for results:
Albian.abundace<- vector()
# For each quorum level:
for (q in 1:length(quorum.levels)) {
  # Calculate sqs diversity:
  Albian.abundace[[q]] <- sqs(abundance = Albian, quota  = 0.2)}

# Create output vector for results:
Aptian.abundace<- vector()
# For each quorum level:
for (q in 1:length(quorum.levels)) {
  # Calculate sqs diversity:
```

```
  Aptian.abundace[[q]] <- sqs(abundance = Aptian, quota  = 0.2)}

# Create output vector for results:
Barremian.abundace<- vector()
# For each quorum level:
for (q in 1:length(quorum.levels)) {
  # Calculate sqs diversity:
  Barremian.abundace[[q]] <- sqs(abundance = Barremian, quota  = 0.2)}

# Create output vector for results:
Hauterivian.abundace<- vector()
# For each quorum level:
for (q in 1:length(quorum.levels)) {
  # Calculate sqs diversity:
  Hauterivian.abundace[[q]] <- sqs(abundance = Hauterivian, quota  = 0.2)}

# Create output vector for results:
Tithonian.abundace<- vector()
# For each quorum level:
for (q in 1:length(quorum.levels)) {
  # Calculate sqs diversity:
  Tithonian.abundace[[q]] <- sqs(abundance = Tithonian, quota  = 0.2)}

# Create output vector for results:
Kimmeridgian.abundace<- vector()
# For each quorum level:
for (q in 1:length(quorum.levels)) {
  # Calculate sqs diversity:
  Kimmeridgian.abundace[[q]] <- sqs(abundance = Kimmeridgian, quota  = 0.2)}

# Create output vector for results:
Callovian.abundace<- vector()
# For each quorum level:
for (q in 1:length(quorum.levels)) {
  # Calculate sqs diversity:
```

```r
  Callovian.abundace[[q]] <- sqs(abundance = Callovian, quota  = 0.2)}

# Create output vector for results:
Bathonian.abundace<- vector()
# For each quorum level:
for (q in 1:length(quorum.levels)) {
  # Calculate sqs diversity:
  Bathonian.abundace[[q]] <- sqs(abundance = Bathonian, quota  = 0.2)}

# Create output vector for results:
Aalenian.abundace<- vector()
# For each quorum level:
for (q in 1:length(quorum.levels)) {
  # Calculate sqs diversity:
  Aalenian.abundace[[q]] <- sqs(abundance = Aalenian, quota  = 0.2)}

# Create output vector for results:
Toarcian.abundace<- vector()
# For each quorum level:
for (q in 1:length(quorum.levels)) {
  # Calculate sqs diversity:
  Toarcian.abundace[[q]] <- sqs(abundance = Toarcian, quota  = 0.2)}

# Create output vector for results:
Valanginian.abundace<- vector()
# For each quorum level:
for (q in 1:length(quorum.levels)) {
  # Calculate sqs diversity:
  Valanginian.abundace[[q]] <- sqs(abundance = Valanginian, quota  = 0.2)}

# Create output vector for results:
Oxfordian.abundance<- vector()
# For each quorum level:
for (q in 1:length(quorum.levels)) {
  # Calculate sqs diversity:
```

```
  Oxfordian.abundance[[q]] <- sqs(abundance = Oxfordian, quota  = 0.2)}


# Create output vector for results:
Berriasian.abundance<- vector()
# For each quorum level:
for (q in 1:length(quorum.levels)) {
  # Calculate sqs diversity:
  Berriasian.abundance[[q]] <- sqs(abundance = Berriasian, quota  = 0.2)}


#show results copy in exel to create table
Holocene.abundace
U_Pleistocene.abundace
M_Pleistocene.abundance
Calabrian.abundace
Gelasian.abundace
Piacenzian.abundace
Zanclean.abundace
Messinian.abundace
Tortonian.abundace
Serravallian.abundace
Langhian.abundace
Burdigalian.abundace
Aquitanian.abundace
Chattian.abundace
Rupelian.abundace
Priabonian.abundace
Bartonian.abundace
Lutetian.abundace
Ypresian.abundace
Thanetian.abundace
Selandian.abundace
Danian.abundace
Maastrictian.abundace
Campanian.abundace
Santonian.abundace
```

```
Coniacian.abundace
Turonian.abundace
Cenomanian.abundace
Albian.abundace
Aptian.abundace
Barremian.abundace
Hauterivian.abundace
Valanginian.abundace
Berriasian.abundance
Tithonian.abundace
Kimmeridgian.abundace
Oxfordian.abundance
Callovian.abundace
Bathonian.abundace
Aalenian.abundace
Toarcian.abundace

# Input time bins (geological stages):
time.bins <- read.table("time.bins.txt", header = TRUE, row.names = 1)

# Get mid-point age of each interval (data in Appendix B.6):
time <- apply(time.bins, 1, median)

#taxic diversity: genus level
sqs.results <- read.csv("sqs.results.csv", header = T, row.names = 1)

#Obtain maxumum value in quorums
max(sqs.results$Quorum1,sqs.results$Quorum2,sqs.results$Quorum3,sqs.results$Quorum4,sqs.results$Quorum5,sqs.results$Quorum6,sqs.result
s$Quorum7,sqs.results$Quorum8,sqs.results$Quorum9)

#Obtain minumum value in quorums
min(sqs.results$Quorum1,sqs.results$Quorum2,sqs.results$Quorum3,sqs.results$Quorum4,sqs.results$Quorum5,sqs.results$Quorum6,sqs.result
s$Quorum7,sqs.results$Quorum8,sqs.results$Quorum9)

#quorum values
```

```
quorum.values <- seq(0,3.8, by= 0.09)

quorum1<- as.vector(sqs.results$Quorum1, mode = "any")
quorum2<- as.vector(sqs.results$Quorum2, mode = "any")
quorum3<- as.vector(sqs.results$Quorum3, mode = "any")
quorum4<- as.vector(sqs.results$Quorum4, mode = "any")
quorum5<- as.vector(sqs.results$Quorum5, mode = "any")
quorum6<- as.vector(sqs.results$Quorum6, mode = "any")
quorum7<- as.vector(sqs.results$Quorum7, mode = "any")
quorum8<- as.vector(sqs.results$Quorum8, mode = "any")
quorum9<- as.vector(sqs.results$Quorum9, mode = "any")

#quorum values as a dataframe
sqs.results <- data.frame(time,quorum1,quorum2,quorum3,quorum4,quorum5,quorum6,quorum7,quorum8,quorum9)

#plot results
gen.sqs <- ggplot(sqs.results, aes(x =time, y=quorum1)) +
  geom_line(aes(y = quorum1, colour= "quorum1")) +
  geom_line(aes(y = quorum2, colour= "quorum2")) +
  geom_line(aes(y = quorum3, colour= "quorum3"))+
  geom_line(aes(y = quorum4, colour= "quorum4"))+
  geom_line(aes(y = quorum5, colour= "quorum5"))+
  geom_line(aes(y = quorum6, colour= "quorum6"))+
  geom_line(aes(y = quorum7, colour= "quorum7"))+
  geom_line(aes(y = quorum8, colour= "quorum8"))+
  geom_line(aes(y = quorum8, colour= "quorum9"))+
  xlab("Time (Ma)") +
  ylab("Quorum_Value") +
  scale_y_continuous(breaks = seq(0,4,0.5)) +
  scale_x_reverse(breaks = seq(0,190,10)) +
  theme(panel.grid.minor = element_blank(), panel.grid.major = element_blank(),axis.line = element_line())
plot(gen.sqs)

# Calculate bin durations (i.e., legnth of each geological stage)
durations <- abs(apply(time.bins, 1, diff))
```

```r
# Scatter plot of SQS quorum4 and duration:
plot(durations, sqs.results$quorum4)

# Get test statistic: Cor. 0.167 p= 0.2828
cor.test(log10(durations + 1),log10(sqs.results$quorum4 + 1), method = "pearson")

#Load TDE
Genus.ages <- read.csv("Genus.csv", header = TRUE, row.names = 1)

# Calculate the taxic diversity estimate (TDE: i.e., taxonomic richness):
tde.genus <- taxicDivCont(timeData =Genus.ages, int.times = time.bins)[,3]

#create list that contains the stage time and taxa time
genus.ranges <- list(time.bins, tde.genus)

#Median of time bins
midtime <- apply(time.bins, 1, median)

# Scatter plot of TDE and duration:
plot(durations, tde.genus)

# Correlation after removal of Recent:
cor.test(durations[-c(1)], tde.genus[-c(1)], method = "pearson") #cor= -0.0385 p = 08083
cor.test(log10(durations + 1),log10(tde.genus + 1), method = "pearson") #cor= -0.2044 p = 0. 1884

# Call Graeme T. Lloyd's generalised differencing function:
gen.diff <- function(x, time) {
  # Suppress warning message:
  if(cor.test(time, x)$p.value > 0.05) print("Warning: variables not significantly correlated, generalised differencing not
recommended.")
  dt <- x - ((lsfit(time, x)$coefficients[2] * time) + lsfit(time, x)$coefficients[1])
  m <- lsfit(dt[1:(length(dt)-1)], dt[2:length(dt)])$coefficients[2]
  gendiffs <- dt[1:(length(dt) - 1)]- (dt[2:length(dt)] * m)
  gendiffs}
```

```
# Perform generalised differencing function on each variable:
gd.sqs <- gen.diff(sqs.results$quorum4, midtime)
gd.tde <- gen.diff(tde.genus, midtime)


#correlation test between diversity estimation methods
cor.test(gd.sqs, gd.tde, method = "spearman")
cor.test(gd.sqs, gd.tde, method = "kendall")


#plot results
plot(gd.sqs, gd.tde)
abline(lm(gd.sqs ~ gd.tde), col = "red")


#plotting tde and quorum
#create data frmae with variables

# Plot TDE and divergence ages estimated by the present analysis:
dframe1 <- data.frame(time, tde.genus)
tdeMe <- ggplot(dframe1, aes(x =time, y = tde.genus)) +
geom_line(size = 0.6, colour = "black") +
  xlab("Time (Ma)") +
  ylab("Genus (TDE)") +
  scale_y_continuous(breaks = seq(0,200,10)) +


  scale_x_reverse(breaks = seq(0,300,10)) +
  ggtitle('TDE. Vs Present results')+
  geom_rect(data = dframe1, aes(xmin = 130.91, xmax = 176.20), ymin = -Inf, ymax = Inf,
            fill= NA, color = "red", linetype = "dashed", alpha= 0.01, inherit.aes = FALSE)+#jurassic
  geom_rect(data = dframe1, aes(xmin = 97.98 , xmax = 147.47), ymin = -Inf, ymax = Inf,
             fill= NA, color = "blue", linetype = "dashed", alpha= 0.01, inherit.aes = FALSE)+#jurassic+cretaceous
  geom_rect(data = dframe1, aes(xmin = 93.92, xmax = 120.22), ymin = -Inf, ymax = Inf,
            fill= NA, color = "green", linetype = "dashed", alpha= 0.01, inherit.aes = FALSE)+#rhinopristiformes
```

```
    geom_rect(data = dframe1, aes(xmin = 86.64, xmax = 126.61), ymin = -Inf, ymax = Inf,
              fill= NA, color = "brown", linetype = "dashed", alpha= 0.01, inherit.aes = FALSE)+#Torpediniformes
    geom_rect(data = dframe1, aes(xmin = 98.56, xmax = 133.75), ymin = -Inf, ymax = Inf,
              fill= NA, color = "orange", linetype = "dashed", alpha= 0.01, inherit.aes = FALSE)+#rajiformes
    geom_rect(data = dframe1, aes(xmin = 93.48, xmax = 32.24), ymin = -Inf, ymax = Inf,
              fill= NA, color = "purple", linetype = "dashed", alpha= 0.01, inherit.aes = FALSE)+#modern batoids
    theme(panel.grid.minor = element_blank(), panel.grid.major = element_blank(), axis.line = element_line(), panel.background =
element_blank())

plot(tdeMe)

# Plot TDE and divergence ages estimated by the present analysis:
tdeAsch <- ggplot(dframe1, aes(x =time, y = tde.genus)) +
  geom_line(size = 0.6, colour = "black") +
  xlab("Time (Ma)") +
  ylab("Genus (TDE)") +
  scale_y_continuous(breaks = seq(0,200,10)) +

  scale_x_reverse(breaks = seq(0,300,10)) +
  ggtitle('TDE vs Aschliman et al. 2012')+
geom_rect(data = dframe1, aes(xmin = 153, xmax = 203.5), ymin = -Inf, ymax = Inf,
              fill= NA, color = "red", linetype = "dashed", alpha= 0.01, inherit.aes = FALSE)+#jurassic 1
  geom_rect(data = dframe1, aes(xmin =135 , xmax = 164), ymin = -Inf, ymax = Inf,
              fill= NA, color = "blue", linetype = "dashed", alpha= 0.01, inherit.aes = FALSE)+#jurassic+cretaceous
  geom_rect(data = dframe1, aes(xmin = 50, xmax = 115), ymin = -Inf, ymax = Inf,
              fill= NA, color = "green", linetype = "dashed", alpha= 0.01, inherit.aes = FALSE)+#rhinopristiformes+modern batoids
  geom_rect(data = dframe1, aes(xmin = 134.5, xmax = 151.3), ymin = -Inf, ymax = Inf,
              fill= NA, color = "yellow", linetype = "dashed", alpha= 0.01, inherit.aes = FALSE)+#myliobatiformes
  geom_rect(data = dframe1, aes(xmin = 164.9, xmax = 191.9), ymin = -Inf, ymax = Inf,
              fill= NA, color = "brown", linetype = "dashed", alpha= 0.01, inherit.aes = FALSE)+#Torpediniformes
  geom_rect(data = dframe1, aes(xmin = 66, xmax = 98), ymin = -Inf, ymax = Inf,
              fill= NA, color = "orange", linetype = "dashed", alpha= 0.01, inherit.aes = FALSE)+#rajiformes
  theme(panel.grid.minor = element_blank(), panel.grid.major = element_blank(), axis.line = element_line(), panel.background =
element_blank())
```

```
plot(tdeAsch)

#Plot sqs
dfquorum4 <- data.frame(time, quorum4)
quorum4plotME <- ggplot(dfquorum4, aes(x=time, y=quorum4))+
  geom_line(size = 0.6, colour = "black") +
  geom_line(size=0.6, colour= "black")+
  xlab("Time (Ma)") +
  ylab("Q.value") +
  scale_y_continuous(breaks = seq(0,15,0.5)) +
  scale_x_reverse(breaks = seq(0,190,10)) +
  ggtitle('SQS Vs Present results')+
  geom_rect(data = dfquorum4, aes(xmin = 130.91, xmax = 176.20), ymin = -Inf, ymax = Inf,
            fill= NA, color = "red", linetype = "dashed", alpha= 0.01, inherit.aes = FALSE)+#jurassic
  geom_rect(data = dfquorum4, aes(xmin = 97.98 , xmax = 147.47), ymin = -Inf, ymax = Inf,
            fill= NA, color = "blue", linetype = "dashed", alpha= 0.01, inherit.aes = FALSE)+#jurassic+cretaceous
  geom_rect(data = dfquorum4, aes(xmin = 93.92, xmax = 120.22), ymin = -Inf, ymax = Inf,
            fill= NA, color = "green", linetype = "dashed", alpha= 0.01, inherit.aes = FALSE)+#rhinopristiformes
  geom_rect(data = dfquorum4, aes(xmin = 61.77, xmax = 101.13), ymin = -Inf, ymax = Inf,
            fill= NA, color = "yellow", linetype = "dashed", alpha= 0.01, inherit.aes = FALSE)+#myliobatiformes
  geom_rect(data = dfquorum4, aes(xmin = 86.64, xmax = 126.61), ymin = -Inf, ymax = Inf,
            fill= NA, color = "brown", linetype = "dashed", alpha= 0.01, inherit.aes = FALSE)+#Torpediniformes
  geom_rect(data = dfquorum4, aes(xmin = 98.56, xmax = 133.75), ymin = -Inf, ymax = Inf,
            fill= NA, color = "orange", linetype = "dashed", alpha= 0.01, inherit.aes = FALSE)+#rajiformes
  geom_rect(data = dfquorum4, aes(xmin = 93.48, xmax = 32.24), ymin = -Inf, ymax = Inf,
            fill= NA, color = "purple", linetype = "dashed", alpha= 0.01, inherit.aes = FALSE)+#modern batoids
  theme(panel.grid.minor = element_blank(), panel.grid.major = element_blank(), axis.line = element_line(), panel.background =
element_blank())

plot(quorum4plotME)

quorum4plotAsh <- ggplot(dfquorum4, aes(x=time, y=quorum4))+
  geom_line(size = 0.6, colour = "black") +
  geom_line(size=0.6, colour= "black")+
```

```r
  xlab("Time (Ma)") +
  ylab("Q.value") +
  scale_y_continuous(breaks = seq(0,15,0.5)) +
  scale_x_reverse(breaks = seq(0,240,10)) +
  ggtitle('SQS Vs Aschliman et al. 2012')+
  geom_rect(data = dfquorum4, aes(xmin = 153, xmax = 203.5), ymin = -Inf, ymax = Inf,
            fill= NA, color = "red", linetype = "dashed", alpha= 0.01, inherit.aes = FALSE)+#jurassic
   geom_rect(data = dfquorum4, aes(xmin =135 , xmax = 164), ymin = -Inf, ymax = Inf,
            fill= NA, color = "blue", linetype = "dashed", alpha= 0.01, inherit.aes = FALSE)+#jurassic+cretaceous
  geom_rect(data = dfquorum4, aes(xmin = 50, xmax = 115), ymin = -Inf, ymax = Inf,
            fill= NA, color = "green", linetype = "dashed", alpha= 0.01, inherit.aes = FALSE)+#rhinopristiformes+modern batoids
  geom_rect(data = dfquorum4, aes(xmin = 134.5, xmax = 151.3), ymin = -Inf, ymax = Inf,
            fill= NA, color = "yellow", linetype = "dashed", alpha= 0.01, inherit.aes = FALSE)+#myliobatiformes
  geom_rect(data = dfquorum4, aes(xmin = 164.9, xmax = 191.9), ymin = -Inf, ymax = Inf,
            fill= NA, color = "brown", linetype = "dashed", alpha= 0.01, inherit.aes = FALSE)+#Torpediniformes
  geom_rect(data = dfquorum4, aes(xmin = 66, xmax = 98), ymin = -Inf, ymax = Inf,
            fill= NA, color = "orange", linetype = "dashed", alpha= 0.01, inherit.aes = FALSE)+#rajiformes
  theme(panel.grid.minor = element_blank(), panel.grid.major = element_blank(), axis.line = element_line(), panel.background =
element_blank())
plot(quorum4plotAsh)

#Plot together
plot <- ggarrange(tdeMe,tdeAsch, quorum4plotME, quorum4plotAsh, nrow = 4)
plot(plot)
```

Appendix 6.6

Time bins used for the diversity curves analyses

```
stage            int.start   int.end
Holocene         0.0117      0
U_Pleistocene    0.126       0.0117
M_Pleistocene    0.781       0.126
Calabrian        1.8         0.781
Gelasian         2.58        1.8
Piacenzian       3.6         2.58
Zanclean         5.333       3.6
Messinian        7.246       5.333
Tortonian        11.63       7.246
Serravallian     13.82       11.63
Langhian         15.97       13.82
Burdigalian      20.44       15.97
Aquitanian       23.03       20.44
Chattian         27.82       23.03
Rupelian         33.9        27.82
Priabonian       37.8        33.9
Bartonian        41.2        37.8
Lutetian         47.8        41.2
Ypresian         56          47.8
Thanetian        59.2        56
Selandian        61.6        59.2
Danian           66          61.6
Maastrictian     72.1        66
Campanian        83.6        72.1
Santonian        86.3        83.6
Coniacian        89.8        86.3
Turonian         93.9        89.8
Cenomanian       100.5       93.9
Albian           113         100.5
Aptian           125         113
Barremian        129.4       125
Hauterivian      132.9       129.4
Valanginian      139.8       132.9
Berriasian       145         139.8
Tithonian        152.1       145
Kimmeridgian     157.3       152.1
Oxfordian        163.5       157.3
Callovian        166.1       163.5
Bathonian        168.3       166.1
Bajocian         170.3       168.3
Aalenian         174.1       170.3
Toarcian         182.7       174.1
Pliensbachian    190         182.7

#the interval star and interval end for each period were taken from the
international chronostratigraphic chart 2017/02
```

Appendix 6.7

Ages used for the Tip-dating analysis using the oldest known occurrence in the fossil record for Sclerorhynchoidei

```
Calibrate Raja = uniform(0,70.6);
Calibrate Bathyraja = uniform(0, 70.6);
Calibrate Torpedo =uniform(0,58.7);
Calibrate Hypnos =uniform(0,58.7);
Calibrate Narcine =uniform(0,58.7);
Calibrate Narke =uniform(0,58.7);
Calibrate Temera =uniform(0,58.7);
Calibrate Titanonarke = uniform(48.6,55.8);
Calibrate Platyrhina =uniform(0,56);
Calibrate Platyrhinoidis = uniform(0,56);
Calibrate Zanobatus =uniform(0,65.5);
Calibrate Urolophus =uniform(0,56);
Calibrate Urobatis =uniform(0,56);
Calibrate Urotrygon =uniform(0,65.5);
Calibrate Gymnura =uniform(0,58.7);
Calibrate Myliobatis =uniform(0,65.5);
Calibrate Aetobatus =uniform(0,58.7);
Calibrate Rhinoptera =uniform(0,58.7);
Calibrate Mobula =uniform(0,33.9);
Calibrate Pristis =uniform(0,55.8);
Calibrate Rhynchobatus =uniform(0,55.8);
Calibrate Glaucostegus =uniform(0,55.8);
Calibrate Rhina =uniform(0,23);
Calibrate Rhinobatos =uniform(0,55.8);
Calibrate Zapteryx =uniform(0,55.8);
Calibrate Trygonorrhina =uniform(0,55.8);
Calibrate Asflapristis = uniform(89.8,129.4);
Calibrate Sclerorhynchus = uniform(59.2,129.4);
Calibrate Libanopristis = uniform(93.5,129.4);
Calibrate Ptychotrygon = uniform(89.8,129.4);
Calibrate Tingitanius = uniform(89.8,93.9);
Calibrate Tethybatis = uniform(72.1,83.6);
Calibrate G__intermedius = uniform(83.6,85.8);
Calibrate G__latus = uniform(83.6,86.3);
Calibrate G__maronita = uniform(93.9,100.5);
Calibrate G__tenuirostris = uniform(83.6,86.3);
Calibrate G__hakelensis = uniform(93.5,100.5);
Calibrate Rhombopterygia = uniform(93.5,99.6);
Calibrate G__grandis = uniform(93.5,100.5);
Calibrate Cyclobatis = uniform(93.5,99.6);
Calibrate Raja_davisi = uniform(83.6,86.3);
Calibrate Tlalocbatus = uniform(100.5,113);
Calibrate Sthalraja = uniform(100.5,113);
Calibrate G__whitfieldi = uniform(93.5,100.5);
Calibrate Britobatos = uniform(84.9,86);
Calibrate Kimmerobatis = uniform(145,152.1);
Calibrate Asterodermus = uniform(145.5,150.8);
Calibrate Spathobatis = uniform(125,175.6);
Calibrate Belemnobatis = fixed(177.7);
Calibrate Iansan = uniform(100.5,113);
Calibrate Aptychotrema =uniform(0,55.8);
Calibrate Asterotrygon = uniform(47.8,56);
Calibrate Heliobatis = uniform(47.8,56);
Calibrate G__zignii = uniform(47.8,56);
Calibrate Promyliobatis = uniform(47.8,56);
```

Appendix 6.8

Tip dated tree estimated using the oldest known age for the Suborder Sclerorhynchoidei

	Estimate interval ages (Ma.)		
Node	Low HPD	Mean	Upper HPD
1	144.4	159.01	172.69
2	113.52	131.46	150.83
3	97.02	115.17	135.54
4	94.42	112.03	130.82
5	94.02	106.33	120.2
6	87.11	99.15	110.5
7	29.99	46.78	63.34
8	12.27	32.76	50.5
9	138.07	152.97	167.84
10	103.82	121.34	139.45
11	77.98	102.54	124.25
12	49.5	77.32	101.21
13	42	58.76	74.3
14	84.89	101.97	119.71
15	94.53	111.48	128.38
16	77.67	92.67	107.25
17	35.6	51.18	65.84
18	65.77	79.28	93.25
19	29.96	44.15	57.49
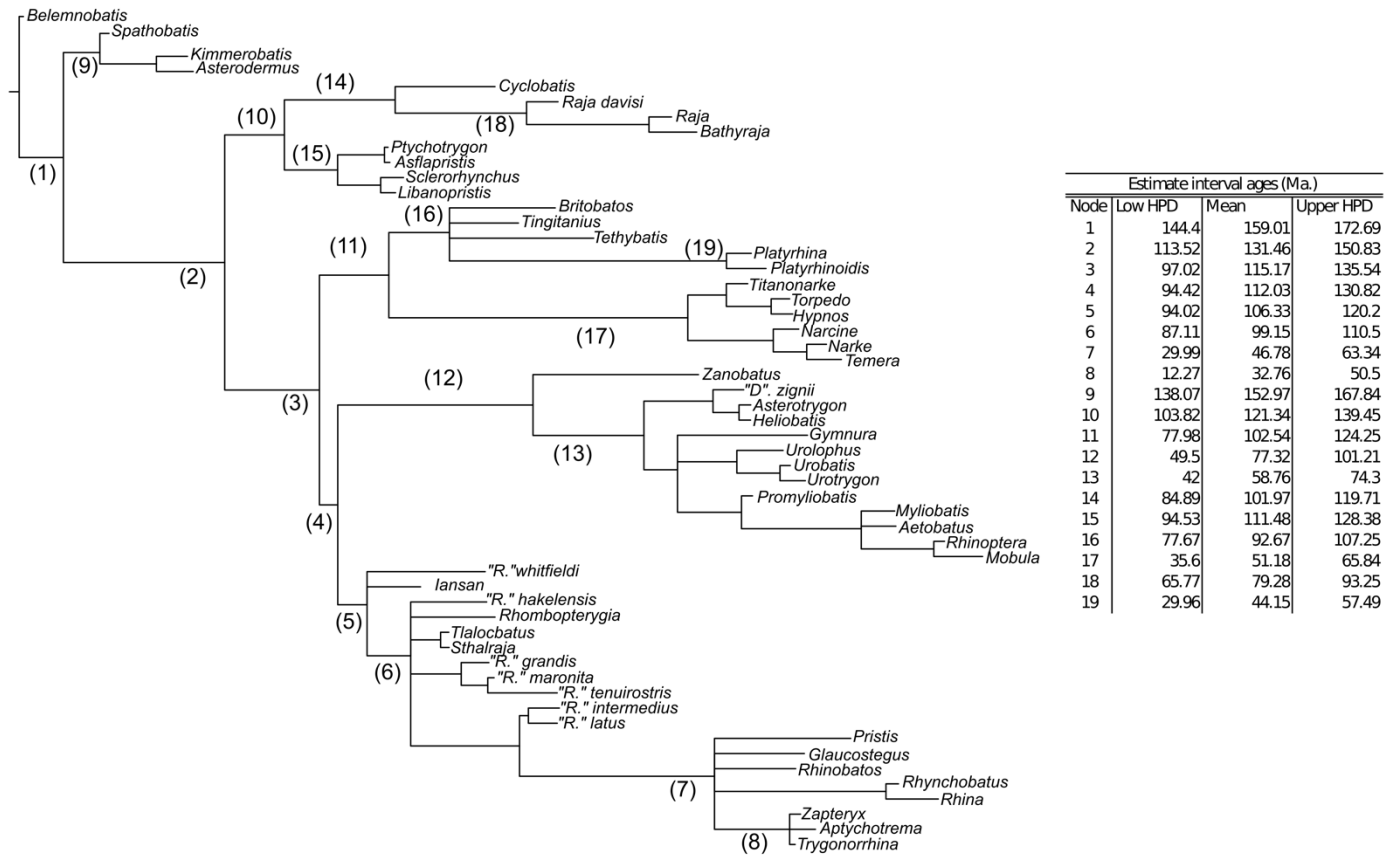
Appendix 7.1

Table with number of publications reviewed for the taxonomic review of the Sclerorhynchoidei

Locality	Interval	Category interval	Publications	Locality	Interval	Category interval	Publications
Africa	1885-1890	5	1	Middle East	1985-1990	21	1
Africa	1905-1910	7	1	Middle East	1990-1995	22	1
Africa	1925-1930	8	1	Middle East	1995-2000	23	1
Africa	1930-1935	9	4	Middle East	2000-2005	24	12
Africa	1935-1940	10	5	North America	1855-1860	3	1
Africa	1940-1945	11	6	North America	1945-1950	12	1
Africa	1950-1955	13	3	North America	1960-1965	15	3
Africa	1955-1960	14	2	North America	1965-1970	16	1
Africa	1960-1965	15	1	North America	1970-1975	18	2
Africa	1970-1975	17	1	North America	1975-1980	19	10
Africa	1980-1985	20	1	North America	1980-1985	20	1
Africa	1985-1990	21	8	North America	1985-1990	21	7
Africa	1990-1995	22	5	North America	1990-1995	22	5
Africa	1995-2000	23	2	North America	1995-2000	23	17
Africa	2000-2005	24	6	North America	2000-2005	24	9
Africa	2015-2019	27	6	North America	2005-2010	25	6
Europe	1845-1850	1	1	North America	2010-2015	26	4
Europe	1850-1855	2	1	North America	2015-2020	27	2
Europe	1880-1885	4	1	Pacific	1985-1990	21	1
Europe	1960-1965	15	7	Pacific	2010-2015	26	1
Europe	1980-1985	20	1	South America	1885-1890	5	1
Europe	1990-1995	22	1	South America	1930-1935	9	1
Europe	1995-2000	23	5	South America	1950-1955	13	1
Europe	2000-2005	24	4	South America	1960-1965	15	1
Europe	2005-2010	25	4	South America	1975-1980	19	3
Europe	2010-2015	26	5	South America	1990-1995	22	2
Middle East	1885-1890	5	1	South America	2000-2005	24	2
Middle East	1900-1905	6	6	South America	2005-2010	25	2
Middle East	1955-1960	14	4				
Total Publications in Locality	Africa =53	Europe = 30	Pacific = 2	Middle east = 11	North America = 69	South America = 13	
Total Publications in Zogeographica region	Gondwana=	Laurassia= 100					

Appendix 7.2

Table with geographical affiliations for the known species of the Sclerorhynchoidei

Species	Zoogeographical	Cat	Species	Zoogeograph	Cat
Dalpiazia stromeri	Cosmopolitan	1	*Colombusia roessingi*	Laurasia	3
Ganopristis leptodon	Cosmopolitan	1	*Colombusia deblieuxi*	Laurasia	3
Ganopristis karakensis	Cosmopolitan	1	*Iberotrygon plagiolophus*	Laurasia	3
Micropristis solomonis	Cosmopolitan	1	*Ischyrhiza mira*	Laurasia	3
Onchosaurus pharo	Cosmopolitan	1	*Ischyrhiza georgiensis*	Laurasia	3
Schizorhiza stromeri	Cosmopolitan	1	*Ischyrhiza monasterica*	Laurasia	3
Archingeayia sistaci	Gondwana	2	*Ischyrhiza viaudi*	Laurasia	3
Atlanticopristis equatorialis	Gondwana	2	*Kiestus texana*	Laurasia	3
Australopristis wiffeni	Gondwana	2	*Onchopristis dunklei*	Laurasia	3
Baharipristis bastetiae	Gondwana	2	*Sclerorhynchus fanninensis*	Laurasia	3
Biropristis landbecki	Gondwana	2	*Sclerorhynchus pettersi*	Laurasia	3
Ctenopristis nougareti	Gondwana	2	*Sclerorhynchus priscus*	Laurasia	3
Ctenopristis jordanicus	Gondwana	2	*Texatrygon hooveri*	Laurasia	3
Ischyrhiza chilensis	Gondwana	2	*Texatrygon avonicola*	Laurasia	3
Ischyrhiza hartenbergeri	Gondwana	2	*Texatrygon copei*	Laurasia	3
Ischyrhiza nigeriensis	Gondwana	2	*Texatrygon stouti*	Laurasia	3
Ischyrhiza serra	Gondwana	2	*Texatrygon benningensis*	Laurasia	3
Libanopristis hiram	Gondwana	2	*Ptychotrygon triangularis*	Laurasia	3
Marckgrafia libyca	Gondwana	2	*Ptychotrygon agujaensis*	Laurasia	3
Onchopristis numidus	Gondwana	2	*Ptychotrygon blainensis*	Laurasia	3
Onchosaurus radicalis	Gondwana	2	*Ptychotrygon boothi*	Laurasia	3
Plicatopristis strougoi	Gondwana	2	*Ptychotrygon chattahoocheensis*	Laurasia	3
Pucapristis branisi	Gondwana	2	*Ptychotrygon cuspidata*	Laurasia	3
Renpetia labiicarinata	Gondwana	2	*Ptychotrygon ellae*	Laurasia	3
Sclerorhynchus atavus	Gondwana	2	*Ptychotrygon eutawensis*	Laurasia	3
Ptychotrygon henkeli	Gondwana	2	*Ptychotrygon geyeri*	Laurasia	3
Ptychotrygon rostrispatula	Gondwana	2	*Ptychotrygon gueveli*	Laurasia	3
Asflapristis cristadentis	Gondwana	2	*Ptychotrygon ledouxi*	Laurasia	3
Agaleorhynchus britannicus	Laurasia	3	*Ptychotrygon pustulata*	Laurasia	3
Ankistrorhynchus lonzeensis	Laurasia	3	*Ptychotrygon rugosa*	Laurasia	3
Ankistrorhynchus major	Laurasia	3	*Ptychotrygon slaughteri*	Laurasia	3
Ankistrorhynchus washakiensis	Laurasia	3	*Ptychotrygon striata*	Laurasia	3
Borodinopristis schwimmeri	Laurasia	3	*Ptychotrygon vermiculata*	Laurasia	3
Borodinopristis ackermani	Laurasia	3	*Ptychotrygon winni*	Laurasia	3
Celtipristis herreroi	Laurasia	3	*Ptychotrygonoides pouiti*	Laurasia	3
Colombusia fragilis	Laurasia	3	*Ptychotrygonoides sabatieri*	Laurasia	3
Total					
Cosmopolitan = 6					
Gondwana = 22					
Laurasia = 44					

Appendix 7.3

Table with geographical affiliations for the known genera of the Sclerorhynchoidei

Genus	Zoological gerion	Genus	Zoological gerion
Dalpiazia	Cosmopolitan	*Libanopristis*	Gondwana
Ganopristis	Cosmopolitan	*Marckgrafia*	Gondwana
Ischyrhiza	Cosmopolitan	*Plicatopristis*	Gondwana
Micropristis	Cosmopolitan	*Pucapristis*	Gondwana
Onchopristis	Cosmopolitan	*Renpetia*	Gondwana
Onchosaurus	Cosmopolitan	*Agaleorhynchus*	Laurasia
Ptychotrygon	Cosmopolitan	*Ankistrorhynchus*	Laurasia
Schizorhiza	Cosmopolitan	*Archingeayia*	Laurasia
Sclerorhynchus	Cosmopolitan	*Borodinopristis*	Laurasia
Asflapristis	Gondwana	*Columbusia*	Laurasia
Atlanticopristis	Gondwana	*Kiestus*	Laurasia
Australopristis	Gondwana	*Ptychotrygonoides*	Laurasia
Baharipristis	Gondwana	*Texatrygon*	Laurasia
Biropristis	Gondwana	*Celtipristis*	Laurasia
Ctenopristis	Gondwana	*Iberotrygon*	Laurasia
Total			
Cosmopolitan	9		
Gondwana	12		
Laurasia	11		

Table with coordinates of the occurrences of the known genera of the Sclerorhynchoidei from the bibliographical review

Name	Cat	Fam	X	Y	Name	Cat	Fam	X	Y	Name	Cat	Fam	X	Y
Agaleorhynchus	1	Sclerorhynchidae	-1.18	51.47	Ischyrhiza	2	Onchopristidae	-89.40	32.35	Plicatopristis	1	Sclerorhynchidae	38.29	34.57
Agaleorhynchus	1	Sclerorhynchidae	-1.35	51.45	Ischyrhiza	2	Onchopristidae	-74.41	40.06	Pucapristis	3	Incertae	-65.76	-18.14
Agaleorhynchus	1	Sclerorhynchidae	-0.81	51.81	Ischyrhiza	2	Onchopristidae	-79.02	35.76	Ptychotrygon	1	Sclerorhynchidae	13.78	50.55
Agaleorhynchus	1	Sclerorhynchidae	-0.69	51.53	Ptychotrygon	1	Sclerorhynchidae	-103.40	29.16	Ptychotrygon	1	Sclerorhynchidae	-109.65	47.67
Ankistrorhynchus	1	Sclerorhynchidae	4.73	50.55	Renpetia	1	Sclerorhynchidae	28.91	28.39	Ptychotrygon	1	Sclerorhynchidae	-107.73	41.50
Ankistrorhynchus	1	Sclerorhynchidae	-74.17	40.36	Sclerorhynchus	1	Sclerorhynchidae	-96.16	33.55	Ptychotrygon	1	Sclerorhynchidae	-84.87	32.23
Ankistrorhynchus	1	Sclerorhynchidae	-107.70	43.80	Sclerorhynchus	1	Sclerorhynchidae	-96.16	33.19	Ptychotrygon	1	Sclerorhynchidae	-74.38	41.21
Atlanticopristis	3	Incertae	-45.86	-2.24	Sclerorhynchus	1	Sclerorhynchidae	-96.92	30.16	Ptychotrygon	1	Sclerorhynchidae	0.82	47.29
Australopristis	3	Incertae	173.42	-41.63	Sclerorhynchus	1	Sclerorhynchidae	35.65	33.99	Ptychotrygon	1	Sclerorhynchidae	-1.11	40.34
Baharipristis	1	Sclerorhynchidae	28.91	28.38	Asflapristis	1	Sclerorhynchidae	-4.93	31.85	Ptychotrygon	1	Sclerorhynchidae	28.91	28.38
Biropristis	1	Sclerorhynchidae	-71.67	-33.37	Ischyrhiza	2	Onchopristidae	-91.83	35.20	Ptrychotrygon	1	Sclerorhynchidae	-103.45	43.21
Borodinopristis	1	Sclerorhynchidae	-84.82	32.11	Ischyrhiza	2	Onchopristidae	-75.53	38.91	Ptrychtrygon	1	Sclerorhynchidae	-0.70	40.67
Borodinopristis	1	Sclerorhynchidae	-84.82	32.29	Ischyhiza	2	Onchopristidae	-99.18	31.87	Ptychotrygon	1	Sclerorhynchidae	-107.70	43.83
Celtipristis	1	Sclerorhynchidae	-0.70	40.95	Ischirhyza	2	Onchopristidae	-86.90	32.32	Ptychotrygon	1	Sclerorhynchidae	-4.91	31.87
Celtipristis	1	Sclerorhynchidae	-0.67	41.00	Ischyrhiza	2	Onchopristidae	-86.58	35.51	Ptrychotrygon	1	Sclerorhynchidae	-97.35	32.77
Columbusia	1	Sclerorhynchidae	-84.96	32.35	Ischyrhiza	2	Onchopristidae	-82.90	32.17	Ptychotrygon	1	Sclerorhynchidae	-0.63	40.85
Colombusia	1	Sclerorhynchidae	-108.04	44.38	Ischyrhiza	2	Onchopristidae	-106.35	56.13	Ptychotrygon	1	Sclerorhynchidae	-96.13	33.17
Colombusia	1	Sclerorhynchidae	-103.40	30.70	Ischyrhiza	2	Onchopristidae	-71.54	-35.68	Ptychotrygon	1	Sclerorhynchidae	-116.58	53.93
Colombusia	1	Sclerorhynchidae	-111.82	37.83	Ischyrhiza	2	Onchopristidae	-63.60	-16.28	Ptychotrygonoides	1	Sclerorhynchidae	4.63	49.76
Ctenopristis	1	Sclerorhynchidae	12.20	-5.58	Ischyrhiza	2	Onchopristidae	8.08	17.61	Ptychotrygonoides	1	Sclerorhynchidae	-0.77	45.75
Ctenopristis	1	Sclerorhynchidae	34.85	31.05	Ischyrhiza	2	Onchopristidae	64.58	41.38	Ptychotrygonoides	1	Sclerorhynchidae	-5.39	43.36
Ctenopristis	1	Sclerorhynchidae	-6.92	32.91	Ischyrhiza	2	Onchopristidae	-1.91	46.75	Texatrygon	1	Sclerorhynchidae	-104.49	43.00
Ctenopristis	1	Sclerorhynchidae	35.76	31.16	Kiestus	1	Sclerorhynchidae	-99.90	31.97	Texatrygon	1	Sclerorhynchidae	-101.87	30.16
Ctenopristis	1	Sclerorhynchidae	21.76	-4.04	Libanopristis	1	Sclerorhynchidae	35.89	34.01	Texatrygon	1	Sclerorhynchidae	-96.80	32.78
Ctenopristis	1	Sclerorhynchidae	43.15	31.92	Marckgrafia	1	Sclerorhynchidae	28.91	28.39	Texatrygon	1	Sclerorhynchidae	-110.08	34.39
Ctenopristis	1	Sclerorhynchidae	38.98	34.76	Micropristis	1	Sclerorhynchidae	35.86	33.96	Texatrygon	1	Sclerorhynchidae	-96.15	33.54
Dalpiazia	1	Sclerorhynchidae	13.19	32.89	Micropristis	1	Sclerorhynchidae	4.47	50.50	Texatrygon	1	Sclerorhynchidae	-106.59	34.99
Dalpiazia	1	Sclerorhynchidae	-7.05	31.77	Micropristis	1	Sclerorhynchidae	10.15	51.04	Texatrygon	1	Sclerorhynchidae	-84.79	32.27
Dalpiazia	1	Sclerorhynchidae	30.11	26.77	Micropristis	1	Sclerorhynchidae	-5.20	43.30	Texatrygon	1	Sclerorhynchidae	-112.19	37.59
Dalpiazia	1	Sclerorhynchidae	8.99	17.47	Onchopristis	2	Onchopristidae	5.10	36.68	Archingeayia	3	Incertae	-0.79	45.72
Dalpiazia	1	Sclerorhynchidae	18.02	-10.94	Onchopristis	2	Onchopristidae	28.91	28.39	Iberotrygon	3	Incertae	-0.64	40.86
Dalpiazia	1	Sclerorhynchidae	-3.75	40.46	Onchopristis	2	Onchopristidae	-4.66	30.53	Schizorhiza	3	Incertae	33.57	25.99
Dalpiazia	1	Sclerorhynchidae	21.76	-4.04	Onchopristis	2	Onchopristidae	-99.59	31.73	Schizorhiza	3	Incertae	-102.09	25.40
Dalpiazia	1	Sclerorhynchidae	36.24	30.59	Onchopristis	2	Onchopristidae	-1.11	40.35	Schizorhiza	3	Incertae	-100.03	31.31
Dalpiazia	1	Sclerorhynchidae	38.99	34.79	Onchopristis	2	Onchopristidae	-97.70	31.85	Schizorhiza	3	Incertae	-92.02	34.74
Ganopristis	1	Sclerorhynchidae	-6.92	32.91	Onchosaurus	3	Incertae	2.24	48.81	Schizorhiza	3	Incertae	-6.43	31.69
Ganopristis	1	Sclerorhynchidae	9.54	33.89	Onchosaurus	3	Incertae	-77.98	-0.82	Schizorhiza	3	Incertae	16.92	25.67
Ganopristis	1	Sclerorhynchidae	5.29	52.13	Onchosaurus	3	Incertae	-106.63	35.02	Schizorhiza	3	Incertae	8.35	8.01
Ganopristis	1	Sclerorhynchidae	-3.75	40.46	Onchosaurus	3	Incertae	-3.70	42.34	Schizorhiza	3	Incertae	22.00	-4.50
Ganopristis	1	Sclerorhynchidae	43.68	33.22	Onchosaurus	3	Incertae	31.13	29.97	Schizorhiza	3	Incertae	36.12	30.48
Ganoptistis	1	Sclerorhynchidae	-127.63	53.73	Onchosaurus	3	Incertae	16.45	-10.43	Schizorhiza	3	Incertae	39.07	34.74
Ganopristis	1	Sclerorhynchidae	36.24	30.59	Onchosaurus	3	Incertae	-74.41	10.41	Schizorhiza	3	Incertae	43.86	32.69
Ganopristis	1	Sclerorhynchidae	39.00	34.80	Onchosaurus	3	Incertae	2.11	13.57	Schizorhiza	3	Incertae	-63.73	-17.05
Ganopristis	1	Sclerorhynchidae	17.87	-11.20	Onchosaurus	3	Incertae	140.89	37.05	Schizorhiza	3	Incertae	-71.86	-35.89
Ischyrhiza	2	Onchopristidae	-96.92	30.16	Onchosaurus	3	Incertae	-104.10	29.95	Schizorhiza	3	Incertae	-6.58	32.85
Ischyrhiza	2	Onchopristidae	-83.10	31.81	Onchosaurus	3	Incertae	-78.59	-7.52	Schizorhiza	3	Incertae	-6.92	32.89
Ischyrhiza	2	Onchopristidae	-106.72	33.88	Plicatopristis	1	Sclerorhynchidae	34.20	26.26	Schizorhiza	3	Incertae	-100.35	28.74
Ischyrhiza	2	Onchopristidae	-98.48	39.01	Plicatopristis	1	Sclerorhynchidae	38.29	34.57					

Appendix 7.5

Table with the number of publications found in ISI Web of Knowledge under different combinations of key words

Year	cat	Title: Fossil assemblage or fossil fauna. Topic: Taxonomy, description, vertebrates	Title: description and fossil assemblage or fossil fauna. Topic: Taxonomy	Title: Fossil assemblage or fossil fauna Topic: Taxonomy, description	Title: Fossil assemblage or fossil fauna. Topic: Taxonomy, description, chodrichthyes
1965-1970	1	2	13	4	2
1971-1975	2	5	75	15	4
1976-1980	3	8	21	17	5
1981-1985	4	6	20	22	3
1986-1990	5	13	22	25	2
1991-1995	6	15	23	27	7
1996-2000	7	3	10	9	3
2001-2005	8	5	6	14	3
2006-2010	9	7	6	9	7
2011-2015	10	17	19	21	11
2016-2019	11	3	5	7	0

Appendix 7.6

Number of genera in time interval and locality

Locality	Interval	Cat	#Localities	Count_gen	Locality	Interval	Cat	#Localities	Count_gen
Africa	1885-1890	5	1	1	Middle East	1985-1990	21	1	4
Africa	1905-1910	7	1	2	Middle East	1990-1995	22	1	4
Africa	1925-1930	8	1	3	Middle East	1995-2000	23	1	5
Africa	1930-1935	9	1	5	Middle East	2000-2005	24	2	9
Africa	1935-1940	10	1	7	North America	1855-1860	3	1	1
Africa	1940-1945	11	2	7	North America	1945-1950	12	1	2
Africa	1950-1955	13	1	7	North America	1960-1965	15	1	4
Africa	1955-1960	14	2	7	North America	1965-1970	16	1	4
Africa	1960-1965	15	1	8	North America	1970-1975	18	2	6
Africa	1970-1975	17	1	8	North America	1975-1980	19	2	8
Africa	1980-1985	20	1	8	North America	1980-1985	20	1	8
Africa	1985-1990	21	2	11	North America	1985-1990	21	1	11
Africa	1990-1995	22	1	12	North America	1990-1995	22	3	11
Africa	1995-2000	23	1	12	North America	1995-2000	23	4	12
Africa	2000-2005	24	1	13	North America	2000-2005	24	1	13
Africa	2015-2020	27	1	15	North America	2005-2010	25	1	14
Europe	1845-1850	1	1	1	North America	2010-2015	26	3	14
Europe	1850-1855	2	1	2	North America	2015-2020	27	2	14
Europe	1880-1885	4	1	3	Pacific	1985-1990	21	1	1
Europe	1960-1965	15	1	6	Pacific	2010-2015	26	1	2
Europe	1980-1985	20	1	6	South America	1885-1890	5	1	1
Europe	1990-1995	22	1	7	South America	1930-1935	9	1	2
Europe	1995-2000	23	1	10	South America	1950-1955	13	1	3
Europe	2000-2005	24	2	10	South America	1960-1965	15	1	4
Europe	2005-2010	25	1	12	South America	1975-1980	19	1	5
Europe	2010-2015	26	3	13	South America	1990-1995	22	2	5
Middle East	1885-1890	5	1	1	South America	2000-2005	24	1	5
Middle East	1900-1905	6	3	2	South America	2005-2010	25	1	7
Middle East	1955-1960	14	1	4					

Appendix 7.7

Table with the year of description and redescription of the genera within Sclerorhynchoidei

Genus	Year	Redescrition
Onchosaurus	1852	
Ischyrhiza	1856	
Sclerorhynchus	1889	
Libanopristis	1903	1980
Micropristis	1903	1980
Onchopristis	1905	1917
Schizorhiza	1930	
Dalpiazia	1933	
Ganopristis	1935	
Marckgrafia	1935	
Ctenopristis	1940	
Pucapristis	1963	
Ankistrorhynchus	1964	
Kiestus	1975	
Ptychotrygon	1984	2009
Borodinopristis	1987	
Baharipristis	1989	
Renpetia	1989	
Plicatopristis	1991	
Ptychotrygonoides	1991	2012
Celtipristis	1999	
Texatrygon	1999	
Colombusia	2001	2012
Biropristis	2004	
Archingeayia	2007	
Atlanticopristis	2008	
Iberotrygon	2009	
Agaleorhynchus	2012	
Australopristis	2012	
Asflapristis	2019	

Appendix 7.8

Table with the year of description of the species within Sclerorhynchoidei

Species	Year	Species	Year
Ptychotrygon triangularis	1844	*Ptychotrygon henkeli*	1989
Onchosaurus radicalis	1852	*Renpetia labiicarinata*	1989
Ischyrhiza mira	1856	*Plicatopristis strougoi*	1991
Ischyrhiza chilensis	1887	*Ptychotrygonoides pouiti*	1991
Onchosaurus pharo	1887	*Colombusia deblieuxi*	1992
Sclerorhynchus atavus	1889	*Ischyrhiza monasterica*	1997
Libanopristis hiram	1903	*Ischyrhiza serra*	1997
Micropristis solomonis	1903	*Ptychotrygon winni*	1997
Onchopristis numidus	1905	*Sclerorhynchus pettersi*	1997
Schizorhiza stromeri	1930	*Celtipristis herreroi*	1999
Dalpiazia stromeri	1933	*Ptychotrygon geyeri*	1999
Ganopristis leptodon	1935	*Sclerorhynchus fanninensis*	1999
Marckgrafia libyca	1935	*Sclerorhynchus priscus*	1999
Ctenopristis nougareti	1940	*Texatrygon copei*	1999
Onchopristis dunklei	1962	*Borodinopristis ackermani*	2001
Ischyrhiza nigeriensis	1963	*Colombusia fragilis*	2001
Pucapristis branisi	1963	*Ischyrhiza georgiensis*	2001
Ankistrorhynchus lonzeensis	1964	*Ptychotrygon chattahoocheensis*	2001
Texatrygon avonicola	1964	*Ptychotrygon eutawensis*	2001
Ptychotrygon agujaensis	1972	*Ptychotrygon rugosa*	2001
Texatrygon hooveri	1972	*Texatrygon benningensis*	2001
Ptychotrygon ledouxi	1973	*Ctenopristis jordanicus*	2002
Ankistrorhynchus major	1975	*Ganopristis karakensis*	2002
Ischyrhiza hartenbergeri	1975	*Biropristis landbecki*	2004
Kiestus texana	1975	*Ptychotrygon gueveli*	2004
Ptychotrygon cuspidata	1975	*Archingeayia sistaci*	2007
Ptychotrygon slaughteri	1975	*Atlanticopristis equatorialis*	2008
Ptychotrygon vermiculata	1975	*Iberotrygon plagiolophus*	2009
Ptychotrygon blainensis	1978	*Ptychotrygon pustulata*	2009
Ischyrhiza viaudi	1981	*Ptychotrygon striata*	2009
Ankistrorhynchus washakiensis	1987	*Texatrygon stouti*	2011
Borodinopristis schwimmeri	1987	*Agaleorhynchus britannicus*	2012
Colombusia roessingi	1987	*Australopristis wiffeni*	2012
Ptychotrygon boothi	1987	*Ptychotrygonoides sabatieri*	2012
Ptychotrygon ellae	1987	*Asflapristis cristadentis*	2019
Baharipristis bastetiae	1989	*Ptychotrygon rosetta*	2019